

UNCLASSIFIED

AD NUMBER: AD0837223

LIMITATION CHANGES

TO:

Approved for public release; distribution is unlimited.

FROM:

Distribution authorized to US Government Agencies and their Contractors; Export Control; 1 May 1968. Other requests shall be referred to Air Force Materials Laboratory, Wright-Patterson AFB, OH 45433.

AUTHORITY

ARML notice dtd 11 Jul 1972

AFML-TR-66-186
Part II

AD837223

EVALUATION AND IMPROVEMENT OF COATINGS
FOR COLUMBIUM ALLOY GAS TURBINE ENGINE COMPONENTS

H. A. Hauser and J. F. Holloway, Jr.

PRATT & WHITNEY AIRCRAFT
DIVISION OF UNITED AIRCRAFT CORPORATION

Technical Report AFML-TR-66-186, Part II

May 1968

This document is subject to special export controls and each transmittal to foreign governments or foreign nationals may be made only with prior approval of the Metals and Ceramics Division (MAM), Air Force Materials Laboratory, Wright-Patterson AFB, Ohio 45433.

Air Force Materials Laboratory
Research and Technology Division
Air Force Systems Command
Wright-Patterson Air Force Base, Ohio

AD 837223
AUG 7 1968

**EVALUATION AND IMPROVEMENT OF COATINGS
FOR COLUMBIUM ALLOY GAS TURBINE ENGINE COMPONENTS**

Part II

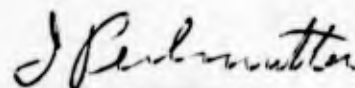
H. A. Hauser and J. F. Holloway, Jr.

This document is subject to special export controls and each transmittal to foreign governments or foreign nationals may be made only with prior approval of the Metals and Ceramics Division (MAM), Air Force Materials Laboratory, Wright-Patterson AFB, Ohio 45433.

FOREWORD

This report discusses the work performed by Pratt & Whitney Aircraft Division of United Aircraft Corporation, East Hartford, Connecticut on evaluation and improvement of coatings for columbium alloy gas turbine engine components during the period from 1 May 1966 to 31 December 1967. The work was performed in accordance with Contract No. AF33(615)-2117 under the direction of Mr. Norman M. Geyer (MAMP), Metals Branch, Metals and Ceramics Division of the Air Force Materials Laboratory. This contract was conducted under Project 7312, "Metal Surface Deterioration and Protection", Task 731201, "Metal Surface Protection", and was supported in part by the AFML Director's Fund. The report was originally submitted 31 August 1967 in compliance with Line Item 1c of DD Form 1423, dated 13 February 1965, attached to the original contract and amended by Contract Modification No. S5(67-3265), dated 10 April 1967; and with Exhibit C, Part I, paragraph C of Contract Modification No. S2(66-1258), dated 1 April 1966. So that the report would be of greater value to the reader, it was resubmitted, by agreement between the contractor and the Air Force Materials Laboratory, on 15 May 1968, with complete results of the laboratory evaluation portion of the program, which had not been scheduled for completion by the original submission date. The contractor has assigned the number PWA-3172 to the report.

This technical report has been reviewed and is approved.



I. PERLMUTTER
Chief, Metals Branch
Metals and Ceramics Division
AF Materials Laboratory

ABSTRACT

Data generated using laboratory tests such as oxidation-erosion, thermal fatigue, ballistic impact, and wear-galling to simulate turbine engine environments are reported for 14 coated columbium alloy composites, 12 in preliminary screening evaluations, 3 of which were pursued through advanced evaluation, and 2 others involved only in the advanced evaluation. Applications considered were turbine vane and turbine blade airfoils operating in the 1800°-2500°F temperature range and turbine blade roots at 1300°-1600°F. Oxidation-erosion, thermal fatigue, and ballistic impact test results for five vane and blade airfoil coating-substrate systems are reported and reviewed through preliminary screening and, where applicable, coating improvement phases. The Sylvania SiCrTi slurry/B-66 alloy and Solar MoTi-Si(TNV-12SE4)/Cb-132M alloy systems demonstrated the best overall performance of the five systems evaluated. As a result of the advanced evaluation program, it was recommended that the Sylvania SiCrTi slurry coating be engine tested on columbium alloy turbine vanes in the final phase of the contract program. Both the TRW TiCr-Si/Cb-132M and the Sylvania SiCrTi/XB-88 systems demonstrated potential for turbine blade application based on adequate oxidation-erosion, thermal fatigue, and 2200°F mechanical fatigue, creep, and stress-rupture performance in advanced evaluation. However, low ductility was observed in tensile tests at intermediate temperatures (1300°-1800°F). Since this characteristic would cause a high risk of premature failure during thermal cycling of a turbine blade, it was recommended that testing of coated columbium alloy turbine blades not be conducted under this contract. Of eight candidate turbine blade root systems evaluated, the Sylvania SiCrFe slurry coated alloy composites proved superior in 1300°-1600°F oxidation, wear-galling resistance, and fatigue performance. The NiCr and NiPt coatings demonstrated potential for the blade root application, especially with regard to coating ductility and minimum effect on composite properties, but, as applied in this program, were poor in 1300° and 1600°F oxidation. Additional development work on these two systems was recommended.

This abstract is subject to special export controls and each transmittal to foreign governments or foreign nationals may be made only with prior approval of the Metals and Ceramics Division (MAM), Air Force Materials Laboratory, Wright-Patterson AFB, Ohio 45433.

BLANK PAGE

TABLE OF CONTENTS

Section		Page
I	INTRODUCTION	1
II	SUMMARY	3
III	TECHNICAL DISCUSSION	6
	1. Items 1, 2, 3, 5, and 7. Literature Survey, Preliminary Screening Evaluation, Coating Improvement, and Advanced Evaluation of Vane and Blade Root Composite Properties	6
	2. Items 4 and 6. Advanced Evaluation	12
	2.1 Substrate Materials	12
	2.2 Coating Application	16
	2.3 Systems Evaluation, Test Procedures and Results	21
	3. Item 8. Preliminary Screening Evaluation of Additional Systems	40
	3.1 Substrate Materials	42
	3.2 Coatings Application, High-Temperature Systems	50
	3.3 Evaluation Testing, High-Temperature Systems	55
	3.4 Extracontractual High-Temperature Systems	93
	3.5 Coatings Application, Low-Temperature Systems	93
	3.6 Evaluation Testing, Low-Temperature Systems	110
	3.7 Performance Comparisons, Low-Temperature Systems	136
	4. Item 9. Coating Improvement of Additional Systems	137
	4.1 Substrate Materials	137
	4.2 Coatings Application	139
	4.3 Evaluation Testing	146
	4.4 Performance Comparisons of the Phase V and Phase VI High-Temperature Systems	156
	5. Items 10 and 11. Advanced Evaluation of Additional Systems	163
	5.1 Composite Materials, High-Temperature Systems	163
	5.2 Coatings Application, High-Temperature Systems	165
	5.3 Systems Evaluation, High-Temperature Systems	173
	5.4 Composite Materials, Low-Temperature Systems	202
	5.5 Coatings Application, Low-Temperature Systems	202
	5.6 Systems Evaluation, Low-Temperature Systems	205
IV	CONCLUSIONS AND RECOMMENDATIONS	228
	1. Conclusions	228
	2. Recommendations	230

TABLE OF CONTENTS (Cont'd)

Section	Page
V FUTURE WORK	231
REFERENCES	232

ILLUSTRATIONS

Figure		Page
1	Flow Chart for Phase I of Program (Items 1 and 2)	7
2	Flow Chart for Phase II of Program (Item 3)	9
3	Flow Chart for Phases III and IV of Program (Items 4 through 7)	10
4	Flow Chart for Items 4 and 6 Portions of Phases III and IV of Program	13
5	Typical Microstructure of As-Received Cb-132M Columbium Alloy Billets	15
6	Microstructure of the As-Extruded Cb-132M Columbium Alloy Bar	17
7	Microstructure of Remodified TRW TiCr-Si (Vacuum) Pack Coated Cb-132M Alloy	19
8	Concentration Profiles for Remodified TRW TiCr-Si (Vacuum) Pack Coated Cb-132M Alloy as Determined by Electron Microprobe Analyses	20
9	Erosion Bar Specimen Configuration for Oxidation-Erosion Tests	22
10	Burner Test Rig for Oxidation-Erosion Studies	22
11	Oxidation-Erosion Life of Remodified TRW TiCr-Si (Vacuum) Pack Coated Cb-132M Alloy as a Function of Test Temperature	23
12	Typical Localized Oxidation-Erosion Failures (Arrows) on Remodified TRW TiCr-Si (Vacuum) Pack Coated Cb-132M Alloy	24
13	Forged Paddle Specimen Configuration for Thermal Cycling Tests	25
14	Thermal Fatigue Life of Phase III TRW TiCr-Si (Vacuum) Pack Coated Cb-132M Alloy as a Function of Test Temperature	27
15	TRW TiCr-Si (Vacuum) Pack Coated Cb-132M Alloy Specimen (Convex Surface) After Thermal Fatigue Testing for 1000 Cycles to 2200°F	28

ILLUSTRATIONS (Cont'd)

Figure		Page
16	Surface of Remodified TRW TiCr-Si (Vacuum) Pack Coated Cb-132M Alloy After 1600°F Ballistic Impact at 500 Feet Per Second Showing Failure Which Occurred After 7 Hours Subsequent Static Oxidation Exposure at 2200°F	30
17	Surface of Remodified TRW TiCr-Si (Vacuum) Pack Coated Cb-132M Alloy After 2200°F Ballistic Impact at 500 Feet Per Second and 20 Hours Subsequent Static Oxidation Exposure at 2200°F	32
18	Microstructure of the Transition Area Between the Specimen Surface and Impact Depression for Remodified TRW TiCr-Si (Vacuum) Pack Coated Cb-132M Alloy Showing Coating Integrity	33
19	Bar Creep-Rupture Specimen Configuration	34
20	Fatigue Specimen Configuration	36
21	Fracture Surface of Remodified TRW TiCr-Si (Vacuum) Pack Coated Cb-132M Alloy After Fatigue Testing in Air at 2200°F	37
22	Flow Chart for Phase V of Program (Item 8)	41
23	Typical Microstructure of As-Received B-66 Columbium Alloy Bar	44
24	Typical Microstructure of As-Received B-66 Columbium Alloy Sheet	45
25	Typical Microstructure of As-Received XB-88 Columbium Alloy Bar	47
26	Typical Microstructure of XB-88 Columbium Alloy Bar After Heat Treatment for 1 Hour at 3000°F	48
27	Radiograph (Positive Print) of XB-88 Columbium Alloy Bars Showing Typical Stringers (Arrows)	49
28	Typical Microstructure of the As-Applied Sylvania SiCrTi Slurry Coating on B-66 Alloy	51
29	As-Coated TRW TiCr-Si/XB-88 Alloy Oxidation-Erosion Bar (Left) and Thermal Fatigue Paddle (Right)	52

ILLUSTRATIONS (Cont'd)

Figure		Page
30	Microstructure of the As-Deposited TRW TiCr-Si Coating on XB-88 Alloy	53
31	Microstructure of the As-Applied Solar V-CrTi-Si Coating on Cb-132M Alloy	54
32	Typical Microstructure of the As-Applied Solar MoTi-Si (TNV-12SE4) Coating on Cb-132M Alloy	56
33	Thermal Fatigue Bow Rig Showing Position of Specimens in Relation to Burner Nozzles	58
34	Vane Airfoil Specimen Configuration for Thermal Fatigue Tests	59
35	Single-Vane Thermal Fatigue Test Rig	59
36	Sylvania SiCrTi Slurry Coated B-66 Alloy Bar After Oxidation-Erosion Testing for 100 Hours at 2200°F Plus 100 Hours at 2400°F Plus 20 Hours at 2500°F	60
37	Sylvania SiCrTi Slurry Coated B-66 Alloy Bar After Oxidation-Erosion Testing for 100 Hours at 2200°F Plus 60 Hours at 2400°F	62
38	Oxide Penetration Through the Outer Coating Layers of Sylvania SiCrTi Slurry Coated B-66 Alloy Specimen After Oxidation-Erosion Testing for 100 Hours at 2200°F Plus 60 Hours at 2400°F	63
39	TRW TiCr-Si Coated XB-88 Alloy Bars After Oxidation-Erosion Testing for 20 Hours at 2200°F	64
40	Typical Oxidation Failure on TRW TiCr-Si Coated XB-88 Alloy Specimen Oxidation-Erosion Tested for 20 Hours at 2200°F	65
41	Typical Solar V-CrTi-Si Coated Cb-132M Alloy Erosion Bars After 80 Hours of Oxidation-Erosion Testing at 2200°F	66
42	Typical Microstructure of Solar V-CrTi-Si Coated Cb-132M Alloy After 80 Hours of Oxidation-Erosion Testing at 2200°F	67

ILLUSTRATIONS (Cont'd)

Figure		Page
43	Microstructure of Solar V-CrTi-Si Coated Cb-132M Alloy in Area of Local Oxidation Failure During 2200°F Oxidation-Erosion Testing	68
44	Microstructure of Cb-132M Alloy Substrate Showing Grain Boundary Oxygen Enrichment Beneath a Typical Solar V-CrTi-Si Coating Failure in 2200°F Oxidation-Erosion	69
45	Solar MoTi-Si Coated Cb-132M Alloy Bar After Oxidation-Erosion Testing for 100 Hours at 2200°F Plus 60 Hours at 2400°F	70
46	Solar MoTi-Si Coated Cb-132M Alloy Bar After Oxidation-Erosion Testing for 100 Hours at 2200°F Plus 100 Hours at 2400°F Plus 40 Hours at 2500°F	72
47	Solar MoTi-Si Coated Cb-132M Alloy Bar After Oxidation-Erosion Testing for 100 Hours at 2200°F Plus 100 Hours at 2400°F Plus 40 Hours at 2500°F	73
48	Microstructure of Solar MoTi-Si Coated Cb-132M Alloy After Oxidation-Erosion Testing for 100 Hours at 2200°F Plus 100 Hours at 2400°F Plus 40 Hours at 2500°F	74
49	Microstructure of Solar MoTi-Si Coated Cb-132M Alloy Showing Formation of Amorphous and Devitrified Glassy Structures During Oxidation-Erosion Testing	75
50	Microstructure of Solar MoTi-Si Coated Cb-132M Alloy Showing Substrate Oxidation Beneath Bisque-Colored Glassy Areas After Oxidation-Erosion Testing	76
51	Sylvania SiCrTi Slurry Coated B-66 Alloy Vane Airfoils After 600 Thermal Fatigue Cycles to 2200°F	77
52	Sylvania SiCrTi Slurry Coated B-66 Alloy Vane Airfoils After 600 Thermal Fatigue Cycles to 2200°F Plus 400 Cycles to 2400°F	78
53	Sylvania SiCrTi Slurry Coated B-66 Alloy Vane Airfoil After 600 Thermal Fatigue Cycles to 2200°F Plus 400 Cycles to 2400°F Plus a 30-Minute Exposure at 2500°F	79

ILLUSTRATIONS (Cont'd)

Figure		Page
54	Craze Cracking and Oxide Penetration Through Outer Coating Layers of Sylvania SiCrTi Slurry Coated B-66 Alloy After 600 Thermal Fatigue Cycles to 2200°F Plus 400 Cycles to 2400°F Plus a 30-Minute Exposure at 2500°F	80
55	Sylvania SiCrTi Slurry Coated B-66 Alloy Vane Airfoil Convex Surface After 600 Thermal Fatigue Cycles to 2200°F Plus 400 Cycles to 2400°F Plus 500 Cycles to 2500°F; No Coating Failure	81
56	Sylvania SiCrTi Slurry Coated B-66 Alloy Vane Airfoil After 600 Thermal Fatigue Cycles to 2200°F Plus 400 Cycles to 2400°F Plus 700 Cycles to 2500°F; No Coating Failure	82
57	TRW TiCr-Si Coated XB-88 Alloy Specimens After 200 Thermal Fatigue Cycles to 2200°F	84
58	Solar V-CrTi-Si Coated Cb-132M Alloy Thermal Fatigue Specimens (Convex Surfaces) After 200 Cycles to 2200°F	85
59	Solar V-CrTi-Si Coated Cb-132M Alloy Thermal Fatigue Specimens After 400 Cycles to 2200°F	86
60	Typical Microstructure of Solar V-CrTi-Si Coated Cb-132M Alloy After 400 Thermal Fatigue Cycles to 2200°F	87
61	Microstructure of Solar V-CrTi-Si Coated Cb-132M Alloy in Area of Local Oxidation Failure During 2200°F Thermal Fatigue Testing	88
62	Microstructure of Solar V-CrTi-Si Coated Cb-132M Alloy in Area of 2200°F Thermal Fatigue Failure at the Airfoil Trailing Edge	89
63	Solar MoTi-Si Coated Cb-132M Alloy Specimen After 600 Thermal Fatigue Cycles to 2200°F Plus 400 Cycles to 2400°F Plus 1200 Cycles to 2500°F	90
64	Solar MoTi-Si Coated Cb-132M Alloy Specimen (Convex Surface) After Thermal Fatigue Testing for 600 Cycles to 2200°F Plus 400 Cycles to 2400°F Plus 1400 Cycles to 2500°F	91

ILLUSTRATIONS (Cont'd)

Figure		Page
65	Schematic Cross Section of a Typical Coated Specimen After Ballistic Impact Test	92
66	Surfaces of Sylvania SiCrTi Slurry Coated B-66 Alloy After Room Temperature Impact Testing at 500 Feet Per Second (No Oxidation Exposure)	95
67	Solar (WMoVTi)-Si (TNV-7SE4) Coated Cb-132M Alloy Bar After Oxidation-Erosion Testing for 100 Hours at 2200°F Plus 40 Hours at 2400°F	96
68	Solar V-(CrTi)-Si Coated Cb-132M Alloy Bar After Oxidation-Erosion Testing for 100 Hours at 2200°F Plus 100 Hours at 2400°F Plus 20 Hours at 2500°F	97
69	Geometry of a Typical Blade Root Section Showing Conditions Suggesting the Duplex Coating Concept	99
70	Typical Microstructure of As-Applied Sylvania SiCrV Slurry Coating on Cb-132M Alloy	100
71	Typical Microstructure of As-Applied Sylvania SiCrFe Slurry Coating on Cb-132M Alloy	101
72	Typical Microstructure of As-Applied TRW TiAl (Vacuum) Pack Coating on Cb-132M Alloy	103
73	Typical Microstructure of the As-Applied TRW TiCr (Vacuum) Pack Coating on Cb-132M Alloy	104
74	Typical Microstructure of TRW TiCr-Al (Vacuum) Pack Coating on Cb-132M Alloy	105
75	Microstructure of the TRW TiCr-Si (Vacuum) Pack Coating on Cb-132M Alloy	107
76	Typical Microstructure of the Vacuum-Deposited NiCr Coating on Cb-132M Alloy	109
77	Microstructure of the PtRh Coating on Cb-132M Alloy	111

ILLUSTRATIONS (Cont'd)

Figure		Page
78	TRW TiCr (Vacuum) Pack Coated Cb-132M Alloy Test Specimen Showing Typical Localized Failures After 54 Hours Static Oxidation Exposure at 1600°F	113
79	Microstructure of TRW TiCr (Vacuum) Pack Coated Cb-132M Alloy After 54 Hours Static Oxidation Exposure at 1600°F	114
80	Typical Microstructure of TRW TiAl (Vacuum) Pack Coated Cb-132M Alloy After 400 Hours Oxidation Exposure at 1600°F	115
81	TRW TiCr-Al (Vacuum) Pack Coated Cb-132M Alloy Specimen Showing Edge Failure After 54 Hours Oxidation Exposure at 1600°F	116
82	TRW TiCr-Si (Vacuum) Pack Coated Cb-132M Alloy Specimen Showing Typical Edge Failure After 175 Hours Oxidation Exposure at 1600°F	118
83	Electroplated NiCr Coated Cb-132M Alloy Specimen Showing Typical Coating Failure After 8 Hours Oxidation Exposure at 1600°F	119
84	Microstructure of Electroplated NiCr Coated Cb-132M Alloy Showing Coating Separation and Oxide Formation at the Coating-Substrate Interface	120
85	PtRh Coated Cb-132M Alloy Specimen After 8 Hours Oxidation Exposure at 1300°F	121
86	Typical Microstructure of the NiPt Coated Cb-132M Alloy After 290 Hours Oxidation Exposure at 1300°F With No Failure	122
87	Tensile Specimen Configuration Used for Prestrain/Oxidation Tests	122
88	Typical Microstructure of Sylvania SiCrFe Slurry Coated Cb-132M Alloy After Tensile Testing in Air at 1300°F	125
89	Microstructure of TRW TiAl (Vacuum) Pack Coated Cb-132M Alloy After Tensile Failure at 70°F	126
90	Typical Microstructure of TRW TiCr-Al (Vacuum) Pack Coated Cb-132M Alloy After Tensile Testing at 70°F	127

ILLUSTRATIONS (Cont'd)

Figure		Page
91	Dovetail Specimen Configuration Used for Wear-Galling Test	128
92	Sylvania SiCrFe Slurry Coated Cb-132M Alloy Wear-Galling Specimen Showing Failure Within Dovetail Radius Area After 97,000 Cycles at 1300°F	131
93	Fracture Surface of Failed Sylvania SiCrFe Slurry Coated Cb-132M Alloy Wear-Galling Specimen After 97,000 Cycles at 1300°F and a Tensile Stress of 30,000 Psi	132
94	Sylvania SiCrFe Slurry Coated Cb-132M Alloy Wear-Galling Specimen Showing Wear Surface (Brackets) After 97,000 Cycles at 1300°F and a Tensile Stress of 30,000 Psi	133
95	TRW TiAl (Vacuum) Pack Coated Cb-132M Alloy Wear-Galling Specimen Showing Wear Surface (Brackets) After 500,000 Cycles at 1300°F and a Tensile Stress of 20,000 Psi	134
96	Electroplated NiCr Coated Cb-132M Alloy Wear-Galling Specimen Showing Wear Surface (Brackets) After 500,000 Cycles at 1300°F and a Tensile Stress of 30,000 Psi	135
97	Flow Chart for Phase VI of Program (Item 9)	138
98	Typical Microstructure of the As-Applied Modified Sylvania SiCrTi Slurry Coating on B-66 Alloy	140
99	Microstructure of the As-Applied Modified Sylvania SiCrTi Slurry Coating on B-66 Alloy Showing the Presence of Two Phases Comprising the Coating-Substrate Interface Layer	141
100	Typical Microstructure of As-Applied Modified TRW TiCr-Si (Vacuum) Pack Coating on XB-88 Alloy	143
101	Microstructure of the As-Applied Sylvania SiCrV Slurry Coating on Cb-132M Alloy	144
102	Microstructure of the As-Applied Sylvania SiCrV Slurry Coating on Cb-132M Alloy Showing Absence of Intermediate Phase Region Above the Coating-Substrate Interface Layer	145
103	Modified Sylvania SiCrTi Slurry Coated B-66 Alloy After Oxidation-Erosion Testing for 100 Hours at 2200°F Plus 100 Hours at 2400°F Plus 20 Hours at 2500°F	147

ILLUSTRATIONS (Cont'd)

Figure		Page
104	Modified TRW TiCr-Si (Vacuum) Pack Coated XB-88 Alloy Bar After Oxidation-Erosion Testing for 100 Hours at 2200°F Plus 100 Hours at 2400°F	148
105	Sylvania SiCrV Slurry Coated Cb-132M Alloy Bar Showing Edge Oxidation After Oxidation-Erosion Testing for 100 Hours at 2200°F Plus 60 Hours at 2400°F	150
106	Modified Sylvania SiCrTi Slurry Coated B-66 Alloy Vane Airfoil After Thermal Fatigue Testing for 600 Cycles to 2200°F Plus 400 Cycles to 2400°F Plus 300 Cycles to 2500°F	151
107	Modified Sylvania SiCrTi Slurry Coated B-66 Alloy Vane Airfoil (Same Airfoil Shown in Figure 106) After 300 Additional Thermal Fatigue Cycles to 2200°F (Total Cycles in Order: 600 to 2200°F, 400 to 2400°F, 300 to 2500°F, and 300 to 2200°F)	152
108	Concave Surface of Modified Sylvania SiCrTi Slurry Coated B-66 Alloy Vane Airfoil (Same Airfoil Shown in Figures 106 and 107) After 100 Additional Thermal Fatigue Cycles to 2200°F (Total Cycles in Order: 600 to 2200°F, 400 to 2400°F, 300 to 2500°F, and 400 to 2200°F)	153
109	Convex Airfoil Surface of Modified TRW TiCr-Si (Vacuum) Pack Coated XB-88 Alloy Specimen Showing Spot Oxidation Failures After Thermal Fatigue Testing for 600 Cycles to 2200°F	154
110	Convex Airfoil Surface of Sylvania SiCrV Slurry Coated Cb-132M Alloy Specimen Showing Spot Failures (Arrows) After Thermal Fatigue Testing for 600 Cycles to 2200°F Plus 400 Cycles to 2400°F Plus 600 Cycles to 2500°F	155
111	Convex Airfoil Surface of Sylvania SiCrV Slurry Cb-132M Alloy Specimen Showing Progression of Spot Failure Deterioration (Arrows) After 600 Additional Cycles to 2500°F	157
112	Sylvania SiCrV Slurry Coated Cb-132M Alloy Thermal Fatigue Specimen Showing Handle Defect	158

ILLUSTRATIONS (Cont'd)

Figure		Page
113	Oxidation-Erosion Performance Comparisons for the Phase V, Phase VI, and Additional Solar-Supplied Coating-Substrate Systems	160
114	Thermal Fatigue Performance Comparisons for the Phase V and Phase VI Coating-Substrate Systems	162
115	Flow Chart for Phase VII of Program (Items 10 and 11)	164
116	Typical Microstructure of Phase VII Sylvania SiCrTi Slurry Coating on B-66 Alloy	166
117	Structure of As-Applied Phase VII Sylvania SiCrTi Slurry Coating on B-66 Alloy at the Coating-Substrate Interface	167
118	Electron Micrograph of As-Applied Phase VII Sylvania SiCrTi Slurry Coating on B-66 Alloy Showing Regions of Diffusion Surrounding Precipitated Particles in the Outer Coating Region	168
119	Concentration Profiles for Phase VII Sylvania SiCrTi Slurry Coated B-66 Alloy As Determined By Electron Microprobe Analyses	170
120	Typical Microstructure of Phase VII Sylvania SiCrTi Slurry Coating on XB-88 Alloy	171
121	Electron Micrograph of As-Applied Phase VII Sylvania SiCrTi Slurry Coating on XB-88 Alloy Showing Columnar Growth Within the Diffusion Zone (A) and Intermediate Coating Layer (B)	172
122	Structure of As-Applied Phase VII Sylvania SiCrTi Slurry Coating on XB-88 Alloy Showing Surface Crack Penetration Through the Outer (A) and Intermediate (B) Coating Layers Into the Diffusion Zone (C)	174
123	Electron Micrograph of As-Applied Phase VII Sylvania SiCrTi Slurry Coating on XB-88 Alloy Showing Lateral Microcracks (Arrows) and the Absence of Diffusion Surrounding Precipitated Particles in the Outer Coating Region	175
124	Concentration Profiles for Phase VII Sylvania SiCrTi Coated XB-88 Alloy as Determined by Electron Microprobe Analyses	176
125	Oxidation-Erosion Life of Phase VII Sylvania SiCrTi Slurry Coated B-66 Alloy as a Function of Test Temperature	178

ILLUSTRATIONS (Cont'd)

Figure		Page
126	Phase VII Sylvania SiCrTi Slurry Coated B-66 Alloy Bar After Oxidation-Erosion Testing for 220 Hours at 2200°F	179
127	Phase VII Sylvania SiCrTi Slurry Coated B-66 Alloy Bar After Oxidation-Erosion Testing for 140 Hours at 2400°F	180
128	Phase VII Sylvania SiCrTi Slurry Coated B-66 Alloy Bar After Oxidation-Erosion Testing for 53 Hours at 2500°F	181
129	Phase VII Sylvania SiCrTi Slurry Coated B-66 Alloy Bars After 200 Hours Total Time at 2200°F Plus 50 Minutes Total Transient Time to 2600°F	182
130	Thermal Fatigue Life of Phase VII Sylvania SiCrTi Slurry Coated B-66 Alloy as a Function of Test Temperature	184
131	Surfaces of Phase VII Sylvania SiCrTi Slurry Coated B-66 Alloy Test Specimens After Room Temperature Impacting at 500 Feet Per Second and Subsequent Static Oxidation Exposure for 1 Hour at 2200°F	185
132	Surfaces of Phase VII Sylvania SiCrTi Slurry Coated B-66 Alloy After 2200°F Impacting at 500 Feet Per Second and Subsequent Static Oxidation Exposure for 3 Hours at 2200°F	187
133	Sheet Creep-Rupture Specimen Configuration	188
134	Creep-Rupture Properties of Phase VII Sylvania SiCrTi Slurry Coated B-66 Alloy at 2200° and 2500°F	189
135	Oxidation-Erosion Life of Phase VII Sylvania SiCrTi Slurry Coated XB-88 Alloy as a Function of Test Temperature	190
136	Typical Surface Appearance of Phase VII Sylvania SiCrTi Slurry Coated XB-88 Alloy Bar After Oxidation-Erosion Testing for 180 Hours at 2200°F	192
137	Typical Surface Appearance of Phase VII Sylvania SiCrTi Slurry Coated XB-88 Alloy Bar After Oxidation-Erosion Testing for 380 Hours at 2000°F	193
138	Surface Appearance of Phase VII Sylvania SiCrTi Slurry Coated XB-88 Alloy Bar After Oxidation-Erosion Testing for 60 Hours at 2500°F	194

ILLUSTRATIONS (Cont'd)

Figure		Page
139	Typical Surface Appearance of Phase VII Sylvania SiCrTi Slurry Coated XB-88 Alloy Bar After Melting (Transient Temperature Overshoot) Testing for 160 Hours at 2200°F Plus 40 Minutes Total Transient Time to 2600°F	195
140	Typical Surface Appearance of Phase VII Sylvania SiCrTi Slurry Coated XB-88 Alloy After 2000°F Impact Testing at 500 Feet Per Second and Subsequent Oxidation Exposure for 1 Hour at 2200°F	197
141	Creep-Rupture Properties of Phase VII Sylvania SiCrTi Slurry Coated XB-88 Alloy and Phase IV TRW TiCr-Si Coated Cb-132M Alloy at 2200°F	199
142	Fracture Surfaces of Phase VII Sylvania SiCrTi Slurry Coated XB-88 Alloy After Fatigue Testing at 50,000 Psi Stress in Air at 2200°F	201
143	Appearance of Phase VII Sylvania SiCrTi Slurry Coated XB-88 Alloy After Charpy Impact Testing at 1400°F, 60 Ft-Lb (Left); 1700°F, 120 Ft-Lb (Center); and 2000°F, 120 Ft-Lb (Right)	203
144	Typical Microstructure of As-Applied Sylvania SiCrFe Slurry Coating on XB-88 Alloy	204
145	Typical Microstructure of As-Applied TRW TiAl (Vacuum) Pack Coating on XB-88 Alloy	206
146	Sylvania SiCrFe Slurry Coated XB-88 Alloy Specimen Showing Edge Failure After 571 Hours Static Oxidation Exposure at 1600°F	208
147	TRW TiAl (Vacuum) Pack Coated XB-88 Alloy Specimen Showing Edge Failure After 77 Hours Static Oxidation Exposure at 1600°F	209
148	Typical Microstructure of As-Applied (Left) and Exposed (Right) TRW TiAl (Vacuum) Pack Coated XB-88 Alloy	210
149	Typical Microstructure of As-Applied (Left) and Exposed (Right) Sylvania SiCrFe Slurry Coated XB-88 Alloy	212
150	Sylvania SiCrFe Slurry Coated XB-88 Alloy Specimen Showing Edge Failure After 24-Hour Postcyclic Exposure at 1600°F	214

ILLUSTRATIONS (Cont'd)

Figure		Page
151	TRW TiAl (Vacuum) Pack Coated XB-88 Alloy Specimens Showing Edge and Surface Failures After Postcyclic Exposure at 1400°F	215
152	TRW TiAl (Vacuum) Pack Coated XB-88 Alloy Specimens Showing Typical Edge and Surface Failures After Postcyclic Exposure at 1600°F	216
153	Smooth and Notched ($K_t = 3.2$) Fatigue Specimen Configurations	217
154	Sylvania SiCrFe Slurry Coated XB-88 Alloy Notched ($K_t = 3.2$) Fatigue Specimens Showing Room Temperature Fracture Surface After Testing in Air at 1250°F	220
155	TRW TiAl (Vacuum) Pack Coated XB-88 Alloy Notched ($K_t = 3.2$) Fatigue Specimen Showing Room Temperature Fracture Surface After Testing at 30,000 Psi in Air at 1250°F	221
156	Sylvania SiCrFe Slurry Coated XB-88 Alloy Smooth Fatigue Specimen Showing Room Temperature Fracture Surface After Testing at 55,000 Psi Stress in Air at 1600°F	223
157	TRW TiAl (Vacuum) Pack Coated XB-88 Alloy Smooth Fatigue Specimen Showing Room Temperature Fracture Surface After Testing at 52,500 Psi Stress in Air at 1600°F	224
158	TRW TiAl (Vacuum) Pack Plus Sylvania SiCrTi Slurry Coated Compatibility Fatigue Specimens After Testing in Air at 1250°F	225
159	Sylvania SiCrFe Slurry Plus Sylvania SiCrTi Slurry Coated Compatibility Fatigue Specimens After Testing in Air	226
160	Sylvania SiCrFe Slurry Plus Sylvania SiCrTi Slurry Coated Compatibility Fatigue Specimen Showing Room Temperature Fracture Surface After Testing at 59,000 Psi Stress in Air at 1250°F	227
161	Flow Chart for Phase VIII of Program (Items 12 and 13)	231

TABLES

Table		Page
I	Chemical Analyses of Cb-132M Columbium Alloy Ingot	14
II	Results of Creep-Rupture Testing of Remodified TRW TiCr-Si (Vacuum) Pack Coated Cb-132M Alloy	35
III	Tensile Data For Remodified TRW TiCr-Si (Vacuum) Pack Coated Cb-132M Alloy	35
IV	Results of Fatigue Testing of Remodified TRW TiCr-Si (Vacuum) Pack Coated Cb-132M Alloy in Air at 2200°F	36
V	Results of Smooth Charpy Impact Testing of Remodified TRW TiCr-Si (Vacuum) Pack Coated Cb-132M Alloy	39
VI	Composition of B-66 Columbium Alloy Evaluated for Turbine Vane Application	43
VII	Results of Room Temperature Bend Testing of B-66 Alloy 0.050-Inch Sheet	46
VIII	Results of Phase V Ballistic Impact Testing of the Vane and Blade Airfoil Coating-Substrate Systems	94
IX	Results of Static Oxidation Testing of Phase V Turbine Blade Root Systems	112
X	Results of Prestrain/Oxidation Testing of Phase V Cb-132M Alloy Blade Root Test Specimens	123
XI	Results of Wear-Galling Testing of Phase V Coated Cb-132M Alloy Blade Root Test Specimens at 1300°F	129
XII	Results of Phase VI Ballistic Impact Testing of the Vane and Blade Airfoil Coating-Substrate Systems	159
XIII	Results of Creep-Rupture Testing of Phase VII Sylvania SiCrTi Slurry Coated B-66 Alloy	188
XIV	Results of Creep-Rupture Testing of Phase VII Sylvania SiCrTi Slurry Coated XB-88 Alloy	198
XV	Tensile Data for Phase VII Sylvania SiCrTi Slurry Coated XB-88 Alloy	198

TABLES (Cont'd)

Table		Page
XVI	Results of Fatigue Testing of Phase VII Sylvania SiCrTi Slurry Coated XB-88 Alloy in Air at 2200°F	200
XVII	Results of Smooth Charpy Impact Testing of Phase VII Sylvania SiCrTi Slurry Coated XB-88 Alloy	203
XVIII	Results of Static Oxidation Testing of Phase VII Blade Root Systems	207
XIX	Results of Cyclic Oxidation Testing of Phase VII Blade Root Systems	213
XX	Results of Fatigue Testing of Phase VII Coated XB-88 Alloy at 1250°F	218
XXI	Results of Fatigue Testing of Phase VII Coated XB-88 Alloy at 1600°F	219

BLANK PAGE

SECTION I

INTRODUCTION

The rapid oxidation rate of columbium alloys has prevented or severely restricted their application in high-temperature oxidizing environments. Since protection from oxidation is necessary to maintain desirable mechanical properties, coating development efforts have been very active in recent years. Most development programs, however, have been oriented toward applications such as re-entry vehicle and rocket engines operating for short times in the 2400° to 3000°F range to take maximum advantage of the high melting point, relatively low density, and high strength and ductility of columbium alloys at these temperatures. As a result, evaluations have been very limited under the conditions found in gas turbine engines, where operating temperatures are currently not as extreme and protection at low pressures is not required, but where reliability must be measured in hundreds or thousands of hours and/or cycles (both thermal and mechanical).

In addition to the high-temperature oxidizing environment, turbine blades and vanes must withstand thermal fatigue from cyclic operation, impact damage from ingested foreign objects, high steady-state and vibratory stresses from centrifugal loading (in the case of blades), and corrosion and erosion from the combusted fuel and air stream. The purpose of the subject evaluation program is to assess the performance of a number of coating/columbium alloy composites in two distinct areas: (1) turbine blade airfoil and turbine vane and (2) turbine blade root. Tentative operating temperature requirements for the blade airfoil and vane are 1800° to 2500°F. Blade root temperatures are only 1300° to 1600°F, but the coating alloy composites must operate under conditions of high stress and mechanical wear.

The program consists of a two-year effort to evaluate candidate coating-substrate systems by laboratory testing, followed by a third year to investigate further the best composites by engine testing if the laboratory tests warrant such action. The laboratory evaluations were accomplished in the first seven program phases, which are briefly described on the next page. Phases I and II and portions of Phases III and IV were completed during the first year of the program, and results were reported in Technical Report AFML-TR-66-186, Part I.

<u>Phase No.</u>	<u>Contractual Item No.</u>	<u>Description</u>	<u>Application Area</u>
I	1	Literature survey	Vane, blade airfoil, and blade root
	2	Preliminary screening evaluation	Vane, blade airfoil, and blade root
II	3	Coating improvement	Vane, blade airfoil, and blade root
III	4	Advanced evaluation, coating life properties	Vane, blade airfoil, and blade root
	5	Advanced evaluation, composite properties	Vane
IV	6	Advanced evaluation, composite properties	Blade airfoil
	7	Advanced evaluation, composite properties	Blade root
V	8	Preliminary screening evaluation of additional systems	Vane, blade airfoil, and blade root
VI	9	Coating improvement of additional systems	Vane and blade airfoil
VII	10	Advanced evaluation, coating life, additional systems	Vane, blade airfoil, and blade root
	11	Advanced evaluation, composite properties, additional systems	Vane, blade airfoil, and blade root
VIII	12	Preliminary component design and material procurement	Vane
	13	Simulated engine test	Vane

SECTION II

SUMMARY

The systems tabulated below were selected for evaluation in the second year of the program as a result of the literature survey and discussions with the Air Force Materials Laboratory Project Engineer. These systems were evaluated through preliminary screening tests for gas turbine engine vane and blade applications. These systems were in addition to those evaluated during the first year's effort, the results of which were reported in Technical Report AFML-TR-66-186, Part I.

<u>Application</u>	<u>Coating</u>	<u>Substrate Alloy</u>
Turbine vane	Sylvania SiCrTi slurry	B-66
Turbine blade airfoil	TRW TiCr-Si (vacuum) pack	XB-88
	Solar V-CrTi-Si	Cb-132M
	Solar MoTi-Si (TNV-12SE4)*	Cb-132M
Turbine blade root	Sylvania SiCrV slurry	Cb-132M
	Sylvania SiCrFe slurry	Cb-132M
	TRW TiAl (vacuum) pack	Cb-132M
	TRW TiCr (vacuum) pack	Cb-132M
	TRW TiCr-Al (vacuum) pack	Cb-132M
	TRW TiCr-Si (vacuum) pack	Cb-132M
	Electroplated NiCr	Cb-132M
	NiPt	Cb-132M

* Supplemental system; eligible for Phase V evaluation only

As a result of the Phase V preliminary screening evaluation of the vane and blade airfoil systems in the listing above, the following composites were evaluated in Phase VI, the coating improvement phase.

<u>Application</u>	<u>Coating</u>	<u>Substrate Alloy</u>
Turbine vane	Modified (thicker) Sylvania SiCrTi slurry	B-66
Turbine blade airfoil	Modified (increased titanium) TRW TiCr-Si (vacuum) pack	XB-88
	Sylvania SiCrV slurry	Cb-132M

Test results indicated that the Phase V and Phase VI Sylvania SiCrTi slurry/B-66 vane systems and the Solar MoTi-Si(TNV-12SE4)/Cb-132M supplemental blade airfoil system were superior to the other systems in oxidation-erosion performance. In thermal fatigue, the above systems and the Sylvania SiCrV slurry/Cb-132M system exhibited very good performance and were relatively insensitive to the cyclic conditions. Although the TRW TiCr-Si coating on XB-88 alloy and the Solar MoTi-Si (TNV-12SE4) coating on Cb-132M alloy were the only systems tested which demonstrated resistance to ballistic impact, performance was erratic and therefore marginal.

The modified Sylvania SiCrTi slurry coating was selected for Phase VII advanced evaluation on B-66 alloy as a vane system and the same coating on XB-88 alloy as a blade airfoil system.

Good performance in Phase VII oxidation-erosion testing was observed for the SiCrTi/B-66 alloy composite, with lives in excess of 900 hours at 1800°F, 220 hours at 2200°F, and 140 hours at 2400°F being obtained. Periodic cycling to 2600°F showed no significant decrease in 2200°F oxidation-erosion life. The thermal fatigue life of this composite system was outstanding with no failure occurring in 10,000 cycles to both 1800° and 2000°F. Cyclic lives averaging 6000 cycles to 2200°F, 3500 cycles to 2400°F, and 1400 cycles to 2500°F were obtained. Creep-rupture test results at 2200° and 2500°F indicated that this system exhibits marginal strength for turbine stator vanes. The ballistic impact performance was poor regardless of impact temperature.

Testing of the Sylvania SiCrTi slurry/XB-88 alloy composite system demonstrated good oxidation-erosion resistance, with lives in excess of 900 hours at 1800°F, 180 hours at 2200°F, and 80 hours at 2400°F obtained. Periodic cycling to 2600°F had no significant effect on 2200°F oxidation-erosion life. Cyclic lifetime in thermal fatigue was adequate, with performance of 2400 cycles to 2200°F, 1800 cycles to 2400°F, and 1400 cycles to 2500°F being observed. Creep-rupture testing at 2200°F indicated marginal creep strength for the composite. Good 2200°F fatigue strength was noted, with a 10^7 -cycle fatigue limit of 45,000 psi at 2200°F observed. Adequate Charpy impact strengths were seen between 1400° and 2000°F, but ballistic impact performance was poor regardless of impact temperature.

To complete the scheduled evaluation of systems selected for the first year of the program, Phase III and Phase IV advanced evaluation tests were performed on the "remodified" TRW TiCr-Si (vacuum) pack coated Cb-132M blade airfoil system. Oxidation-erosion performance was adequate, with average lives of 520 hours at 1800°F, 200 hours at 2200°F, and 87 hours at 2400°F observed. Periodic cycling to 2600°F resulted in a 35-percent decrease in 2200°F oxidation-erosion life. Thermal fatigue performance was fair, with lives of 5000 cycles to 1800°F, 1200 cycles to 2200°F, and only 600 cycles to 2500°F being noted. Creep-rupture data was limited due to difficulties with the test fixture and the low ductility of the coating-alloy composite.

Charpy impact and fatigue strengths were inferior to those obtained from the Sylvania SiCrTi/XB-88 system. These results were influenced by the low ductility of the Cb-132M alloy substrate. No brittle-to-ductile transition was observed in impact testing from 70° to 2000°F. A 2200°F fatigue limit of 35,000 psi was noted, with fracture occurring in a brittle manner.

Preliminary screening of eight blade root systems in Phase V indicated that the Sylvania SiCrFe slurry and the TRW TiAl (vacuum) pack coatings demonstrated superior overall performance on Cb-132M columbium alloy. Poor or marginal oxidation resistance at 1300° and/or 1600°F was noted for the TRW TiCr, TiCr-Al, and TiCr-Si coatings and the NiCr and NiPt coatings. All of the coating systems demonstrated good resistance to wear-galling.

Phase VII advanced evaluation for blade root coatings was conducted on Sylvania SiCrFe slurry and TRW TiAl (vacuum) pack coatings on XB-88 columbium alloy. Oxidation testing resulted in superior performance for the Sylvania SiCrFe coating, with 17 of 20 specimens surviving 1000 hours of testing at 1400° and 1600°F (10 specimens tested at each temperature). Only 8 of 20 TRW TiAl (vacuum) pack coated specimens survived 1000 hours in similar tests. Fatigue testing resulted in the superior performance of the Sylvania SiCrFe slurry coated XB-88 alloy, with fatigue limits of 49,000 psi at 1250°F and 48,500 psi at 1600°F being exhibited on notched specimens. The TRW TiAl (vacuum) pack coated XB-88 alloy exhibited lower performance, with a fatigue limit of less than 30,000 psi at 1250°F observed on notched specimens. The compatibility of a blade airfoil coating (Sylvania SiCrTi) and blade root coatings (Sylvania SiCrFe and TRW TiAl) on XB-88 alloy was excellent at both 1250° and 1600°F with fatigue strengths of approximately 50,000 psi observed on smooth specimens.

It is recommended in this report, based on the results obtained during the two-year evaluation effort, that Sylvania SiCrTi slurry be engine tested as a turbine vane coating in Phase VIII, Simulated Engine Test.

SECTION III

TECHNICAL DISCUSSION

1. ITEMS 1, 2, 3, 5, AND 7

LITERATURE SURVEY, PRELIMINARY SCREENING EVALUATION, COATING IMPROVEMENT, AND ADVANCED EVALUATION OF VANE AND BLADE ROOT COMPOSITE PROPERTIES

All work under contract Items 1, 2, 3, 5, and 7 was completed during the first 13 months of the contract period, and the results were reported in Technical Report AFML-TR-66-186, Part I.

In brief summary, selection of the initial eight coating-substrate systems tabulated below was based on the results of the literature survey (Item 1, Phase I) and discussions between the contractor and the Air Force Materials Laboratory Project Engineer. These systems were evaluated through preliminary screening tests for gas turbine engine vane and blade applications (Item 2, Phase I) according to the plan presented in Figure 1.

<u>Application</u>	<u>Classification</u>	<u>Coating</u>	<u>Substrate Alloy</u>
Turbine vane	Original	TRW TiCr-Si (vacuum) pack	C-129Y
	Original	Sylvania Ti-CrTi-Si (triplex) pack	D-43
	Supplemental	Sylvania SiCrTi slurry	D-43
Turbine blade airfoil	Original	TRW TiCr-Si (vacuum) pack	Cb-132M
	Supplemental	TRW TiCr-Si (slip) pack	Cb-132M
Turbine blade root	Original	Sylvania SnAl (505-F)	Cb-132M
	Original	Sylvania Ag-Al-Si (508-C)	Cb-132M
	Original	Zn	Cb-132M

The supplemental systems were not candidates for Phase II improvement or Phase III and Phase IV advanced evaluation because of time limitations due to their late incorporation into the program.

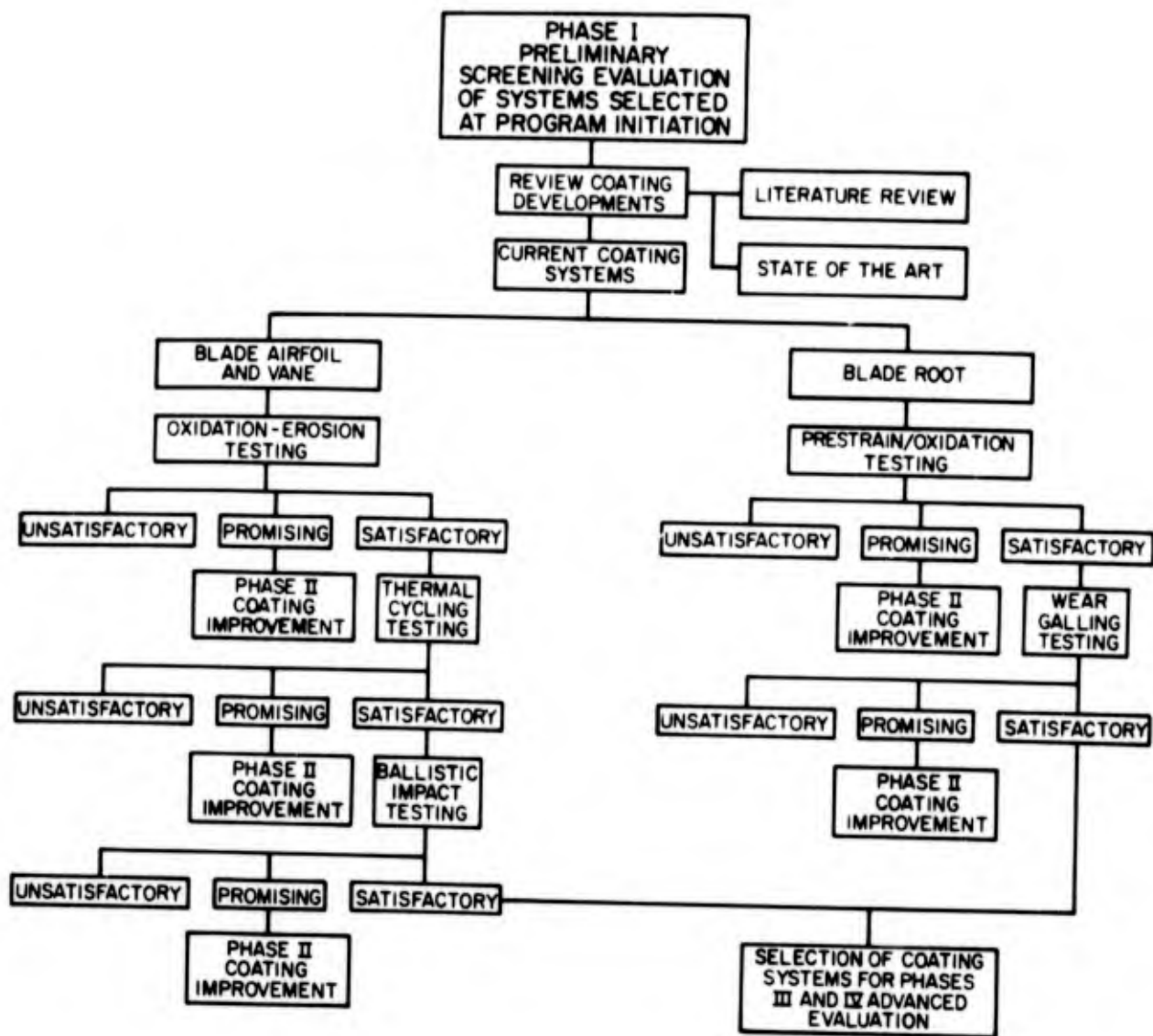


Figure 1. Flow Chart for Phase I of Program (Items 1 and 2)

Modification of the original systems constituted Phase II of the program (Item 3). Appropriate compositional and/or coating application process modifications were performed on those systems demonstrating substandard, but promising, performance in Phase I tests. The technical flow chart for Phase II is shown in Figure 2.

Evaluation of the Phase II modified coatings led to the selection of the following three systems for Phase III and Phase IV advanced evaluation:

<u>Application</u>	<u>Coating</u>	<u>Substrate Alloy</u>
Turbine vane	Modified TRW TiCr-Si (vacuum) pack	D-43
Turbine blade airfoil	Remodified TRW TiCr-Si (vacuum) pack	Cb-132M
Turbine blade root	Sylvania Ag-Al-Si (508-F)	Cb-132M

Item 4 constituted the portion of Phase III pertaining to coating life properties for the three systems listed above. Since the turbine blade airfoil work in Item 4 was not completed during the first year of the contract program, Item 4 work is described later in this report (see paragraph 2., Items 4 and 6).

As written in the Statement of Work in the original contract, Item 5 consisted of Phase III composite properties evaluation of all three advanced systems; this work was accordingly reported as Item 5, Phase III work in Technical Report AFML-TR-66-186, Part I. However, a contract amendment at the end of the first year of work transferred composite properties evaluation of the blade airfoil system to a new Item 6, Phase IV and of the blade root system to Item 7, Phase IV, leaving only the evaluation (stress-rupture and ballistic impact testing) of the TRW TiCr-Si/D-43 vane system in Item 5, Phase III (Figure 3). Since complete composite properties evaluation of the vane system was reported in AFML-TR-66-186, Part I, the Item 5 work was considered to be complete (reference Section V, Future Work, of that report).

Since work under Item 6, the composite properties evaluation of the blade airfoil system, was not completed during the first year, it is described in this report under paragraph 2., Items 4 and 6.

Work under Item 7, the blade root portion of the Phase IV composite properties evaluation, consisted of mechanical fatigue testing of Sylvania Ag-Al-Si (508-F) coated Cb-132M alloy at 1300°F in air plus oxidation exposure at 1300° and 1600°F, cyclic oxidation from 1300° and 1600° to 2000°F, and duplex coating compatibility, i. e. overlap compatibility between the Sylvania Ag-Al-Si and the TRW TiCr-Si coatings. Except for the mechanical fatigue testing, all work on the Sylvania Ag-Al-Si/Cb-132M system was completed during the first year, with the results reported in Technical Report AFML-TR-66-186, Part I.

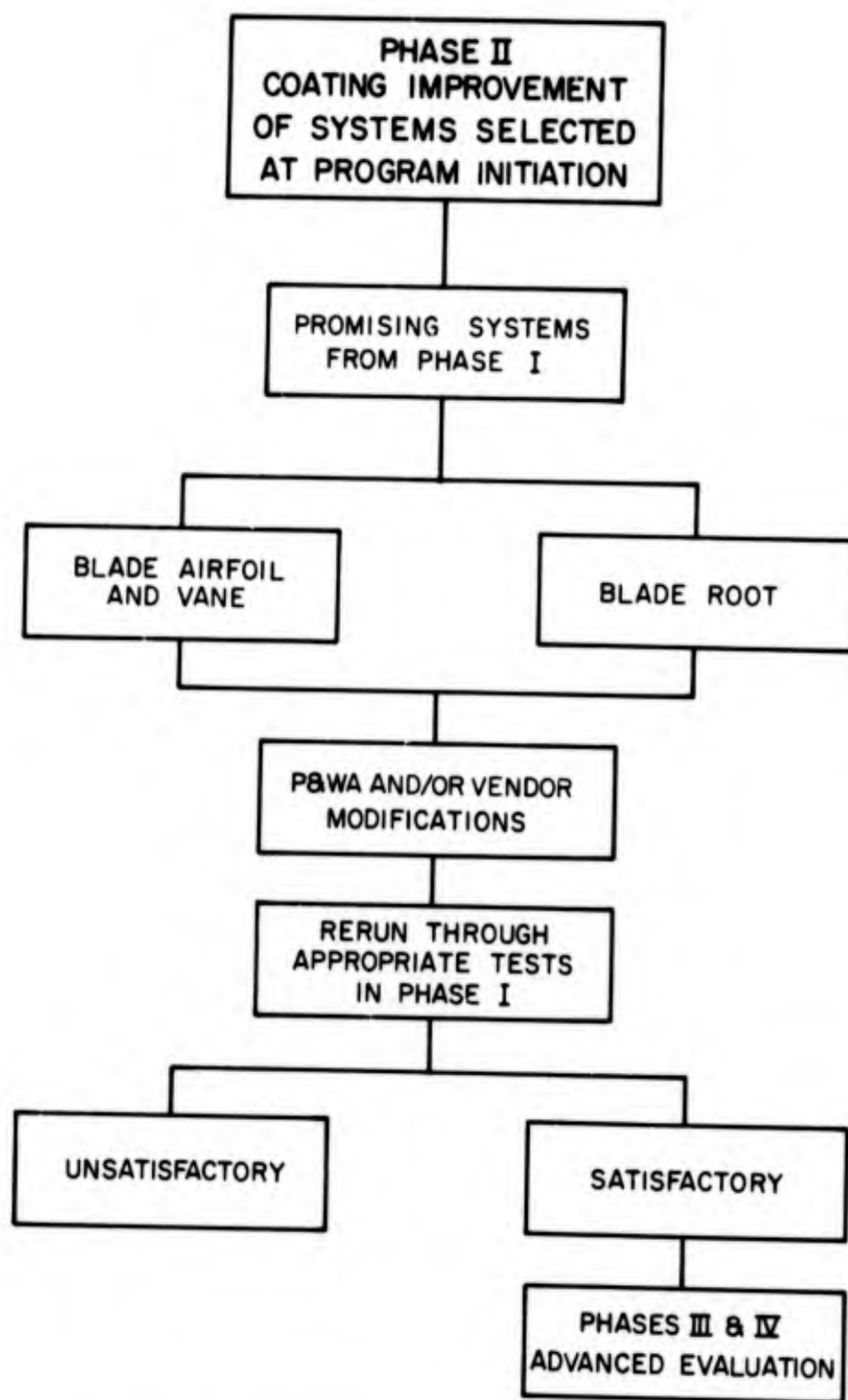


Figure 2. Flow Chart for Phase II of Program (Item 3)

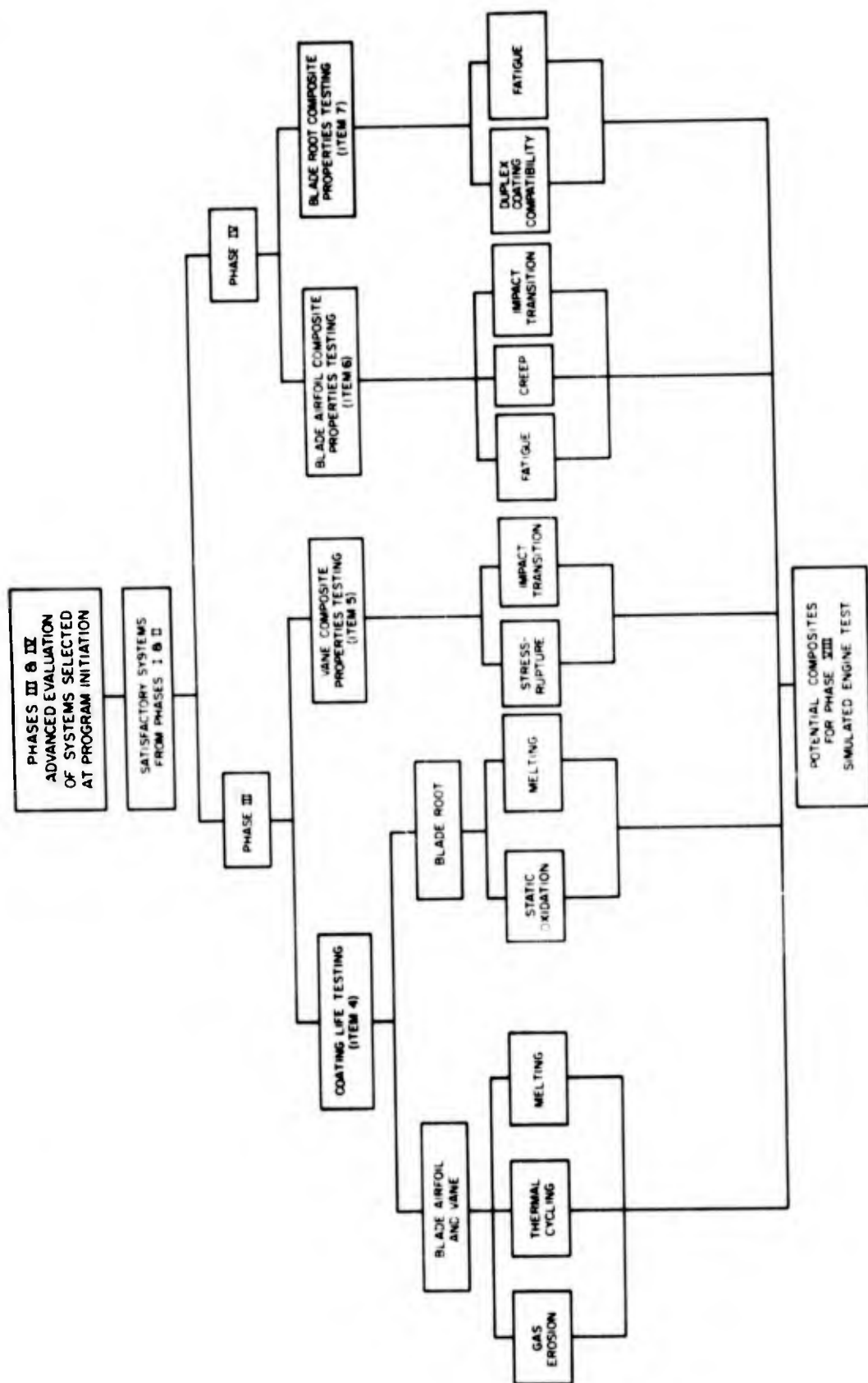


Figure 3. Flow Chart for Phases III and IV of Program (Items 4 through 7)

Since the performance of the Sylvania Ag-Al-Si coating was considered marginal for the blade root application, the fatigue testing of this system was deleted, in early 1967, from Item 7 with the approval of the Air Force Materials Laboratory Project Engineer. The change permitted the evaluation of one additional blade root composite in Phase VII, Items 10 and 11 and completed the Phase IV, Item 7 requirements.

2. ITEMS 4 AND 6

ADVANCED EVALUATION

Contract Item 4, the coating life evaluation portion of Phase III of the program, requires that the contractor perform oxidation-erosion, thermal cycling, and melting tests until failure on the optimized blade airfoil and vane coating systems and also static oxidation and melting tests on the optimized blade root coating system. These tests are to determine protectiveness, diffusional stability, and reliability as well as ability to withstand transient temperature overshoots.

Modified TRW TiCr-Si (vacuum) pack coated D-43 alloy for vane applications and Sylvania Ag-Al-Si (508-F) coated Cb-132M alloy for blade root applications completed the Item 4 evaluation during the first year of the contract period; the results were reported in Technical Report AFML-TR-66-186, Part I. Item 4 evaluation of remodified TRW TiCr-Si (vacuum) pack coated Cb-132M alloy for blade airfoil applications is reported below.

Under contract Item 6, the blade airfoil portion of the Phase IV composite properties evaluation, the properties of remodified TRW TiCr-Si (vacuum) pack coated Cb-132M alloy were determined for blade airfoil application. This evaluation includes fatigue, creep, and ballistic impact testing.

The flow chart for work under Items 4 and 6 is shown in Figure 4.

2.1 SUBSTRATE MATERIALS

Turbine blade alloys must have high fatigue strength, resistance to creep, and the ability to absorb impact forces without fracture. Sufficient yield strength at lower temperatures, i. e. below 1600°F, is also required to satisfy attachment (blade root) requirements. Since Cb-132M columbium alloy had demonstrated potential properties for fulfilling these requirements, it was selected at the beginning of the program as the Phase I blade alloy. Because Cb-132M was the only blade alloy in Phases I and II of the program, it was necessarily forwarded to Phase III and Phase IV advanced evaluation.

Nominal 3-inch-diameter extruded Cb-132M alloy billets were obtained from Fansteel Metallurgical Corporation. The chemical analyses of the 5-inch-diameter ingot after electron beam melting are presented in Table I. The material exhibited a completely worked microstructure after extrusion (Figure 5). Further extrusion of the billets to a 1.25-inch-diameter size was performed at the Nuclear Metals

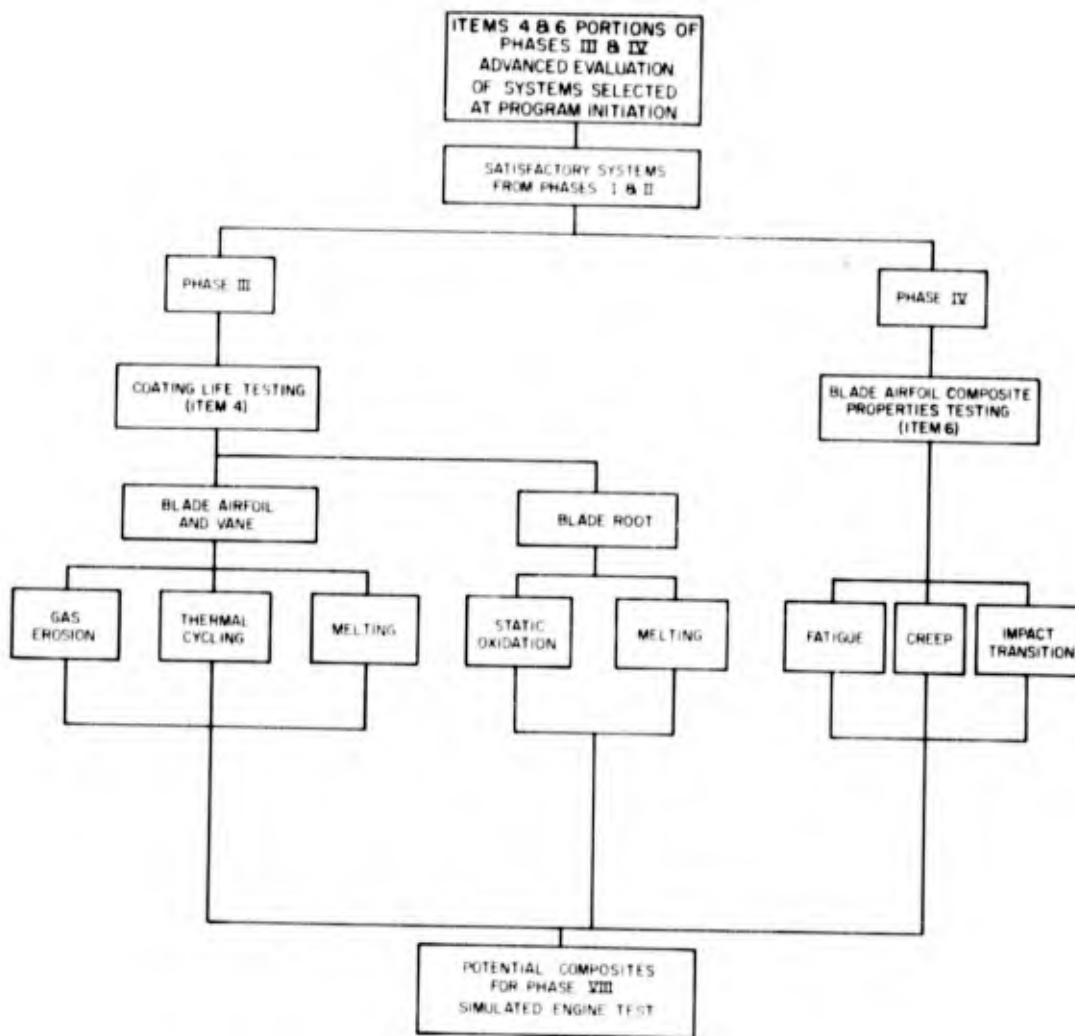


Figure 4. Flow Chart for Items 4 and 6 Portions of Phases III and IV of Program

TABLE I
 CHEMICAL ANALYSES OF Cb-132M
 COLUMBIUM ALLOY INGOT

Analysis Location	Composition (percent)						Interstitial (Gas) Impurities (parts per million)		
	Cb	Ta	W	Mo	Zr	C	O	H	N
Top of Ingot	Balance	20.50	15.20	4.59	1.27	0.10	133	5	1
Bottom of Ingot	Balance	19.80	14.70	4.60	1.70	0.11	126	5	1

Note: Chemical analyses for Heat No. 132-B-1868 supplied by Fansteel Metallurgical Corporation.



PLANE: NORMAL TO EXTRUSION DIRECTION
ETCH: 33% HYDROFLUORIC ACID, 33% NITRIC ACID, 33% WATER

MAG: 100X



PLANE: PARALLEL TO EXTRUSION DIRECTION (ARROW)
ETCH: 33% HYDROFLUORIC ACID, 33% NITRIC ACID, 33% WATER

MAG: 100X

Figure 5. Typical Microstructure of As-Received Cb-132M Columbian Alloy Billets

Division of the Whittaker Corporation. After encapsulation in molybdenum, extrusion was carried out in ZrO₂-lined dies utilizing the parameters tabulated below.

<u>Billet No.</u>	<u>Reduction</u>	<u>Extrusion Temp. (°F)</u>	<u>Force (tons)</u>	
			<u>Upset</u>	<u>Running</u>
A-1	6.0X	3350	750	700
A-2	6.0X	3350	670	650
A-3	6.3X	3350	700	650
B-1	5.7X	3350	720	650
B-2	5.7X	3350	720	650
B-3	5.8X	3350	700	650
C	5.5X	3000	700	680
D	5.0X	3350	600	550

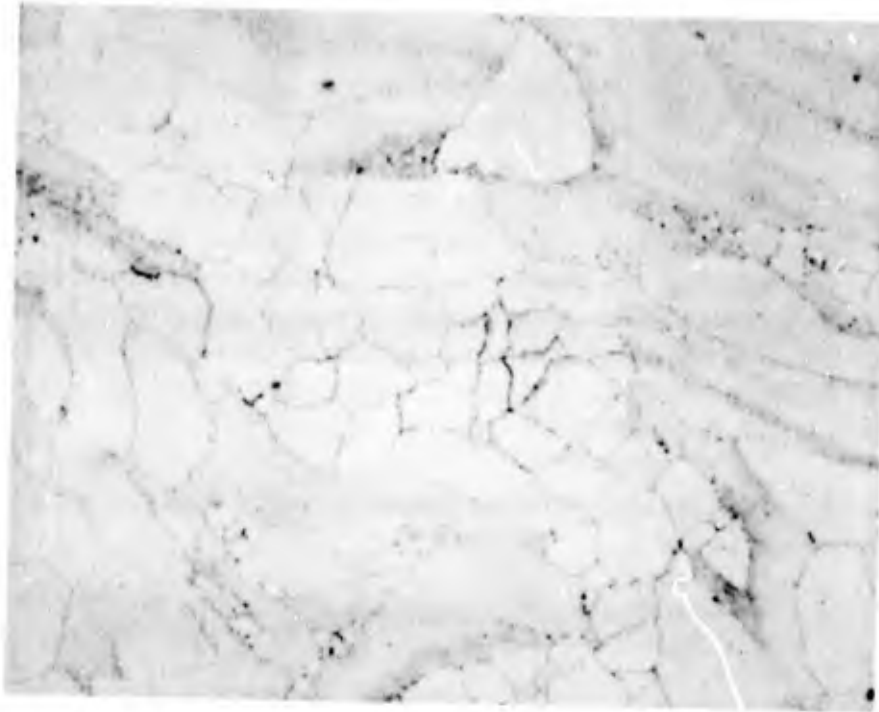
Metallographic examinations performed on representative samples from each extruded billet revealed no significant microstructural differences between billets, including billet C, which was purposely extruded at a lower temperature. In general, the material exhibited a predominantly worked microstructure (Figure 6).

2.2 COATING APPLICATION

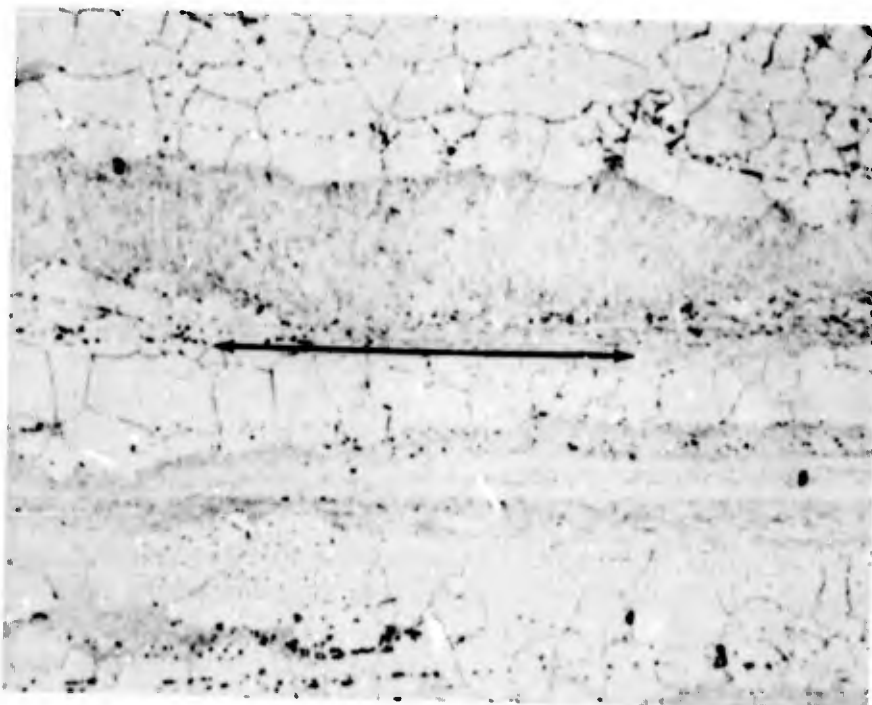
Application of the remodified TRW TiCr-Si (vacuum) pack coating (or "second modification"--see Technical Report AFML-TR-66-186, Part I, paragraph 3.2.2, pages 114-116) for Phase III and Phase IV evaluation was performed utilizing the following parameters:

- Cycle 1: A 50Cr-50Ti weight percent pack prepared from crushed, pre-alloyed material was used. Deposition was carried out in vacuum at 2340°F for 8 hours utilizing a potassium fluoride activator.
- Cycle 2: The second low-pressure cycle, a siliconizing process, was conducted at 2050°F for a period of 4 hours using a potassium fluoride activator.

Good coverage at specimen corners and edges was obtained with the gray, dense-appearing coating. However, specimen surfaces were extremely mottled in appearance; i. e., regions of dark coloration were noted.



PLANE: NORMAL TO EXTRUSION DIRECTION **MAG: 500X**
ETCH: 33% HYDROFLUORIC ACID, 33% NITRIC ACID, 33% WATER



PLANE: PARALLEL TO EXTRUSION DIRECTION (ARROW) **MAG: 500X**
ETCH: 33% HYDROFLUORIC ACID, 33% NITRIC ACID, 33% WATER

Figure 6. Microstructure of the As-Extruded Cb-132M Columbian Alloy Bar

Metallographic examination of the 2.5-mil-thick coating revealed three distinct coating-substrate regions: an outer coating zone, an intermediate coating zone adjacent to the substrate, and a solid solution region within the alloy (Figure 7). Although the outer coating layer of 1.0 mil in thickness contained regions of second phase, these areas were relatively isolated and occurred in a direction perpendicular to the coating-substrate interface. The intermediate coating region of 1.5 mils thickness was predominantly two phase. However, within approximately 0.5 mil of the alloy interface, regions of second phase decreased significantly. The 1-mil-thick solid solution zone beneath the coating contained a second-phase precipitate, presumably a (Cb, Ti)Cr₂-type Laves phase. Precipitation appeared to be at substrate grain boundaries (Figure 7).

Results of diamond pyramid hardness measurements, made using a 20-gram load, are summarized below.

<u>Region</u>	<u>Distance From Coating-Substrate Interface (mils)</u>	<u>Hardness (DPH)</u>
Outer coating layer	2.4	1600
	2.0	1236
	1.5	1846
	1.2	1600
Intermediate coating layer	1.0	3052
	0.4	1600
	0.1	2544
Substrate, solid solution zone	-0.2	800
	-0.75	479
Substrate	-1.6	414
	-2.5	329
	-3.5	319
	-4.5	329

Concentration profiles obtained by electron microprobe scanning from the base metal through the coating to the nickel-plate overlay produced the results presented in Figure 8. The high titanium and chromium concentrations, i. e. 29.1 and 50.7 weight percent respectively, are within regions of (Cb, Ti)Cr₂ Laves phase which precipitated in the solid solution zone.



ETCH: 33% HYDROFLUORIC ACID, 33% NITRIC ACID, 33% WATER MAG: 500X

Figure 7. Microstructure of Remodified TRW TiCr-Si (Vacuum) Pack Coated Cb-132M Alloy

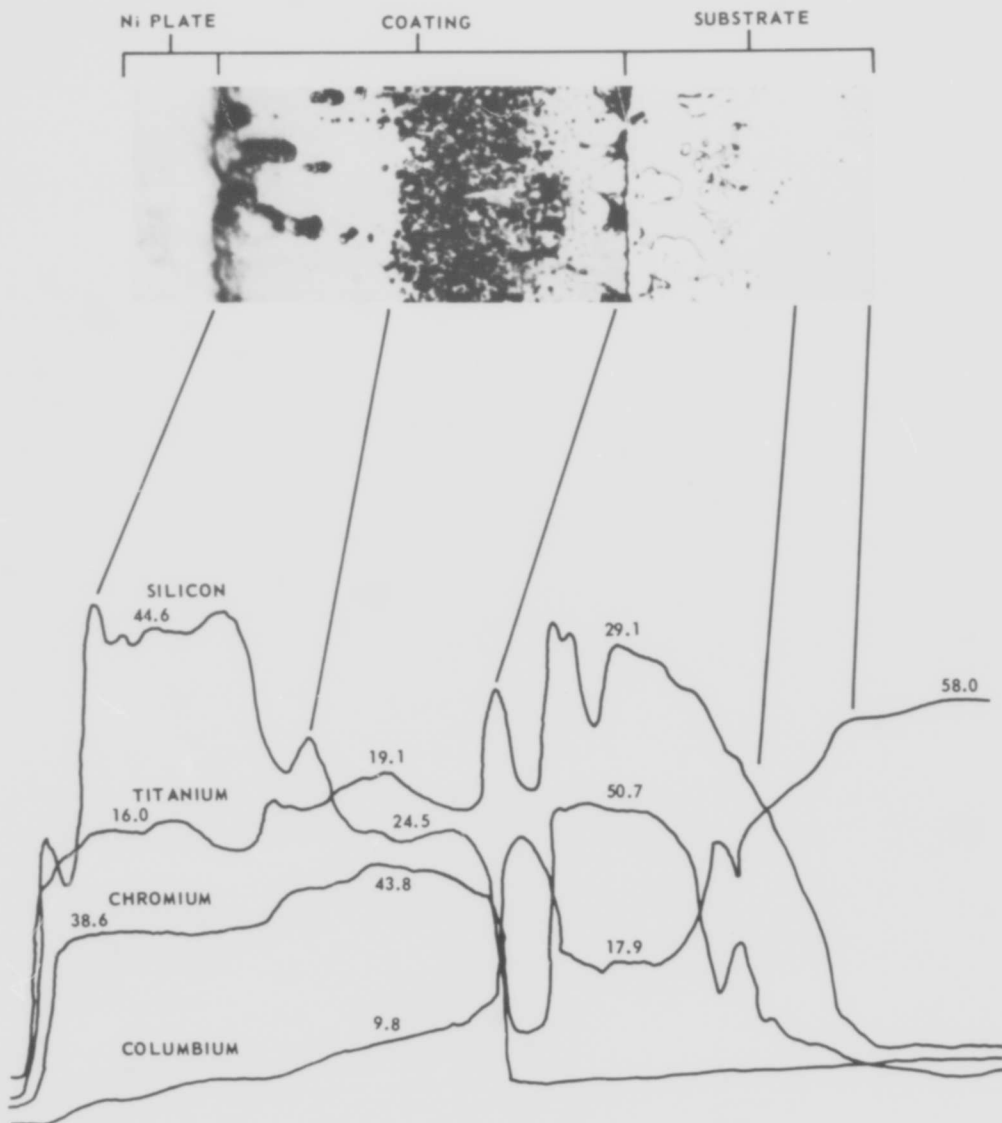


Figure 8. Concentration Profiles for Remodified TRW TiCr-Si (Vacuum) Pack Coated Cb-132M Alloy as Determined by Electron Microprobe Analyses

Weight percentage figures are given at representative points on traces.

2.3 SYSTEMS EVALUATION, TEST PROCEDURES AND RESULTS

2.3.1 Oxidation-Erosion Testing

Oxidation-erosion test bars were machined from 0.5-inch-diameter bar to the required "airfoil" geometry (Figure 9). Phase III testing was conducted at 1800°, 2000°, 2200°, 2400°, and 2500°F until failure, as constituted by the appearance of substrate oxide on the specimen airfoil surfaces. A minimum of two specimens were tested at each temperature. Testing in the rig shown in Figure 10 was performed in a combusted JP-5 fuel and air stream with an inspection interval not exceeding 20 test hours. At each temperature, dummy specimens were used for rig balancing purposes, and the bars were rotated in an 8-specimen holder at 1750 rpm to maintain temperature uniformity. Temperature was monitored with an optical pyrometer.

The performance of the TRW TiCr-Si/Cb-132M system is illustrated in Figure 11. In summary, the results were as follows:

- 1800°F: Failures after 460 hours and 580 hours for two specimens.
- 2000°F: Failures after 400 hours and 420 hours for two specimens.
- 2200°F: Failures after 200 hours for two specimens.
- 2400°F: Failures after 80 hours for two specimens and 100 hours for one specimen.
- 2500°F: Failures after 60 hours for two specimens and 80 hours for one specimen.

All failures resulted from localized oxidation on specimen airfoil surfaces (Figure 12). These areas of substrate oxidation were confined and occurred at random airfoil locations. Continued testing after failure did not significantly degrade the specimens further after 20 to 100 additional hours. This lack of further degradation was highly temperature dependent, i. e., the higher the test temperature, the shorter the time period during which further specimen degradation occurs.

2.3.2 Thermal Fatigue Testing

The Phase III thermal fatigue tests were performed on forged Cb-132M blade alloy paddles of the type shown in Figure 13. Testing at 1800°, 2000°, 2200°, 2400°, and 2500°F consisted of heating to the desired peak temperature in a combusted JP-5 fuel and air stream, stabilizing at this temperature for 30 minutes, and cycling by alternate heating to peak temperature and cooling to approximately 200°F with an ambient temperature air blast at 60-65 psi. Each thermal cycle consisted of 1 minute at the elevated temperature followed by a 30-second cooling period. For temperature uniformity, the specimens were rotated at 1850 rpm in groups of 12 (TRW TiCr-Si/Cb-132M test pieces plus dummy specimens). All specimens were inspected at the end of each 200 thermal

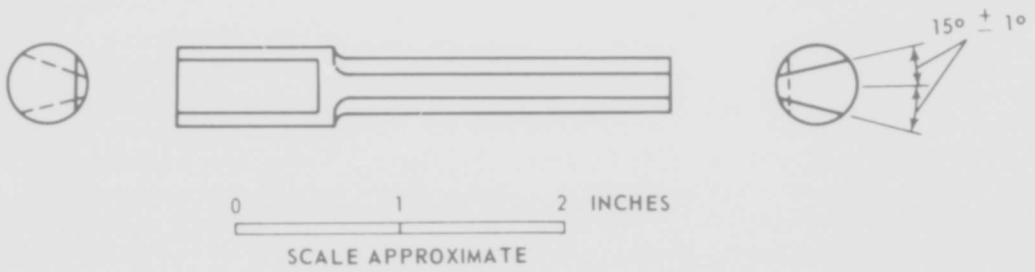


Figure 9. Erosion Bar Specimen Configuration for Oxidation-Erosion Tests

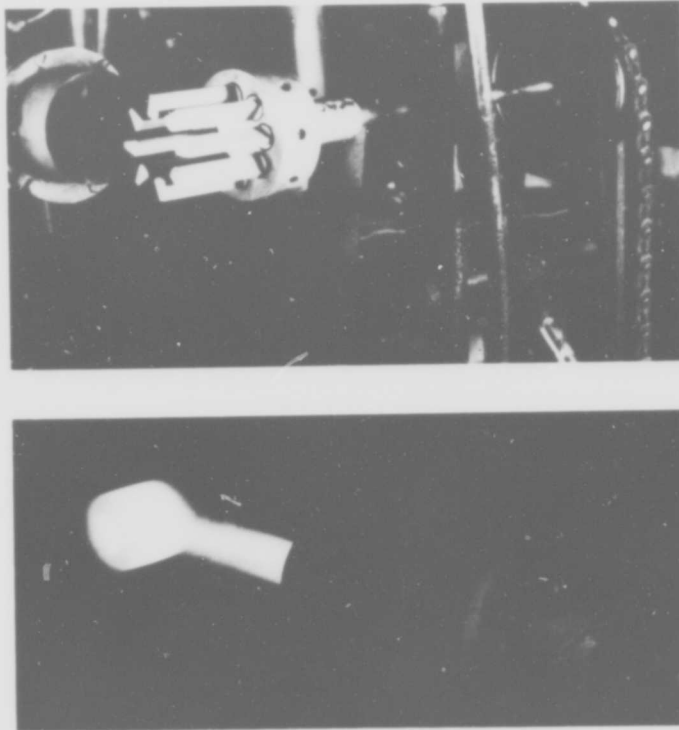


Figure 10. Burner Test Rig for Oxidation-Erosion Studies

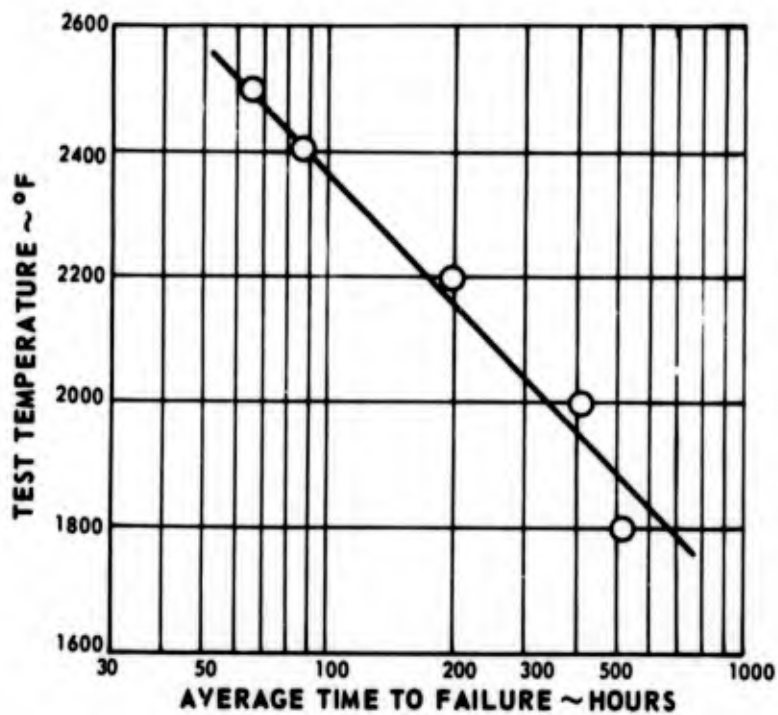
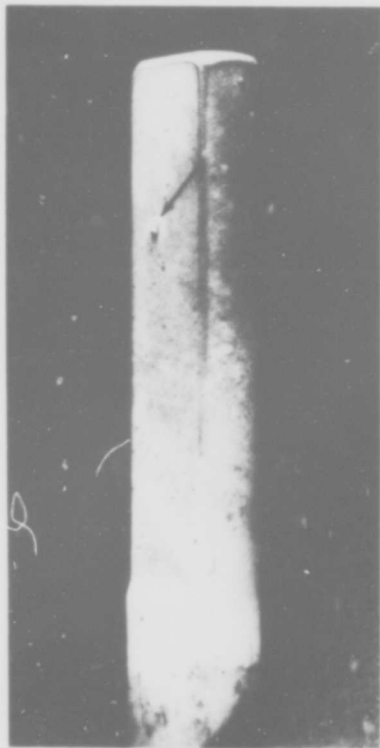
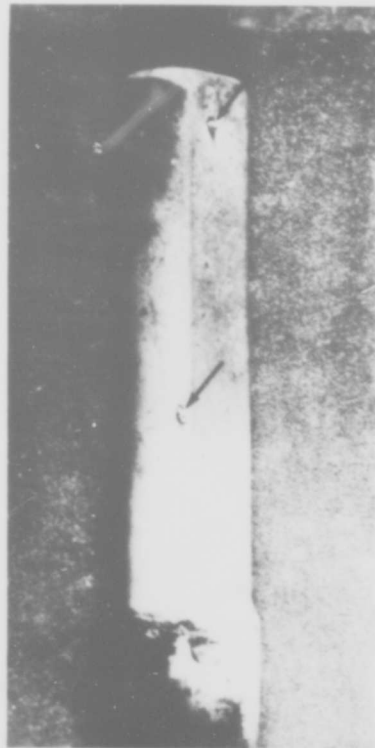


Figure 11. Oxidation-Erosion Life of Remodified TRW TiCr-Si (Vacuum) Pack Coated Cb-132M Alloy as a Function of Test Temperature



AFTER 60 HOURS AT 2500°F



AFTER 100 HOURS AT 2400°F

MAG: 1.6X

Figure 12. Typical Localized Oxidation-Erosion Failures (Arrows) on Remodified TRW TiCr-Si (Vacuum) Pack Coated Cb-132M Alloy

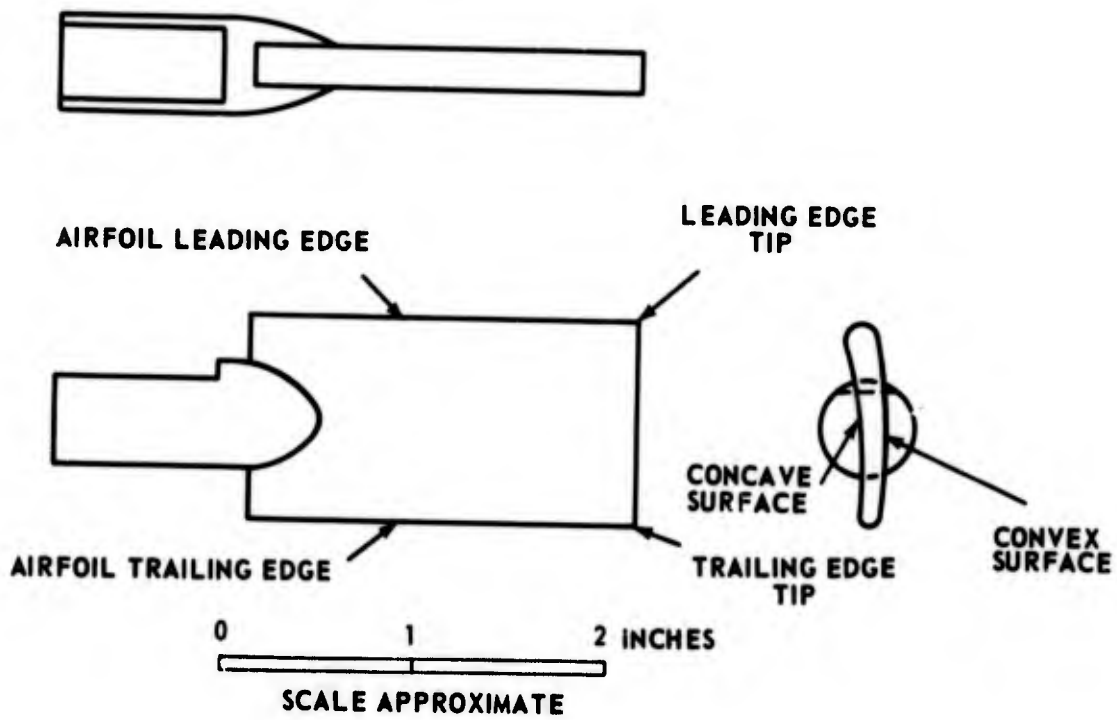


Figure 13. Forged Paddle Specimen Configuration for Thermal Cycling Tests

cycles, and during continued testing a 5-minute stabilization period at the elevated temperature was utilized prior to cycling. Two specimens were tested at each temperature.

Thermal fatigue test results are summarized below and are presented graphically in Figure 14.

- 1800°F: Failures after 4200 and 5800 cycles.
- 2000°F: Failures after 1600 cycles.
- 2200°F: Failures after 1000 and 1400 cycles.
- 2400°F: Failures after 800 cycles.
- 2500°F: Failures after 600 cycles.

For the 2200°, 2400°, and 2500°F tests, failure occurred by extensive coating spalling and subsequent substrate oxidation along airfoil leading edge surfaces (Figure 15). The 1800° and 2000°F failures were also confined principally to the airfoil leading edge surfaces, but failure was less extensive and resulted from the formation of substrate oxide extending out through coating surface craze cracks.

2.3.3 Melting Testing

To determine the effects of occasional transient temperature overshoots, a cyclic oxidation-erosion test was performed (Phase II). Each cycle consisted of the following:

- 10 hours at 2200°F, followed by
- 5 minutes at 2600°F, followed by
- 10 hours at 2200°F.

The test specimens were rotated at 1750 rpm for temperature uniformity in a combusted JP-5 fuel and air stream. The specimens were inspected at the end of each cycle.

Failures as evidenced by localized formations of substrate oxide were observed after 100 hours total time at 2200°F plus 25 minutes total transient time to 2600°F for one specimen and after 140 hours total time at 2200°F plus 35 minutes total transient time to 2600°F for two remaining specimens. Failures were very similar in appearance to those noted during isothermal oxidation-erosion testing.

Comparison of these cyclic test results with the 2200°F isothermal oxidation-erosion performance revealed that the 5-minute transient periods to 2600°F during

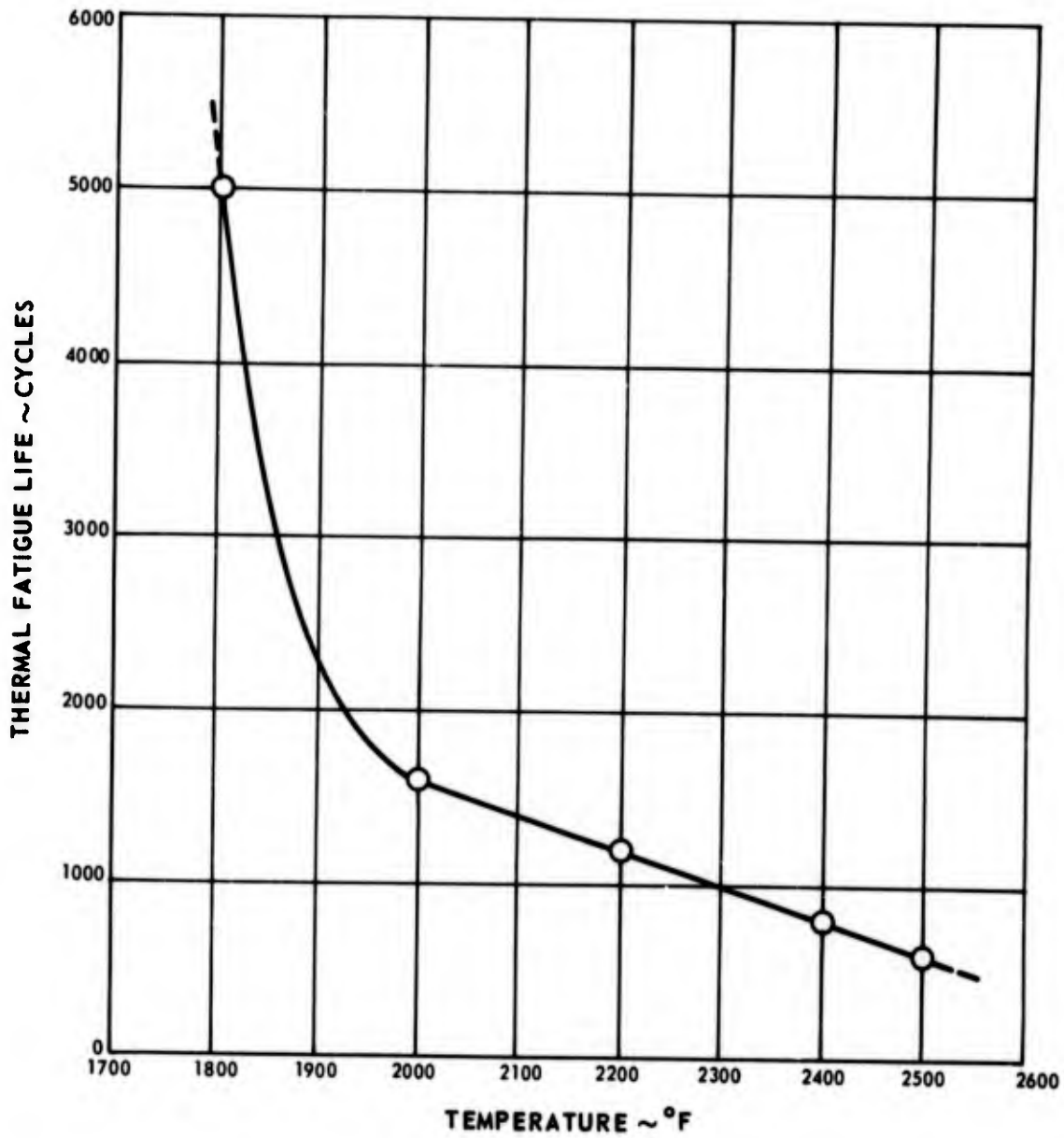
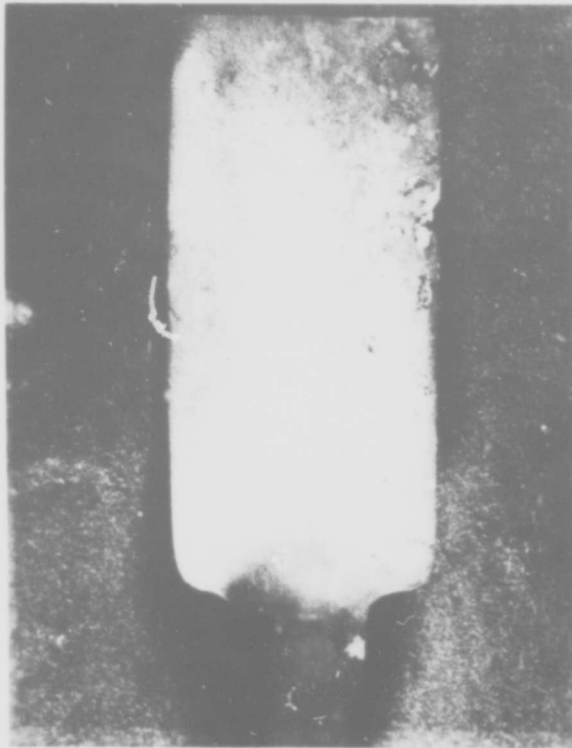


Figure 14. Thermal Fatigue Life of Phase III TRW TiCr-Si (Vacuum) Pack Coated Cb-132M Alloy as a Function of Test Temperature



MAG: 1.6X

Figure 15. TRW TiCr-Si (Vacuum) Pack Coated Cb-132M Alloy Specimen (Convex Surface) After Thermal Fatigue Testing for 1000 Cycles to 2200°F

Note areas of localized oxidation on leading edge surface.

each 20 hours at 2200°F reduced the reliability of the system by approximately 35 percent.

As in the case of the oxidation-erosion failures, 60 additional test hours at 2200°F combined with an additional total transient time of 15 minutes to 2600°F did not significantly degrade the specimens further. That is, gross substrate oxidation was not observed.

2.3.4 Ballistic Impact Testing

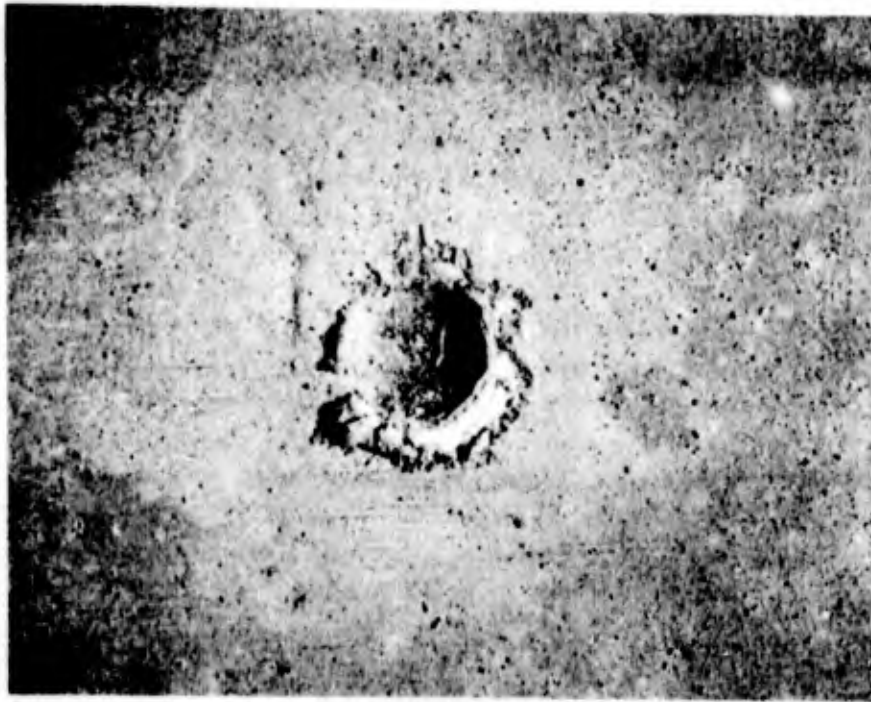
Rectangular 0.125-inch-thick specimens were impacted at a velocity of 500 feet per second with a 0.75-gram steel pellet after a 5-minute stabilization at 70°, 1600°, 2000°, 2200°, 2400°, and 2600°F. The specimens were mounted in grips utilizing transite coverings to avoid local coating damage, and heating was accomplished with an acetylene torch. Two specimens were evaluated at each temperature.

Appearance of the impacted area was characterized by the condition of the outer silicide coating layers. Three zones were defined after impacting, i.e. an impact depression consisting of crushed and compressed coating, a scab area surrounding the impact depression in which the outer silicide layers were removed, and a third zone of unaffected coating. These regions are discussed more thoroughly in paragraph 3.3.2.3 under Item 8. Increasing temperature of the specimen at impact resulted in decreased degradation of the outer silicide coating layers.

After impacting and inspection, static oxidation exposure in air at 2200°F was performed to assess the extent of coating damage. The first appearance of substrate oxide constituted failure. The following Phase IV results were obtained:

<u>Impact Temperature (°F)</u>	<u>Oxidation Exposure Time at 2200°F; Results</u>
70	5 hours; failure
1600	7 hours; failure
2000	9 hours; failure
2200	20 hours; no failure, test stopped
2400	20 hours; no failure, test stopped
2600	5 hours; failure

In all cases failure resulted from substrate oxidation surrounding the impact depression (Figure 16). Due to specimen thickness, no adverse effects occurred on the specimen surface behind the point of impact.



POINT OF IMPACT

MAG: 10X

Figure 16. Surface of Remodified TRW TiCr-Si (Vacuum) Pack Coated Cb-132M Alloy After 1600°F Ballistic Impact at 500 Feet Per Second Showing Failure Which Occurred After 7 Hours Subsequent Static Oxidation Exposure at 2200°F

The excellent performance of the system in the 2200° and 2400°F ballistic impact testing indicates a transition between 2000° and 2400°F. Within this region a temperature is reached at which ductility of the coating has increased to the extent that spalling of outer silicide layers and disruption of the coating layer adjacent to the substrate are minimized. The surface appearance of the specimen (Figure 17) and metallographic examination of the impact depression (Figure 18) support this conclusion.

2.3.5 Creep-Rupture Testing

Phase IV creep testing in air at 1800° and 2200°F was performed at Metcut Research Associates using the specimen configuration shown in Figure 19. Testing was conducted in a resistance-heated furnace, and temperature was monitored with an optical pyrometer which had been calibrated with thermocouples prior to test initiation. The specimens were placed into the furnace, aligned, and placed under a nominal load during the furnace heating cycle. After stabilization at the test temperature, the test load was applied. The specimen gage cross-sectional area prior to coating application was used to calculate the load required to produce the desired stress level.

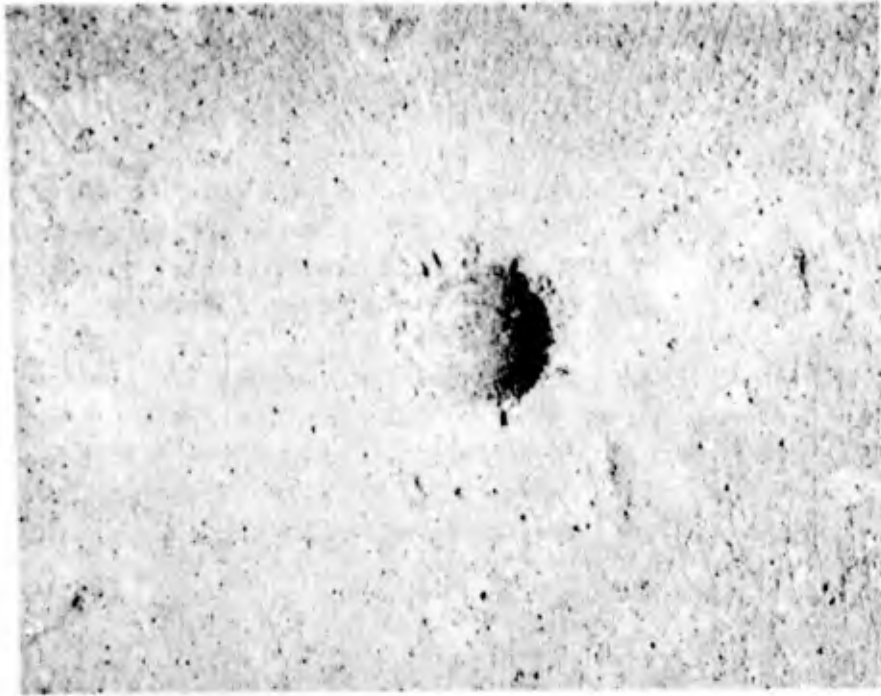
Difficulties with the specimen grips limited the data generated in this phase of the work. The results of the testing on the TRW TiCr-Si coated Cb-132M alloy are presented in Table II. These results may be compared with the results of similar tests on Phase VII Sylvania SiCrTi coated XB-88 alloy in paragraph 5.3.2.5. Tensile data for TRW TiCr-Si coated Cb-132M alloy are shown in Table III.

2.3.6 Fatigue Testing

Reverse-bending fatigue in air at 2200°F was performed using the smooth specimen configuration shown in Figure 20. The TRW TiCr-Si coated Cb-132M test specimens were calibrated using static weight deflection. Testing was performed at a resonant frequency of 600 cycles per second with an electrodynamic table shaker. The specimens were heated in a resistance furnace with temperature monitored optically. The optical pyrometer was calibrated using dummy specimens with attached thermocouples prior to testing the coated alloy specimens.

A summary of the Phase IV fatigue test results is in Table IV. Three specimens failed during static load calibration.

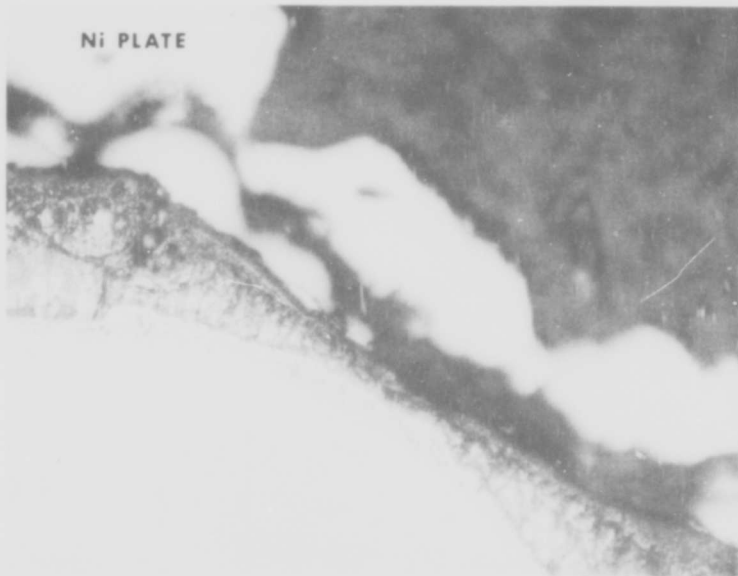
The fracture surfaces of the specimens tested at 40,000 and 50,000 psi revealed a predominantly granular surface, with a very small outer region of fatigue progression (Figure 21). The fatigue limit of 35,000 psi for 10^7 cycles reflects a stress level of approximately 50 percent of the ultimate tensile strength for uncoated Cb-132M alloy at 2200°F.



POINT OF IMPACT

MAG: 10X

Figure 17. Surface of Remodified TRW TiCr-Si (Vacuum) Pack Coated Cb-132M Alloy After 2200°F Ballistic Impact at 500 Feet Per Second and 20 Hours Subsequent Static Oxidation Exposure at 2200°F



ETCH: 33% HYDROFLUORIC ACID, 33% NITRIC ACID, 33% WATER MAG: 200X

Figure 18. Microstructure of the Transition Area Between the Specimen Surface and Impact Depression for Remodified TRW TiCr-Si (Vacuum) Pack Coated Cb-132M Alloy Showing Coating Integrity

The specimen was impacted at 500 feet per second at 2400°F and subsequently exposed to oxidation at 2200°F for 20 hours with no failure. The specimen surface outside the impact-affected zone continues to the left of photograph; the surface of the impact depression continues down and to the right.

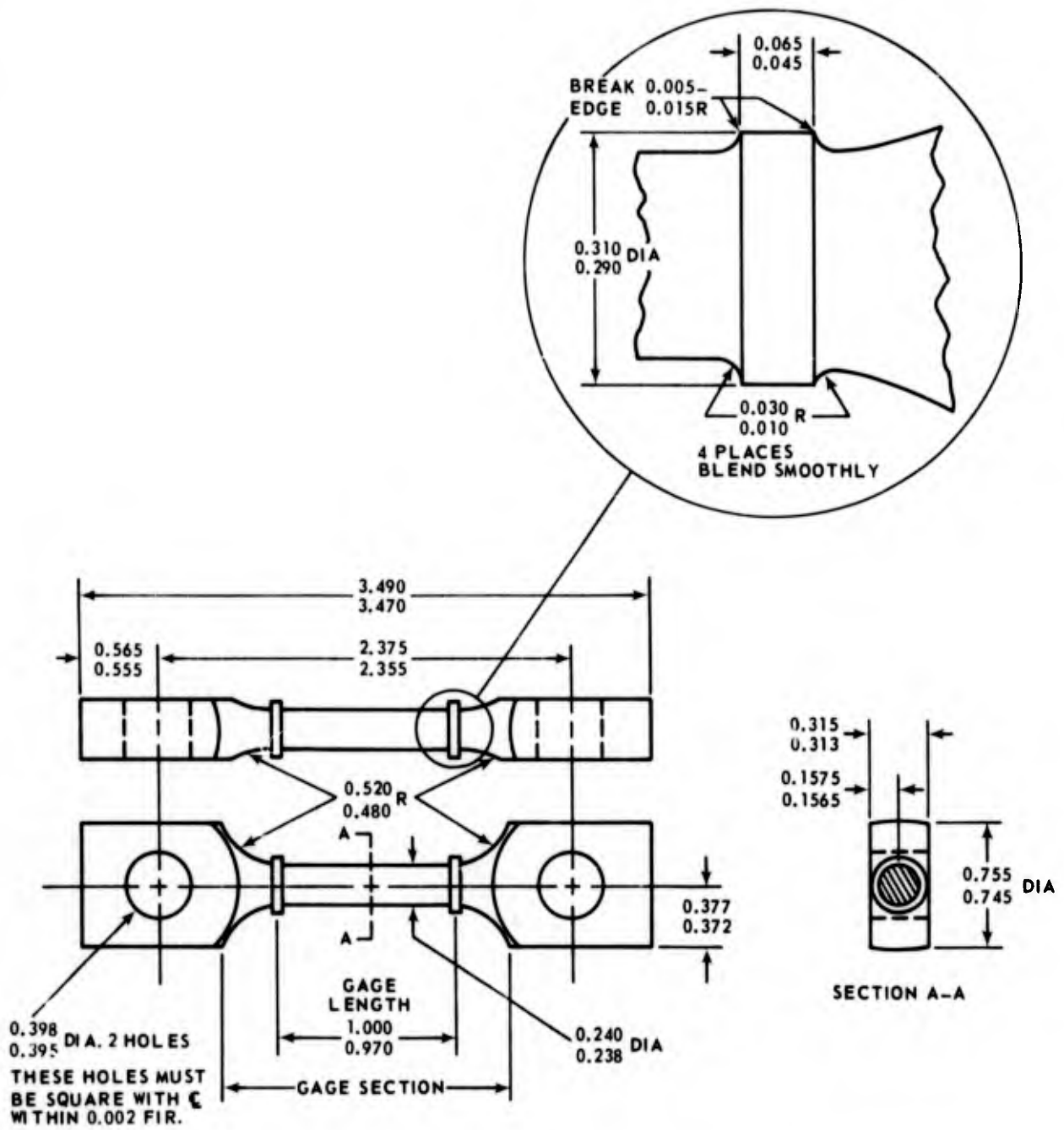


Figure 19. Bar Creep-Rupture Specimen Configuration

TABLE II

RESULTS OF CREEP-RUPTURE TESTING OF REMODIFIED TRW TiCr-Si (VACUUM) PACK COATED Cb-132M ALLOY

Specimen No.	Test Temperature (°F)	Stress (psi)	Time (hours)					Rupture	Elongation at Rupture (%)
			0.1% Creep	0.2% Creep	0.5% Creep	1.0% Creep	2.0% Creep		
MCR-4-4	1800	46,500	0.3	1.0	---	---	---	16.6 ^a	Nil
MCR-4-6	2200	35,000	0.2	0.7	---	---	---	4.6	1.0
MCR-4-8	2200	35,000	b	b	b	1.0	---	9.9	2.0
MCR-4-9	2200	35,000	---	---	---	---	---	0.5 ^c	---
MCR-4-7	2200	30,000	1.6	3.7	10.5	21.0	38.0	96.7	10.5

Notes: a. Pin bent; failure not considered valid.
 b. 0.5% extension occurred on loading.
 c. Pull bar failed.

TABLE III

TENSILE DATA FOR REMODIFIED TRW TiCr-Si (VACUUM) PACK COATED Cb-132M ALLOY

Specimen No.	Test Temperature (°F)	Ultimate Tensile Strength (psi)	0.2% Yield Strength (psi)	Elongation (%)
MCR-4-1	1500	24,200	---	---
MCR-4-2	1500	30,700	---	---
MCR-4-3	1500	55,000	46,700	Nil

Note: The first two specimens failed before 0.2% yield stress was obtained.

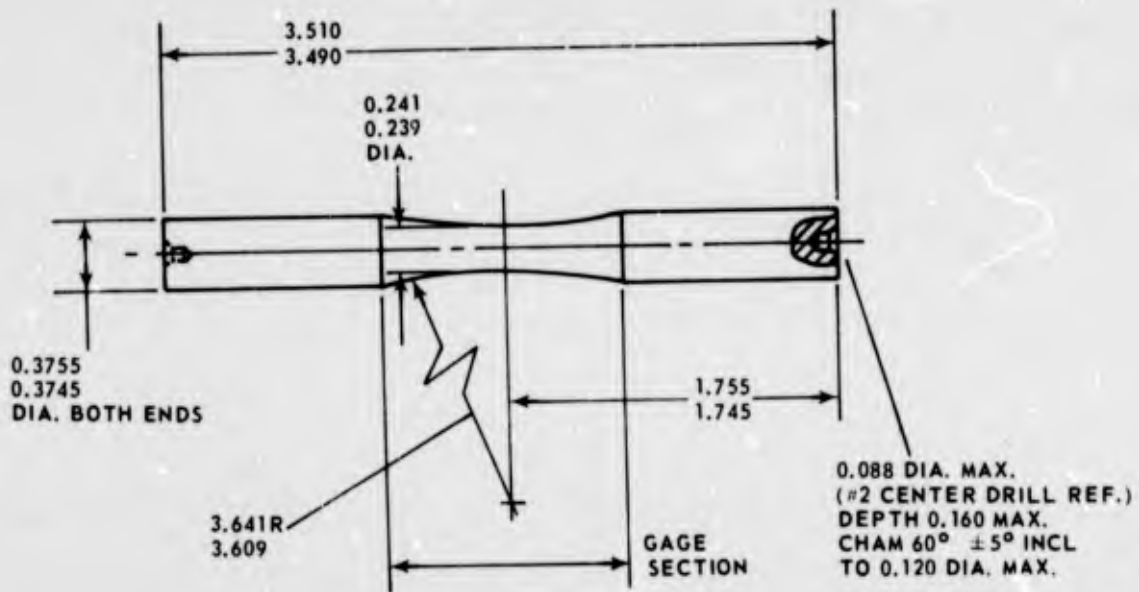


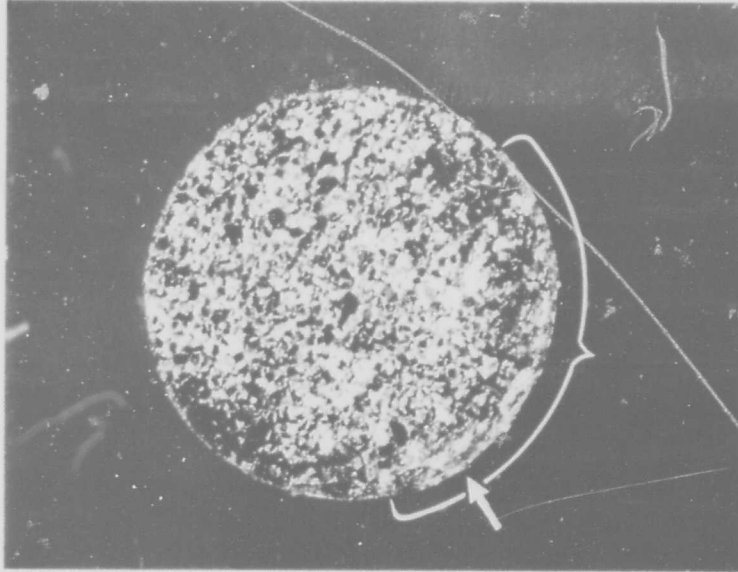
Figure 20. Fatigue Specimen Configuration

TABLE IV

RESULTS OF FATIGUE TESTING OF REMODIFIED
TRW TiCr-Si (VACUUM) PACK COATED Cb-132M
ALLOY IN AIR AT 2200°F

Test No.	Stress (psi)	Results
1	50,000	Failure at 0.25×10^7 cycles
2	40,000	Failure at 0.47×10^7 cycles
3	35,000	No failure after 10^7 cycles; test stopped
4	35,000	No failure after 10^7 cycles; test stopped
5	35,000	No failure after 10^7 cycles; test stopped

Note: All tests were conducted in reverse bending using a resonant frequency of 600 cycles per second.



MAG: 10X

Figure 21. Fracture Surface of Remodified TRW TiCr-Si (Vacuum) Pack Coated Cb-132M Alloy After Fatigue Testing in Air at 2200°F

Fracture occurred at a stress level of 40,000 psi after 0.47×10^7 cycles. Note area of fracture initiation (arrow) and region of fatigue wear (bracket). Remaining fracture area is extremely granular.

2.3.7 Charpy Impact Testing

In addition to the scheduled Phase III and Phase IV tests, smooth Charpy impact tests were conducted on remodified TRW TiCr-Si (vacuum) pack coated Cb-132M alloy specimens at 70°, 1400°, 1700°, and 2000°F. Uncoated Cb-132M columbium alloy specimens were also tested at 70°F. The results are in Table V. The low room temperature impact strengths for the uncoated specimens indicate poor toughness for the Cb-132M alloy. The tests revealed that the coated specimens had much lower impact resistance at room temperature and that the toughness of these specimens did not increase significantly with temperature until 2000°F was reached.

TABLE V

RESULTS OF SMOOTH CHARPY IMPACT TESTING OF
 REMODIFIED TRW TiCr-Si (VACUUM) PACK COATED Cb-132M ALLOY

Test No.	Specimen Condition	Specimen Temperature at Impact (°F)	Impact Strength (ft-lb)
1	Uncoated	70	6.57
2	Uncoated	70	3.65
3	Coated	70	0.51
4	Coated	70	1.0
5	Coated	1400	2.0
6	Coated	1400	2.5
7	Coated	1700	2.0
8	Coated	1700	0.5
9	Coated	2000	5.0
10	Coated	2000	4.5

3. ITEM 8

PRELIMINARY SCREENING EVALUATION OF ADDITIONAL SYSTEMS

Contract Item 8, which constitutes Phase V of the program, requires that the contractor perform preliminary screening tests on four additional coating-substrate combinations for turbine vane and blade airfoil applications and on eight coating-substrate combinations for blade root application. Three blade airfoil systems were selected; one of these was a supplemental system which was evaluated only in Phase V and, according to the original schedule, was not eligible for Phase VI, coating improvement, or Phase VII, advanced evaluation. The selected vane, blade airfoil, and blade root systems, which are tabulated below, were evaluated according to the preliminary screening procedure presented in Figure 22. The Solar TNV-12SE4 coating on Cb-132M alloy was selected as the supplemental blade airfoil system during the Seventh Quarter of the program.

<u>Application</u>	<u>Coating</u>	<u>Substrate Alloy</u>
Turbine vane	Sylvania SiCrTi slurry	B-66
Turbine blade airfoil	TRW TiCr-Si (vacuum) pack	XB-88
	Solar V-CrTi-Si	Cb-132M
	Solar MoTi-Si (TNV-12SE4)	Cb-132M
Turbine blade root	Sylvania SiCrV slurry	Cb-132M
	Sylvania SiCrFe slurry	Cb-132M
	TRW TiAl (vacuum) pack	Cb-132M
	TRW TiCr (vacuum) pack	Cb-132M
	TRW TiCr-Al (vacuum) pack	Cb-132M
	TRW TiCr-Si (vacuum) pack	Cb-132M
	Electroplated NiCr	Cb-132M
NiPt	Cb-132M	

Phase V substrate materials are discussed in the following paragraphs. Discussion of characteristics and procedures and reporting of test data for Phase V systems under the headings of Coatings Application and Evaluation Testing are presented first for the high-temperature systems (vane and blade airfoil applications) and then for the low-temperature systems (blade root).

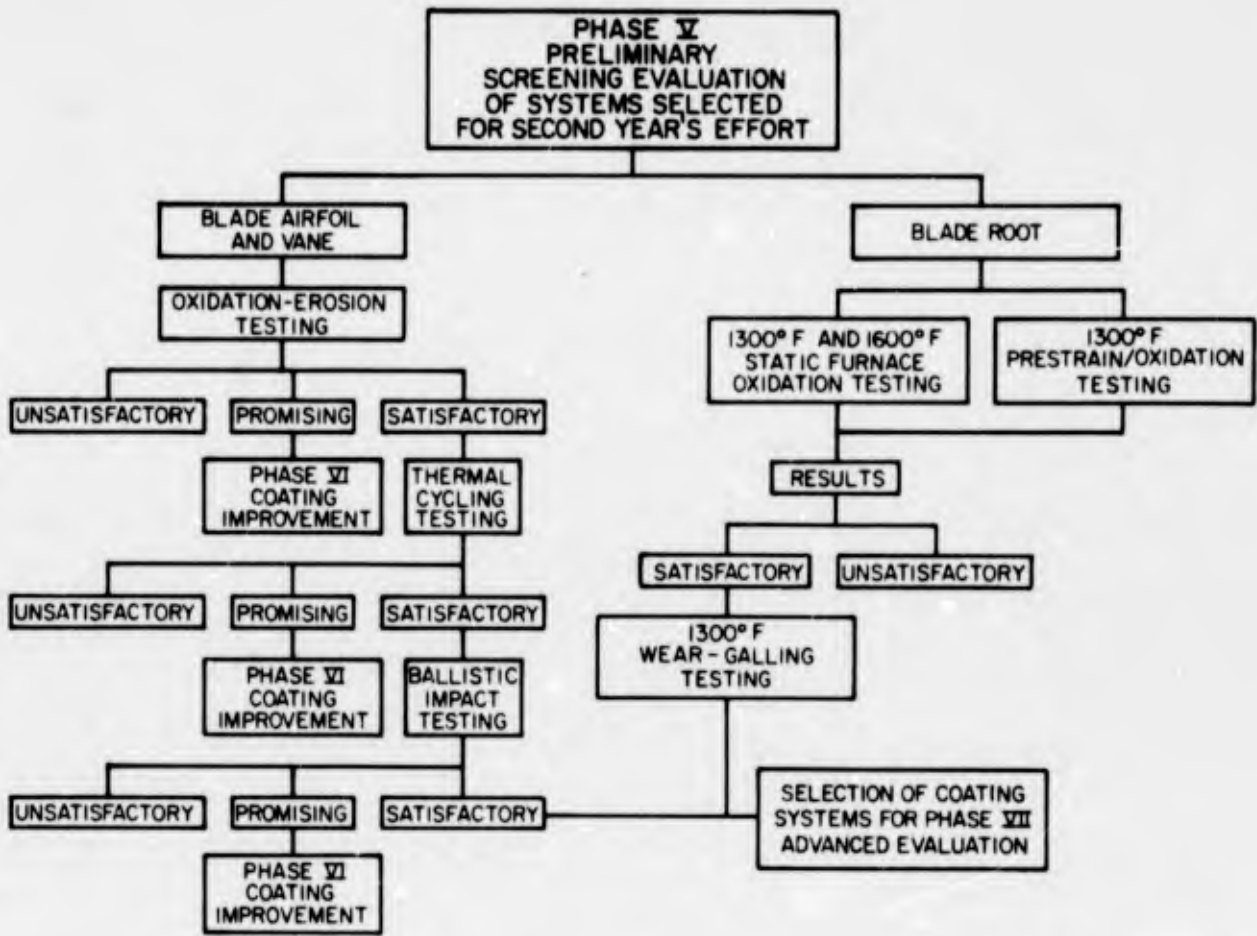


Figure 22. Flow Chart for Phase V of Program (Item 8)

3.1 SUBSTRATE MATERIALS

Alloys for turbine vane applications should possess moderate strength, be resistant to thermal fatigue, be weldable, and possess sufficient ductility to allow fabrication to the desired configuration. B-66 alloy was selected as the Phase V vane alloy and was supplied by Westinghouse Electric Corporation Astronuclear Laboratory in sheet and bar form. Chemical analyses of the two heats are presented in Table VI, and typical microstructures are shown in Figures 23 and 24.

The vane alloy thermal fatigue test necessitates cold forming of a sheet airfoil with a leading edge radius of two and one-half times the thickness ($2.5T$) for 0.050-inch-thick material. Results of bend tests, conducted to assure this capability prior to airfoil forming, are summarized in Table VII. The B-66 as-received sheet material met the ductility requirement both normal and parallel to the sheet roll direction.

As mentioned under Items 4 and 6, turbine blade alloys must have high fatigue strength, good creep resistance, and the ability to absorb impact forces without fracture. The Cb-132M blade alloy was supplied by Fansteel Metallurgical Corporation and extruded further at Nuclear Metals Division of the Whittaker Corporation. Composition, extrusion parameters, and microstructures are described in Items 4 and 6, paragraph 2.1, Substrate Materials. The XB-88 blade alloy was supplied by Westinghouse Astronuclear Laboratory in 0.50- and 0.75-inch-diameter bar form. The as-received material was in the as-swaged condition and exhibited a completely worked microstructure (Figure 25).

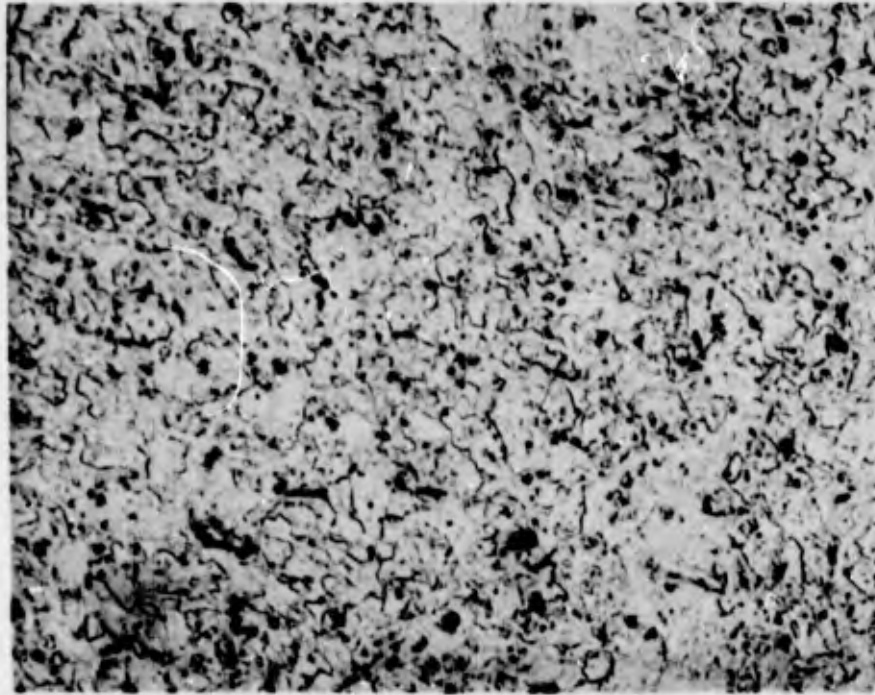
To develop high-temperature strength properties while maintaining room temperature ductility, heat treatment was required for XB-88 creep, fatigue, and Charpy impact test specimens. Westinghouse personnel suggested a 1-hour heat treatment at 3090°F , but at the same time cautioned that slight variations from this "optimum" temperature might be necessary for different heats. An investigation was therefore performed by heat treating test specimens for 1-hour periods at 3000° , 3090° , and 3180°F in vacuum. Appropriate micrographs of the heat treated structures were compared with micrographs supplied by Westinghouse. Comparative examination indicated that a 1-hour heat treatment at 3000°F corresponded to the "reference" condition for optimization of properties. The alloy structure was partially recrystallized (Figure 26). The XB-88 creep, fatigue, and Charpy impact specimens were therefore heat treated at 3000°F for 1 hour in vacuum.

Inspection of XB-88 alloy test specimens utilizing radiographic techniques revealed occasional high-density stringers within the alloy (Figure 27). The stringers, believed to be tungsten rich, were isolated and oriented parallel to the swaging direction. Stringer locations for all inspected test specimens were documented should premature coating failures occur where these areas are in contact with the coating. Care was also utilized to avoid stringers in the gage sections of the creep and fatigue test specimens.

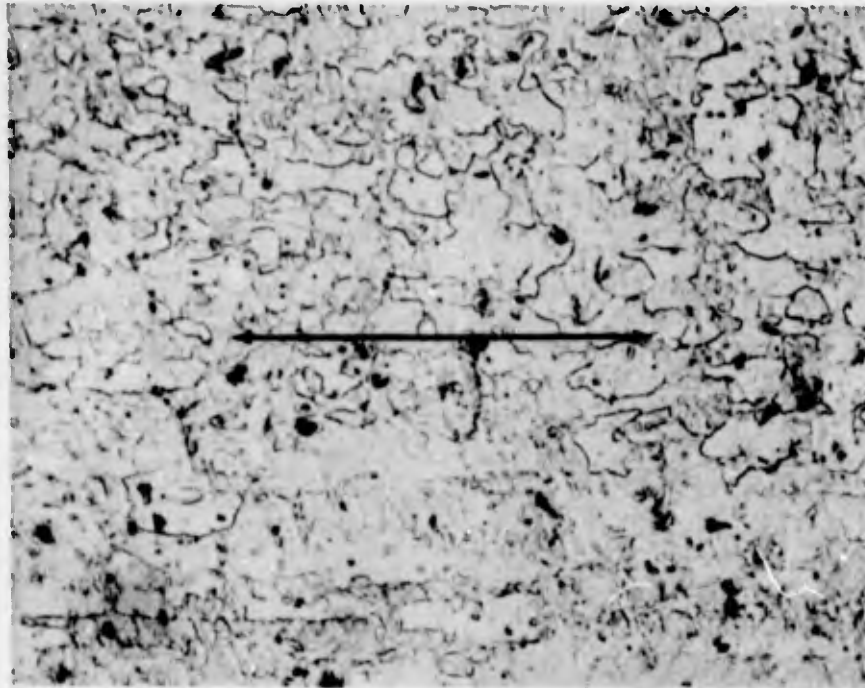
TABLE VI

COMPOSITION OF B-66 COLUMBIUM ALLOY
EVALUATED FOR TURBINE VANE APPLICATION

Westinghouse Heat No.	Metallics (percent)				Interstitials (parts per million)		
	Mo	V	Zr	Cb	O	H	C
FV-139	4.9	5.0	0.86	Balance	110	76	23
FV-151	5.2	5.0	0.97	Balance	127	53	55

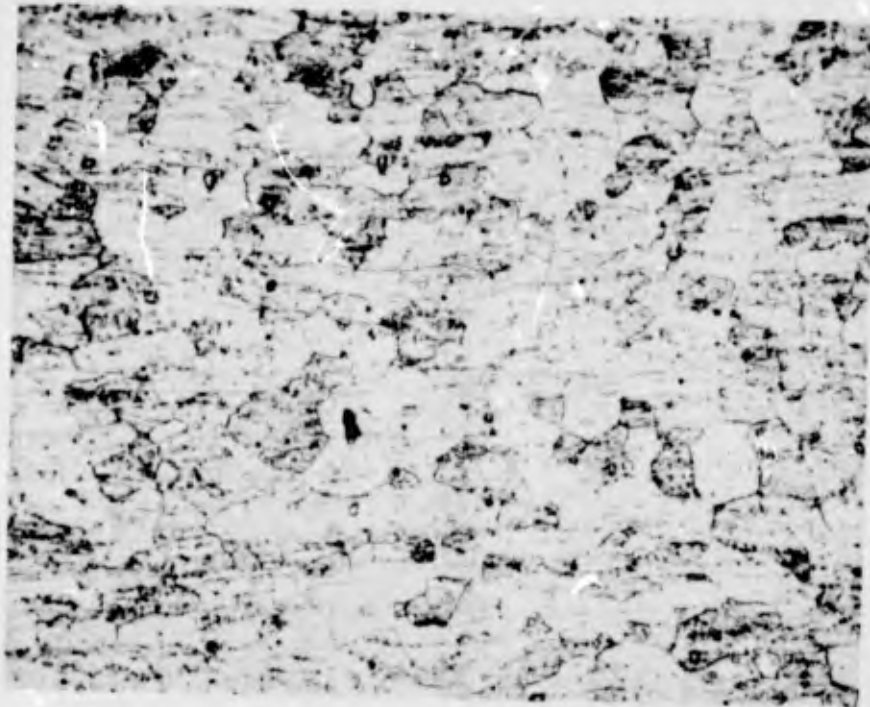


ALLOY: B-66, EXTRUDED BAR WESTINGHOUSE HEAT: NO. FV-139
PLANE: NORMAL TO EXTRUSION DIRECTION MAG: 500X
ETCH: 33% HYDROFLUORIC ACID, 33% NITRIC ACID, 33% WATER



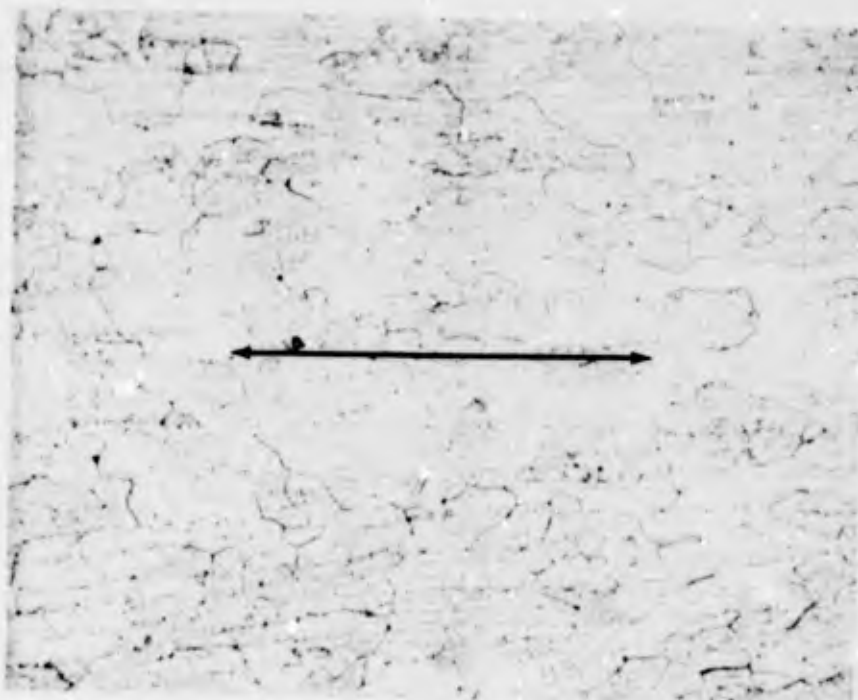
ALLOY: B-66, EXTRUDED BAR WESTINGHOUSE HEAT: NO. FV-139
PLANE: PARALLEL TO EXTRUSION DIRECTION (ARROWS) MAG: 500X
ETCH: 33% HYDROFLUORIC ACID, 33% NITRIC ACID, 33% WATER

Figure 23. Typical Microstructure of As-Received B-66 Columbium Alloy Bar



ALLOY: B-66, SHEET
PLANE: NORMAL TO ROLL DIRECTION
ETCH: 33% HYDROFLUORIC ACID, 33% NITRIC ACID, 33% WATER

WESTINGHOUSE HEAT: NO. FV-151
MAG: 500X



ALLOY: B-66 SHEET
PLANE: PARALLEL TO ROLL DIRECTION (ARROWS)
ETCH: 33% HYDROFLUORIC ACID, 33% NITRIC ACID, 33% WATER

WESTINGHOUSE HEAT: NO. FV-151
MAG: 500X

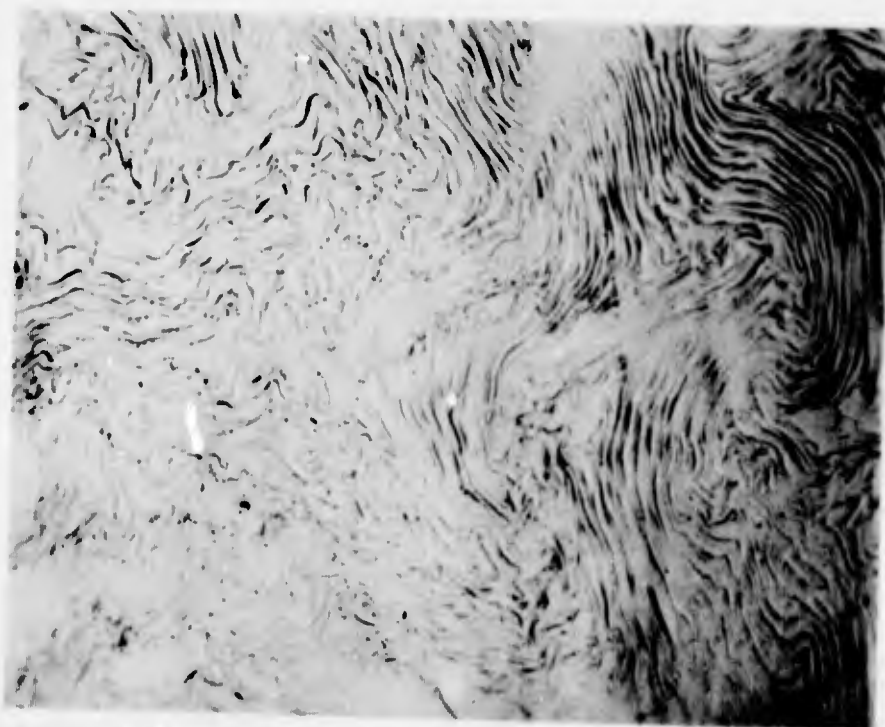
Figure 24. Typical Microstructure of As-Received B-66 Columbian Alloy Sheet

TABLE VII

RESULTS OF ROOM TEMPERATURE BEND TESTING OF
B-66 ALLOY 0.050-INCH SHEET

Mandrel Axis Relative to Sheet Roll Direction	No. of Specimens Tested	Bend Radius*	Test Results
Normal	1	3T	Passed 135° bend
Parallel	1	3T	Passed 135° bend
Normal	2	2T	Passed 135° bend
Parallel	2	2T	Passed 135° bend
Normal	2	1.5T	Passed 135° bend
Parallel	2	1.5T	One specimen passed 135° bend; second specimen failed at 90°
Normal	3	T	Passed 135° bend
Parallel	3	T	All specimens failed between 80° and 90°
Normal	2	0.5T	Both specimens failed at 110°

*T represents thickness of sheet



ALLOY: XB-88, SWAGED BAR
PLANE: NORMAL TO BAR AXIS
ETCH: 33% HYDROFLUORIC ACID, 33% NITRIC ACID, 33% WATER

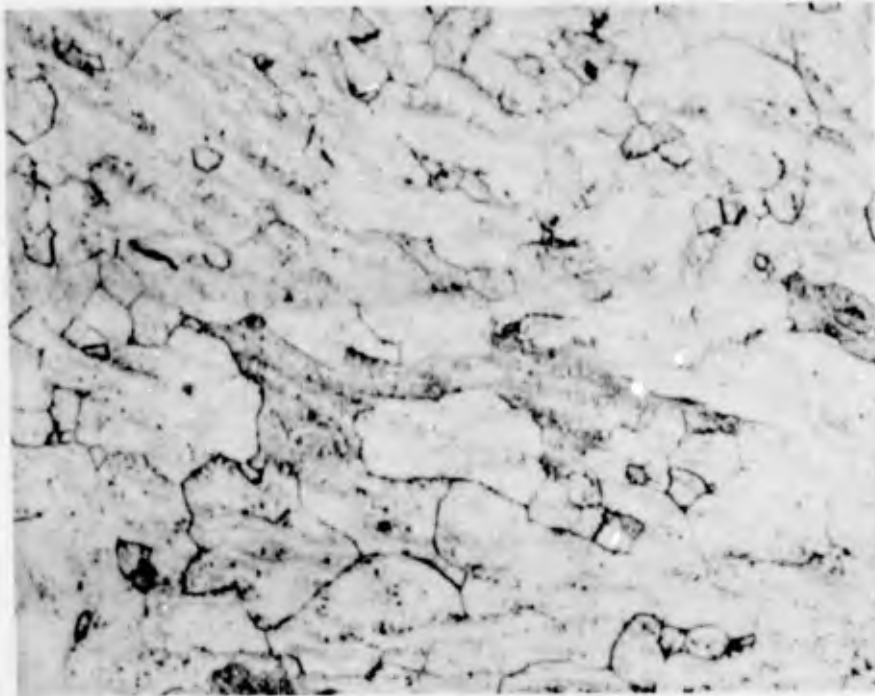
MAG: 500X



ALLOY: XB-88, SWAGED BAR
PLANE: PARALLEL TO BAR AXIS (ARROW)
ETCH: 33% HYDROFLUORIC ACID, 33% NITRIC ACID, 33% WATER

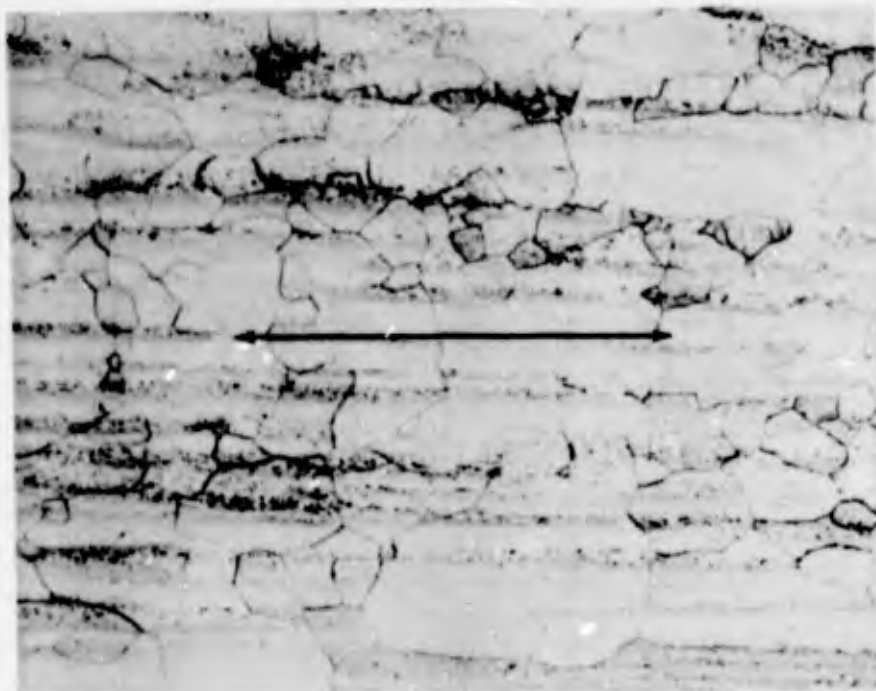
MAG: 500X

Figure 25. Typical Microstructure of As-Received XB-88 Columbian Alloy Bar



PLANE: NORMAL TO BAR AXIS
ETCH: 33% HYDROFLUORIC ACID, 33% NITRIC ACID, 33% WATER

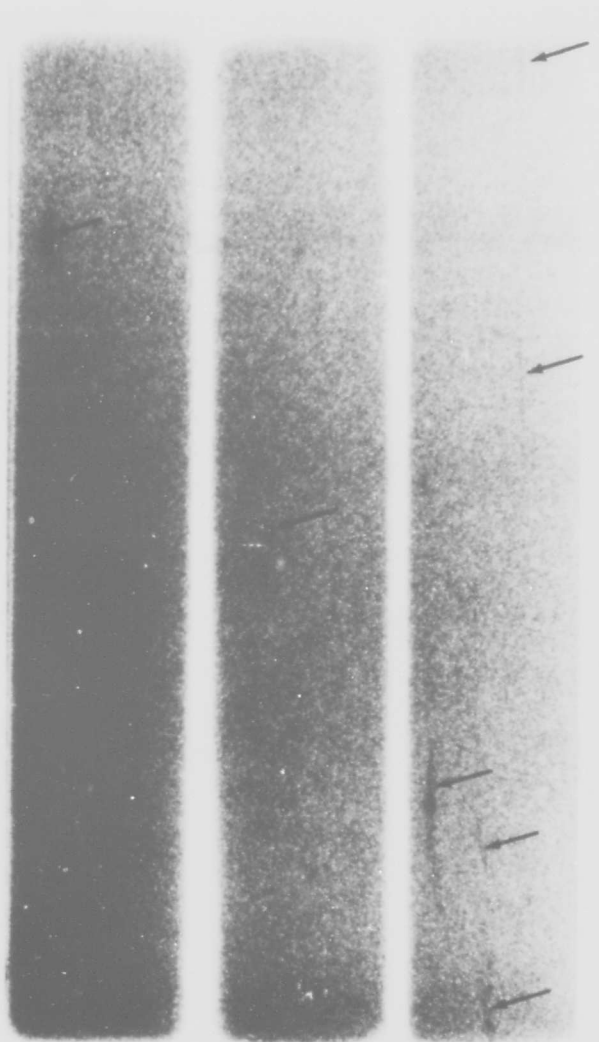
MAG: 500X



PLANE: PARALLEL TO BAR AXIS (ARROW)
ETCH: 33% HYDROFLUORIC ACID, 33% NITRIC ACID, 33% WATER

MAG: 500X

Figure 26. Typical Microstructure of XB-88 Columbian Alloy Bar After Heat Treatment for 1 Hour at 3000°F



MAG: 2X

Figure 27. Radiograph (Positive Print) of XB-88 Columbian Alloy Bars Showing Typical Stringers (Arrows)

3.2 COATINGS APPLICATION, HIGH-TEMPERATURE SYSTEMS

3.2.1 Sylvania SiCrTi Slurry/B-66

A Si-20Cr-5Ti and vehicle mixture was applied by Sylvania Division of General Telephone and Electronics, Inc. using a spray and/or dipping procedure. Heat treatment for 1 hour at 2550° F produced a coating exhibiting a very uniform surface appearance with excellent coverage of corner and edge surfaces. Metallographic examination revealed an average coating thickness of 2.5 to 2.6 mils and three microstructurally distinct regions within the coating (Figure 28). A continuous 0.2-mil-thick layer was present at the coating-substrate interface. Above this a 0.6-mil-thick zone exhibited columnar phase growth and was denuded of second-phase material. The outer coating layer, 1.8 mils in thickness, contained a discontinuous second phase resembling the columnar-type intermediate layer in appearance.

3.2.2 TRW TiCr-Si (Vacuum) Pack/XB-88

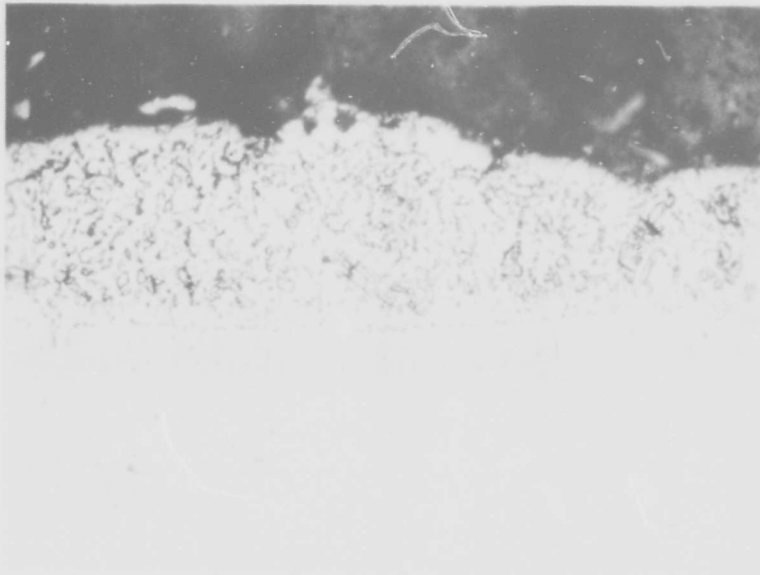
Application of the TiCr-Si coating on XB-88 alloy was accomplished at TRW, Incorporated with a two-cycle vacuum pack process and the parameters outlined below:

- Cycle 1: The first low-pressure cycle consisted of chromium-titanium deposition at 2200° F for 8 hours from a 60Cr-40Ti weight percent pack utilizing a potassium fluoride activator.
- Cycle 2: The second low-pressure cycle, a siliconizing process, was conducted at 2040° F for a period of 4 hours.

The coating had an extremely mottled surface appearance (Figure 29). Discussions with TRW, Inc. revealed that these darker surface areas were high in chromium. Metallographic examination showed that coating thickness varied from 3.2 to 3.6 mils. Poor uniformity of the (Cb, Ti)Cr₂-type Laves phase and outer silicide coating layers was noted (Figure 30). No solid solution zone beneath the coating-substrate interface was apparent.

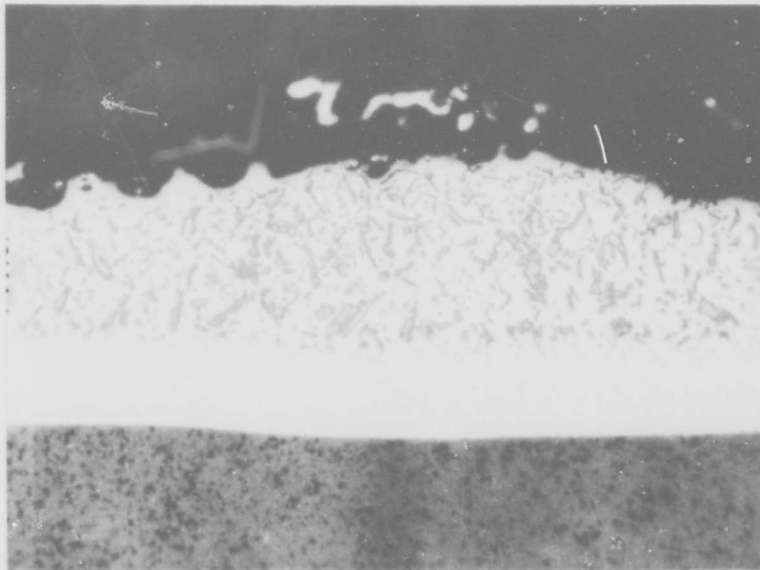
3.2.3 Solar V-CrTi-Si/Cb-132M

A V-CrTi-Si coating of 2.3 to 2.6 mils was developed on the Cb-132M test specimens by Solar Division of International Harvester Company, with coating weights ranging from 25.6 to 31.4 milligrams per square centimeter. Coating coverage on specimen edges and corners was good. Metallographic examination of the composite revealed three microstructurally distinct coating regions (Figure 31). The outer coating layer of about 2.0 mils contained a discontinuous second phase of fairly uniform distribution. A second region of 0.4 mil at the coating-substrate interface also contained discontinuous phases; i.e., no discrete coating interfacial compound was observed. The third region consisted of a 0.5-mil solid solution zone beneath the coating.



ETCH: 20% HYDROFLUORIC ACID, 20% NITRIC ACID, 60% WATER

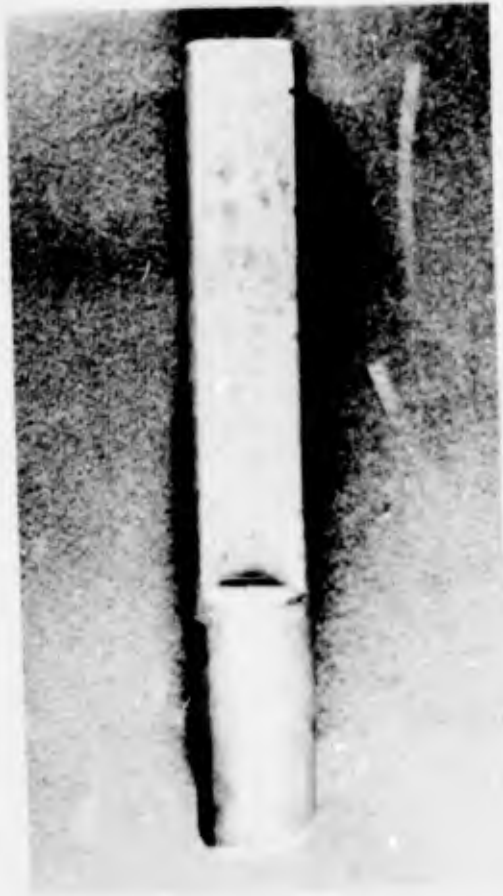
MAG: 500X



ETCH: ANODIZED

MAG: 500X

Figure 28. Typical Microstructure of the As-Applied Sylvania SiCrTi Slurry Coating on B-66 Alloy



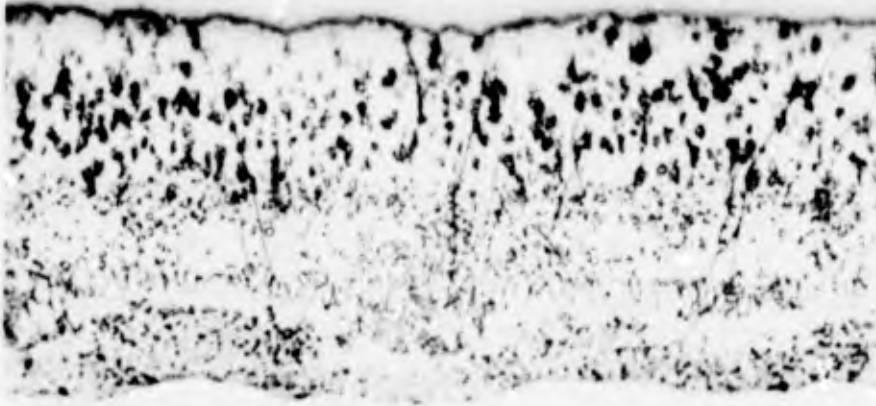
MAG: 1.3X



MAG: 1.3X

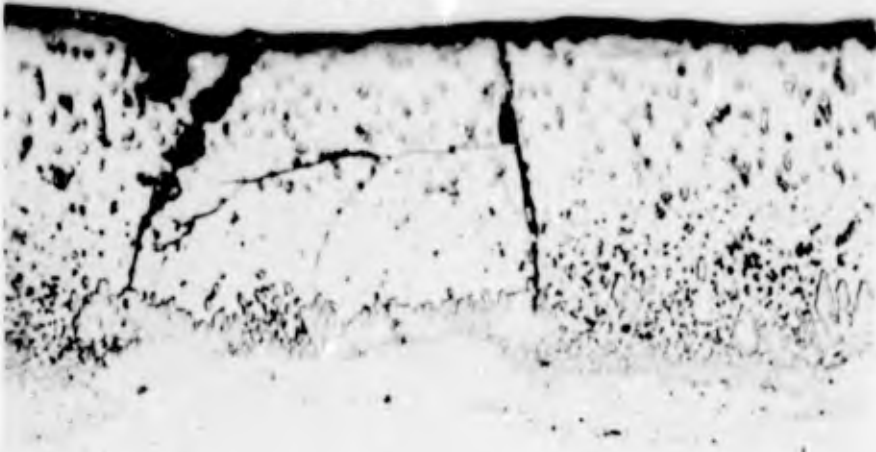
Figure 29. As-Coated TRW TiCr-Si/XB-88 Alloy Oxidation-Erosion Bar (Left) and Thermal Fatigue Paddle (Right)

Ni PLATE



ETCH: 20% HYDROFLUORIC ACID, 20% NITRIC ACID, 60% WATER MAG: 500X

Ni PLATE



ETCH: 20% HYDROFLUORIC ACID, 20% NITRIC ACID, 60% WATER MAG: 500X

Figure 30. Microstructure of the As-Deposited TRW TiCr-Si Coating on XB-88 Alloy

Ni PLATE



ETCH: 20% HYDROFLUORIC ACID, 20% NITRIC ACID, 60% WATER MAG: 500X

Figure 31. Microstructure of the As-Applied Solar V-CrTi-Si Coating on Cb-132M Alloy

3.2.4 Solar MoTi-Si (TNV-12SE4)/Cb-132M

MoTi-Si coating of Cb-132M alloy was accomplished at Solar by slurry application of a layer of 95Mo-5Ti composition and vacuum sintering at 2750° F. This layer was subsequently silicided by a pack cementation process, impregnated with a borosilicate glass, and oxidized for 1 hour at 2400° F in air. The surface of the coating appeared very uniform with good coverage of specimen corners and edges.

Metallographic examination of the 6-mil coating revealed two coating regions, i.e. a continuous, irregular layer of approximately 1/2-mil thickness at the coating-substrate interface and a 5.5-mil (average) outer coating layer (Figure 32). This outer region appeared sintered with considerable porosity and no distinctive structure.

3.3 EVALUATION TESTING, HIGH-TEMPERATURE SYSTEMS

3.3.1 Test Procedures

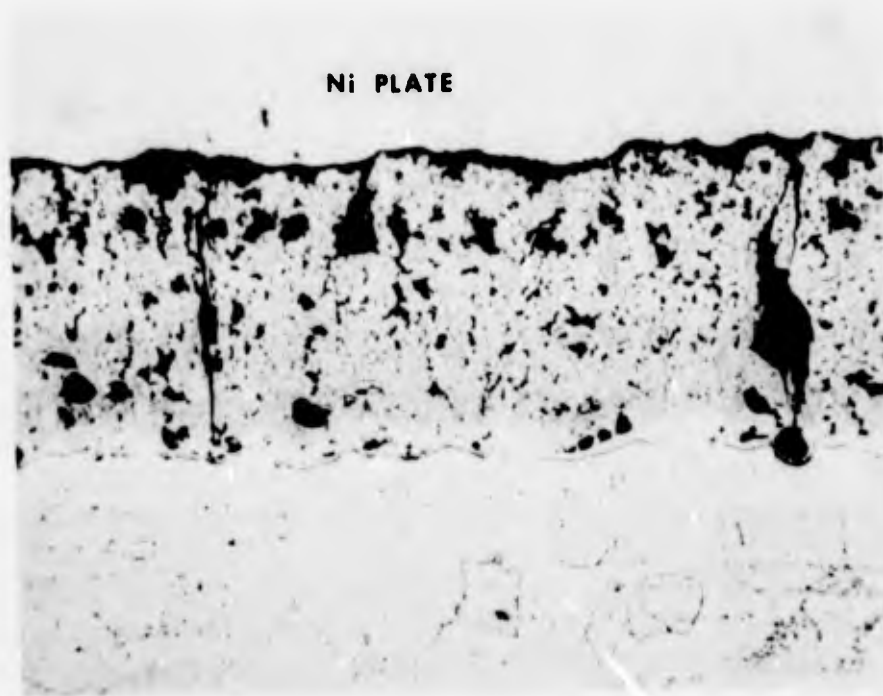
Evaluation of the high-temperature systems for blade airfoil and/or vane application included three complementary preliminary screening tests: oxidation-erosion, thermal fatigue, and ballistic impact. The purpose of these tests was to obtain qualitative data from which potential comparisons could be assessed and made between candidate systems for a given application. Therefore, in cases of promising but inadequate performance, modifications could be made (Phase VI, coating improvement) or, in the case of outstanding performance, a system could be forwarded directly to Phase VII, advanced evaluation, for the generation of quantitative data. The parameters of each test are discussed below.

3.3.1.1 Oxidation-Erosion Procedure

The erosion test specimens were machined from 0.5-inch-diameter bar stock to the required "airfoil" shape (Figure 9). Testing was conducted in a combusted JP-5 fuel and air stream at 2200° and 2400° F using the test rig shown in Figure 10. Specimens were rotated at 1750 rpm in groups of eight for temperature uniformity. Temperature during testing was determined by an optical pyrometer and checked at 30-minute intervals. Coating-substrate systems not exhibiting failure after 100 hours at 2200° F were tested further at 2400° F for a maximum of 100 hours and at 2500° F until failure. Specimens were visually inspected and weighed after each 20 hours of testing. Four specimens were tested for each system evaluated.

3.3.1.2 Thermal Fatigue Procedure

Blade alloy thermal fatigue specimens were forged by TRW, Inc. from 0.5-inch-diameter bar stock (Figure 13). During testing, the specimens were rotated at 1850 rpm in groups of 12 for temperature uniformity. In cases where less than 12 specimens



ETCH: 20% HYDROFLUORIC ACID, 20% NITRIC ACID, 60% WATER MAG: 250X

Figure 32. Typical Microstructure of the As-Applied Solar MoTi-Si (TNV-12SE4) Coating on Cb-132M Alloy

were being tested, dummy blanks were used to complete the set for rig-balancing purposes. The test rig is shown in Figure 33. Two specimens per system were tested.

The vane alloy thermal fatigue specimens (Figure 34) were fabricated from sheet and bar material. The airfoils were cold-formed from 0.050-inch-thick sheet with a leading edge bend radius of two and one-half times the sheet thickness. Joining of the trailing edge was accomplished by manual TIG (tungsten inert gas) welding with parent metal filler rod in an argon atmosphere dry box. Atmosphere dew point was maintained at -40° F or lower. The resultant joint was blended to the desired trailing edge contour. Remaining details of the completed assembly were similarly joined by welding. The specimens were tested utilizing the single-vane test rig shown in Figure 35. Duplicate specimens were tested.

Test parameters for both the blade and vane alloy thermal fatigue specimens consisted of heating to the desired peak temperature in a combusted JP-5 fuel and air stream, stabilizing at this temperature for 30 minutes, and cycling by alternate heating to the peak temperature and cooling to approximately 200° F with an ambient temperature air blast. Parts were visually inspected at the end of each 100 or 200 cycles. On resumption of testing at the initial elevated temperature, a 10-minute stabilization was used for the blade airfoil specimens and a 30-minute stabilization for the vane alloy specimens. Each cycle consisted of 1 minute at the elevated temperature followed by a 30-second ambient temperature air blast of 60-65 psi. Temperatures were determined with an optical pyrometer.

3.3.1.3 Ballistic Impact Procedure

The ballistic impact tests were conducted on 0.050 x 1 x 2-inch coupons for the vane system and 0.125 x 0.5 x 2-inch coupons for the blade airfoil systems. During testing, the specimens were mounted in grips utilizing transite coverings to avoid local coating damage. A 0.75-gram steel pellet was fired at velocities of 200 and 500 feet per second at a point one-half inch above the grips to avoid bending moment variations between tests. Heating was accomplished with an acetylene torch with impact occurring at the end of a 10-minute stabilization period. Specimens were impacted at room temperature and at 2200° F. Temperature measurements were made with an optical pyrometer. To determine the amount of resulting coating damage, the specimens were subjected to 2200° F static-air oxidation after impact.

3.3.2 Test Results

3.3.2.1 Oxidation-Erosion Results

Sylvania SiCrTi Slurry/B-66. Failure was observed for the Sylvania SiCrTi/B-66 system within a range from 100 hours at 2200° F plus 40 hours at 2400° F to 100 hours at 2200° F plus 100 hours at 2400° F plus 20 hours at 2500° F. Failure generally occurred by localized oxidation at random airfoil locations (Figure 36). In two instances, however, oxidation occurred in areas used for specimen support during coating

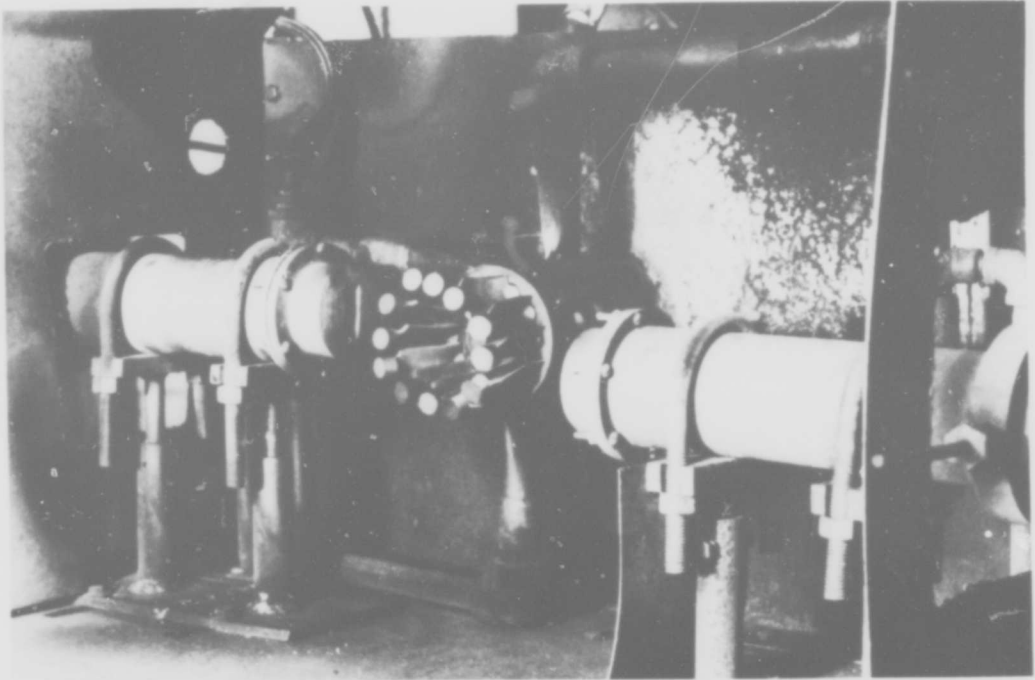


Figure 33. Thermal Fatigue Bow Rig Showing Position of Specimens in Relation to Burner Nozzles

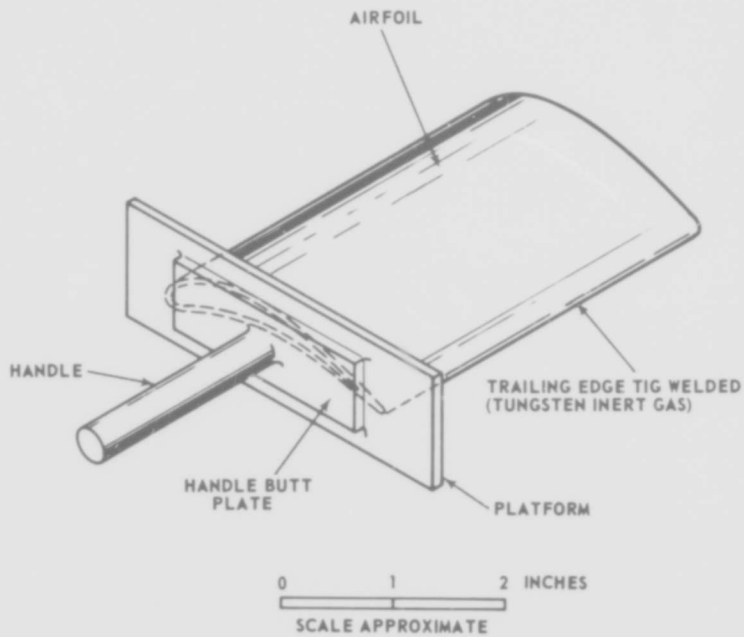


Figure 34. Vane Airfoil Specimen Configuration for Thermal Fatigue Tests

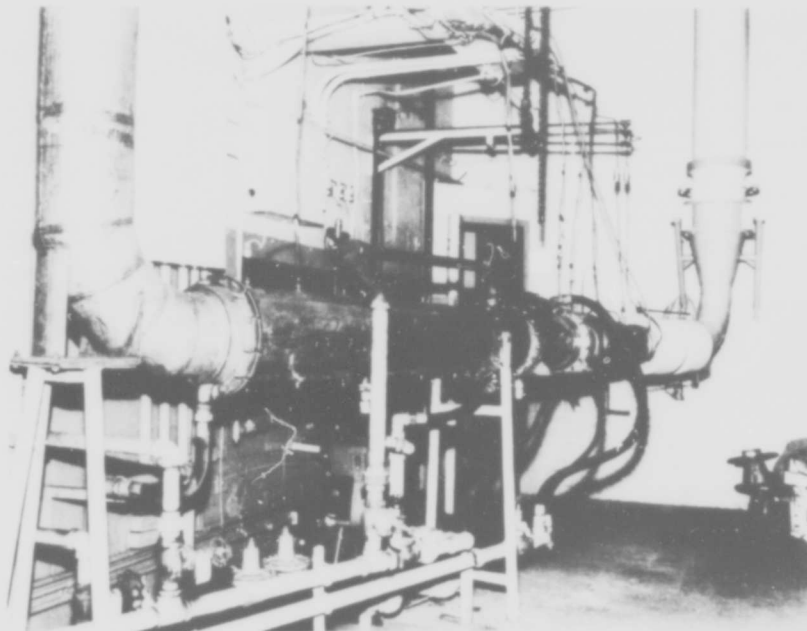
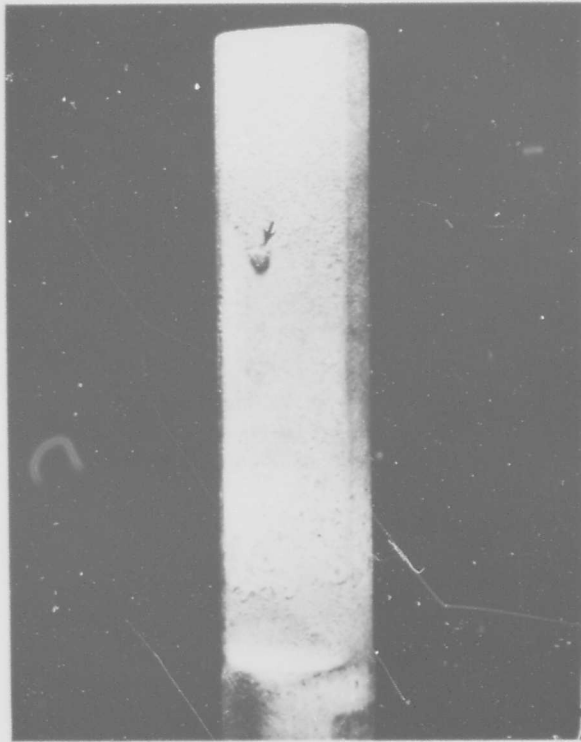


Figure 35. Single-Vane Thermal Fatigue Test Rig



MAG: 2X

Figure 36. Sylvania SiCrTi Slurry Coated B-66 Alloy Bar After Oxidation-Erosion Testing for 100 Hours at 2200°F Plus 100 Hours at 2400°F Plus 20 Hours at 2500°F

Localized failure after 20 hours at 2500°F is indicated by arrow.

application (Figure 37). These support areas were evidenced prior to testing by a slightly different coloration of the coating.

Metallographic examination of the coating after erosion testing revealed numerous areas of oxide penetration through the outer coating layers (Figure 38). Substrate attack, however, was absent except in those areas where oxidation was visible on the specimen surfaces.

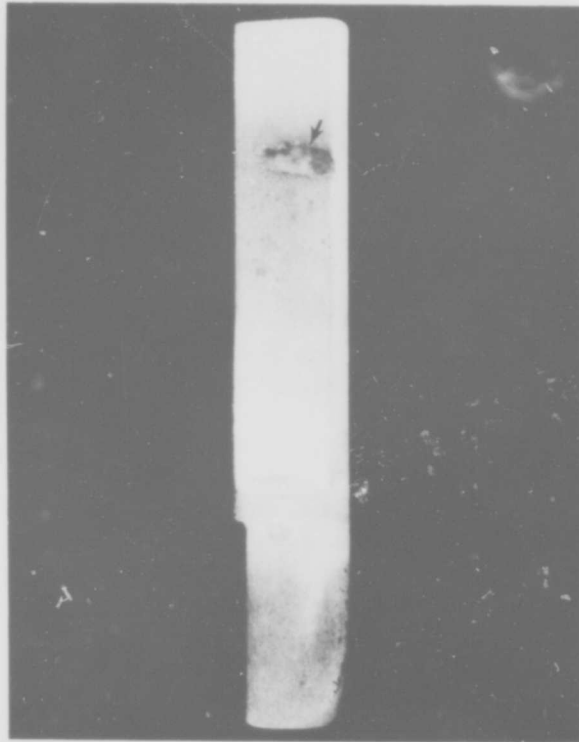
TRW TiCr-Si (Vacuum) Pack/XB-88. Failure of four specimens, as judged by visible substrate oxide (Figure 39), was observed for the TRW TiCr-Si/XB-88 system after 20 hours at 2200° F. Metallographic examination revealed complete oxygen penetration of the coating in areas of surface craze cracking. Subsequent oxidation occurred along the coating-substrate interface (Figure 40).

Solar V-CrTi-Si/Cb-132M. Failure was detected after 20 hours at 2200° F for three of the Solar V-CrTi-Si/Cb-132M specimens and after 100 hours at 2200° F plus 20 hours at 2400° F for the fourth specimen. Those specimens exhibiting failure after 20 hours were tested for an additional 60 hours at 2200° F to determine whether the areas of local oxidation represented coating defects or signified the onset of general failure. Although progressive extension of the local oxidation occurred, no additional areas of failure were observed. Local oxidation generally occurred along the trailing edge and airfoil tip surfaces (Figure 41).

Metallographic examination of the specimens after test revealed general oxide penetration through coating cracks to the coating-substrate diffusion zone (Figure 42). The areas of local failure showed appreciable amounts of substrate oxide (Figure 43), and, in some cases, oxygen enrichment along grain boundaries extended for an appreciable distance (2 to 3 mils) beneath the oxide layer (Figure 44).

Solar MoTi-Si (TNV-12SE4)/Cb-132M. Oxidation-erosion failures were observed for the Solar MoTi-Si/Cb-132M system after 100 hours at 2200° F plus 100 hours at 2400° F plus 40 hours at 2500° F. The condition of the coating during and at the conclusion of this test series is summarized below:

- After 100 hours at 2200° F: Coating was unaffected.
- After 100 hours at 2200° F plus 40 hours at 2400° F: Surface craze crack pattern developed with small glassy spots on airfoil surfaces. No substrate oxidation was apparent.
- After 100 hours at 2200° F plus 60 hours at 2400° F: A portion of the glassy spots (concentrated primarily along the airfoil trailing edges) developed a milky-white appearance as shown in Figure 45.
- After 100 hours each at 2200° and 2400° F plus 20 hours at 2500° F: Glassy areas became more prominent with increase in milky-white coloration.



MAG. 1.25X

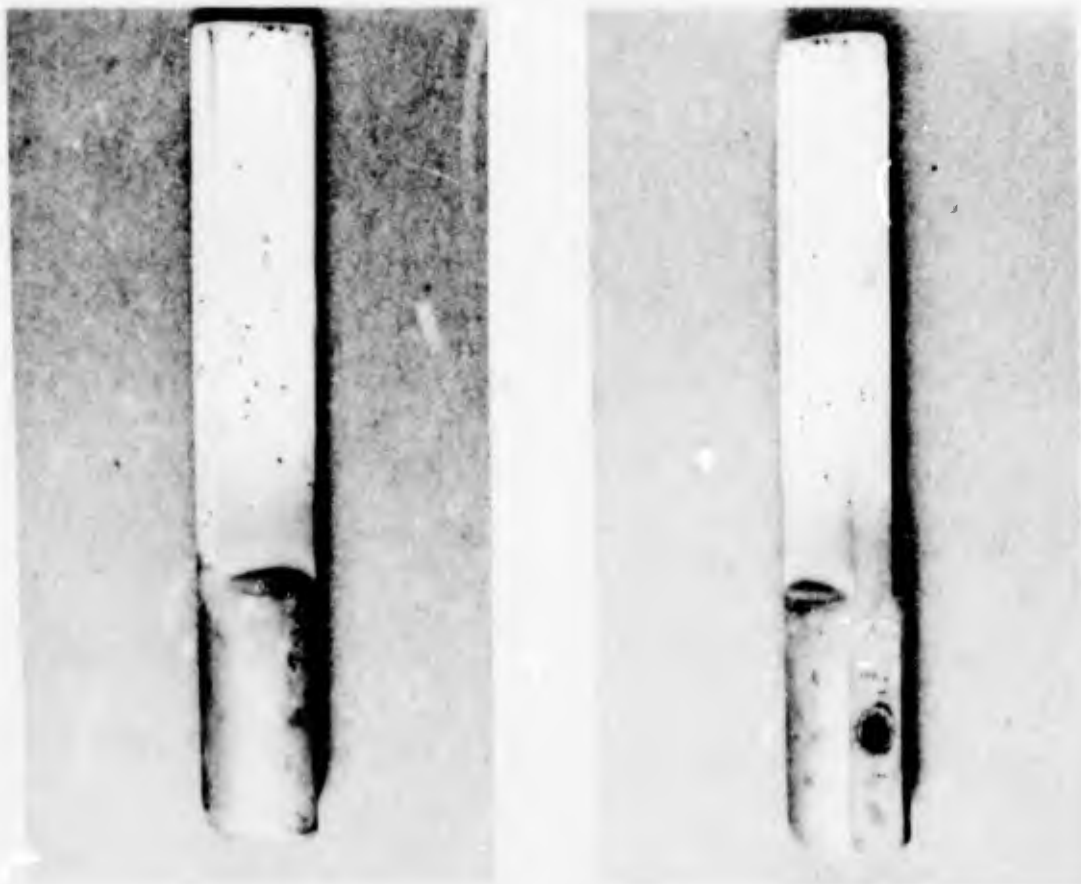
Figure 37. Sylvania SiCrTi Slurry Coated B-66 Alloy Bar After Oxidation-Erosion Testing for 100 Hours at 2200°F Plus 60 Hours at 2400°F

Failure occurred after 140 hours in area at which specimen was supported during coating application (arrow).



ETCH: 20% HYDROFLUORIC ACID, 20% NITRIC ACID, 60% WATER MAG: 500X

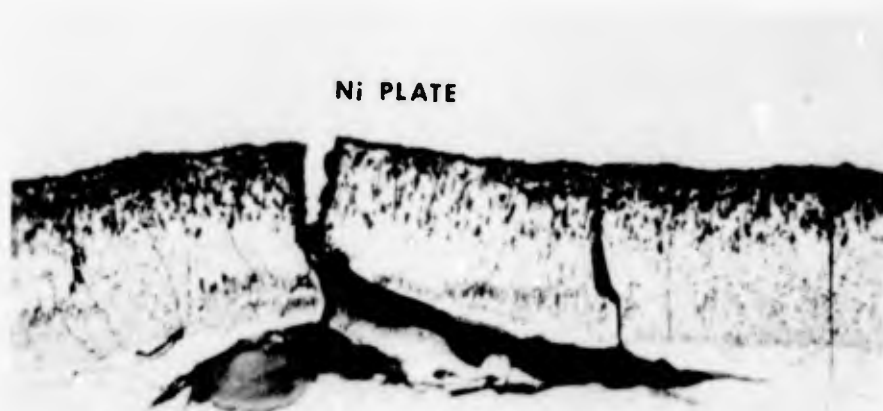
Figure 38. Oxide Penetration Through the Outer Coating Layers of Sylvania SiCrTi Slurry Coated B-66 Alloy Specimen After Oxidation-Erosion Testing for 100 Hours at 2200°F Plus 60 Hours at 2400°F



MAG: 1.3X

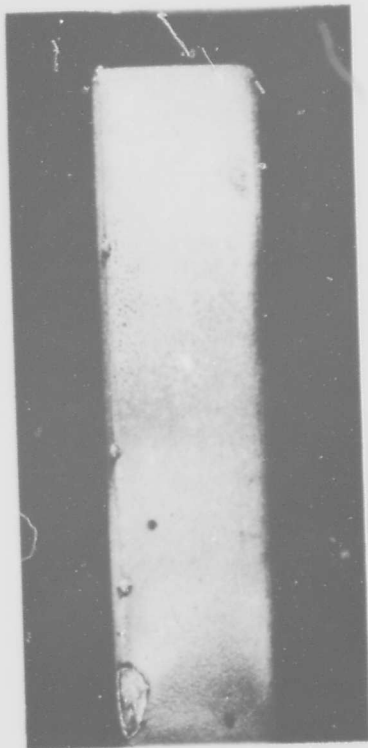
Figure 39. TRW TiCr-Si Coated XB-88 Alloy Bars After Oxidation-Erosion Testing for 20 Hours at 2200°F

Note numerous localized oxidation failures on airfoil surfaces.



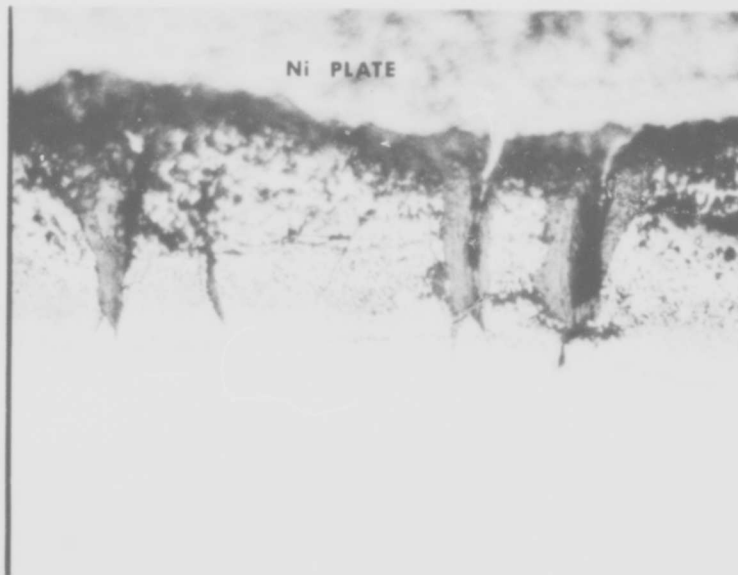
ETCH: 20% HYDROFLUORIC ACID, 20% NITRIC ACID, 60% WATER MAG: 250X

Figure 40. Typical Oxidation Failure on TRW TiCr-Si Coated XB-88 Alloy Specimen Oxidation-Erosion Tested for 20 Hours at 2200°F



MAG: 2X

Figure 41. Typical Solar V-CrTi-Si Coated Cb-132M Alloy Erosion Bars After 80 Hours of Oxidation-Erosion Testing at 2200°F

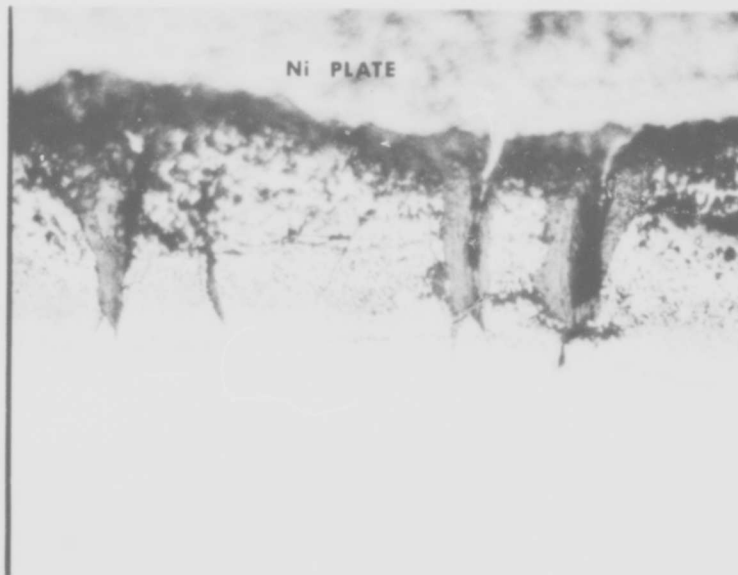


ETCH: 20% HYDROFLUORIC ACID, 20% NITRIC ACID, 60% WATER

MAG: 500X

Figure 42. Typical Microstructure of Solar V-CrTi-Si Coated Cb-132M Alloy After 80 Hours of Oxidation-Erosion Testing at 2200°F

No external failure was noted in this area.

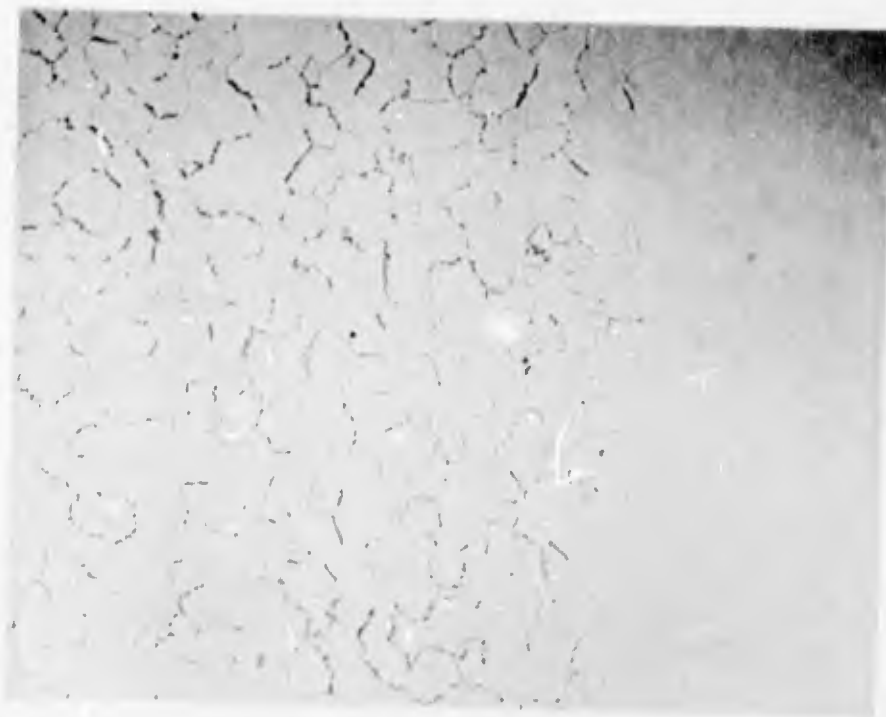


ETCH: 20% HYDROFLUORIC ACID, 20% NITRIC ACID, 60% WATER

MAG: 500X

Figure 42. Typical Microstructure of Solar V-CrTi-Si Coated Cb-132M Alloy After 80 Hours of Oxidation-Erosion Testing at 2200°F

No external failure was noted in this area.



ETCH: 20% HYDROFLUORIC ACID, 20% NITRIC ACID, 60% WATER
DIRECTION OF OXYGEN PENETRATION →

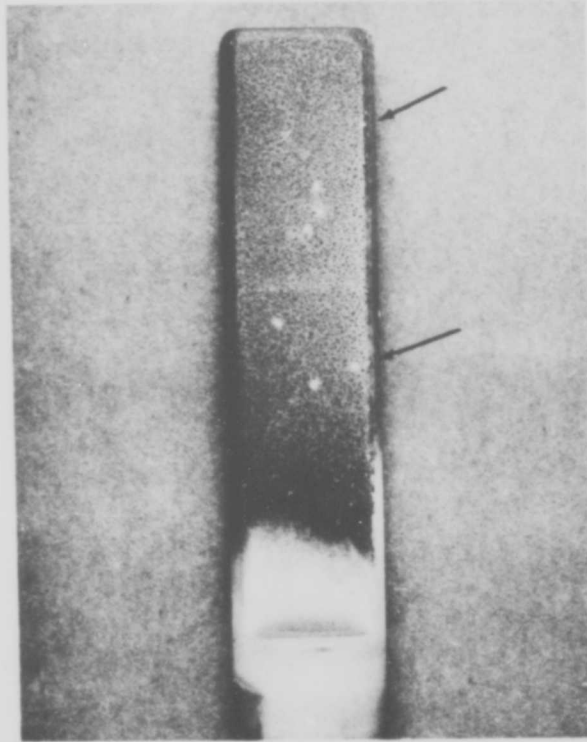
MAG: 75X



ETCH: 20% HYDROFLUORIC ACID, 20% NITRIC ACID, 60% WATER

MAG: 250X

Figure 44. Microstructure of Cb-132M Alloy Substrate Showing Grain Boundary Oxygen Enrichment Beneath a Typical Solar V-CrTi-Si Coating Failure in 2200°F Oxidation-Erosion



MAG: 1.6X

Figure 45. Solar MoTi-Si Coated Cb-132M Alloy Bar After Oxidation-Erosion Testing for 100 Hours at 2200°F Plus 60 Hours at 2400°F

Note small dark glassy beads, some of which have turned a milky-white color (arrows).

- After 100 hours each at 2200° and 2400° F plus 40 hours at 2500° F: Substrate oxidation was observed along the trailing edge surface as shown in Figure 46. In other specimen airfoil areas, subcoating substrate oxidation appeared to be imminent as shown in Figure 47.

Metallographic examinations confirmed that surface beads were glassy formations. The glassy spots which were dark gray in color indicated glass devitrification on specimen cooling (Figure 48); the milky white spots, however, retained an amorphous structure (Figure 49). Coating structure beneath these glassy surface formations consisted of craze cracks extending to the coating-substrate interface. These cracks were filled with devitrified glass. During testing, an additional coating layer was formed at the coating-substrate interface. This layer also appeared glassy in nature. Additional layer formation was notably absent in substrate regions immediately beneath the glass-filled craze cracks (Figure 48). At failure, the glassy areas were bisque-colored in appearance, denoting substrate oxidation (Figure 50).

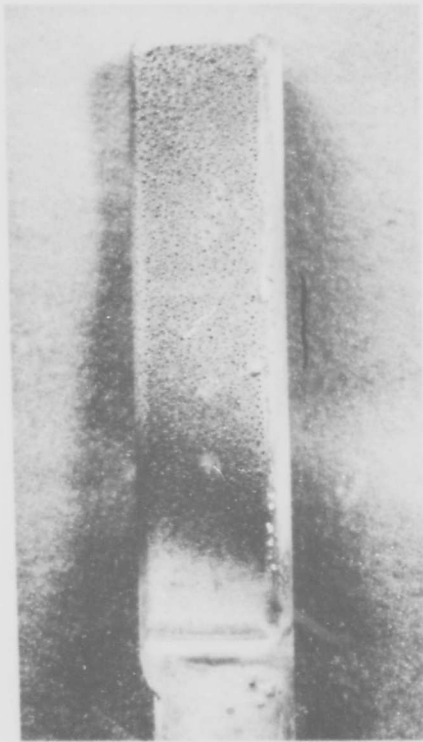
3.3.2.2 Thermal Fatigue Results

Sylvania SiCrTi Slurry/B-66. After thermal fatigue testing of the coated B-66 alloy vane airfoil specimens for 600 cycles to 2200°F (Figure 51) followed by 400 cycles to 2400°F (Figure 52), the Sylvania SiCrTi slurry coating was in good condition on both internal and external airfoil surfaces. However, oxidation had occurred on faying surfaces between the handle butt plate and airfoil platform (see Figure 34). During initial thermal fatigue testing to 2500° F, the embrittling effect of continued oxidation in this area led to weld cracking and subsequent handle-airfoil separation.

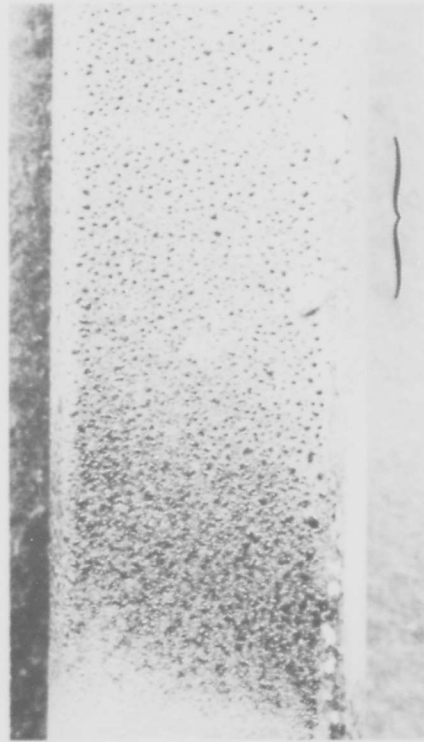
On the first of the two specimens, separation occurred after the 30-minute stabilization period at 2500° F prior to cycling. The coating on the airfoil (Figure 53) was damaged, and testing was necessarily terminated. Metallographic examination of the airfoil section revealed craze cracking and subsequent oxide penetration through outer coating layers (Figure 54). Substrate oxidation, however, was not observed in these areas.

The second specimen was tested further at 2500° F for the stabilization period plus 100 cycles. Testing was discontinued immediately prior to handle-airfoil separation. Since the airfoil coating areas remained in good condition, a suitable fixturing technique was devised to allow continued testing at 2500° F. An additional 400 cycles to 2500° F (500 cycles total at 2500° F) was accumulated before airfoil cracking (convex surface) was observed along a line parallel to the trailing edge (Figure 55). Although an additional 200 cycles to 2500° F (700 cycles total at 2500° F) resulted in continued oxidation along the cracked surface and additional crack formation along the concave surface, the airfoil leading edge remained in good condition (Figure 56). The leading edge exhibited local coating depletion, but coating failure and leading edge oxidation did not occur.

TRW TiCr-Si (Vacuum) Pack/XB-88. Both TRW TiCr-Si/XB-88 specimens failed after 200 thermal fatigue cycles to 2200° F. Numerous areas of local substrate oxidation



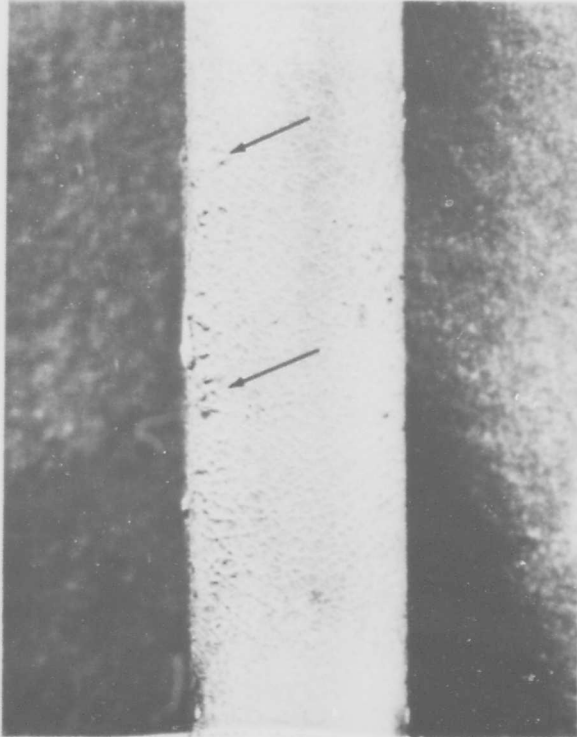
MAG: 1.75X



MAG: 4X

Figure 46. Solar MoTi-Si Coated Cb-132M Alloy Bar After Oxidation-Erosion Testing for 100 Hours at 2200°F Plus 100 Hours at 2400°F Plus 40 Hours at 2500°F

Note oxidation along trailing edge surface (bracket).



MAG: 4X

Figure 47. Solar MoTi-Si Coated Cb-132M Alloy Bar After Oxidation-Erosion Testing for 100 Hours at 2200°F Plus 100 Hours at 2400°F Plus 40 Hours at 2500°F

Note area of apparent subcoating oxidation (arrows).



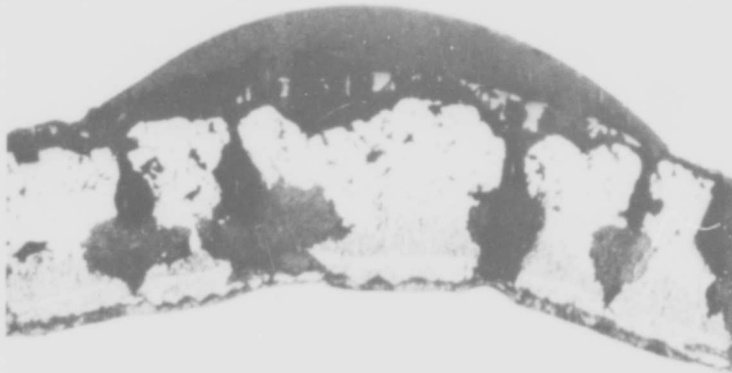
ETCH: 20% HYDROFLUORIC ACID, 20% NITRIC ACID, 60% WATER

MAG: 250X

Figure 48. Microstructure of Solar MoTi-Si Coated Cb-132M Alloy After Oxidation-Erosion Testing for 100 Hours at 2200°F Plus 100 Hours at 2400°F Plus 40 Hours at 2500°F

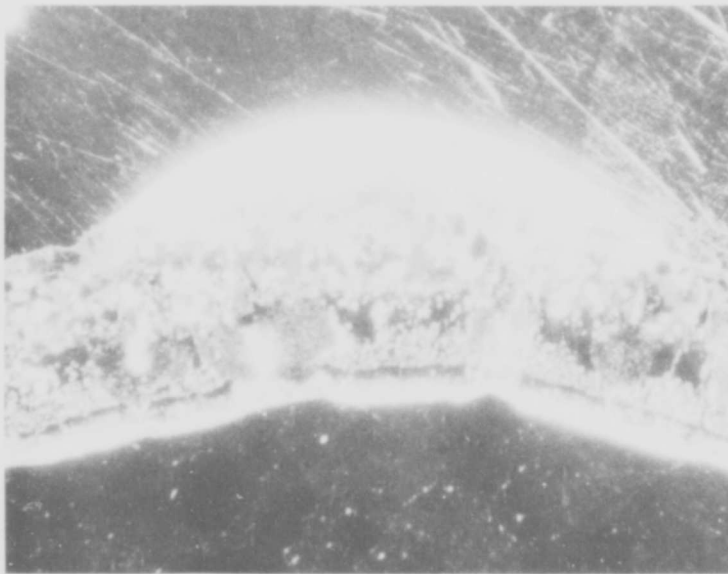
Note devitrified glassy spot on coating surface (arrow) and the formation and penetration of second phase into the alloy substrate (brackets).

Ni PLATE



ETCH: 20% HYDROFLUORIC ACID, 20% NITRIC ACID, 60% WATER

MAG: 200X



POLARIZED LIGHT

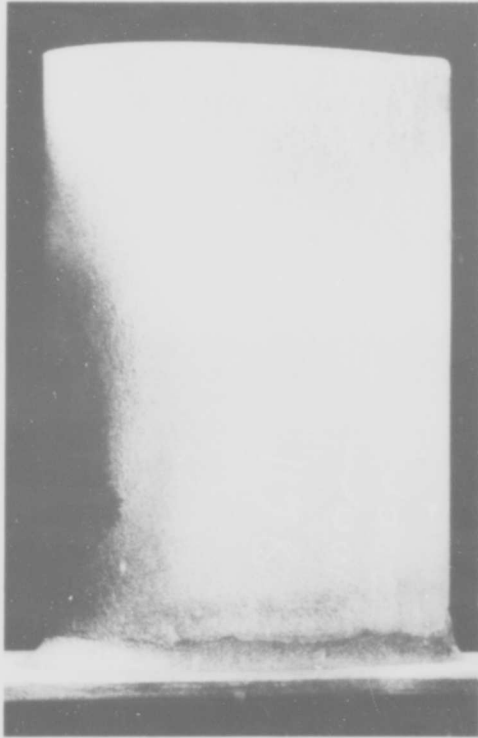
MAG: 200X

Figure 49. Microstructure of Solar MoTi-Si Coated Cb-132M Alloy Showing Formation of Amorphous and Devitrified Glassy Structures During Oxidation-Erosion Testing

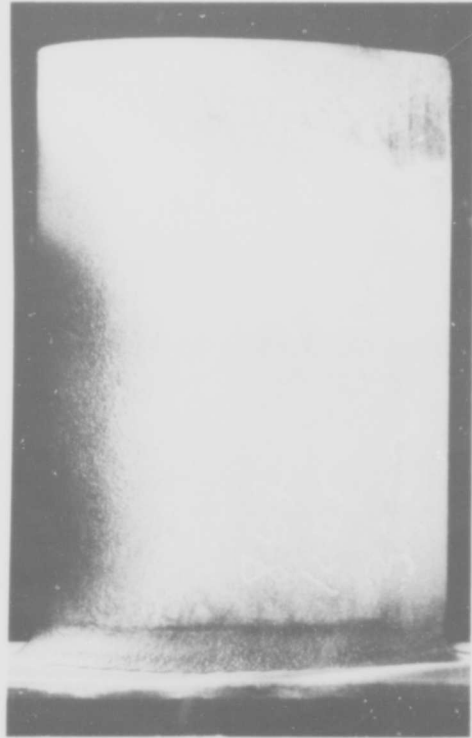


ETCH: 20% HYDROFLUORIC ACID, 20% NITRIC ACID, 60% WATER MAG: 100X

Figure 50. Microstructure of Solar MoTi-Si Coated Cb-132M Alloy Showing Substrate Oxidation Beneath Bisque-Colored Glassy Areas After Oxidation-Erosion Testing



SPECIMEN 1



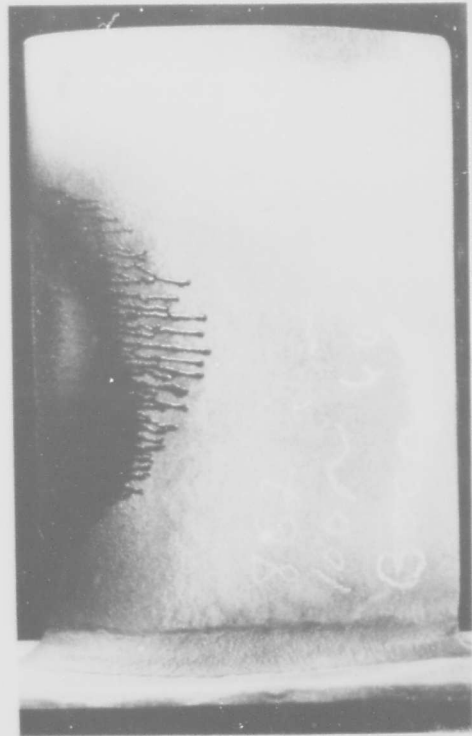
SPECIMEN 2

MAG: 1X

Figure 51. Sylvania SiCrTi Slurry Coated B-66 Alloy Vane Airfoils After 600 Thermal Fatigue Cycles to 2200°F



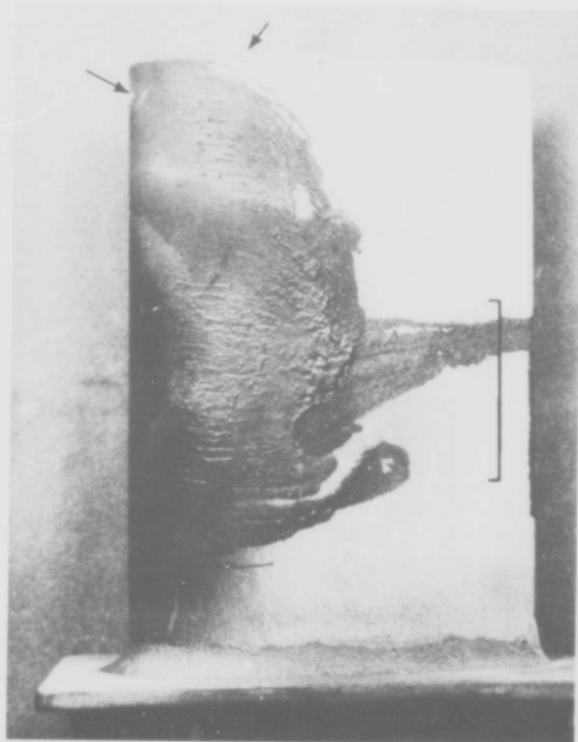
SPECIMEN 1



SPECIMEN 2

MAG: 1X

Figure 52. Sylvania SiCrTi Slurry Coated B-66 Alloy Vane Airfoils After 600 Thermal Fatigue Cycles to 2200°F Plus 400 Cycles to 2400°F



SPECIMEN 1

MAG: 0.9X

Figure 53. Sylvania SiCrTi Slurry Coated B-66 Alloy Vane Airfoil After 600 Thermal Fatigue Cycles to 2200°F Plus 400 Cycles to 2400°F Plus a 30-Minute Exposure at 2500°F

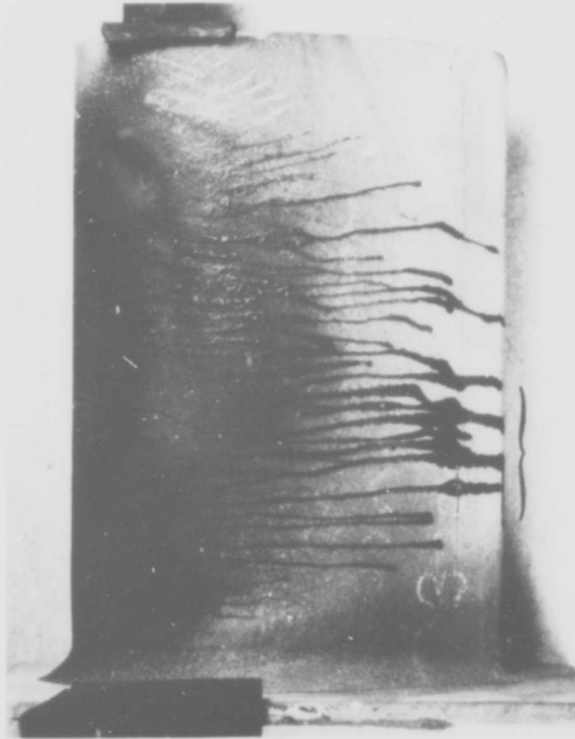
Note localized coating and specimen damage (arrow). Bracket denotes location of a hairline crack.



ETCH: 20% HYDROFLUORIC ACID, 20% NITRIC ACID, 60% WATER

MAG: 500X

Figure 54. Craze Cracking and Oxide Penetration Through Outer Coating Layers of Sylvania SiCrTi Slurry Coated B-66 Alloy After 600 Thermal Fatigue Cycles to 2200°F Plus 400 Cycles to 2400°F Plus a 30-Minute Exposure at 2500°F

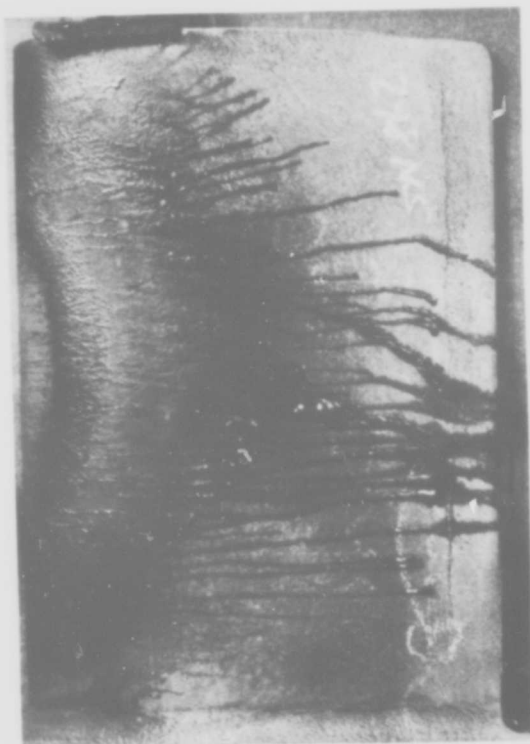


SPECIMEN 2

MAG: 0.9X

Figure 55. Sylvania SiCrTi Slurry Coated B-66 Alloy Vane Airfoil Convex Surface After 600 Thermal Fatigue Cycles to 2200°F Plus 400 Cycles to 2400° F Plus 500 Cycles to 2500°F; No Coating Failure

Bracket locates hairline crack.



CONVEX AIRFOIL SURFACE



CONCAVE AIRFOIL SURFACE

MAG: 1.2X

SPECIMEN 2

Figure 56. Sylvania SiCrTi Slurry Coated B-66 Alloy Vane Airfoil After 600 Thermal Fatigue Cycles to 2200°F Plus 400 Cycles to 2400°F Plus 700 Cycles to 2500°F; No Coating Failure

Brackets locate hairline cracks.

were observed on airfoil surfaces (Figure 57). Composite microstructure after failure was similar to that observed for the system after failure in oxidation-erosion (see Figure 40); i.e., oxide penetration within coating craze cracks led to rupture of the coating and subsequent substrate oxidation.

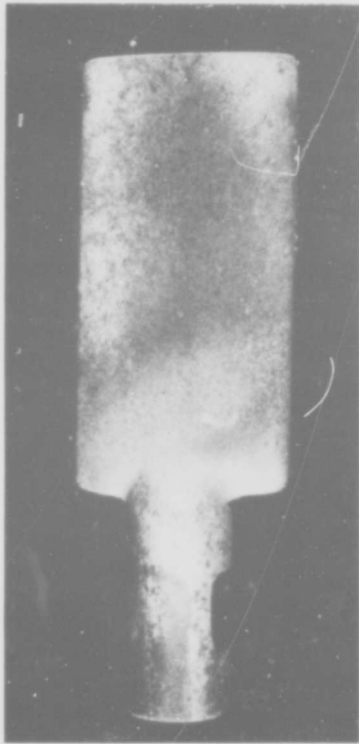
Solar V-CrTi-Si/Cb-132M. Spalling and local oxidation of the Solar V-CrTi-Si coated Cb-132M thermal fatigue specimens was first observed after 200 cycles to 2200° F (Figure 58) and became more severe during the next 200 cycles (Figure 59). Metallography revealed substrate oxidation extending from coating craze cracks (Figure 60). In some cases, this oxidation led to complete rupture of the coating (Figure 61). Oxidation at the trailing edge of one specimen was severe (Figure 62).

Solar MoTi-Si (TNV-12SE4)/Cb-132M. No evidence of coating spalling or failure was observed for two Solar MoTi-Si/Cb-132M specimens after 600 cycles to 2200° F followed by 400 cycles to 2400° F followed by 1200 cycles to 2500° F (Figure 63). An additional 200 cycles to 2500° F (1400 cycles total at 2500° F) produced failure in the form of localized oxidation along the airfoil trailing edge surfaces (Figure 64). Failure characteristics were microstructurally similar to those observed and described for the oxidation-erosion specimens.

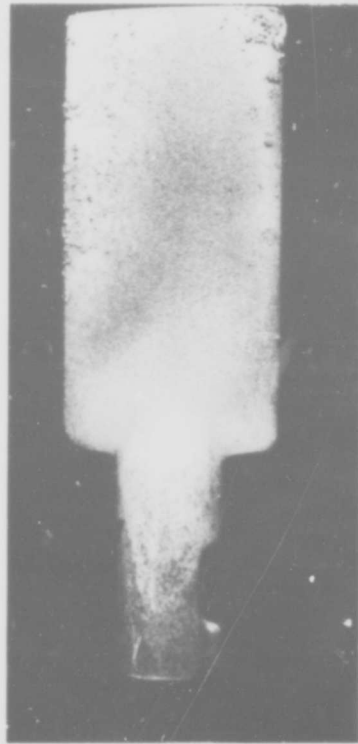
3.3.2.3 Ballistic Impact Results

Impact test results were similar for both vane and blade airfoil coating-substrate systems. The impact areas were characterized by five zones, depending on the condition of the outer silicide layers after impact and before oxidation exposure (Figure 65). These zones were as follows:

- Zone I, impact depression: A region consisting of crushed and compressed coating. The outer silicide layers exhibit complete structure disregistry after impact.
- Zone II, scab area surrounding impact depression: This area is characterized by complete removal of the outer silicide coating layers. An increase in impact velocity results in extension of this zone; whereas scabbing is reduced as impact temperature is increased.
- Zone III, unaffected coating: The areas of the specimen lying outside of the impact-affected zones.
- Zone IV: This zone is characterized by coating adherence with perpendicular cracking and separation of the outer silicide layers in the area of specimen directly behind the impact point.
- Zone V, scab area surrounding the protrusion of Zone IV: The scabbing surrounding Zone IV is similar in nature but less severe than that observed in Zone II.



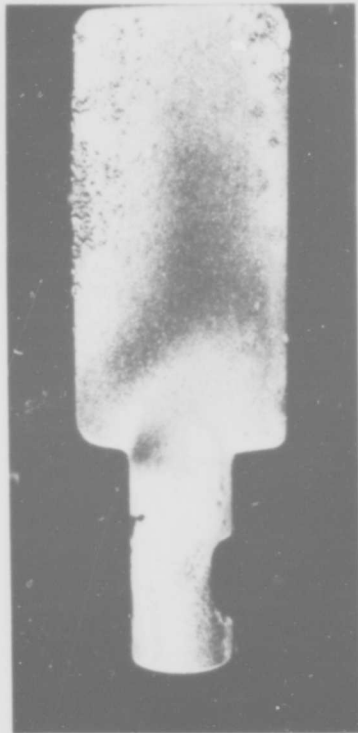
SPECIMEN 1



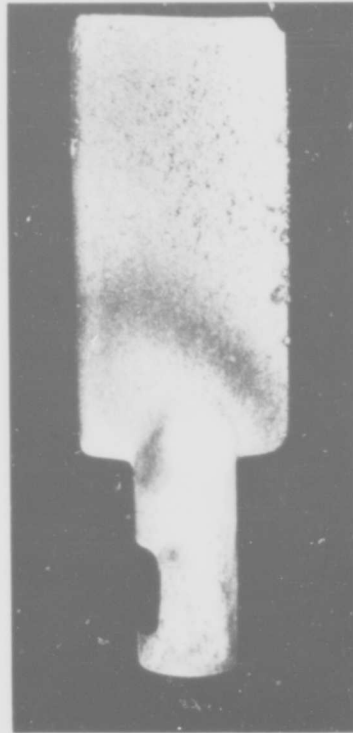
SPECIMEN 2

MAG: 1.3X

Figure 58. Solar V-CrTi-Si Coated Cb-132M Alloy Thermal Fatigue Specimens (Convex Surfaces) After 200 Cycles to 2200°F



SPECIMEN 1
CONVEX SURFACE



SPECIMEN 2
CONCAVE SURFACE

MAG: 1.3X

Figure 59. Solar V-CrTi-Si Coated Cb-132M Alloy Thermal Fatigue Specimens
After 400 Cycles to 2200°F



CONCAVE AIRFOIL SURFACE

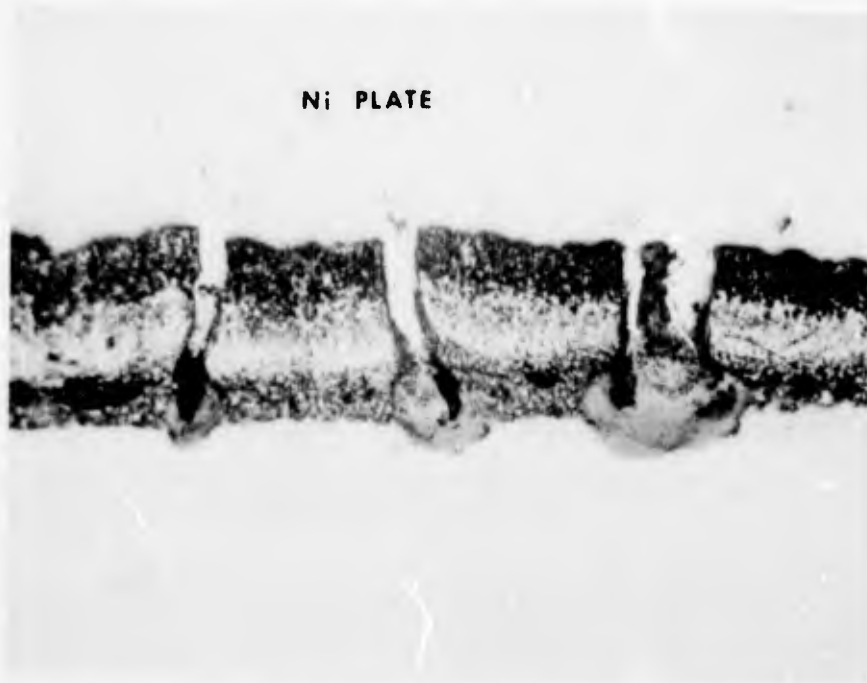


CONVEX AIRFOIL SURFACE

MAG: 1.3X

Figure 57. TRW TiCr-Si Coated NB-88 Alloy Specimens After 200 Thermal Fatigue Cycles to 2200°F

Note numerous airfoil oxidation failures.



ETCH: 20% HYDROFLUORIC ACID, 20% NITRIC ACID, 60% WATER

MAG: 250X

Figure 60. Typical Microstructure of Solar V-CrTi-Si Coated Cb-132M Alloy After 400 Thermal Fatigue Cycles to 2200°F

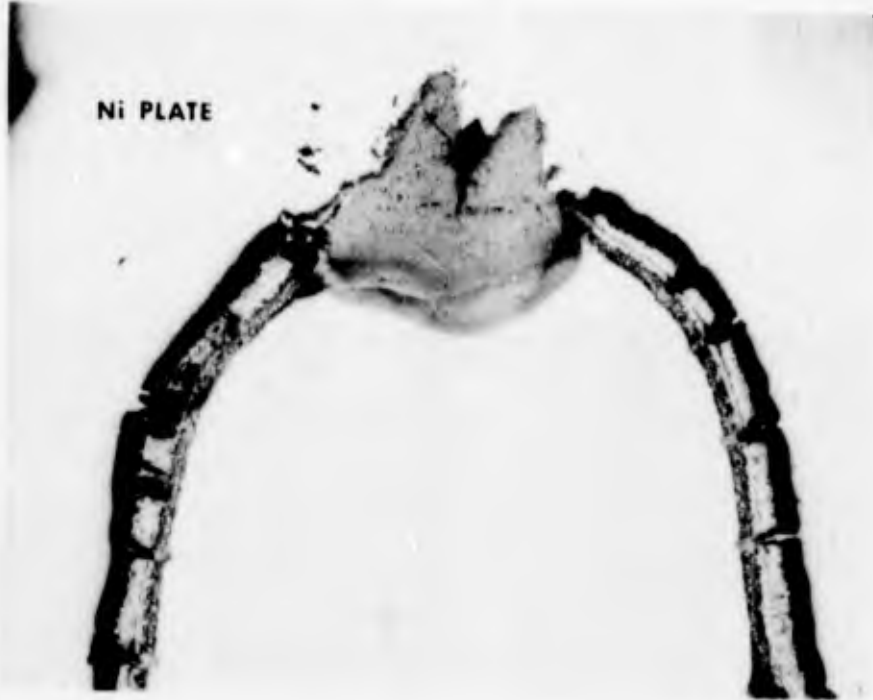
No external failure was noted in this area.



ETCH: 20% HYDROFLUORIC ACID, 20% NITRIC ACID, 60% WATER

MAG: 250X

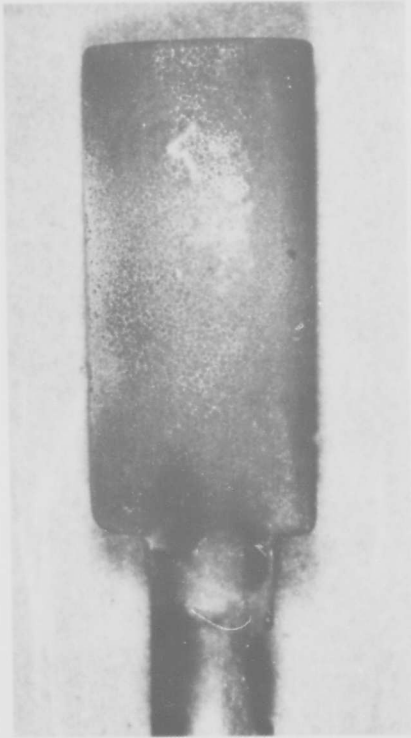
Figure 61. Microstructure of Solar V-CrTi-Si Coated Cb-132M Alloy in Area of Local Oxidation Failure During 2200°F Thermal Fatigue Testing



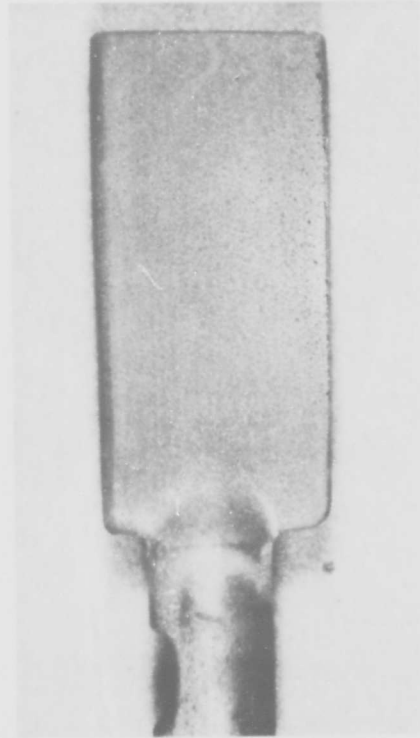
ETCH: 20% HYDROFLUORIC ACID, 20% NITRIC ACID, 60% WATER

MAG: 75X

Figure 62. Microstructure of Solar V-CrTi-Si Coated Cb-132M Alloy in Area of 2200°F Thermal Fatigue Failure at the Airfoil Trailing Edge



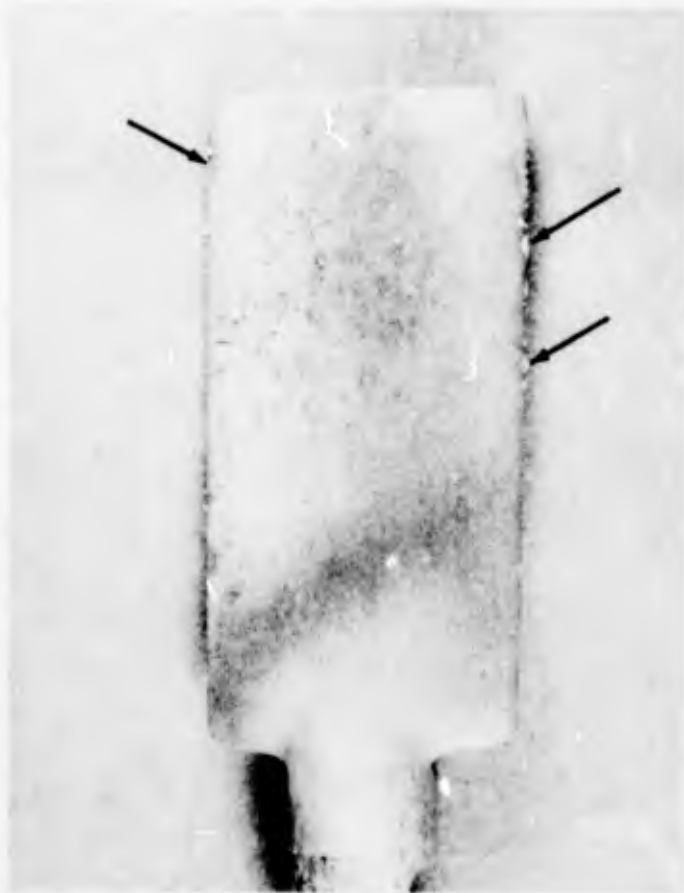
CONVEX AIRFOIL SURFACE



CONCAVE AIRFOIL SURFACE

MAG: 1.5X

Figure 63. Solar MoTi-Si Coated Cb-132M Alloy Specimen After 600 Thermal Fatigue Cycles to 2200°F Plus 400 Cycles to 2400°F Plus 1200 Cycles to 2500°F



MAG: 1.6X

Figure 64. Solar MoTi-Si Coated Cb-132M Alloy Specimen (Convex Surface)
After Thermal Fatigue Testing for 600 Cycles to 2200°F Plus 400
Cycles to 2400°F Plus 1400 Cycles to 2500°F

Note areas of localized oxidation on leading and trailing edge surfaces (arrows).

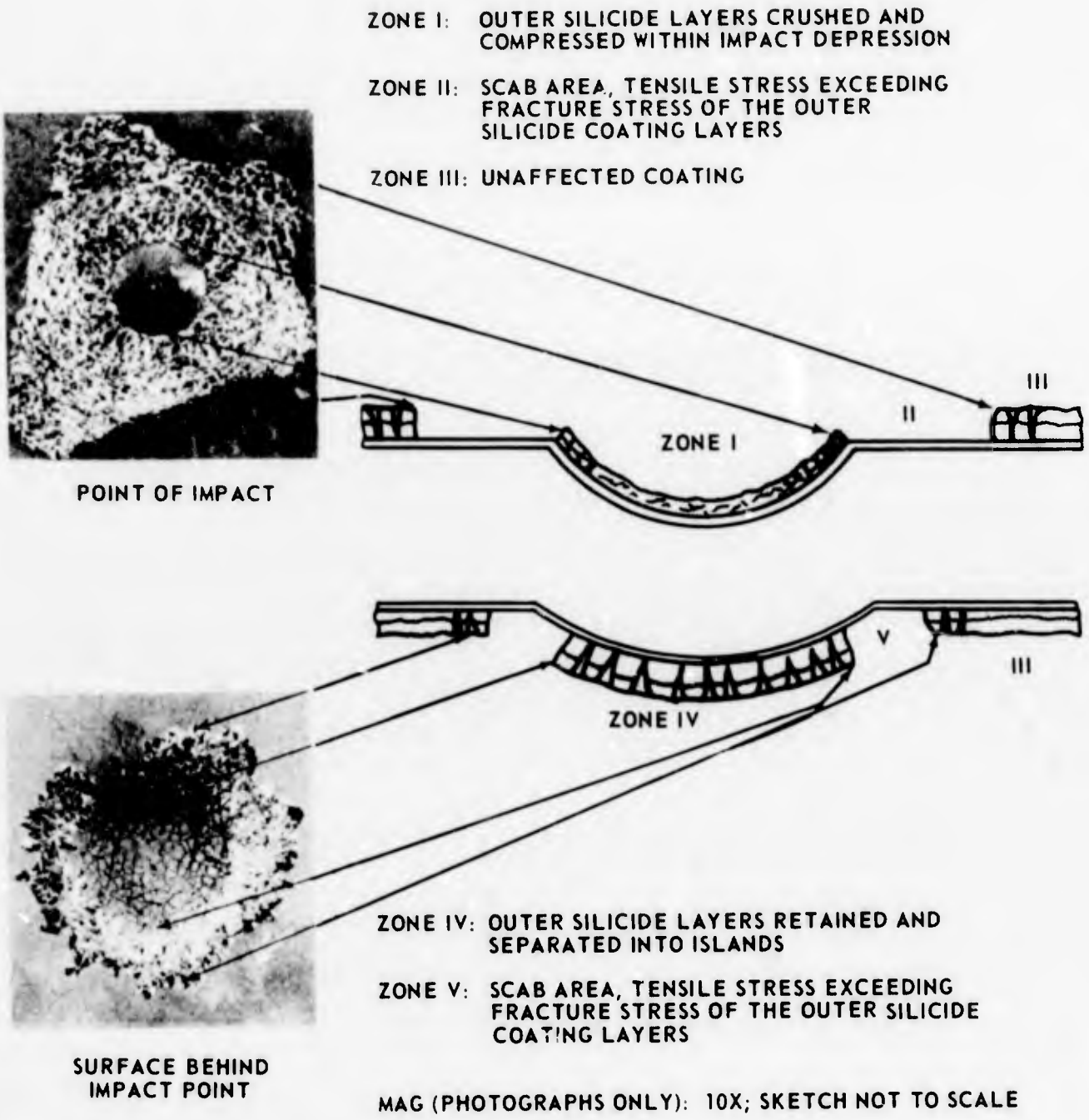


Figure 65. Schematic Cross Section of a Typical Coated Specimen After Ballistic Impact Test

Due to the thickness of the blade airfoil test specimens (0.125 inch compared to 0.050 inch for the vane alloy test specimens), Zones IV and V did not appear on these specimens.

A summary of the ballistic impact test results on all four coating-substrate systems is presented in Table VIII, with the observed condition after oxidation exposure stated for various periods at 2200° F. In all cases, failures were first noted in the scabbed areas (either Zone II or Zone V). Oxidation was generally more prevalent on the impact sides of the specimens. The 500-ft/sec, 70° F impact condition was particularly severe for the Sylvania SiCrTi slurry/B-66 vane system. Both impacts resulted in fracture of the coating-alloy composite (Figure 66).

3.4 EXTRACONTRACTUAL HIGH-TEMPERATURE SYSTEMS

The Solar Division of International Harvester Company supplied to Pratt & Whitney Aircraft Cb-132M alloy oxidation-erosion bars coated with the Solar TNV-7SE4 (35W-35Mo-15V-15Ti-silicide) and V-(CrTi)-Si coatings for evaluation. The V-(CrTi)-Si coating differed from the V-CrTi-Si coating evaluated in Phase V of the program (paragraph 3.2.3) in that increased amounts of vanadium, chromium-titanium, and silicon were deposited.

Though not part of contract requirements, oxidation-erosion testing was performed on these test specimens using parameters identical to those described for the Phase V preliminary screening tests (paragraph 3.3.1.1). Failure as determined by localized oxide formations occurred for all Solar TNV-7SE4 coated Cb-132M alloy specimens after 100 hours at 2200° F plus 40 hours at 2400° F (Figure 67). Oxidation-erosion failures of the Solar V-(CrTi)-Si coated Cb-132M alloy occurred on one specimen after 100 hours at 2200° F plus 60 hours at 2400° F and for two remaining specimens after 100 hours at 2200° F plus 100 hours at 2400° F plus 20 hours at 2500° F. Localized substrate oxide formations on specimen airfoil surfaces were considered to indicate a failure of the coating (Figure 68).

3.5 COATINGS APPLICATION, LOW-TEMPERATURE SYSTEMS

Coatings on the root sections of turbine blades are subjected to conditions considerably different from airfoil coatings. The blade root is not exposed to the high-velocity gas stream and therefore does not require a coating with good erosive properties. The coating must, however, be protective in the 1300° to 1600° F temperature range, exhibit sufficient ductility to deform without cracking, resist mechanical fatigue, and be sufficiently wear resistant to tolerate blade-disk bearing loads.

The blade root operating conditions do not necessarily exclude the coatings currently being considered for blade airfoil application. Ballistic impact data, however, suggest that the silicide-type coatings may not exhibit sufficient ductility in the blade root temperature range to avoid the previously mentioned problems. For this reason,

TABLE VIII
RESULTS OF PHASE V BALLISTIC IMPACT TESTING OF THE
VANE AND BLADE AIRFOIL COATING-SUBSTRATE SYSTEMS

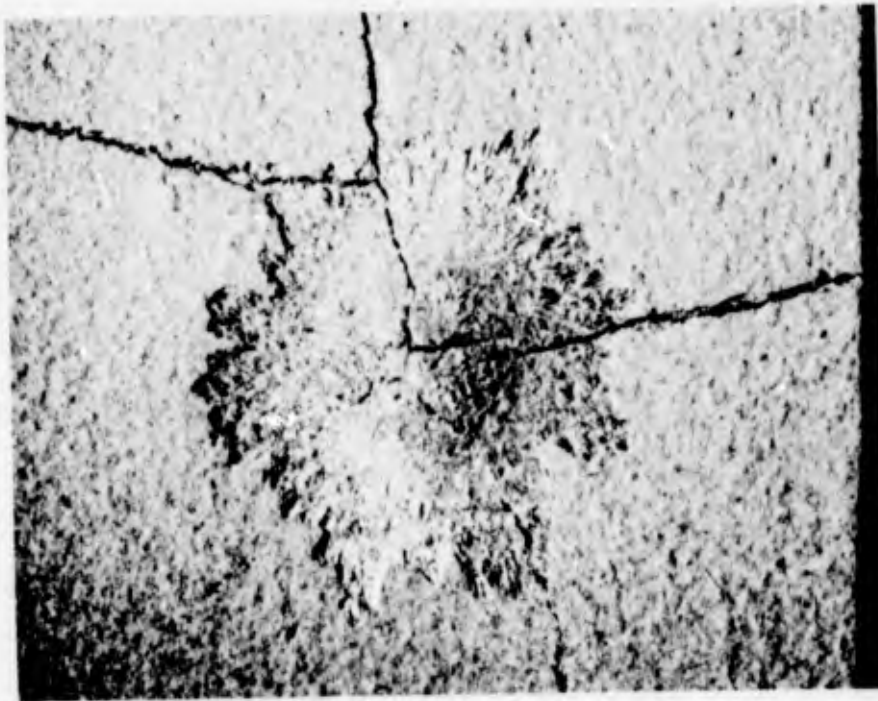
Application	Test No.	Specimen No.	Coating	Substrate Alloy	Specimen Temp. at Impact (°F)	Impact Velocity (ft/sec)	Oxidation Life After Impact		Observed Condition After Oxidation Exposure	
							Temp. (°F)	Time (hrs)	Surface at Impact Point	Surface Directly Behind Impact Point
Vane	1	BH-5-1	Sylvania SiCrTi slurry	B-66	70	200	2200	1	Oxide surrounding impact depression	Oxidation of surface
	2	BH-5-1	Sylvania SiCrTi slurry	B-66	70	200	2200	1	Oxide surrounding impact depression	Oxidation of surface
	3	BH-5-2	Sylvania SiCrTi slurry	B-66	70	500	--	--	Specimen fractured at impact depression	---
	4	BH-5-2	Sylvania SiCrTi slurry	B-66	70	500	--	--	Specimen fractured at impact depression	---
	5	BH-5-3	Sylvania SiCrTi slurry	B-66	2200	200	2200	1	Oxide surrounding impact depression	No oxide noted
	6	BH-5-3	Sylvania SiCrTi slurry	B-66	2200	200	2200	1	Oxide surrounding impact depression	Oxidation of surface
	7	BH-5-4	Sylvania SiCrTi slurry	B-66	2200	200	2200	1	Oxide surrounding impact depression	No oxide noted
	8	BH-5-4	Sylvania SiCrTi slurry	B-66	2200	500	2200	1	Oxide surrounding impact depression	No oxide noted
Blade Airfoil	9	MBI-5-1	Solar V-CrTi-Si	Cb-132M	70	200	2200	2	Oxide surrounding impact depression	
	10	MBI-5-1	Solar V-CrTi-Si	Cb-132M	70	200	2200	3	Oxide surrounding impact depression	
	11	MBI-5-1	Solar V-CrTi-Si	Cb-132M	70	200	2200	1	Oxide surrounding impact depression	
	12	MBI-5-2	Solar V-CrTi-Si	Cb-132M	70	500	2200	--	No failure after 16 hours; test stopped	
	13	MBI-5-2	Solar V-CrTi-Si	Cb-132M	70	500	2200	1	Oxide surrounding impact depression	
	14	MBI-5-3	Solar V-CrTi-Si	Cb-132M	2200	200	2200	--	No failure after 16 hours; test stopped	
	15	MBI-5-3	Solar V-CrTi-Si	Cb-132M	2200	200	2200	1	Oxide surrounding impact depression	
	16	MBI-5-4	Solar V-CrTi-Si	Cb-132M	2200	500	2200	1	Oxide surrounding impact depression	
	17	MBI-5-4	Solar V-CrTi-Si	Cb-132M	2200	500	2200	1	Oxide surrounding impact depression	
	18	XBI-5-1	TRW TiCr-Si (vacuum)	XB-88	70	200	2200	2	Oxide surrounding impact depression	See Note 3
	19	XBI-5-2	TRW TiCr-Si (vacuum)	XB-88	2200	200	2200	--	No failure after 16 hours; test stopped	
	20	XBI-5-3	TRW TiCr-Si (vacuum)	XB-88	70	500	2200	1	Oxide surrounding impact depression	
	21	XBI-5-4	TRW TiCr-Si (vacuum)	XB-88	2200	500	2200	2	Oxide surrounding impact depression	
	22	MBI-B-1	Solar MoTi-Si (TNV-12SE4)	Cb-132M	70	200	2200	1	Oxide surrounding impact depression	See Note 3
	23	MBI-B-2	Solar MoTi-Si (TNV-12SE4)	Cb-132M	2200	200	2200	--	No failure after 16 hours; test stopped	
	24	MBI-B-3	Solar MoTi-Si (TNV-12SE4)	Cb-132M	70	500	2200	1	No failure after 16 hours; test stopped	
	25	MBI-B-4	Solar MoTi-Si (TNV-12SE4)	Cb-132M	2200	500	2200	1	Slight oxide surrounding impact depression	

Notes:

1. Weight of steel projectiles: 0.75 gram each.
2. Thickness of substrate: B-66: 0.050 inch; Cb-132M and XB-88: 0.125 inch.
3. No effects were noted on the surface directly behind the impact point on the coated Cb-132M and XB-88 due to the greater thickness of these specimens (0.125 inch).



POINT OF IMPACT

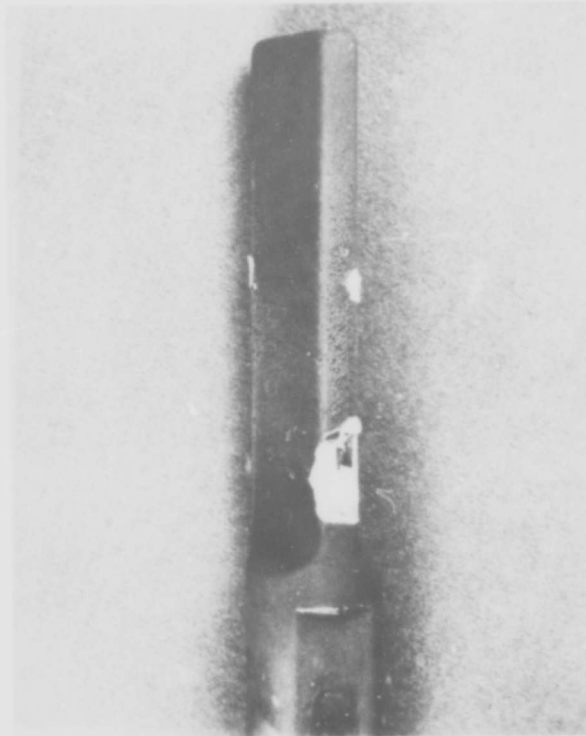


SURFACE BEHIND IMPACT POINT

MAG: 10X

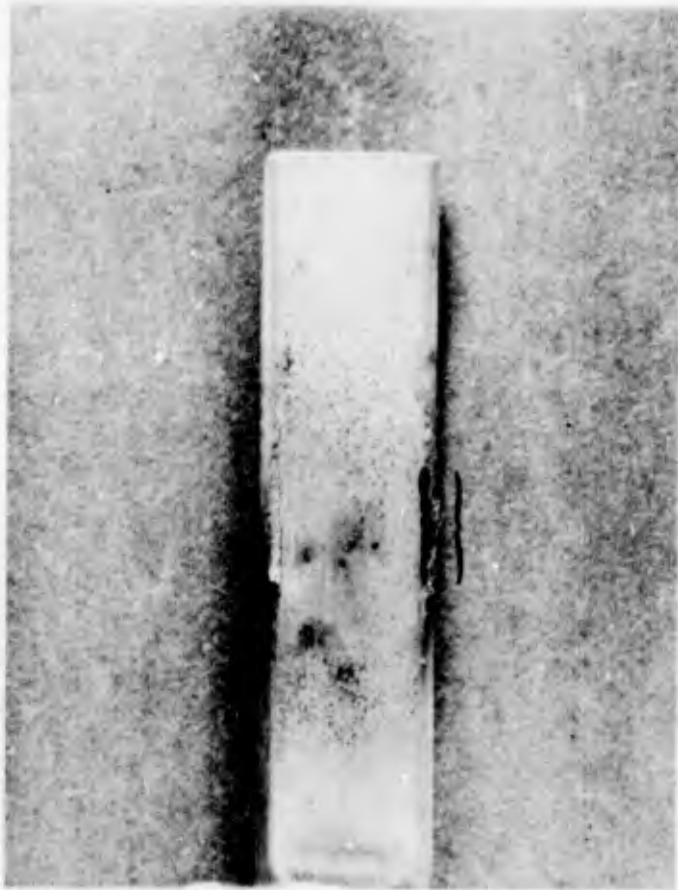
Figure 66. Surfaces of Sylvania SiCrTi Slurry Coated B-66 Alloy After Room Temperature Impact Testing at 500 Feet Per Second (No Oxidation Exposure)

Note coating-alloy composite cracking.



MAG: 1.6X

Figure 67. Solar (WMoVTi)-Si (TNV-7SE4) Coated Cb-132M Alloy Bar After Oxidation-Erosion Testing for 100 Hours at 2200°F Plus 40 Hours at 2400°F



MAG: 1.9X

Figure 68. Solar V-(CrTi)-Si Coated Cb-132M Alloy Bar After Oxidation-Erosion Testing for 100 Hours at 2200°F Plus 100 Hours at 2400°F Plus 20 Hours at 2500°F

Note areas of oxidation along specimen edge surfaces (brackets).

duplex coatings (root-airfoil) are considered to offer the greatest potential for fulfilling the blade coating requirements. This concept is presented schematically in Figure 69.

3.5.1 Sylvania SiCrV Slurry/Cb-132M

A Si-20Cr-5V composition and vehicle mixture was spray applied to the Cb-132M alloy and heat treated for 1 hour at 2550° F in vacuum to produce a coating of uniform surface appearance. Excellent coverage of corner and edge surfaces was obtained. Metallographic examination revealed a 4.4-mil-thick coating consisting of three distinct layers (Figure 70). A continuous 0.18-mil-thick diffusion layer was present at the coating-substrate interface. The intermediate layer, averaging 0.9 mil in thickness, exhibited regions of a columnar-type growth. The outer 3.3-mil-thick layer contained islands of second-phase material which probably precipitated from the continuous matrix. Hairline cracks appeared to extend from the surface through the coating to the coating-substrate interface (Figure 70).

Microstructural characteristics of the coating deviated from those observed for the SiCrV coating on Cb-132M alloy evaluated as a blade airfoil system in Phase VI of the program (Item 9, paragraph 4.2.3).

3.5.2 Sylvania SiCrFe Slurry/Cb-132M

The Sylvania SiCrFe coating was applied to Cb-132M using a Si-20Cr-20Fe mixture-vehicle slurry and heat treating for 1 hour at 2550° F. Excellent coverage of the specimen corner and edge surfaces was obtained with the dull-gray coating.

Five distinct regions were noted during metallographic examination of the 4.4-mil-thick coating (Figure 71). Above a continuous 0.18-mil-thick region at the coating-substrate interface, a dark-colored 0.2-mil region extended into a 0.2-mil third coating layer of dendritic appearance. Above this third layer, a 0.8-mil fourth coating layer was continuous and homogeneous in appearance. The outer coating region of 3.0 mils in thickness was two-phase in appearance (Figure 71). Numerous hairline cracks and voids were present in the coating.

3.5.3 TRW TiAl (Vacuum) Pack/Cb-132M

Application of the TiAl coating was performed at TRW utilizing the following parameters:

- Cycle 1: Titanium was deposited at 2000° F for 13 hours using an argon back-fill.

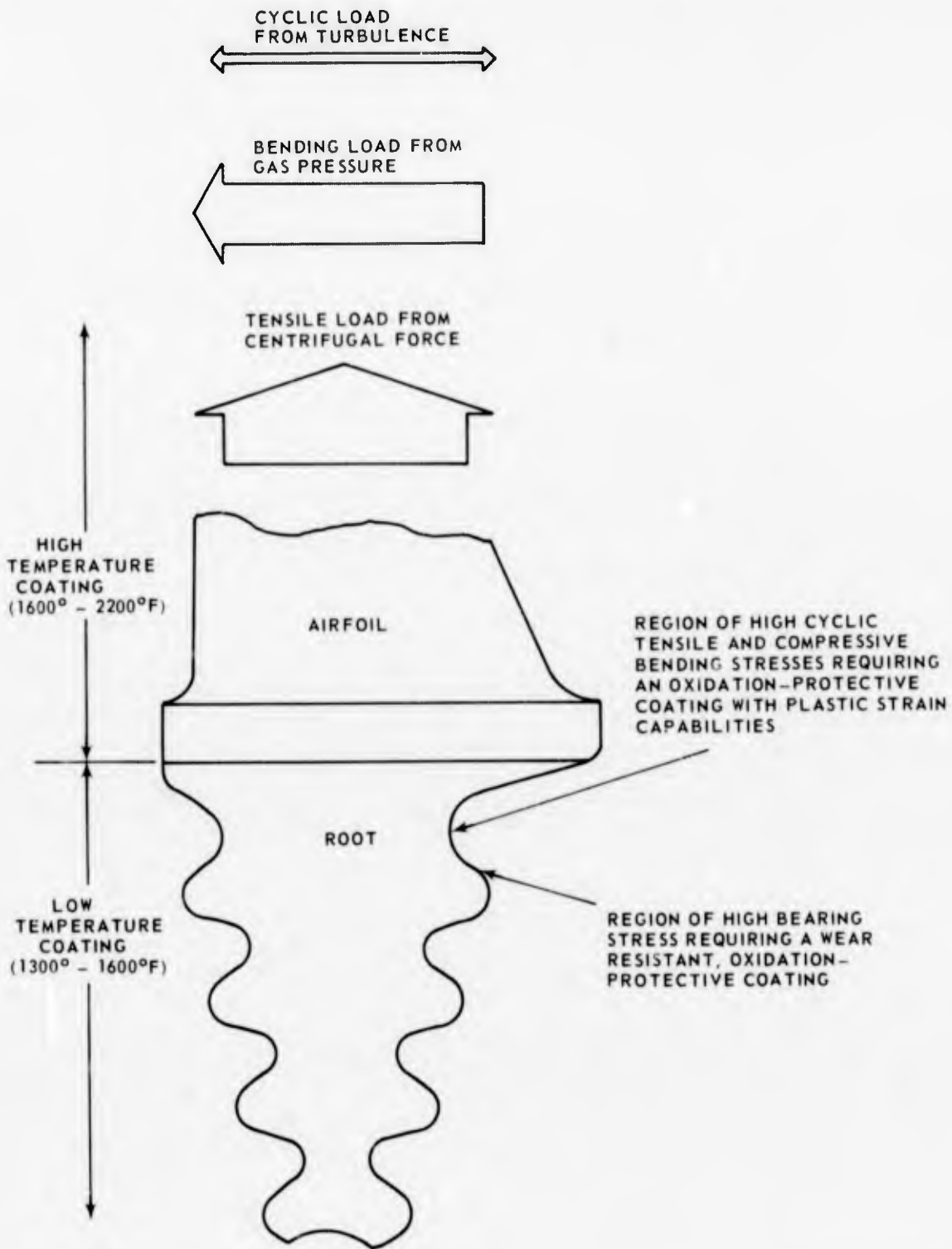
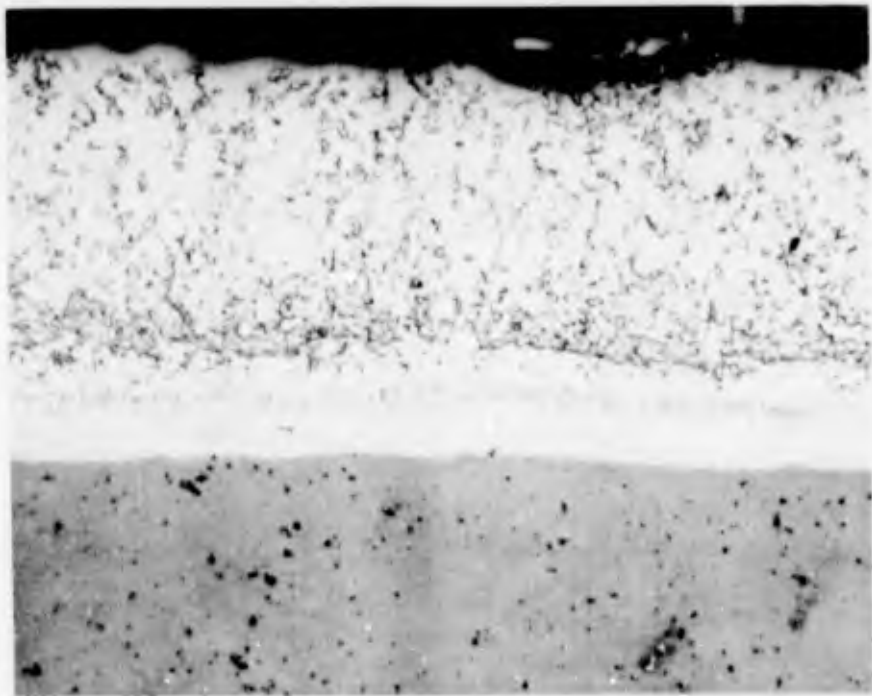
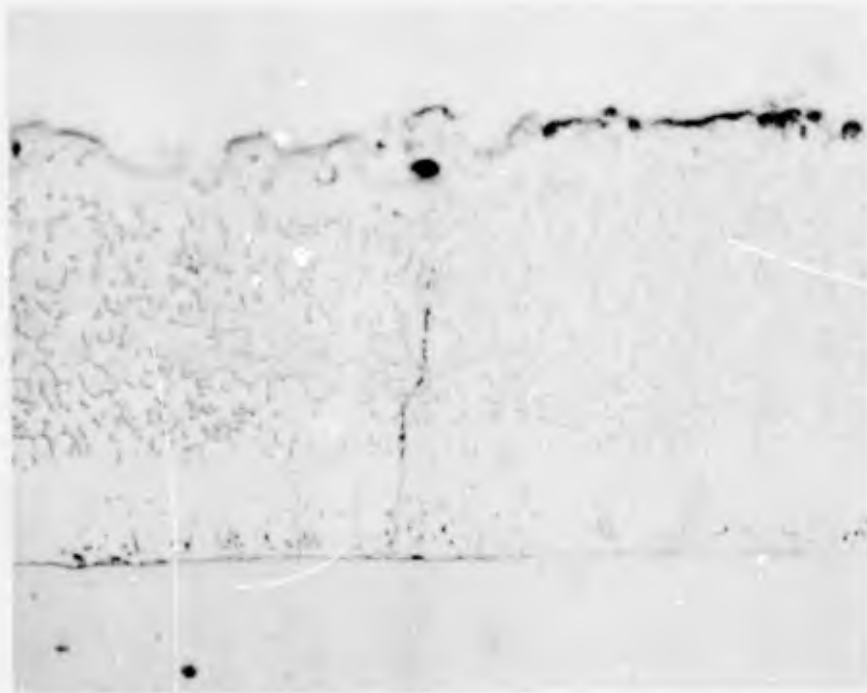


Figure 69. Geometry of a Typical Blade Root Section Showing Conditions Suggesting the Duplex Coating Concept



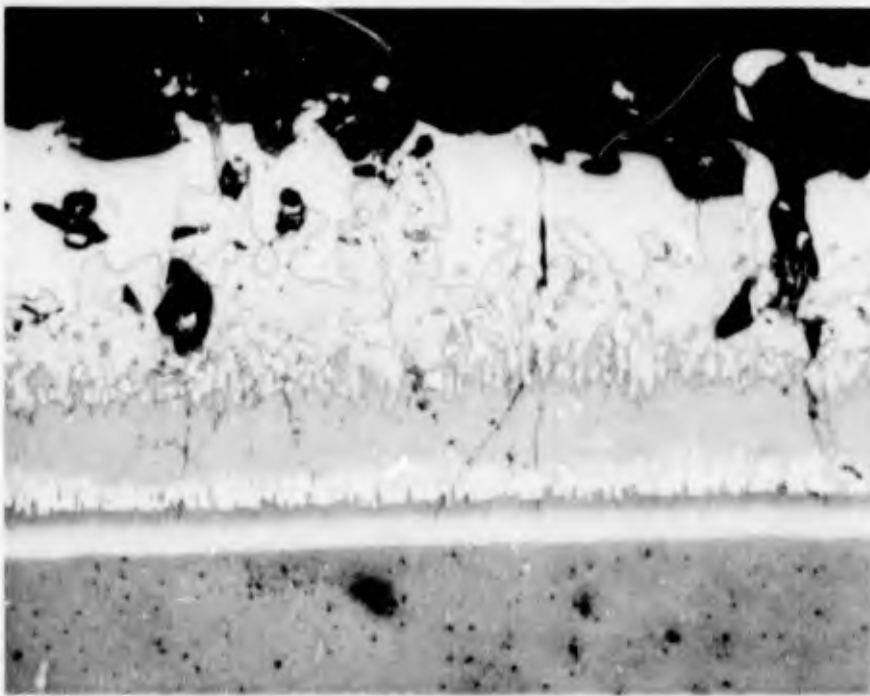
ETCH: ANODIZED

MAG: 500X



ETCH: 33% HYDROFLUORIC ACID, 33% NITRIC ACID, 33% WATER MAG: 500X

Figure 70. Typical Microstructure of As-Applied Sylvania SiCrV Slurry Coating on Cb-132M Alloy



ETCH: ANODIZED

MAG: 500X



ETCH: 33% HYDROFLUORIC ACID, 33% NITRIC ACID, 33% WATER MAG: 500X

Figure 71. Typical Microstructure of As-Applied Sylvania SiCrFe Slurry Coating on Cb-132M Alloy

- Cycle 2: The low-pressure second cycle resulted in a predominantly aluminum layer and was deposited from a 56Cr-44Al prealloyed pack at 1900° F for 4 hours.

Use of the Cr-Al pack during the second cycle resulted in an aluminum layer reportedly containing less than 10 percent chromium.

Metallographic examination revealed three distinct coating regions (Figure 72). Adjacent to the columbium substrate was observed a continuous 2.5- to 3.2-mil-thick region in which titanium was predominant. Etching brought out a grain structure in the outer 1.5-mil region. A 0.25-mil-thick continuous intermediate layer was beneath a 1.0-mil-thick aluminum-rich outer coating layer. The intermediate region possibly consists of either concentrated chromium or a TiAl-Cr compound. The outer layer was very irregular and contained numerous cracks penetrating to the intermediate coating region. In some areas penetration of titanium-rich constituents into the columbium substrate along grain boundaries was observed.

3.5.4 TRW TiCr (Vacuum) Pack/Cb-132M

Titanium and chromium were deposited from a 50Cr-50Ti pack composition in a single-cycle operation at 2340° F for 8 hours in vacuum. This procedure produced a coating of homogeneous appearance with good coverage at corner and edge surfaces.

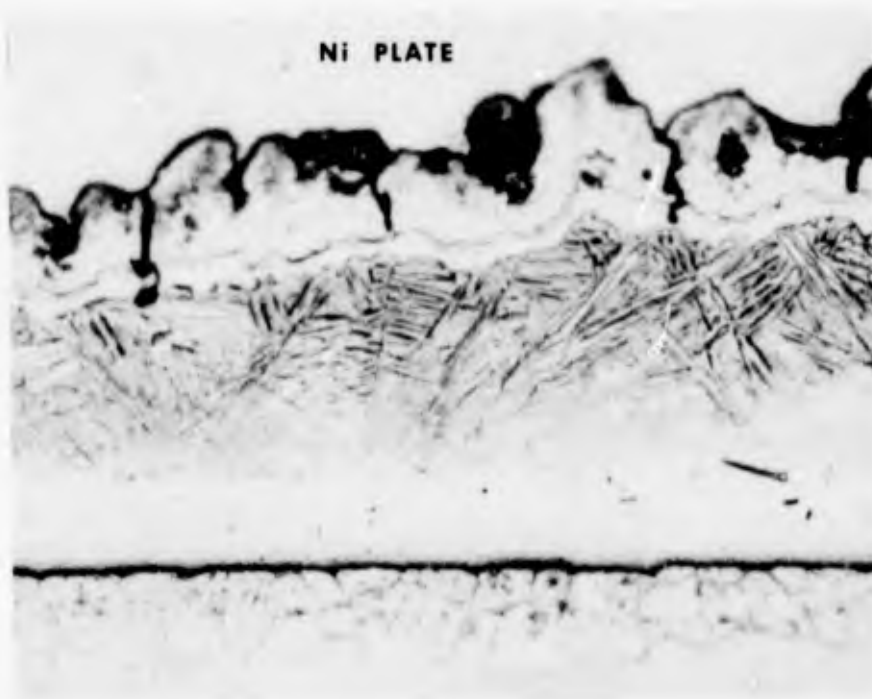
Two regions were observed metallographically for the 1.0-mil-thick coating (Figure 73). The first region, adjacent to the substrate, was approximately 0.25 mil in thickness and penetrated into the substrate approximately 0.5 mil along substrate grain boundaries. The outer 0.75-mil-thick layer was continuous and homogeneous in appearance.

3.5.5 TRW TiCr-Al (Vacuum) Pack/Cb-132M

Application of the TiCr-Al coating was performed in a two-step operation using the parameters summarized below.

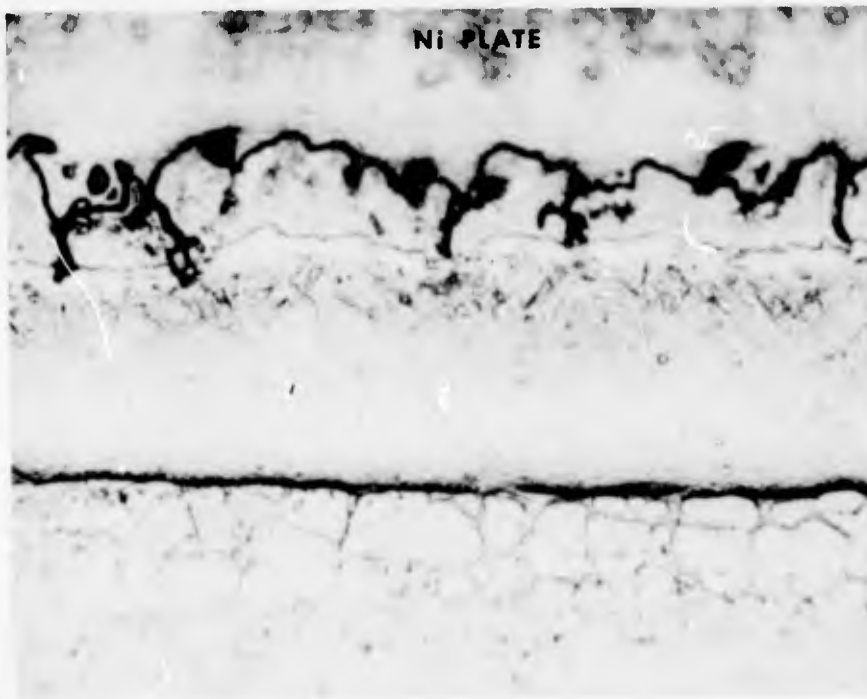
- Cycle 1: Chromium and titanium was deposited from a 50Cr-50Ti prealloyed mixture at 2340° F for 8 hours in vacuum.
- Cycle 2: The aluminum-rich surface layer was applied from a 56Cr-44Al pack at 1900° F for 4 hours. A partial pressure of 150 mm mercury was maintained throughout the cycle.

Metallographic examination of the 2.2-mil-thick coating failed to delineate coating phases in distinct compositionally defined layers (Figure 74). However, penetration of the second phase occurred within a solid solution region extending approximately 1.0 mil into the alloy substrate.



ETCH: 33% HYDROFLUORIC ACID, 33% NITRIC ACID, 33% WATER

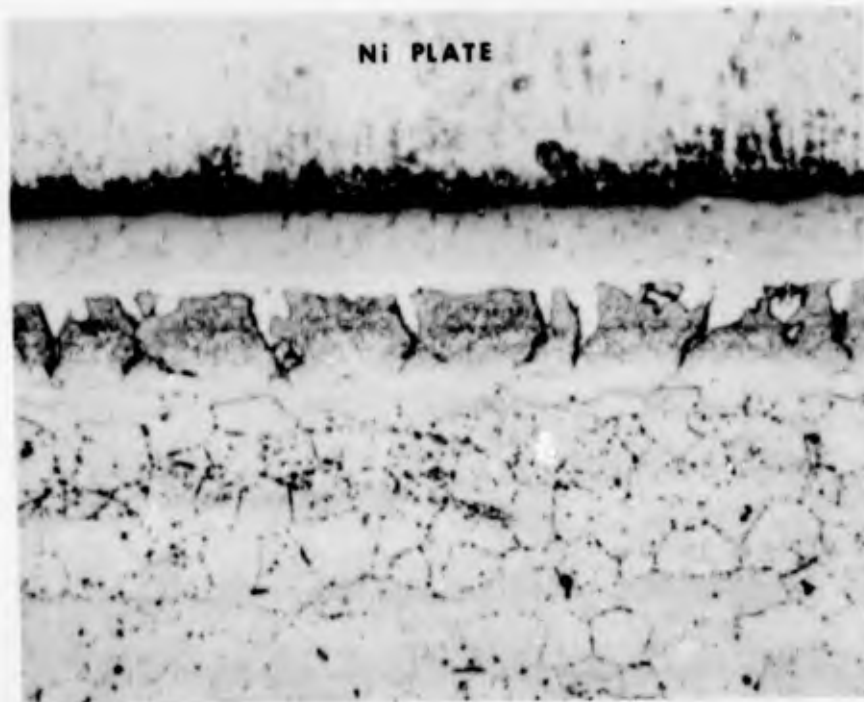
MAG: 500X



ETCH: 33% HYDROFLUORIC ACID, 33% NITRIC ACID, 33% WATER

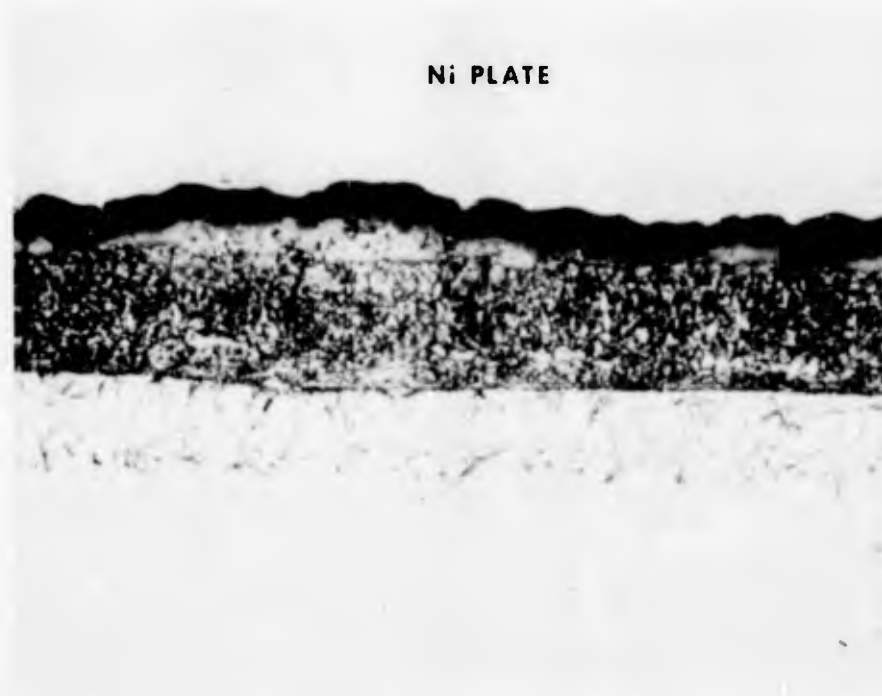
MAG: 500X

Figure 72. Typical Microstructure of As-Applied TRW TiAl (Vacuum) Pack Coating on Cb-132M Alloy



ETCH: 33% HYDROFLUORIC ACID, 33% NITRIC ACID, 33% WATER MAG: 500X

Figure 73. Typical Microstructure of the As-Applied TRW TiCr (Vacuum)
Pack Coating on Cb-132M Alloy



ETCH: 33% HYDROFLUORIC ACID, 33% NITRIC ACID, 33% WATER

MAG: 500X

Figure 74. Typical Microstructure of TRW TiCr-Al (Vacuum) Pack Coating on Cb-132M Alloy

3.5.6 TRW TiCr-Si (Vacuum) Pack/Cb-132M

TRW reported a slight modification in its application of the TiCr-Si coating for blade root application. This deviation consisted of less siliciding than is used for higher temperature coatings. Application parameters were as follows:

- Cycle 1: The first low-pressure cycle consisted of chromium-titanium deposition at 2340°F for 8 hours from a 50Cr-50Ti weight percent prealloyed pack.
- Cycle 2: The second low-pressure cycle, a siliconizing process, was conducted at 2000°F for a period of 1 hour.

Normally (for high-temperature coatings) the second cycle is run for 4 to 10 hours at 2040°F to increase the concentration of silicon within the coating (refer to paragraph 3.2.2).

Metallography revealed a coating structure consisting of two distinct layers (Figure 75). A 0.5-mil-thick layer of predominantly CrTi was observed adjacent to the substrate. This phase penetrated into the alloy substrate a distance of approximately 0.5 mil at intermittent locations. The outer coating region of 1.0 mil thickness contained numerous cracks extending from the surface through the coating to the layer adjacent to the substrate.

3.5.7 Electroplated NiCr/Cb-132M

The use of nickel-chromium compositions as coatings for columbium alloys represents a departure from the conventional silicon- and aluminum-base coatings. The use of such coatings on a turbine blade root, however, appears to offer considerable potential for the following reasons: (1) The 1300° to 1600°F range of interest is sufficiently low to avoid deleterious columbium-nickel reactions, (2) protection of the columbium substrate should be adequate at and below 1600°F, and (3) NiCr coatings should be ductile and should not adversely affect columbium substrate mechanical properties. Preliminary studies have indicated that pure nickel would be reasonably protective in the temperature range of interest. However, the use of chromium was employed to improve oxidation characteristics and to prevent excessive wear and galling of the nickel which would result from the very high bearing loads experienced during blade root operation.

Electroplating of alternate nickel and chromium layers and vacuum codeposition of an 80Ni-20Cr composition were investigated as coating application processes. Prior to electrodeposition, the test specimens were vapor blasted, decreased in acetone, and pickled for two minutes in a solution containing, by volume, 30 percent lactic acid, 10 percent nitric acid, 10 percent hydrofluoric acid, and 50 percent water. After rinsing in a distilled water bath at 180° and 70°F, three to six plating cycles were utilized to produce 0.8- to 1.2-mil-thick coatings. Nickel was deposited from a sulfamate nickel plating solution with nickel chloride salt additions at 120°F.

Ni PLATE



ETCH: 33% HYDROFLUORIC ACID, 33% NITRIC ACID, 33% WATER

MAG: 500X

Figure 75. Microstructure of the TRW TiCr-Si (Vacuum) Pack Coating on Cb-132M Alloy

The chromium deposits were produced at 135°F from a solution containing chromium plating salts. The plating bath composition was prepared from chromic acid and sulfate- and chloride-containing compounds.

Four to six plating cycles were utilized to produce 0.8- to 2.0-mil-thick coatings. Each cycle comprised alternate deposition of nickel and chromium. Some difficulty was experienced initially as a result of poor nickel-chromium adherence in the outer coating layers, but proper adjustment of the plating parameters eliminated this problem. In general, the appearance of the as-plated specimens was uniform and smooth, with excellent coverage of corner and edge surfaces. The coated specimens were heat treated at 1800°F for 2 hours in argon with only slight darkening of the surfaces. The nickel and chromium layers remained stratified after the heat treatment operation.

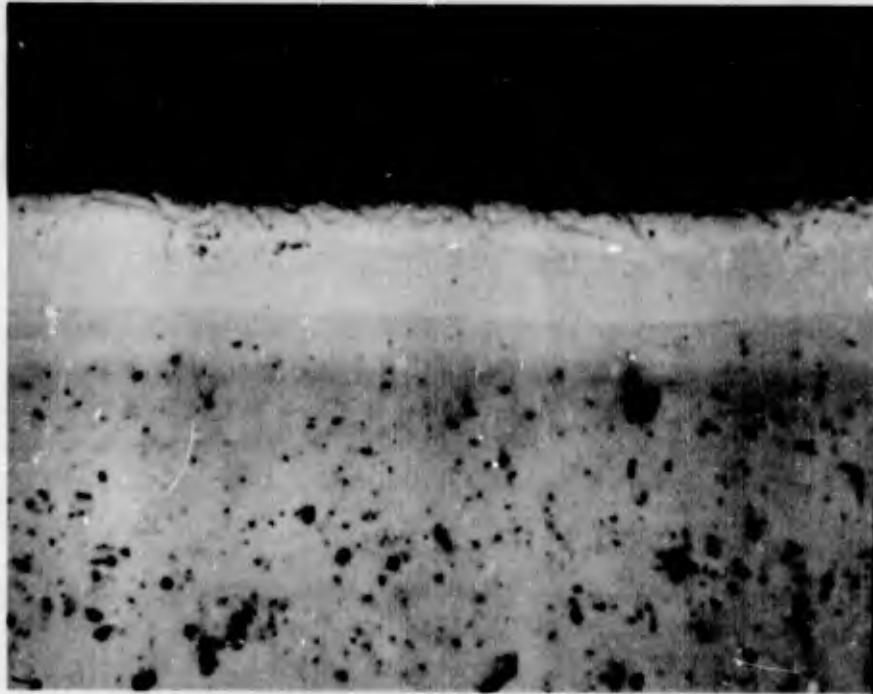
As an alternate coating method, vacuum codeposition of an NiCr coating was investigated through static oxidation tests only. Coatings which ranged from 0.4 to 1.2 mils in thickness were produced. Evaporation of the 80Ni-20Cr source material was accomplished with an electron gun at a vacuum level of 10^{-6} mm of mercury. A 0.2-mil/hour deposition rate was established with the specimen substrate heated to 1150°F to promote adherence and bonding of the coating. It is reasonable to assume that the coating deposit composition deviated somewhat from the source composition, which was 80 parts nickel and 20 parts chromium. The as-deposited coatings were developed further by heat treatment in argon at 1800°F for a period of 2 hours. Metallographic examination revealed good bonding and no stratification of the nickel and chromium constituents (Figure 76).

3.5.8 NiPt/Cb-132M

Combinations of nickel, platinum, and rhodium metal were applied to Cb-132M alloy specimens utilizing several application combinations. After preliminary coating trials, a nickel-platinum coating was selected for blade root screening evaluation. In addition an alternate coating, a platinum-rhodium combination, was investigated in the static oxidation testing only.

The coating application procedure for the NiPt coating was as follows: After cleaning, the specimens were plated with a 0.6- to 1.0-mil-thick layer of nickel. On this nickel layer a platinum resonant coating film (proprietary product of Englehard Industries) was slurry applied and developed to a final 0.5 mil in thickness by baking for 5 minutes at 600°F. The coating was diffused in a 1-hour, 1800°F vacuum heat treatment cycle. The resultant 2.5-mil-thick coating was dense and uniform in appearance with excellent coverage of specimen corner and edge surfaces.

The PtRh coating was applied by flash plating a thin layer of nickel and a 2.5-mil-thick layer of platinum on the test specimens following a cleaning process. A 0.1-mil-thick rhodium layer was then vapor plated from rhodium acetylacetonate vapor at 485°F with the specimen surface heated at 600°F. As an outer coating layer,



UNETCHED

MAG: 1000X

Figure 76. Typical Microstructure of the Vacuum-Deposited NiCr Coating on Cb-132M Alloy

a 0.25- to 0.5-mil-thick layer of platinum coating was developed at 600°F from a platinum resonate solution. Metallographic examination revealed an extremely irregular coating surface and coating substrate interface (Figure 77). Coverage of specimen surfaces appeared good, however.

3.6 EVALUATION TESTING, LOW-TEMPERATURE SYSTEMS

Three tests which simulate the bearing and shear loads and thermal environment experienced by the turbine blade root were utilized in the preliminary screening tests. These tests consisted of static oxidation testing at 1300° and 1600°F, prestrain/oxidation at 70° and 1300°F, and wear-galling at 1300°F. All testing was performed in air.

3.6.1 Static Oxidation Test Procedure and Results

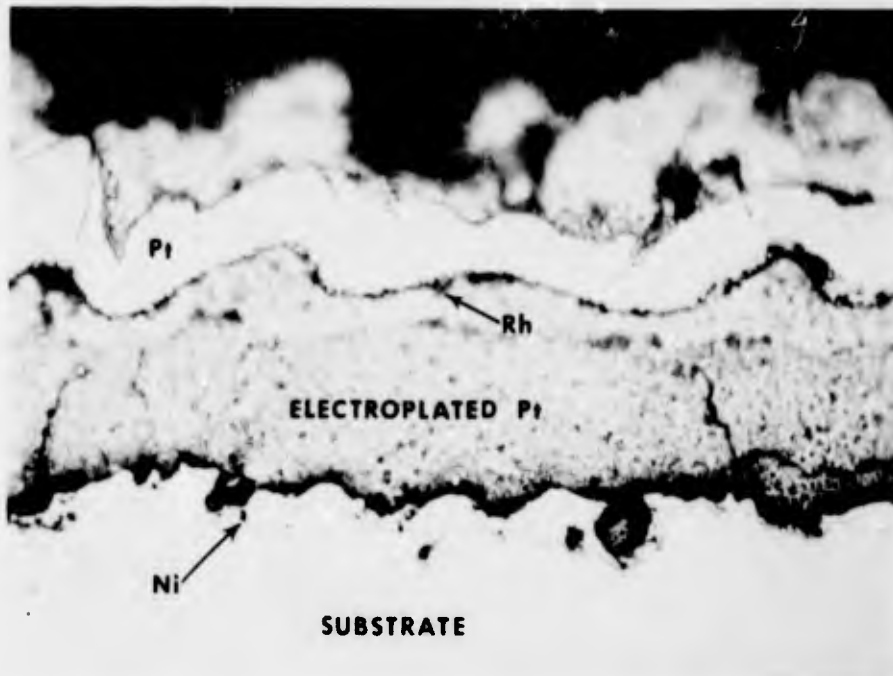
The static oxidation tests at 1300° and 1600°F were performed on coated coupons. Three specimens were exposed at each temperature, with inspection and weight change data recorded after 1, 2, 4, 8, 16, and 24 hours and after each subsequent 20- to 24-hour period. Temperature was monitored continuously and controlled automatically during specimen exposures.

Oxidation test results at both 1300° and 1600°F for the eight primary coating-substrate systems (plus two alternate systems) are presented in Table IX. In summary, the performance of the Sylvania SiCrV and SiCrFe coatings at both 1300° and 1600°F was good. Although one edge failure occurred at 1300°F for the Sylvania SiCrV/Cb-132M system after 216 hours, the remaining Sylvania SiCrV and SiCrFe coated test specimens were in excellent condition after 400 hours of exposure.

Performance of the TRW TiCr, TiAl, TiCr-Al, and TiCr-Si coatings was highly dependent upon composition and temperature. Although no 1300°F oxidation failures occurred for the TRW TiCr/Cb-132M system after 400 hours, all of the specimens exposed at 1600°F failed after 54 test hours. Failure resulted from localized substrate oxidation at numerous surface locations and appeared to be independent of any surface features (Figure 78). Metallography revealed extensive coating heterogeneity (Figure 79) which differed considerably from that observed for the as-coated specimens (refer to Figure 73).

No 1300° or 1600°F failures were noted for the TRW TiAl/Cb-132M system after 400 hours. Metallographic examination of the coating after 1600°F testing revealed good coating continuity, particularly near the coating-substrate interface, and no surface crack penetration to the substrate (Figure 80). Extensive intergranular and intragranular precipitation occurred during exposure within a region extending into the substrate for approximately 1.0 mil (see Figure 80).

The 1600°F failures for the TRW TiCr-Al coating were confined to corners and edges. In other areas, however, the specimen surfaces were rough and appeared nonhomogeneous (Figure 81). No failures occurred after 400 hours at 1300°F.



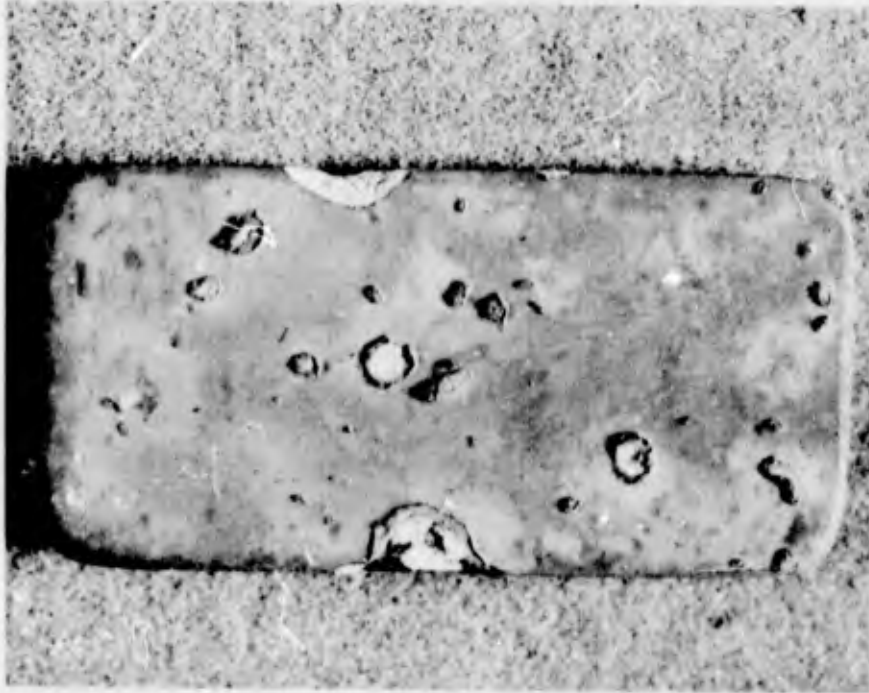
UNETCHED

MAG: 500X

Figure 77. Microstructure of the PtRh Coating on Cb-132M Alloy

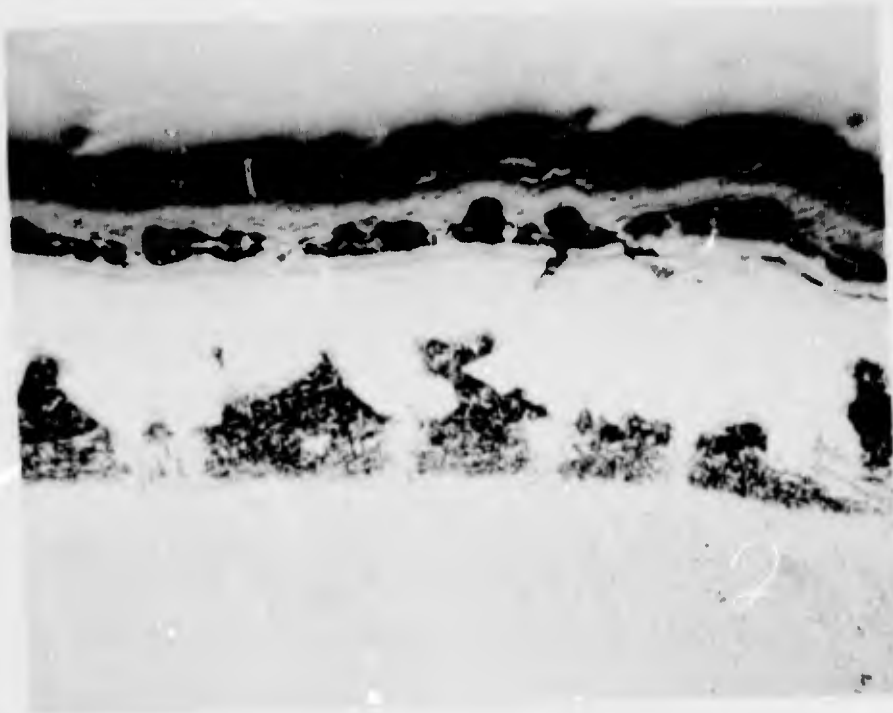
TABLE IX
RESULTS OF STATIC OXIDATION TESTING OF
PHASE V TURBINE BLADE ROOT SYSTEMS

Coating	Temperature (°F)	Test Results
Sylvania SiCrV slurry	1300	Edge failure at 216 hours; no failures on remaining two specimens after 400 hours; test stopped
	1600	No failures after 400 hours; test stopped
Sylvania SiCrFe slurry	1300	No failures after 400 hours; test stopped
	1600	No failures after 400 hours; test stopped
TRW TiAl (vacuum) pack	1300	No failures after 400 hours; test stopped
	1600	No failures after 400 hours; test stopped
TRW TiCr (vacuum) pack	1300	No failures after 400 hours; test stopped
	1600	Three specimens failed after 54 hours
TRW TiCr-Al (vacuum) pack	1300	No failures after 400 hours; test stopped
	1600	Edge or corner failures after 54, 333, and 339 hours
TRW TiCr-Si (vacuum) pack	1300	Surface failure after 3 hours; no failures on remaining two specimens after 400 hours; test stopped
	1600	Edge failures after 175 and 255 hours; no failure on one remaining specimen after 400 hours; test stopped
Electroplated NiCr	1300	Surface failure after 8 hours; no failures on remaining two specimens after 248 hours; test stopped
	1600	Surface failures after 4, 8, and 37 hours
Vacuum Deposited NiCr	1300	Surface failures after 5 hours
NiPt	1300	No failures after 290 hours; test stopped
	1600	Surface failures after 3, 3, and 8 hours
PtRh	1300	Failure for one specimen after 8 hours (only specimen exposed)
	1600	Failure for one specimen after 1 hour (only specimen exposed)



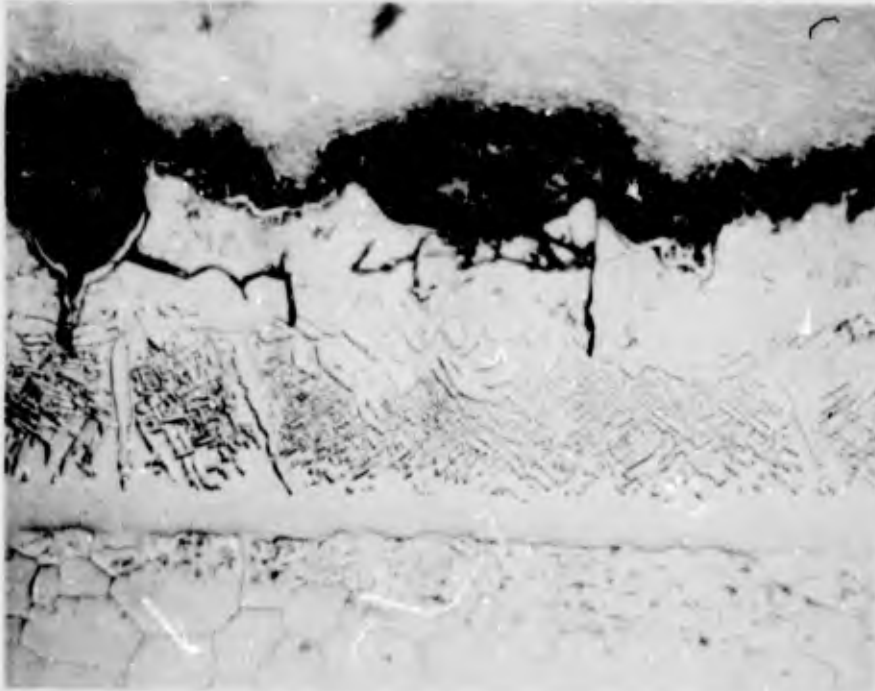
MAG: 4X

Figure 78. TRW TiCr (Vacuum) Pack Coated Cb-132M Alloy Test Specimen Showing Typical Localized Failures After 54 Hours Static Oxidation Exposure at 1600°F



ETCH: 20% HYDROFLUORIC ACID, 20% NITRIC ACID, 60% WATER MAG: 500 X

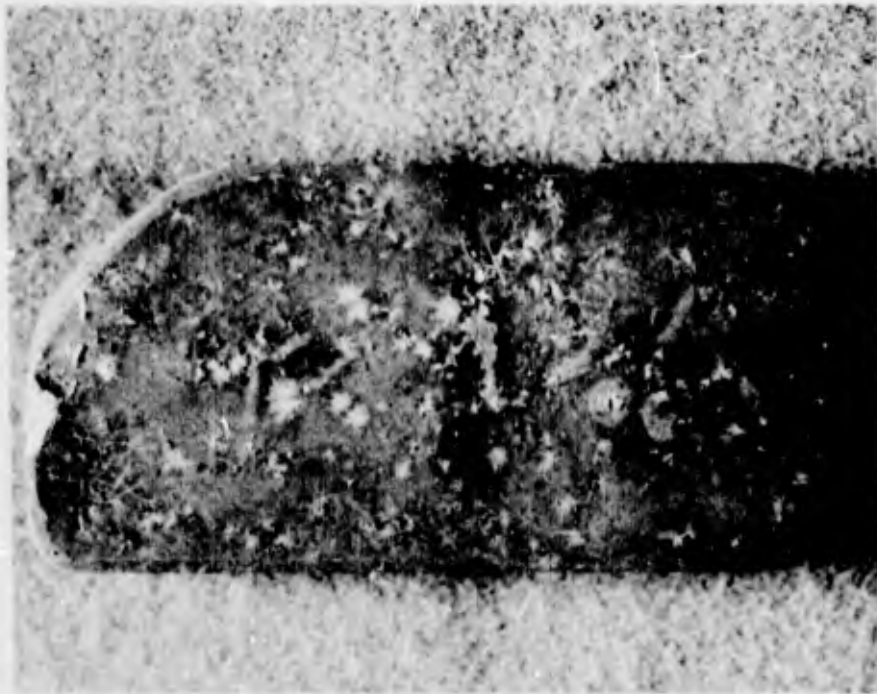
Figure 79. Microstructure of TRW TiCr (Vacuum) Pack Coated Cb-132M Alloy After 54 Hours Static Oxidation Exposure at 1600°F



ETCH: 20% HYDROFLUORIC ACID, 20% NITRIC ACID, 60% WATER MAG: 500X

Figure 80. Typical Microstructure of TRW TiAl (Vacuum) Pack Coated
Cb-132M Alloy After 400 Hours Oxidation Exposure at 1600°F

Note precipitation in substrate region immediately beneath the coating.



MAG: 4X

Figure 81. TRW TiCr-Al (Vacuum) Pack Coated Cb-132M Alloy Specimen Showing Edge Failure After 54 Hours Oxidation Exposure at 1600°F

Performance of the TRW TiCr-Si/Cb-132M system was erratic, with single failures occurring at both 1300° and 1600°F. At each temperature, no failures were observed for the remaining specimens after 400 hours. Failure was generally confined to the edges (Figure 82).

Failure of the electroplated NiCr coatings followed a distinct pattern. Where oxygen had apparently penetrated the NiCr coating layers, continued substrate oxidation buckled the surrounding coating extensively (Figure 83). Failures initially occurred along specimen edges. Metallographic examination of intact coating regions revealed extensive diffusion, coating separation, and oxide formations beneath the outer NiCr layers (Figure 84). In contrast, the vacuum deposited NiCr coating failed only by localized oxidation. Both the NiPt and the PtRh coatings failed by localized oxidation, principally at specimen edges. At failure, oxygen had apparently penetrated the coating and led to the formation of surface irregularities by substrate oxidation (Figure 85). Areas away from the failure points remained in good condition. Very good coating homogeneity was noted metallographically for the NiPt coating, which did not fail after 290 hours at 1300°F (Figure 86).

3.6.2 Prestrain/Oxidation Test Procedure and Results

Prestrain testing was performed to determine (1) whether the coating and/or coating application process led to substrate embrittlement and (2) whether the coating possessed an elastic-plastic strain capability while maintaining oxidation protection. Prestraining at 1300°F followed by static oxidation exposure at 1300°F and metallographic examination were used to evaluate these factors. A 2.0- to 4.0-percent elastic-plastic prestrain at 1300°F was desired.

Three uncoated Cb-132M alloy specimens of the configuration shown in Figure 87 were first tensile tested at room temperature to establish the low-temperature ductility of the alloy. Results of these tests are presented in Table X (test numbers 1 through 3).

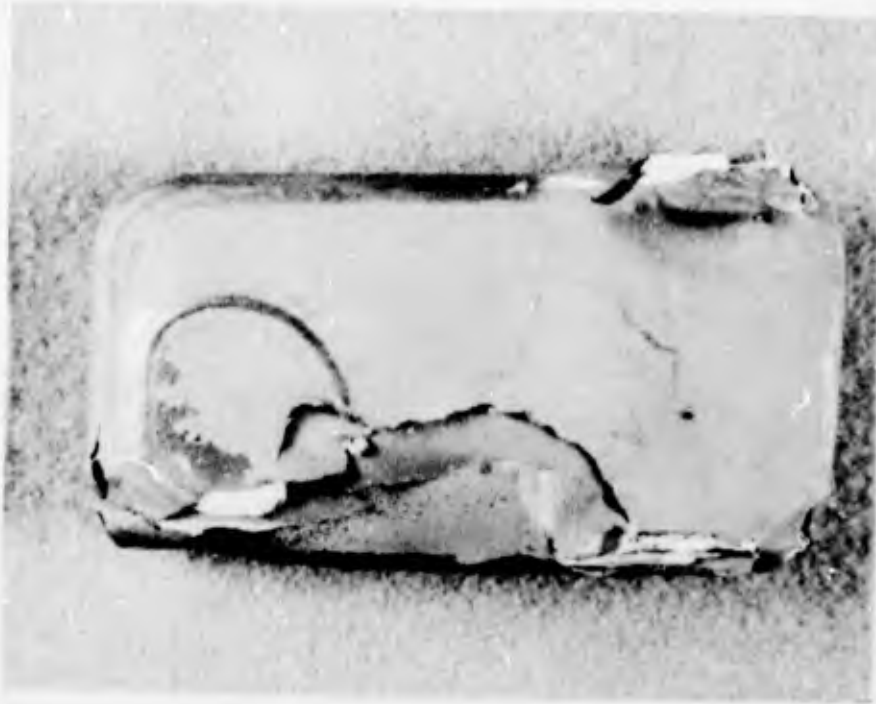
The coated test specimens were aligned and placed under a nominal load during the furnace heating cycle to 1300°F. After a 30-minute stabilization period, the tensile load was applied at a strain rate of 0.005 inch per inch per minute.

The tensile test results for the eight coating-substrate systems are presented in Table X. In all cases, failure occurred in a brittle fashion. In some cases, 70°F tensile tests were performed on the second specimen representing each system to compare properties to those exhibited by the uncoated alloy.



MAG: 4X

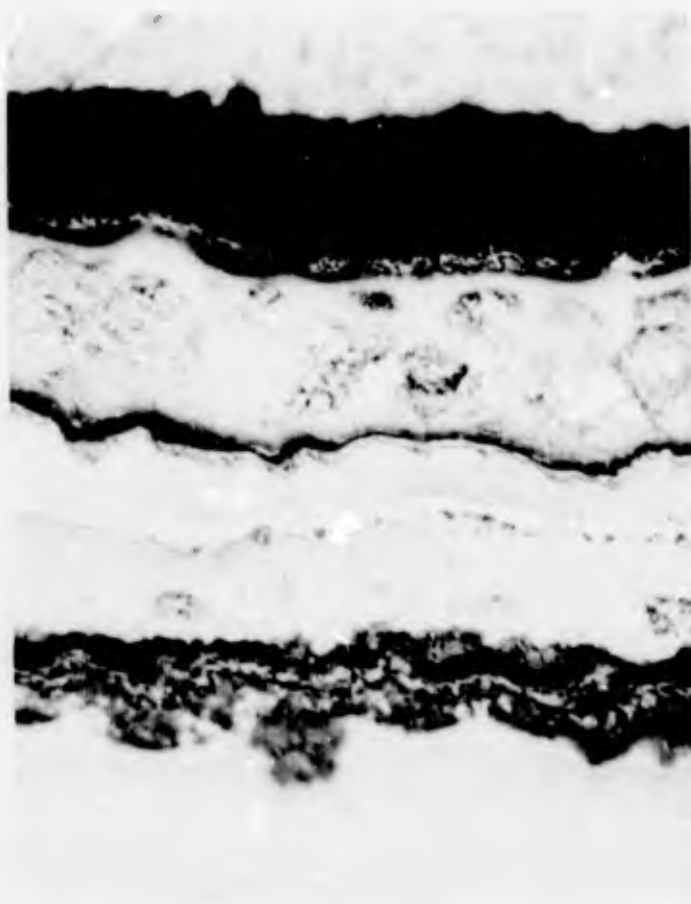
Figure 82. TRW TiCr-Si (Vacuum) Pack Coated Cb-132M Alloy Specimen Showing Typical Edge Failure After 175 Hours Oxidation Exposure at 1600°F



MAG: 4X

Figure 83. Electroplated NiCr Coated Cb-132M Alloy Specimen Showing Typical Coating Failure After 8 Hours Oxidation Exposure at 1600°F

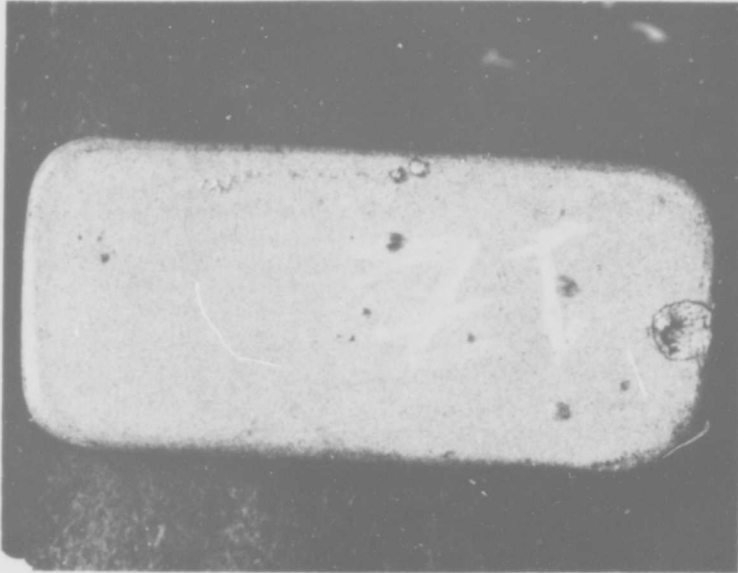
Note undermining and rupture of intact coating regions.



ETCH: 50% NITRIC ACID, 50% ACETIC ACID

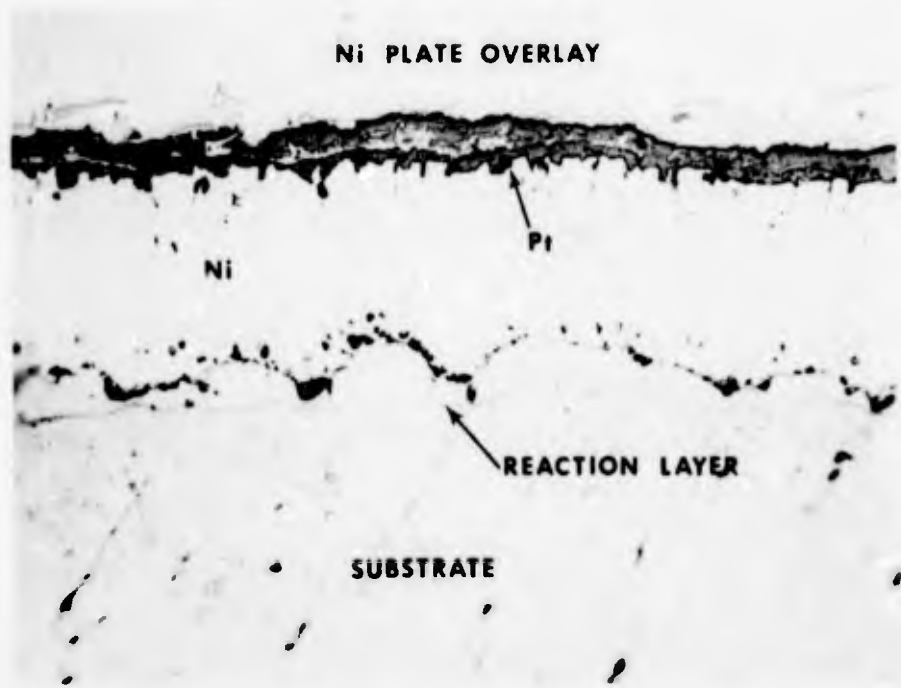
MAG: 500X

Figure 84. Microstructure of Electroplated NiCr Coated Cb-132M Alloy Showing Coating Separation and Oxide Formation at the Coating-Substrate Interface



MAG: 4X

Figure 85. PtRh Coated Cb-132M Alloy Specimen After 8 Hours Oxidation Exposure at 1300°F



UNETCHED

MAG: 500X

Figure 86. Typical Microstructure of the NiPt Coated Cb-132M Alloy After 290 Hours Oxidation Exposure at 1300°F With No Failure

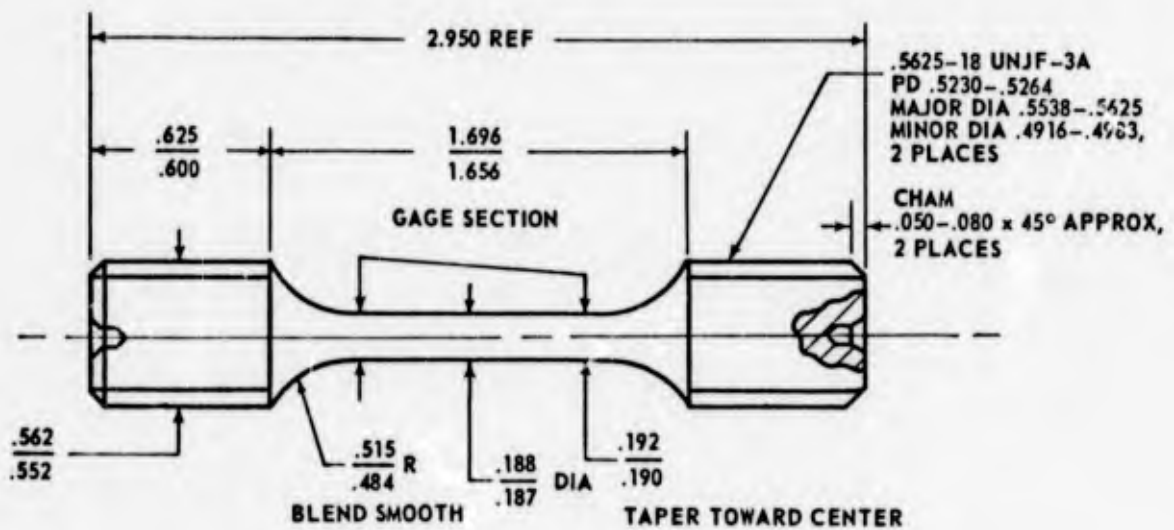


Figure 87. Tensile Specimen Configuration Used for Prestrain/Oxidation Tests

TABLE X

RESULTS OF PRESTRAIN/OXIDATION TESTING OF PHASE V Cb-132M ALLOY BLADE ROOT TEST SPECIMENS

Test No.	Coating	Specimen No.	Prestrain Temperature (°F)	Proportional Limit (psi)	0.2 Yield Strength (psi)	Ultimate Tensile Strength (psi)	Total Strain		Remarks
							Elastic (percent)	Plastic (percent)	
1	Uncoated ¹	Std-1	70	---	127,200	142,000	0.48	2.94	
2	Uncoated ¹	Std-2	70	---	133,500	141,900	0.42	0.80	
3	Uncoated ²	Std-3	70	---	120,600	129,800	0.43	5.0	
4	Sylvania SiCrV	SCV-1	1300	---	---	60,300	---	---	Failed in the elastic region
5	Sylvania SiCrV	SCV-2	70	---	---	76,000	---	---	Failed in the elastic region
6	Sylvania SiCrFe	SCF-1	1300	46,400	60,900	67,300	0.29	1.4	Brittle fracture
7	Sylvania SiCrFe	SCF-2	1300	18,000	57,200	63,300	0.21	1.02	Brittle fracture
8	TRW TiAl	TA-1	1300	---	---	82,100	---	---	Failed in the elastic region
9	TRW TiAl	TA-2	70	109,300	122,700	132,200	0.43	0.92	Brittle fracture within gage area
10	TRW TiCr	TC-1	1300	---	---	---	---	---	Failed on loading
11	TRW TiCr	TC-2	70	---	---	43,700	---	---	Failed in the elastic region
12	TRW TiCr-Al	TCA-1	1300	---	---	---	---	---	Failed on loading
13	TRW TiCr-Al	TCA-2	70	---	---	43,700	---	---	Failed in the elastic region
14	TRW TiCr-S	TCS-1	1300	45,400	51,000	59,300	0.29	0.41	Brittle failure
15	TRW TiCr-S	TCS-2	70	---	---	61,200	---	---	Failed in the elastic region
16	Electroplated NiCr	NC-1	1300	---	59,800	95,000	0.28	2.3	Brittle fracture
17	Electroplated NiCr	NC-2	1300	---	63,600	84,500	0.33	1.4	Brittle fracture
18	NiPt	NP-1	1300	---	57,700	79,300	0.26	1.9	Brittle fracture
19	NiPt	NP-2	1300	---	60,600	68,400	0.25	2.2	Brittle fracture

1. As extruded

2. Heat treated in vacuum for 1 hour at 2900°F

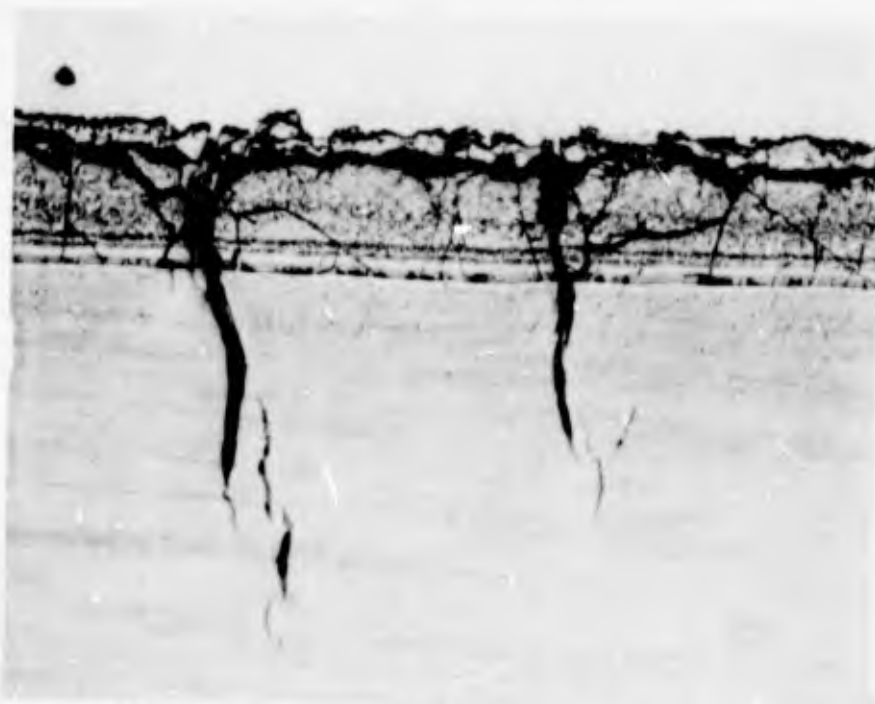
Failure of the test specimens complicated considerably the task of comparing performance of the individual systems. Comparison of the tensile data in Table X and metallographic examination of the failed specimen gage sections resulted in the following conclusions.

- The Sylvania SiCrV coating or coating application process led to specimen embrittlement, as evidenced by both test specimens failing in the elastic region.
- Although the tensile strain data were relatively good for the Sylvania SiCrFe coating, metallographic examination of specimen gage sections after failure revealed numerous cracks originating at the coating surface and extending into the substrate (Figure 88).
- One of the TRW TiAl coated tensile specimens failed in the elastic region. A second specimen tested at 70°F, however, developed plastic strain. Metallographic examination of the gage section showed some coating cracks (Figure 89), but more extensive cracking at the center of the specimen diameter suggests that the coating may not be responsible for the tensile failure.
- The TRW TiCr and TiCr-Al coatings resulted in severe embrittlement. However, metallographic examination suggests that cracks did not originate in the coating (Figure 90).
- The prestrain performance of the electroplated NiCr coating and the NiPt coating on Cb-132M alloy was reasonably good, with no evidence of cracks propagating from the coating-substrate interface.

3.6.3 Wear-Galling Test Procedure and Results

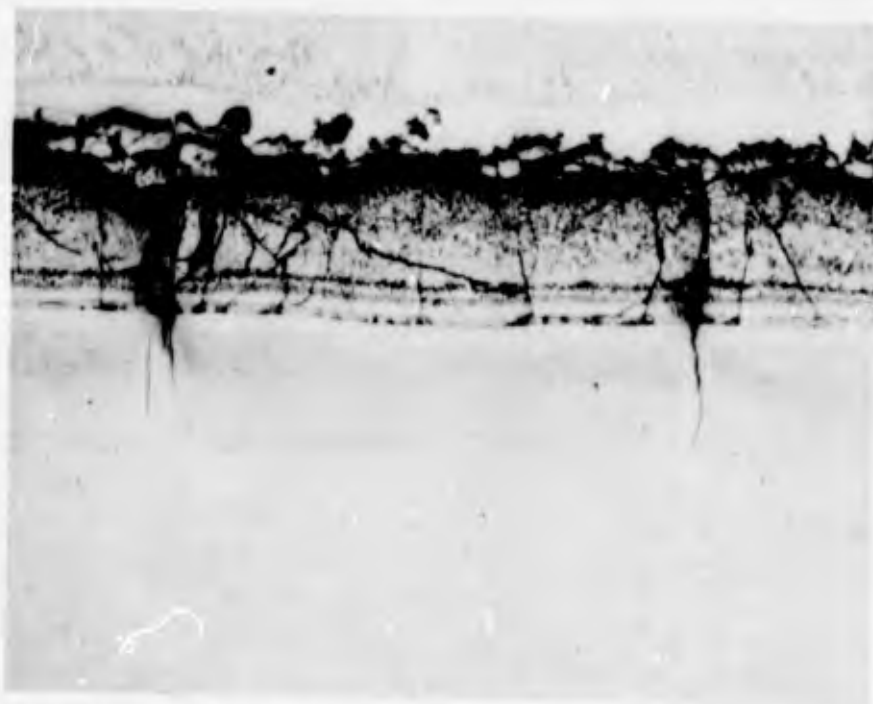
To simulate the vibratory and bearing loads experienced by blade root sections during operation, wear-galling tests were initiated using the dovetail-type specimen configuration presented in Figure 91. During testing, the specimens were held at 1300°F, loaded against a mating surface of PWA 1007 (Waspaloy) nickel-base turbine disk alloy, subjected to a tensile stress of 30,000 psi and a vibratory deflection of 0.007 inch at the specimen end opposite the mating surfaces (this corresponds to a 0.0003-inch total transverse rubbing action at the contact area between the blade root coating and the disk alloy). The tensile stress was calculated based on the cross-sectional area at the specimen shank (see Figure 91). A vibration frequency of 3600 cycles per minute was used with a 500,000-cycle maximum test period. In cases where specimen failure occurred as a result of the 30,000-psi tensile load, a coated second specimen was tested using a constant tensile stress of 20,000 psi.

Wear-galling test results for the eight coating-substrate systems are presented in Table XI. Specimen characteristics and a brief performance summary of the systems are discussed in the following paragraphs.



ETCH: 33% HYDROFLUORIC ACID, 33% NITRIC ACID, 33% WATER

MAG: 150X



ETCH: 33% HYDROFLUORIC ACID, 33% NITRIC ACID, 33% WATER

MAG: 200X

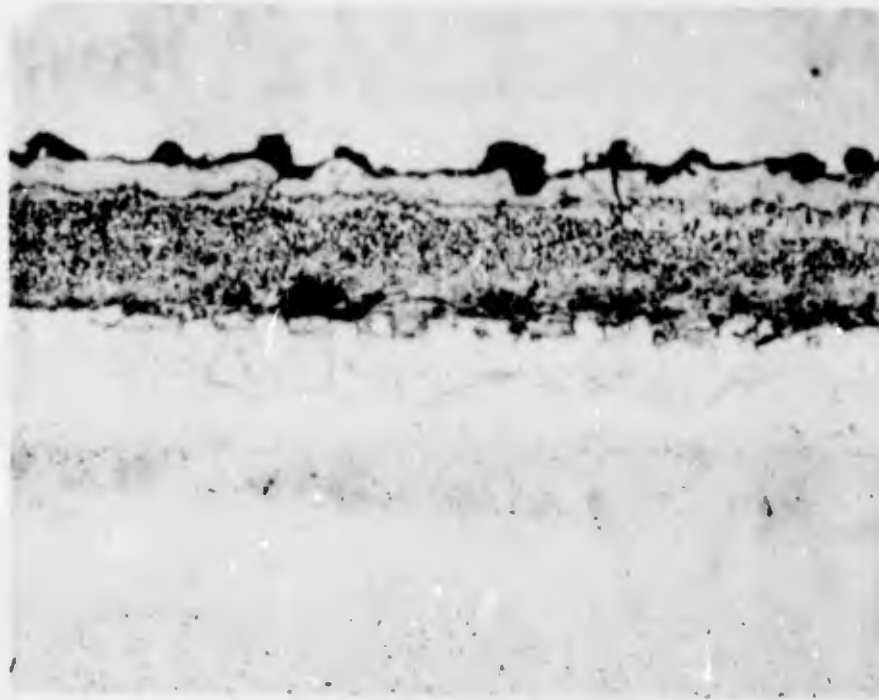
Figure 88. Typical Microstructure of Sylvania SiCrFe Slurry Coated Cb-132M Alloy After Tensile Testing in Air at 1300°F



ETCH: 20% HYDROFLUORIC ACID, 20% NITRIC ACID, 60% WATER MAG: 500X

Figure 89. Microstructure of TRW TiAl (Vacuum) Pack Coated Cb-132M Alloy After Tensile Failure at 70°F

No other areas contained coating cracks extending into the substrate.

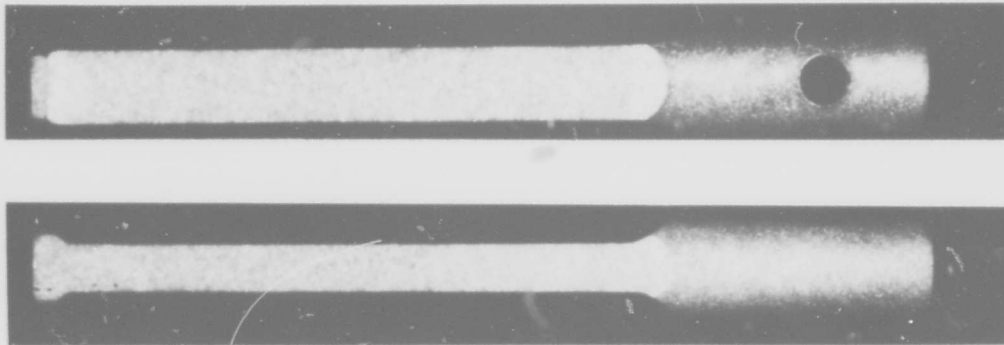


ETCH: 20% HYDROFLUORIC ACID, 20% NITRIC ACID, 60% WATER

MAG: 500X

Figure 90. Typical Microstructure of TRW TiCr-Al (Vacuum) Pack Coated Cb-132M Alloy After Tensile Testing at 70°F

Note absence of crack penetration from the coating into the substrate.



TYPICAL AS-COATED TEST SPECIMEN

MAG: APPROX. 1.2X

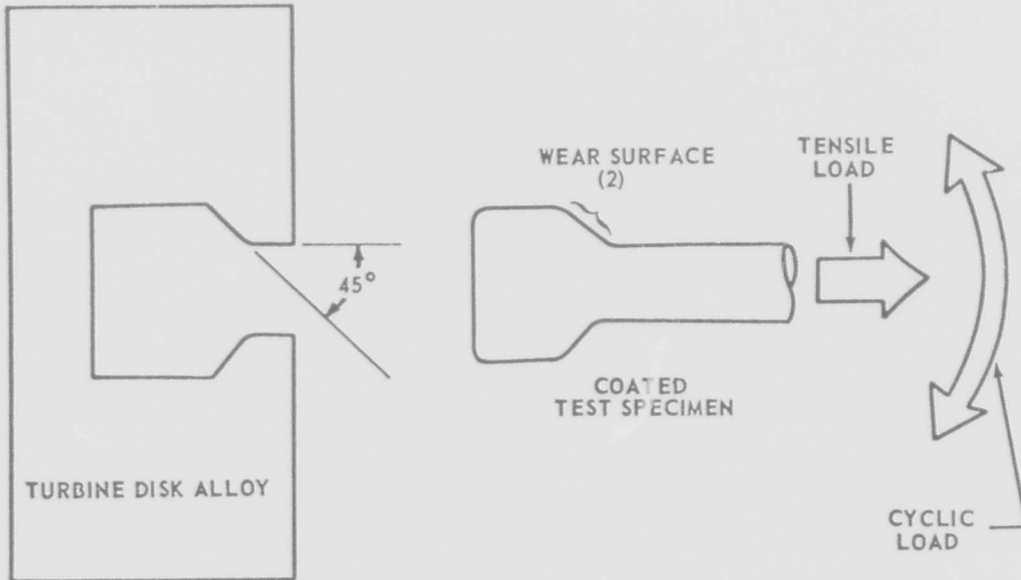


Figure 91. Dovetail Specimen Configuration Used for Wear-Galling Test

TABLE XI

**RESULTS OF WEAR-GALLING TESTING OF PHASE V COATED
Cb-132M ALLOY BLADE ROOT TEST SPECIMENS AT 1300°F**

Rubbing surface: PWA 1007 (Waspaloy) nickel-base turbine disk alloy
 Vibratory deflection: 0.007 inch (0.0003 inch total transverse rubbing
 distance at the coating-alloy contact area)
 Specimen vibration frequency: 3600 cycles per minute
 Inspection interval: 100,000 cycles

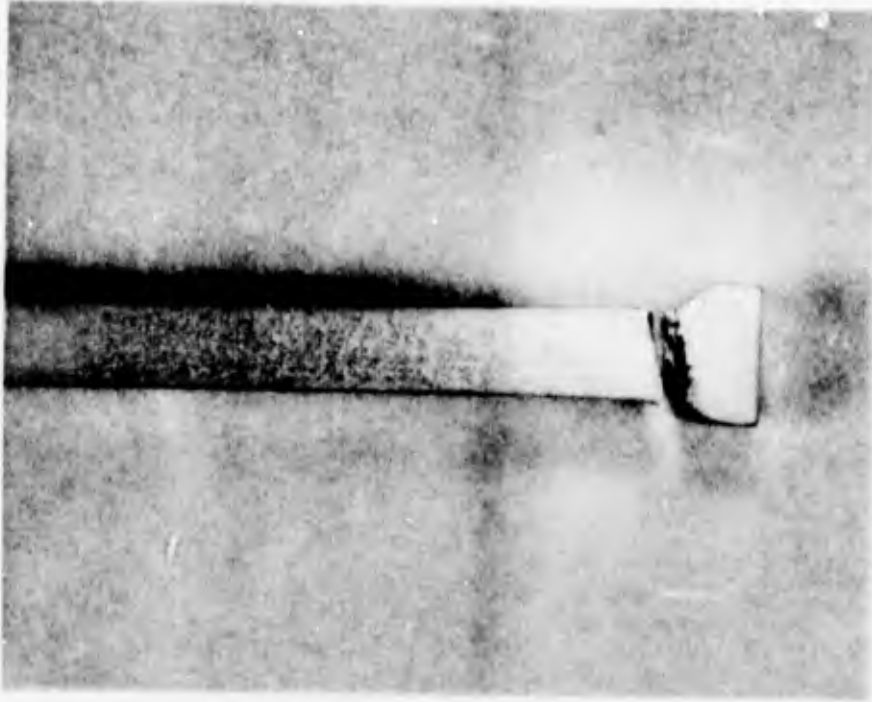
Test No.	Coating	Specimen No.	Tensile Load (psi)	No. of Test Cycles	Test Results
1	Sylvania SiCrV	SCV-1	30,000	---	Specimen failed in handle on application of tensile load
2	Sylvania SiCrV	SCV-2	30,000	104,000	Fracture occurred at dovetail neck; very little wear and no galling was noted
3	Sylvania SiCrFe	SCF-1	30,000	---	Fracture occurred in handle on loading
4	Sylvania SiCrFe	SCF-2	30,000	97,000	Fracture occurred in dovetail neck; the coating was in good condition with very little wear and no galling
5	TRW TiAl	TA-1	30,000	249,000	Fracture occurred in dovetail neck; the coating was in good condition with little wear and no galling
6	TRW TiAl	TA-2	20,000	500,000	Test was stopped; no apparent wear or galling of the coating was noted
7	TRW TiCr	TC-1	30,000	---	Fracture occurred in dovetail neck on loading
8	TRW TiCr	TC-2	20,000	---	Fracture occurred in handle on loading
9	TRW TiCr-Al	TCA-1	30,000	28,000	Fracture occurred in dovetail neck; no wear or galling was noted
10	TRW TiCr-Al	TCA-2	20,000	100,000	Fracture occurred in handle; very little wear and no galling was noted
11	TRW TiCr-Si	TCS-1	30,000	---	Fracture occurred in dovetail neck on loading
12	TRW TiCr-Si	TCS-2	20,000	500,000	Test was stopped; very little wear and no galling was noted
13	Electroplated NiCr	NC-1	30,000	500,000	Test was stopped; very little wear and no galling was noted
14	Electroplated NiCr	NC-2	30,000	500,000	Test was stopped; very little wear or galling was noted
15	NiPt	NP-1	30,000	500,000	Test was stopped; little wear or galling was noted
16	NiPt	NP-2	30,000	500,000	Test was stopped; very little wear and no galling was noted

The wear-galling performance of the Sylvania SiCrV and SiCrFe slurry coatings was reasonably good in that the contact surfaces were in good condition after testing. One specimen from each coating-substrate system failed in the handle region of the specimen on application of the tensile load. These failures were probably due to slight specimen misalignment which led to high local stresses at specimen corners. This slight misalignment was within the plane of vibration. After realignment and recalibration of the testing apparatus, a second specimen from each system was tested. Specimen failure occurred in the dovetail neck section of the specimens after 104,000 cycles for the Sylvania SiCrV coating and 97,000 cycles for the Sylvania SiCrFe coating (Figure 92). The fracture surfaces were brittle in appearance (Figure 93), and for both coatings the contact areas showed very little wear and no galling (Figure 94).

Tensile loads of both 30,000 psi and 20,000 psi were used for testing the TRW TiCr, TiAl, TiCr-Al, and TiCr-Si coatings. At 30,000 psi, the specimens failed either during tensile loading or during initial stages of testing, except for the TRW TiAl/Cb-132M specimen, which failed in the dovetail neck after 249,000 cycles. Results of further 1300°F testing utilizing a 20,000-psi tensile stress indicate that the TRW TiAl and TiCr-Si coatings performed best. Specimen failure was not observed for either coating after 500,000 cycles. All of the TRW coatings exhibited good resistance to wear with no coating galling. The TiAl (vacuum) pack coating ranked as the best TRW coating system evaluated. Although some coating flow was observed on the wear surfaces (Figure 95), the TiAl specimen contact area after testing was in good condition.

Both the electroplated NiCr/Cb-132M and NiPt/Cb-132M systems performed very well in the wear-galling tests. Very little coating wear, no galling, and no specimen failures after 500,000 cycles were observed for either system using a tensile load of 30,000 psi. Of the eight coatings evaluated, these were the only two coatings for which there were no specimen failures using the higher tensile stress level. This performance is attributed to the higher ductility of the coatings and the absence of detrimental conditions during the coating application processes. The wear surfaces of the NiCr coated specimens were particularly good after testing (Figure 96).

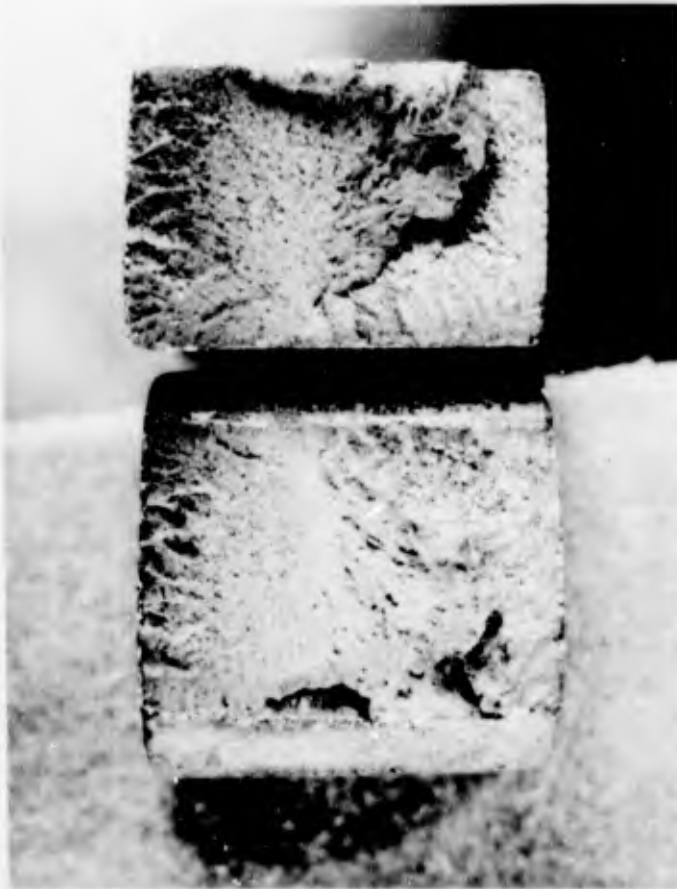
In those systems where performance was good, close examination of the wear surfaces at the 100,000-cycle inspection intervals revealed that misalignment normal to the plane of vibration was possibly occurring during testing. This condition, if present, could cause the slightly uneven wear of the coatings (see Figures 94 through 96) and contribute significantly to fracture of the specimens in the dovetail neck sections. Recalibration of the testing apparatus failed to establish the cause of this misalignment, but alignment adjustments were made, when necessary, at the 100,000-cycle inspection periods. Comparisons of the number of cycles to failure, the amount of tensile load, and the types of specimen failure (where present) for the eight coating-substrate combinations indicate qualitative correlation between these wear-galling results and the tensile prestrain test results (refer to Tables X and XI). These



MAG: 1.9X

Figure 92. Sylvania SiCrFe Slurry Coated Cb-132M Alloy Wear-Galling Specimen Showing Failure Within Dovetail Radius Area After 97,000 Cycles at 1300°F

Tensile stress was 30,000 psi with 0.007 inch deflection.



MAG: 5.5X

Figure 93. Fracture Surface of Failed Sylvania SiCrFe Slurry Coated Cb-132M Alloy Wear-Galling Specimen After 97,000 Cycles at 1300°F and a Tensile Stress of 30,000 Psi

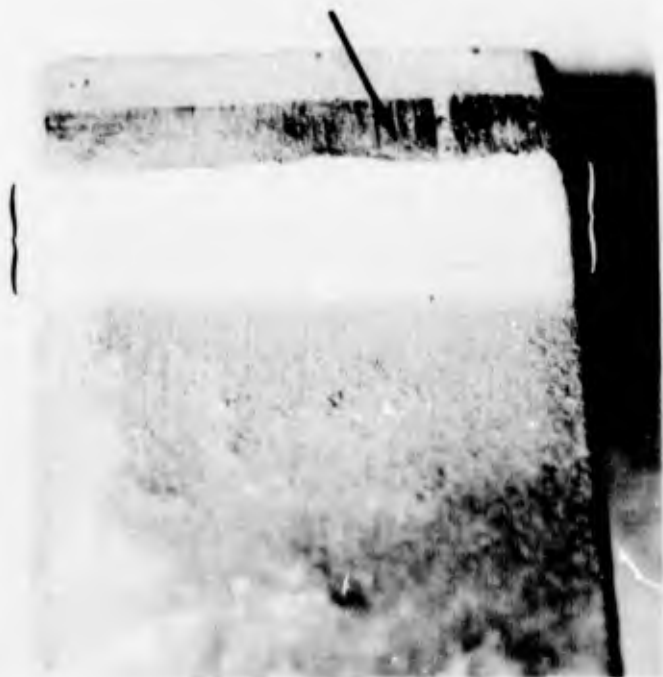
Surface indicates brittle fracture.



MAG: 10X

Figure 94. Sylvania SiCrFe Slurry Coated Cb-132M Alloy Wear-Galling Specimen Showing Wear Surface (Brackets) After 97,000 Cycles at 1300°F and a Tensile Stress of 30,000 Psi

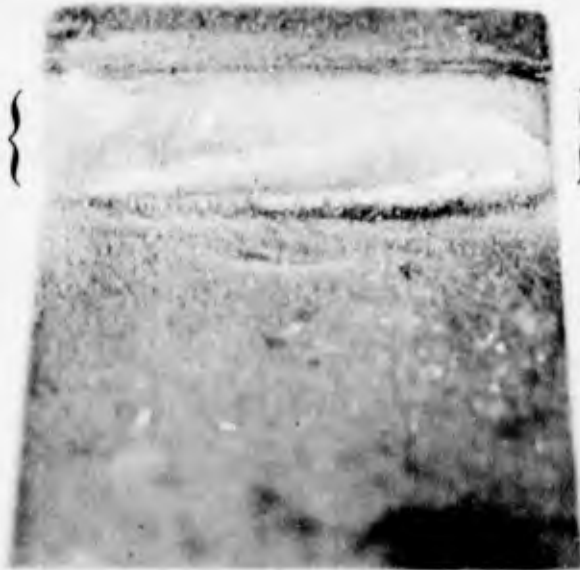
Note absence of distress in contact area.



MAG: 7X

Figure 95. TRW TiAl (Vacuum) Pack Coated Cb-132M Alloy Wear-Galling Specimen Showing Wear Surface (Brackets) After 500,000 Cycles at 1300°F and a Tensile Stress of 20,000 Psi

Note coating flow over dovetail lip (arrow).



MAG: 7X

Figure 96. Electroplated NiCr Coated Cb-132M Alloy Wear-Galling Specimen Showing Wear Surface (Brackets) After 500,000 Cycles at 1300°F and a Tensile Stress of 30,000 Psi

comparisons demonstrate that the coatings and/or coating application processes had a definite influence on fracture during the wear-galling tests.

3.7 PERFORMANCE COMPARISONS, LOW-TEMPERATURE SYSTEMS

In order to present more concisely the relative performance of the eight candidate blade root coatings, the tabulation below summarizes qualitatively the results of the Phase V screening tests for each coating. The performance of each coating, relative to the performance of the other coatings in the same test, was judged and assigned a letter: A (excellent) through E (poor).

<u>Coating</u>	<u>Oxidation Performance, 1300°F</u>	<u>Oxidation Performance, 1600°F</u>	<u>Prestrain Performance, 70° and 1300°F</u>	<u>Wear- Galling Performance</u>
Sylvania SiCrV	B	A	D	C
Sylvania SiCrFe	A	A	C	C
TRW TiAl	A	A	B	B
TRW TiCr	A	E	E	E
TRW TiCr-Al	A	D	E	C
TRW TiCr-Si	B	C	C	C
Electroplated NiCr	C	E	A	A
NiPt	C	E	B	A

The above presentation indicates that the best overall performance was demonstrated by the TRW TiAl, the Sylvania SiCrFe, and the NiCr coatings. Since the primary goal of this program is to evaluate coatings for the protection of columbium alloys from oxidation, greater importance may be attached to the 1300° and 1600°F oxidation test results. In oxidation testing the performance of the Sylvania SiCrV coating was very good, while the performance of the NiCr and NiPt coatings was disappointing in this area. Failure of the NiCr and NiPt coatings appeared to result from improper coating application rather than from chemistry effects; that is, better processing technique would have resulted in greatly improved performance.

Some correlation was noted in the mechanical behavior of the systems in the prestrain and wear-galling tests. The wear-galling test results were apparently influenced by ductility of the coating-substrate composites, and, in this regard, the wear-galling performance of the NiCr and NiPt coated Cb-132M specimens was superior to that of the six other systems. The degree of wear and galling was not significant for any of the coatings.

4. ITEM 9

COATING IMPROVEMENT OF ADDITIONAL SYSTEMS

The work required in Item 9 of the contract is Phase VI of the evaluation program. This phase provides an opportunity to optimize coating-substrate composites for the appropriate applications. Candidate composites for Phase VI were the Sylvania SiCrTi/B-66 vane system and the TRW TiCr-Si/XB-88 and Solar V-CrTi-Si/Cb-132M blade airfoil systems. The Solar MoTi-Si (TNV-12SE4)/Cb-132M blade airfoil system and the eight Phase V blade root systems were not candidates for the Phase VI coating improvement portion of the program.

The results of the Phase V oxidation-erosion and thermal fatigue testing of the Solar V-CrTi-Si coated Cb-132M alloy were discussed with a Solar Division representative, who revealed that the application procedure for the V-CrTi-Si coating was not optimized and that the chief difficulty was one of processing rather than composition. Due to the poor Phase V performance of the coating, it was concluded that short term improvement by process modification was unlikely. In a discussion between the contractor and the Air Force Materials Laboratory Project Engineer it was decided that the Sylvania SiCrV slurry should be investigated as a further evaluation of the vanadium-modified silicide approach.

A technical flow chart showing the progression of composites through Phase VI is presented in Figure 97. The appropriate Phase V tests were conducted on Phase VI composites in order to verify optimization and to justify promotion to Phase VII advanced evaluation.

Systems evaluated in Phase VI are tabulated below.

<u>Application</u>	<u>Coating</u>	<u>Substrate Alloy</u>
Turbine vane	Modified Sylvania SiCrTi slurry	B-66
Turbine blade airfoil	Modified TRW TiCr-Si (vacuum) pack	XB-88
	Sylvania SiCrV slurry	Cb-132M

4.1 SUBSTRATE MATERIALS

Characteristics of the substrate alloys are described in Items 4 and 6, paragraph 2.1, Substrate Materials (Cb-132M) and Item 8, paragraph 3.1, Substrate Materials (B-66 and XB-88).

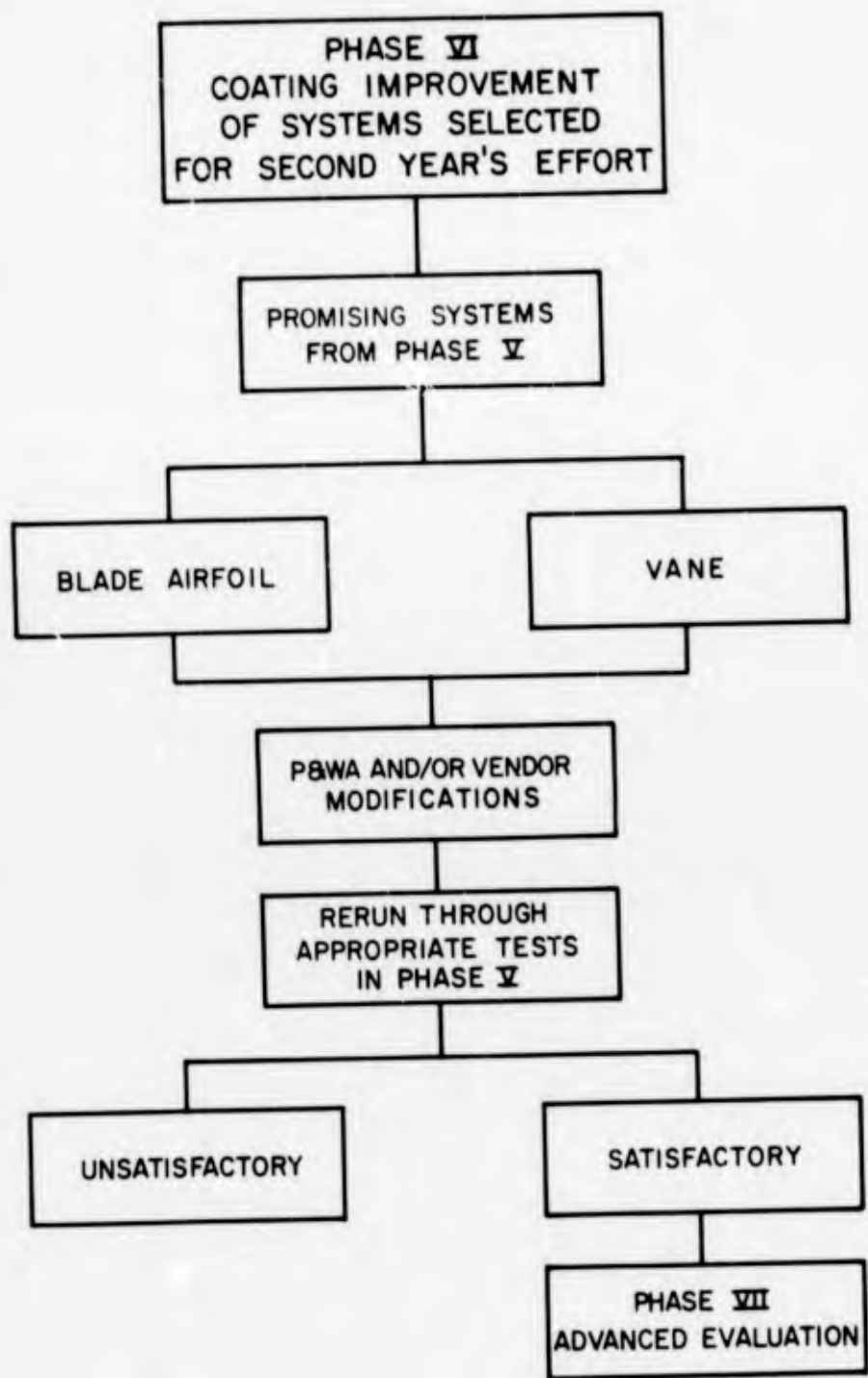


Figure 97. Flow Chart for Phase VI of Program (Item 9)

4.2 COATINGS APPLICATION

4.2.1 Modified Sylvania SiCrTi Slurry/B-66

During a meeting of the contractor with representatives of Sylvania, modification and retesting of the SiCrTi slurry coating on B-66 alloy was discussed. The Sylvania personnel revealed that the coating used in the Phase V (Item 8) evaluation was optimized to the best of their present ability from both compositional and processing standpoints and that improvements would require considerable development time. For this reason and because of the good oxidation-erosion performance of the Phase V coating, it was decided to increase the coating thickness from 2.5 mils to a thickness range between 3.5 and 5 mils. This modification to determine the effects of coating thickness on protective life was subsequently approved by the Air Force Materials Laboratory Project Engineer.

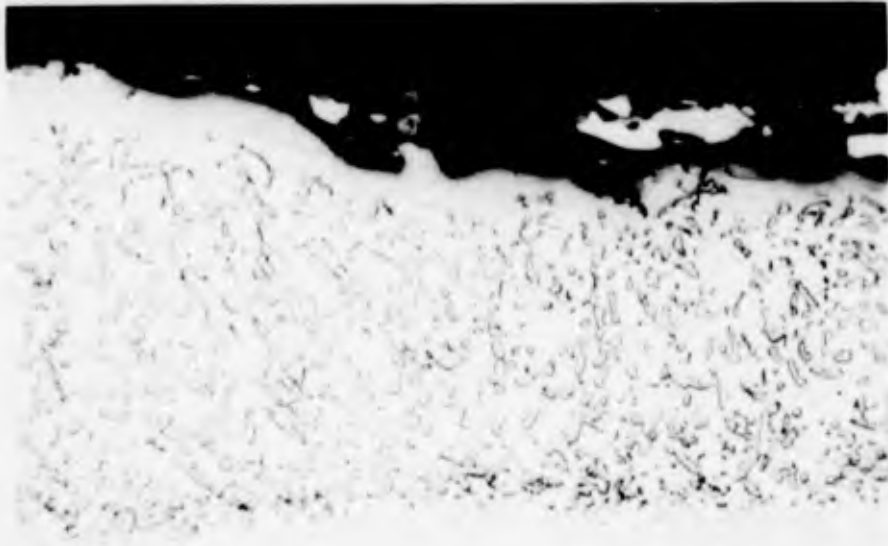
To eliminate oxidation between the handle butt plate and airfoil platform faying surfaces on thermal fatigue specimens, Sylvania suggested application of the coating in these areas by a vacuum dip technique.

Coating application was performed at Sylvania; the above proposed modification suggestions were followed. A Si-20Cr-5Ti and vehicle composition was sprayed and vacuum dip applied. The coating was developed at 2550°F for 1 hour in vacuum.

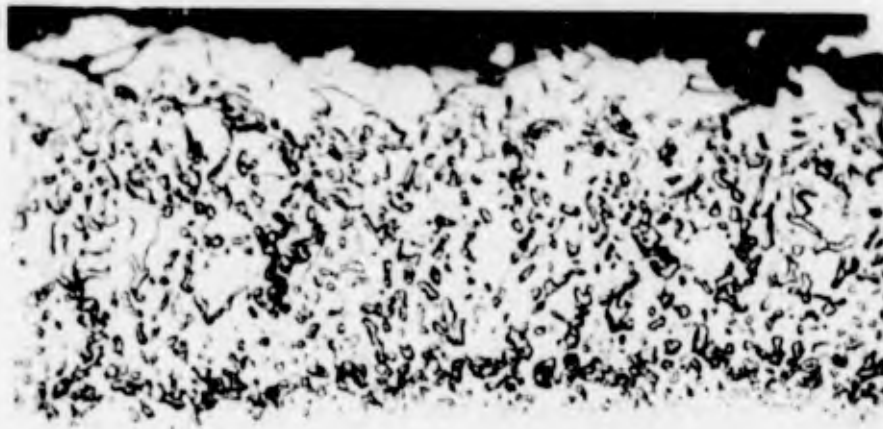
Some coating thickness scatter was observed on the as-received Phase VI test specimens. Total thickness, observed metallographically, was 3.8 to 5.4 mils, with an average of approximately 4.4 mils (Figure 98). The thicknesses of the coating layers are tabulated below.

	<u>Thickness of Phase V Coating (mils)</u>	<u>Thickness of Phase VI Coating (mils)</u>
Coating-substrate interfacial layer	0.2	0.2
Intermediate phase of columnar growth	0.6	0.6 to 0.9
Outer coating layer	1.8	3.6 (average)

Heavy etching of the Phase V and Phase VI coatings revealed two sublayers within the coating-substrate interfacial layer (Figure 99). Microstructurally the Phase V and Phase VI coatings appeared identical.

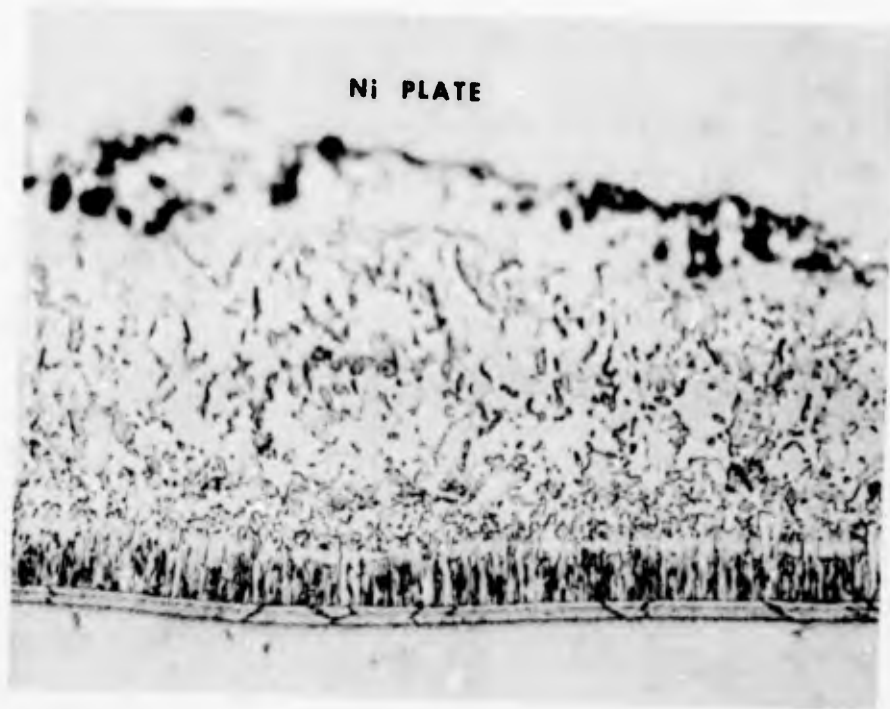


ETCH: 20% HYDROFLUORIC ACID, 20% NITRIC ACID, 60% WATER MAG: 500X



ETCH: 20% HYDROFLUORIC ACID, 20% NITRIC ACID, 60% WATER MAG: 500X

Figure 98. Typical Microstructure of the As-Applied Modified Sylvania SiCrTi Slurry Coating on B-66 Alloy



ETCH: 20% HYDROFLUORIC ACID, 20% NITRIC ACID, 60% WATER MAG: 500X

Figure 99. Microstructure of the As-Applied Modified Sylvania SiCrTi Slurry Coating on B-66 Alloy Showing the Presence of Two Phases Comprising the Coating-Substrate Interface Layer

This coating sample was more heavily etched than the one in Figure 98.

4.2.2 Modified TRW TiCr-Si (Vacuum) Pack/XB-88

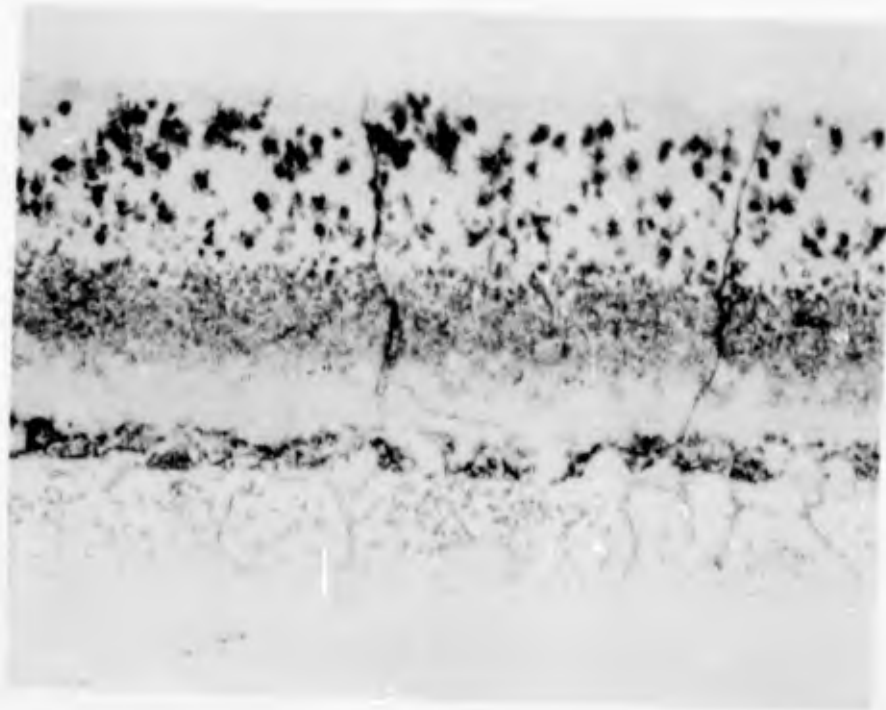
At a meeting with TRW, Inc. it was decided to modify the TiCr-Si coating on XB-88 alloy by increasing the titanium content. This was accomplished through utilization of a 50Cr-50Ti composition in the initial vacuum pack process. It was felt that increased titanium would result in a thicker, more uniform (Cb, Ti)Cr₂-type Laves phase layer and a more highly alloyed titanium and chromium solid solution in the columbium substrate beneath the coating interface. Application procedure was identical to that described in Item 8, paragraph 3.2.2 for the Phase V coating, except for substitution of the 50Cr-50Ti composition for the 60Cr-40Ti pack during the first vacuum deposition treatment.

A metallographic examination of the 3.5-mil-thick metallic-gray coating produced with this modified process revealed three microstructurally different layers in addition to a solution zone extending approximately 0.5 mil into the XB-88 substrate (Figure 100). Precipitation of a second phase within this solid solution zone had occurred in a continuous fashion along the substrate grain boundaries. Precipitation was discontinuous within substrate grains. The coating layer adjacent to the substrate was discontinuous and poorly defined in thickness (Figure 100). The continuous intermediate layer was approximately 1.3 mils thick and was fairly homogeneous except for the outer 0.8 mil, which contained discontinuous regions similar in appearance to portions of the outer layer. The 2.0-mil-thick outer layer was continuous although regions of second phase were present at random locations. Numerous coating cracks extended from the surface through the coating to the coating-substrate layer.

4.2.3 Sylvania SiCrV Slurry/Cb-132M

Coating application was accomplished by spraying a mixture of Si-20Cr-20V and vehicle on the test specimens and developing at 2550°F for 1 hour in vacuum. The coating appeared dense and uniform with good coverage of specimen edge and corner surfaces. Small surface asperities were noted and were believed to be random areas of high vanadium content.

Metallographic examination of the 4.5-mil-thick coating revealed a three-layered structure (Figure 101). A continuous 0.25-mil-thick layer was present at the coating-substrate interface. The second layer (0.35 mil) exhibited a fine columnar structure perpendicular to the coating-substrate interface. This layer was absent in some regions of the coatings (Figure 102). The outer coating layer of approximately 4 mils thickness contained regions of second phase and cracks extending from the surface to the interfacial coating zones.



ETCH: 20% HYDROFLUORIC ACID, 20% NITRIC ACID, 60% WATER MAG: 500X

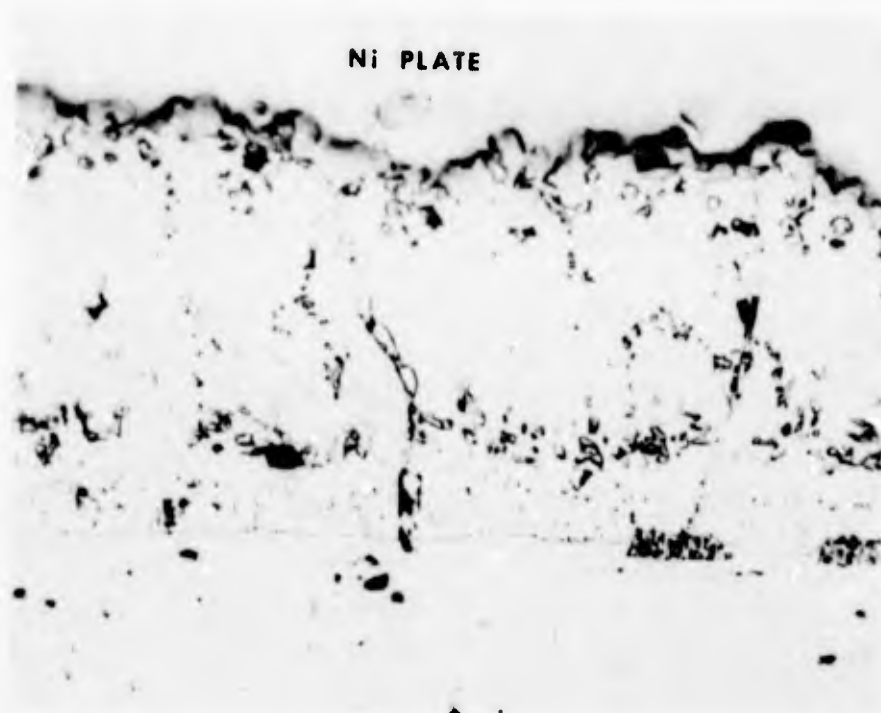
Figure 100. Typical Microstructure of As-Applied Modified TRW TiCr-Si (Vacuum) Pack Coating on XB-88 Alloy



ETCH: 20% HYDROFLUORIC ACID, 20% NITRIC ACID, 60% WATER

MAG: 500X

Figure 101. Microstructure of the As-Applied Sylvania SiCrV Slurry Coating on Cb-132M Alloy



ETCH: 20% HYDROFLUORIC ACID, 20% NITRIC ACID, 60% WATER MAG: 500X

Figure 102. Microstructure of the As-Applied Sylvania SiCrV Slurry Coating on Cb-132M Alloy Showing Absence of Intermediate Phase Region Above the Coating-Substrate Interface Layer

4.3 EVALUATION TESTING

4.3.1 Test Procedures

Evaluation of the Phase VI vane and blade airfoil coatings was by oxidation-erosion, thermal fatigue, and ballistic impact test procedures described for the Phase V high-temperature systems in Item 8, paragraph 3.3.1.

4.3.2 Test Results

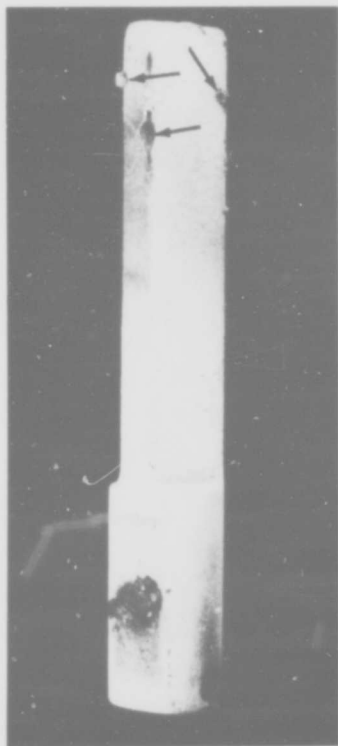
4.3.2.1 Oxidation-Erosion Results

Modified Sylvania SiCrTi Slurry/B-66. For all four test specimens, the modified (thicker) SiCrTi slurry coating on B-66 alloy exhibited a protective life of 100 hours at 2200°F plus 100 hours at 2400°F plus 20 hours at 2500°F. Failure occurred by local oxide formation on specimen airfoil surfaces (Figure 103). Comparison of these results with the Phase V results for the 2.6-mil-thick coating indicates that the greater coating thickness does not extend the maximum oxidation-erosion life, but does increase the reliability of the system. Characteristics of failure, determined metallographically, were similar to those reported for the Phase V coating. Oxide penetration through surface craze cracks led to eventual substrate oxidation at random airfoil locations.

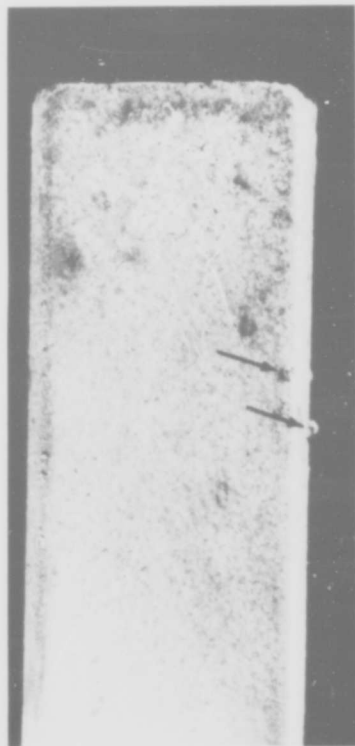
Modified TRW TiCr-Si (Vacuum) Pack/XB-88. During oxidation-erosion testing of the modified TRW TiCr-Si/XB-88 system, failure occurred on four separate test specimens after 100 hours at 2200°F plus 40, 60, 80, and 100 hours, respectively, at 2400°F. Localized formations of substrate oxide penetrating the coating at random locations on specimen airfoil surfaces constituted failure (Figure 104). The progressive failure of these specimens as observed metallographically was similar to that described for the Phase V TRW TiCr-Si/XB-88 oxidation-erosion specimens in paragraph 3.3.2.1.

Pest, or low-temperature (1500°-2000°F), oxidation occurred on specimen grip sections after 100 hours of testing. The holder or grip portions of the specimens operate 200° to 500°F cooler than the airfoil, this temperature difference depending on the airfoil temperature. Oxidation appeared independent of specimen-holder contact locations and progressed continuously during subsequent 2400°F testing of specimen airfoils (see Figure 104).

Increasing the titanium content of the TRW TiCr-Si coating appeared to result in significant improvement over the Phase V performance of this system. It is uncertain to what extent the gain in performance was actually due to the titanium increase, since TRW reported processing difficulties with the 60Cr-40Ti vacuum pack deposition used in Phase V. The 100 hours at 2200°F plus 80 and 100 hours at 2400°F, for two specimens, represented improvements of 20 and 40 hours for the TRW TiCr-Si



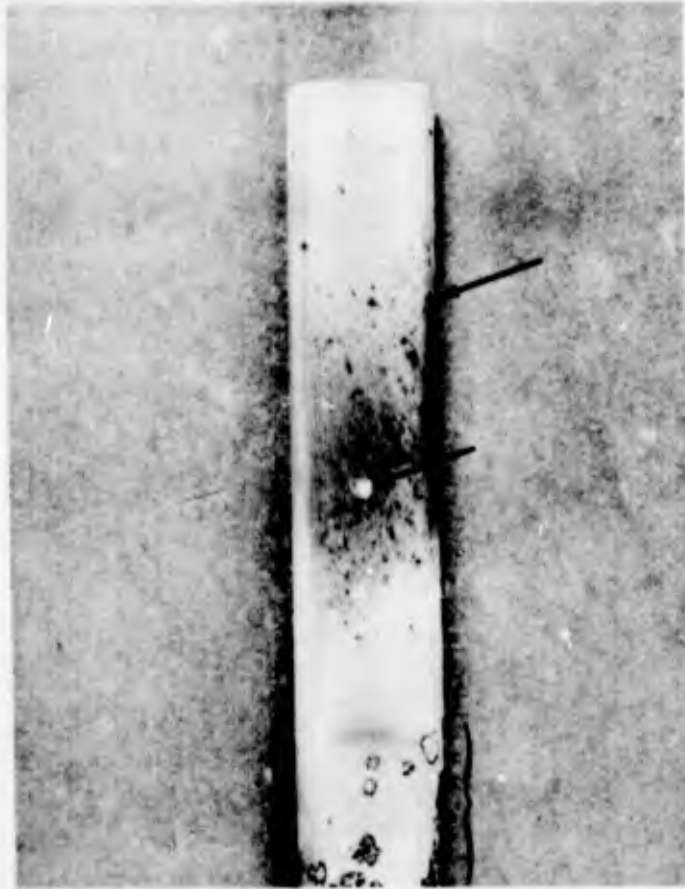
MAG: 1.4X



MAG: 3X

Figure 103. Modified Sylvania SiCrTi Slurry Coated B-66 Alloy After Oxidation-Erosion Testing for 100 Hours at 2200°F Plus 100 Hours at 2400°F Plus 20 Hours at 2500°F

Note areas of local oxidation (arrows).



MAG: 1.6X

Figure 104. Modified TRW TiCr-Si (Vacuum) Pack Coated XB-88 Alloy Bar After Oxidation-Erosion Testing for 100 Hours at 2200°F Plus 100 Hours at 2400°F

Airfoil failures resulted from local oxidation (arrows). Note pest oxidation in specimen grip section (brackets) which was first observed after 100 hours at 2200°F.

coating over the best oxidation-erosion performance observed for the coating on D-43, C-129Y, and Cb-132M alloys (vacuum pack and slip pack, original and modified forms of the coating taken into consideration). The various forms of the coating were evaluated on these three alloys during the first year of the program, under identical test conditions, in Phases I, II, and III; results were reported in Technical Report AFML-TR-66-186. Part I.

Sylvania SiCrV Slurry/Cb-132M. During testing of Sylvania SiCrV/Cb-132M in oxidation-erosion at 2200°F, some erosion of outer silicide coating layers occurred. Partial removal of the outer coating layer appeared to be strictly a surface effect and did not immediately affect performance of the specimens. Failure of all test specimens occurred after 100 hours at 2200°F plus 60 hours at 2400°F. Oxidation along airfoil edge surfaces was extensive (Figure 105) compared to the localized oxidation observed for most of the other systems.

Replacement of the Phase V Solar V-CrTi-Si/Cb-132M system with the Sylvania SiCrV/Cb-132M system resulted in significant improvement in oxidation-erosion performance, (see paragraph 3.3.2.1, Oxidation-Erosion Results, Solar V-CrTi-Si/Cb-132M).

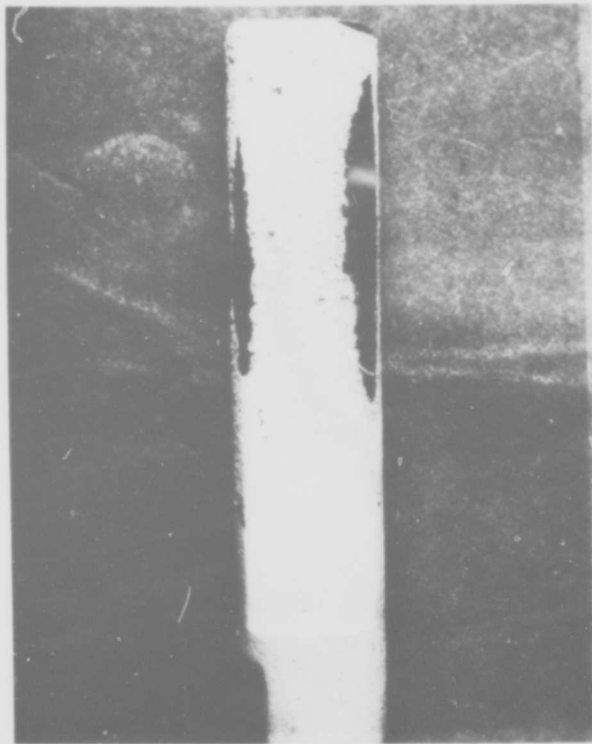
4.3.2.2 Thermal Fatigue Results

Modified Sylvania SiCrTi Slurry/B-66. The thicker SiCrTi coating exhibited a thermal fatigue life of 600 cycles to 2200°F plus 400 cycles to 2400°F plus 300 and 400 cycles to 2500°F for two specimens. Failure, occurring on airfoil leading edge surfaces, resulted from coating depletion due to viscous flow of the outer coating layers during testing. In areas away from this localized oxidation, however, the coating appeared to be in good condition.

To determine the rapidity of specimen deterioration after localized failure on the leading edge, one of the two test airfoils (Figure 106) was subjected to additional thermal fatigue cycles to 2200°F. After 300 additional cycles, oxidation produced only a pinhole through the leading edge (50-mil-thick sheet prior to coating) within the initial failure region (Figure 107). An additional 100 cycles to 2200°F led to continued penetration and enlargement of the oxidized region (Figure 108).

Modified TRW TiCr-Si (Vacuum) Pack/XB-88. Thermal fatigue testing resulted in failure of the modified TRW TiCr-Si/XB-88 system after 400 and 600 cycles to 2200°F (two specimens). Localized (spot) oxidation occurred along random airfoil locations (Figure 109) with coating characteristics after failure similar to those observed after oxidation-erosion testing.

Sylvania SiCrV Slurry/Cb-132M. Local failures at random airfoil locations occurred on one of two specimens after 600 cycles to 2200°F plus 400 cycles to 2400°F plus 600 cycles to 2500°F (Figure 110). These isolated failures progressed only



MAG: 1.75X

Figure 105. Sylvania SiCrV Slurry Coated Cb-132M Alloy Bar Showing Edge Oxidation After Oxidation-Erosion Testing for 100 Hours at 2200°F Plus 60 Hours at 2400°F



CONCAVE AIRFOIL SURFACE

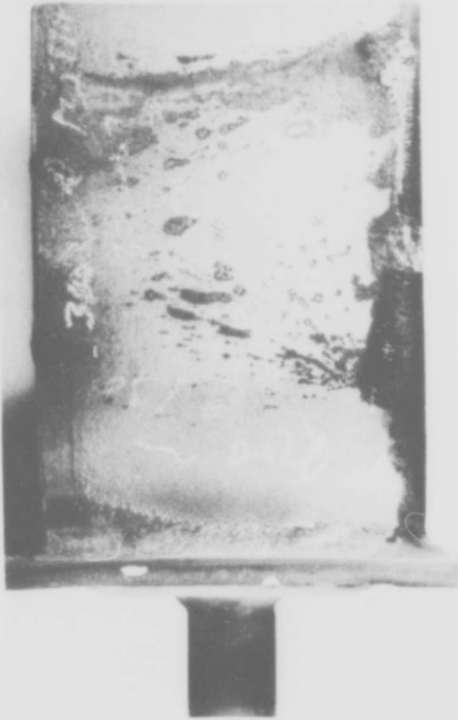


CONVEX AIRFOIL SURFACE

MAG: 1X

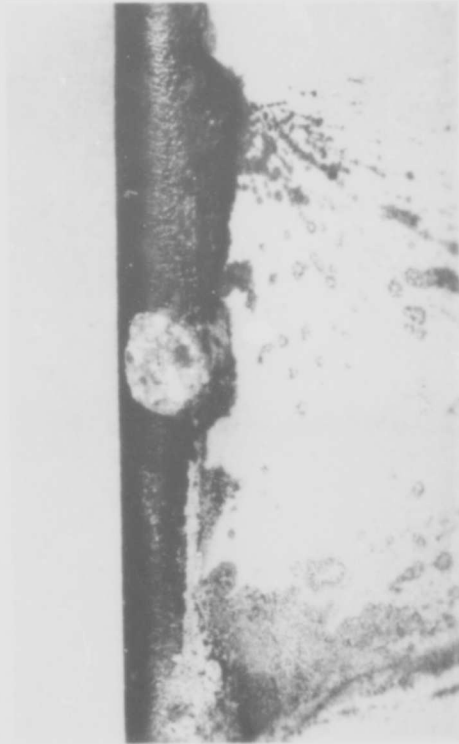
Figure 106. Modified Sylvania SiCrTi Slurry Coated B-66 Alloy Vane Airfoil After Thermal Fatigue Testing for 600 Cycles to 2200°F Plus 400 Cycles to 2400°F Plus 300 Cycles to 2500°F

Arrow locates area of coating failure on leading edge.



CONCAVE AIRFOIL SURFACE

MAG: 1X



LEADING EDGE SURFACE

MAG: 2X

Figure 107. Modified Sylvania SiCrTi Slurry Coated B-66 Alloy Vane Airfoil (Same Airfoil Shown in Figure 106) After 300 Additional Thermal Fatigue Cycles to 2200°F (Total Cycles in Order: 600 to 2200°F, 400 to 2400°F, 300 to 2500°F, and 300 to 2200°F)

Note that substrate oxidation has progressed but has not penetrated the 0.050-inch-thick airfoil wall.



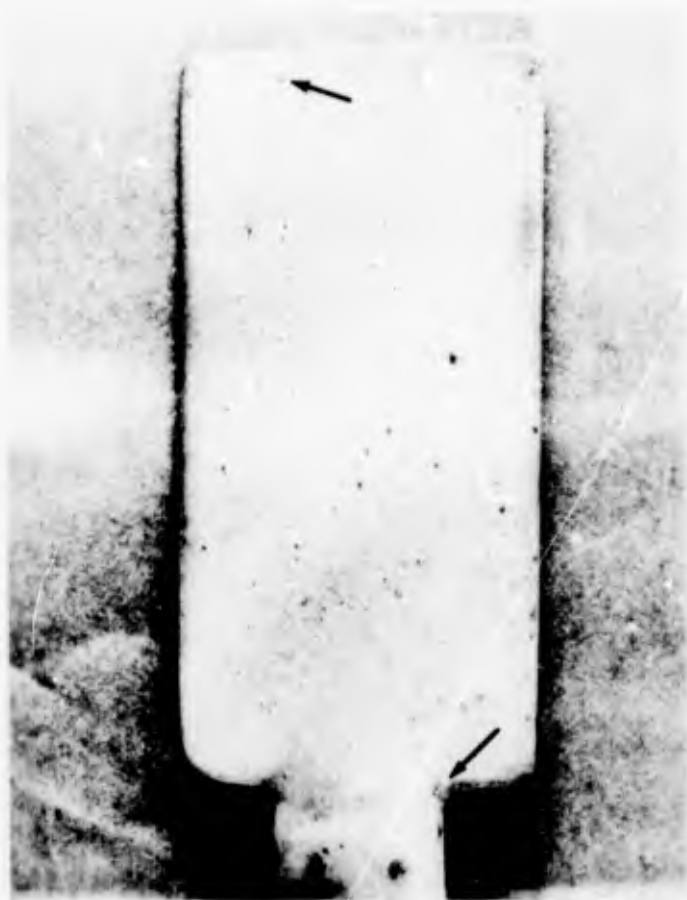
MAG: 1X

Figure 108. Concave Surface of Modified Sylvania SiCrTi Slurry Coated B-66 Alloy Vane Airfoil (Same Airfoil Shown in Figures 106 and 107) After 100 Additional Thermal Fatigue Cycles to 2200°F (Total Cycles in Order: 600 to 2200°F, 400 to 2400°F, 300 to 2500°F, and 400 to 2200°F)

Note oxidation through leading edge wall (arrow) 400 cycles after detection of initial coating failure.



Figure 109. Convex Airfoil Surface of Modified TRW TiCr-Si (Vacuum) Pack Coated XB-88 Alloy Specimen Showing Spot Oxidation Failures After Thermal Fatigue Testing for 600 Cycles to 2200°F



MAG: 1.75X

Figure 110. Convex Airfoil Surface of Sylvania SiCrV Slurry Coated Cb-132M Alloy Specimen Showing Spot Failures (Arrows) After Thermal Fatigue Testing for 600 Cycles to 2200°F Plus 400 Cycles to 2400°F Plus 600 Cycles to 2500°F

slightly during 600 additional thermal fatigue cycles to 2500°F (Figure 111). The second test specimen exhibited failure after 600 cycles to 2200°F plus 400 cycles to 2400°F plus 1400 cycles to 2500°F. Localized failures were similar to those observed for the first test specimen.

The areas of localized oxidation for both thermal fatigue specimens coincided with those spots of high vanadium content visible as surface asperities on the as-coated specimens. Metallographic examination showed no nonuniformity in the 0.35-mil-thick intermediate coating layer in the failure regions.

It is considered significant that a forging lap or crack present in the handle of the second specimen after paddle forging and prior to coating application was protected throughout testing for 600 cycles to 2200°F plus 400 cycles to 2400°F plus 1400 cycles to 2500°F (Figure 112). It is projected that specimen temperature at the defect was in the 1400° to 1900°F temperature range during the 2200°, 2400°, and 2500°F peak temperature portions of the thermal cycles.

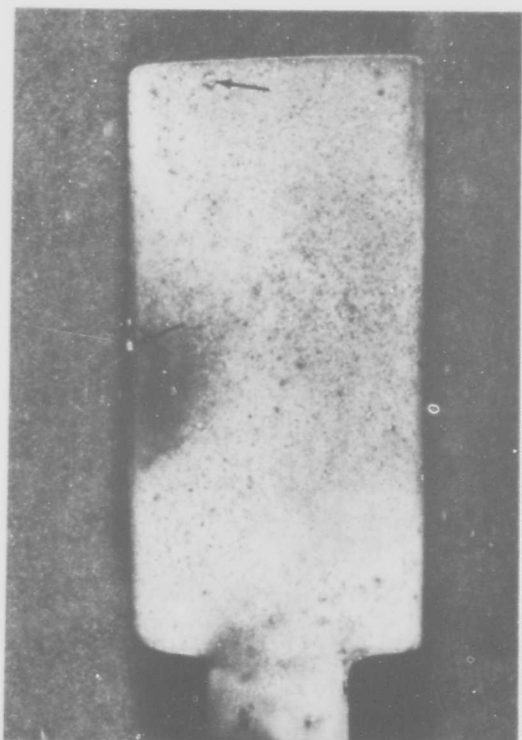
4.3.2.3 Ballistic Impact Results

Impact characteristics of the Phase VI test specimens did not differ appreciably between the coating-substrate systems tested. After ballistic impact and prior to subsequent oxidation exposure, the five characteristic surface features described in paragraph 3.3.2.3 (Phase V ballistic impact results) were noted. Results of post-impact 2200°F oxidation exposure are presented in Table XII. In summary, the room temperature impacts at 200 and 500 feet per second resulted in the shortest exposure lives during subsequent oxidation testing. No failures of the modified TRW TiCr-Si/XB-88 system were observed after 3 hours at 2200°F following impacts at 70°F and 200 ft/sec, 2200°F and 200 ft/sec, and 2200°F and 500 ft/sec. During the fourth hour, a malfunction in the furnace temperature control system led to the destruction of all specimens.

4.4 PERFORMANCE COMPARISONS OF THE PHASE V AND PHASE VI HIGH-TEMPERATURE SYSTEMS

4.4.1 Oxidation-Erosion

The Phase VI modified or replacement coatings in all cases demonstrated better performance, or showed greater reliability, than the Phase V coatings. The oxidation-erosion data are graphically presented in Figure 113.



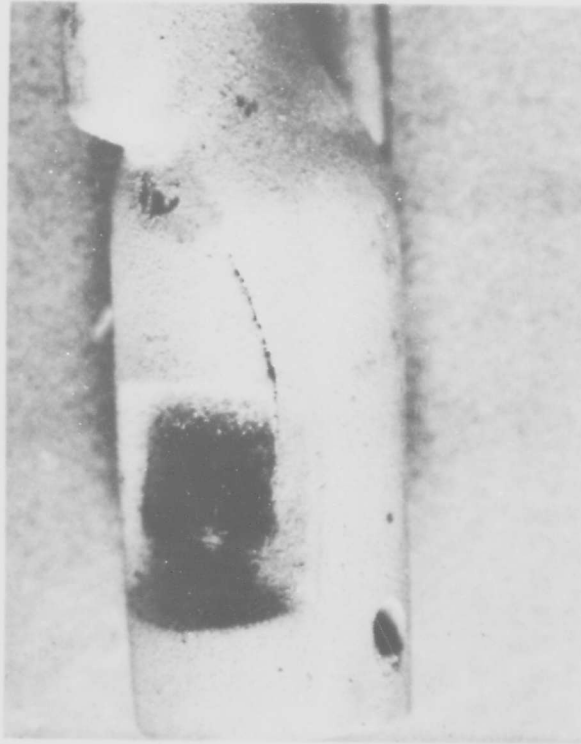
MAG: 2X



MAG: 4X

Figure 111. Convex Airfoil Surface of Sylvania SiCrV Slurry Coated Cb-132M Alloy Specimen Showing Progression of Spot Failure Deterioration (Arrows) After 600 Additional Cycles to 2500°F

Spot failure occurred initially after 600 cycles to 2200°F plus 400 cycles to 2400°F plus 600 cycles to 2500°F (see Figure 110).



MAG: 4X

Figure 112. Sylvania SiCrV Slurry Coated Cb-132M Alloy Thermal Fatigue Specimen Showing Handle Defect

Defect was present prior to coating.

TABLE XII

RESULTS OF PHASE VI BALLISTIC IMPACT TESTING OF THE
VANE AND BLADE AIRFOIL COATING-SUBSTRATE SYSTEMS

Application	Test No.	Specimen No.	Coating	Substrate Alloy	Specimen Temp. at Impact (°F)	Impact Velocity (ft/sec)	Oxidation Life After Impact		Observed Condition After Oxidation Exposure	
							Temp. (°F)	Time (hrs)	Surface at Impact Point	Surface Directly Behind Impact Point
Vane	1	BB1-6-1	Modified Sylvania SiCrTi slurry	B-66	70	200	2200	1	Oxide surrounding impact depression	Oxidation of surface
	2	BB1-6-1	Modified Sylvania SiCrTi slurry	B-66	70	200	2200	1	Oxide surrounding impact depression	No oxide noted
	3	BB1-6-2	Modified Sylvania SiCrTi slurry	B-66	70	500	--	-	Specimen fractured at impact depression	---
	4	BB1-6-2	Modified Sylvania SiCrTi slurry	B-66	70	500	--	-	Specimen fractured at impact depression	---
	5	BB1-6-3	Modified Sylvania SiCrTi slurry	B-66	2200	200	2200	1	Oxide surrounding impact depression	No oxide noted
	6	BB1-6-3	Modified Sylvania SiCrTi slurry	B-66	2200	200	2200	1	Oxide surrounding impact depression	No oxide noted
	7	BB1-6-4	Modified Sylvania SiCrTi slurry	B-66	2200	500	2200	1	Oxide surrounding impact depression	Oxidation of surface
	8	BB1-6-4	Modified Sylvania SiCrTi slurry	B-66	2200	500	2200	1	Oxide surrounding impact depression	Oxidation of surface
Blade Airfoil	9	MB1-6-1	Sylvania SiCrV slurry	CB-132M	70	200	2200	1	Slight oxide surrounding impact depression	See Note 3
	10	MB1-6-2	Sylvania SiCrV slurry	CB-132M	2200	200	2200	-	No failure after 16 hours; test stopped	
	11	MB1-6-3	Sylvania SiCrV slurry	CB-132M	70	500	2200	1	Oxide surrounding impact depression	
	12	MB1-6-4	Sylvania SiCrV slurry	CB-132M	2200	500	2200	-	No failure after 16 hours; test stopped	
	13	NB1-6-1	Modified TRW TiCr-Si (vacuum)	NB-88	70	200	2200	-	No failure after 3 hours; test stopped	
	14	NB1-6-2	Modified TRW TiCr-Si (vacuum)	NB-88	2200	200	2200	-	No failure after 3 hours; test stopped	
	15	NB1-6-3	Modified TRW TiCr-Si (vacuum)	NB-88	70	500	2200	1	Oxide surrounding impact depression	See Note 3
	16	NB1-6-4	Modified TRW TiCr-Si (vacuum)	NB-88	2200	500	2200	-	No failure after 3 hours; test stopped	

Notes:

1. Weight of steel projectiles: 0.75 gram each.
2. Thickness of substrate: B-66; 0.050 inch; CB-132M and NB-88; 0.125 inch.
3. No effects were noted on the surface directly behind the impact point on the coated CB-132M and NB-88 due to the greater thickness of these specimens (0.125 inch).

■ NO FAILURES
 □ RANGE OF SPECIMEN FAILURES

CIRCLED FIGURES INDICATE THE NUMBER OF SPECIMENS WHICH FAILED AT THE RESPECTIVE TEST TIMES

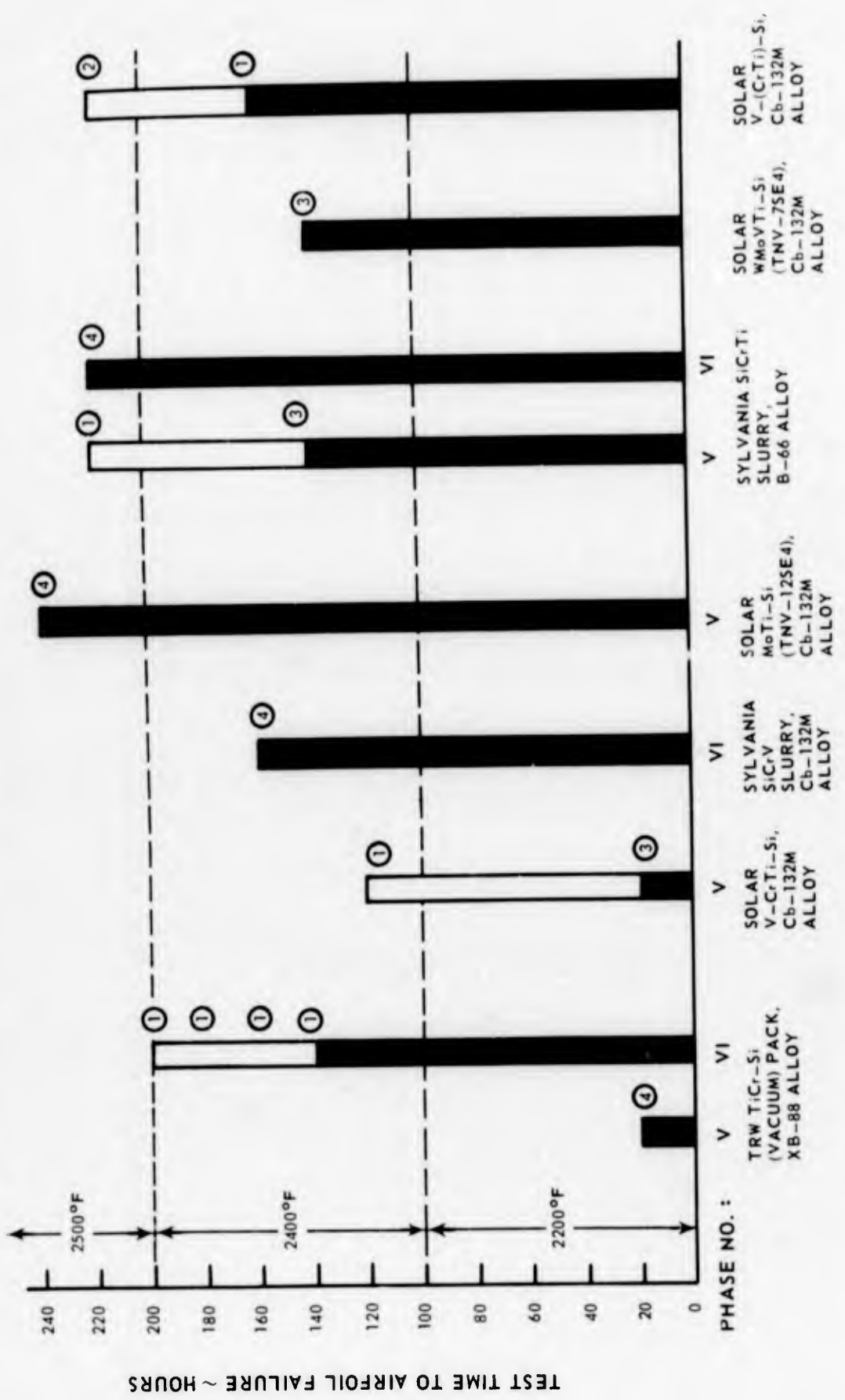


Figure 113. Oxidation-Erosion Performance Comparisons for the Phase V, Phase VI, and Additional Solar-Supplied Coating-Substrate Systems

4.4.2 Thermal Fatigue

Except for the Sylvania SiCrTi/B-66 system, the thermal fatigue performance of the Phase VI coatings was also significantly better than the Phase V performance. These results are summarized in Figure 114.

4.4.3 Ballistic Impact

The Phase V and Phase VI ballistic impact results are summarized in Tables VIII and XII, respectively. In cases where modifications were attempted, no significant differences between the unmodified and modified coatings were observed.

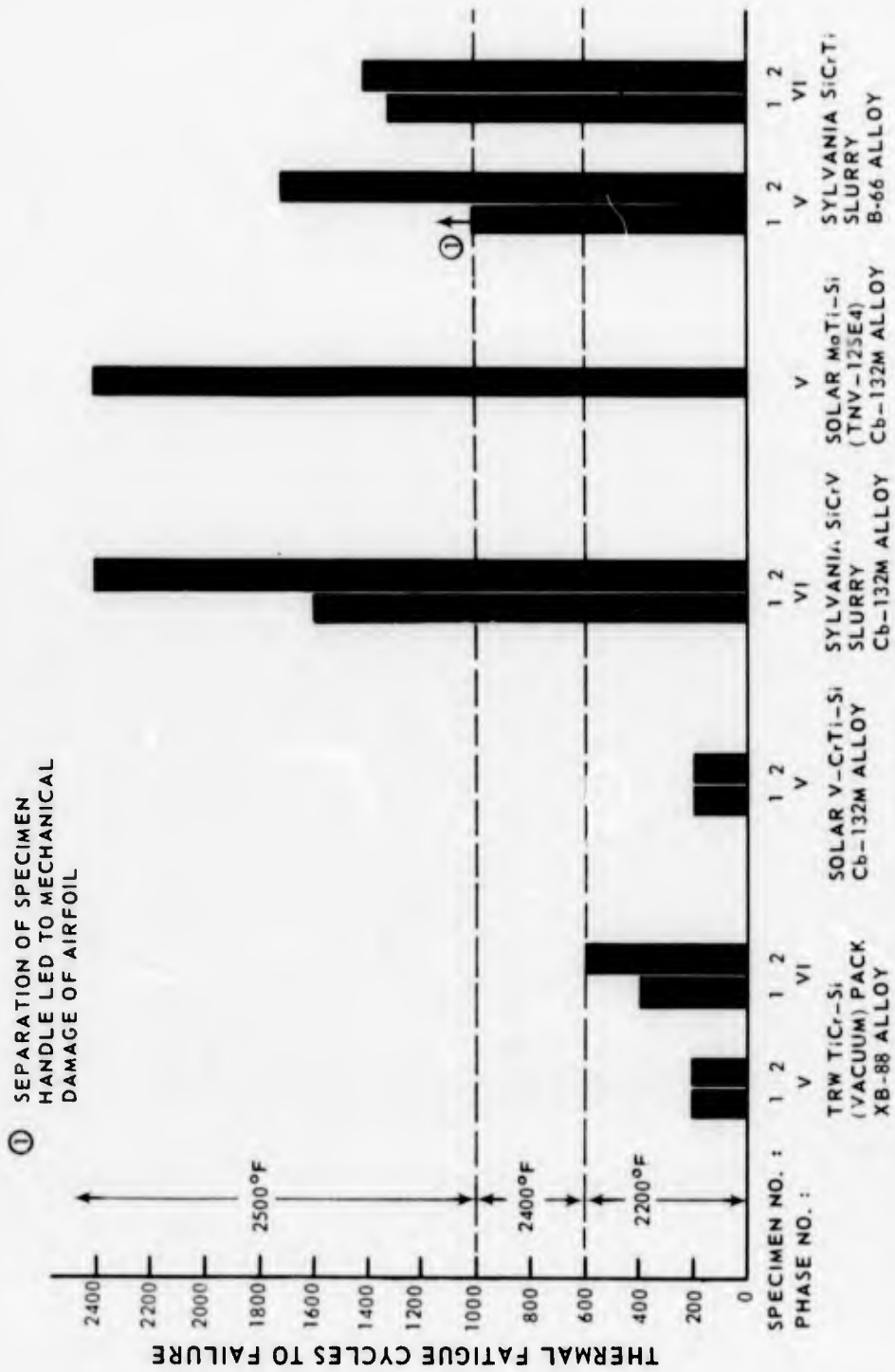


Figure 114. Thermal Fatigue Performance Comparisons for the Phase V and Phase VI Coating-Substrate Systems

5. ITEMS 10 AND 11

ADVANCED EVALUATION OF ADDITIONAL SYSTEMS

Contract Item 10, Coating Life Evaluation, and Item 11, Composite Properties Evaluation, represent Phase VII of the program. As in the case of Phases III and IV, the purpose of this phase was to obtain the quantitative data required to assess the advisability of engine testing coated columbium vane and blade components.

Work under Item 10 involved oxidation-erosion and thermal fatigue testing of the optimized blade airfoil and vane coatings and static oxidation testing of the two blade root coatings exhibiting highest performance to determine the protectiveness, diffusional stability, and reliability of the coating systems, and also melting tests to determine the ability to withstand transient temperature overshoots.

Under Item 11 the following tests to determine thermomechanical properties of the coated alloy composites were conducted: stress-rupture and ballistic impact on the turbine vane composite; mechanical fatigue, creep, and impact on the blade airfoil composite; and mechanical fatigue, including duplex coating compatibility, on blade root composites.

The flow chart for Phase VII is presented in Figure 115.

Phase VII composite materials, coatings application, and systems evaluation are discussed in the following paragraphs first for the high-temperature systems (vane and blade airfoil applications) and finally for low-temperature systems (blade root).

5.1 COMPOSITE MATERIALS. HIGH-TEMPERATURE SYSTEMS

Selection of the Phase VII high-temperature composites was based on the performance of the vane and blade airfoil systems in Phases V and VI.

Selected for advanced evaluation in the vane application area was modified Sylvania SiCrTi slurry coated B-66 alloy. The coating was selected because of its good reliability and, in particular, its favorable performance in both oxidation-erosion and thermal fatigue testing. The B-66 alloy was necessarily the Phase VII substrate since it was the only candidate vane alloy in the second year's effort.

Modified Sylvania SiCrTi slurry coated XB-88 alloy was selected for advanced evaluation for blade airfoil application. Selection of this coating, the same coating as

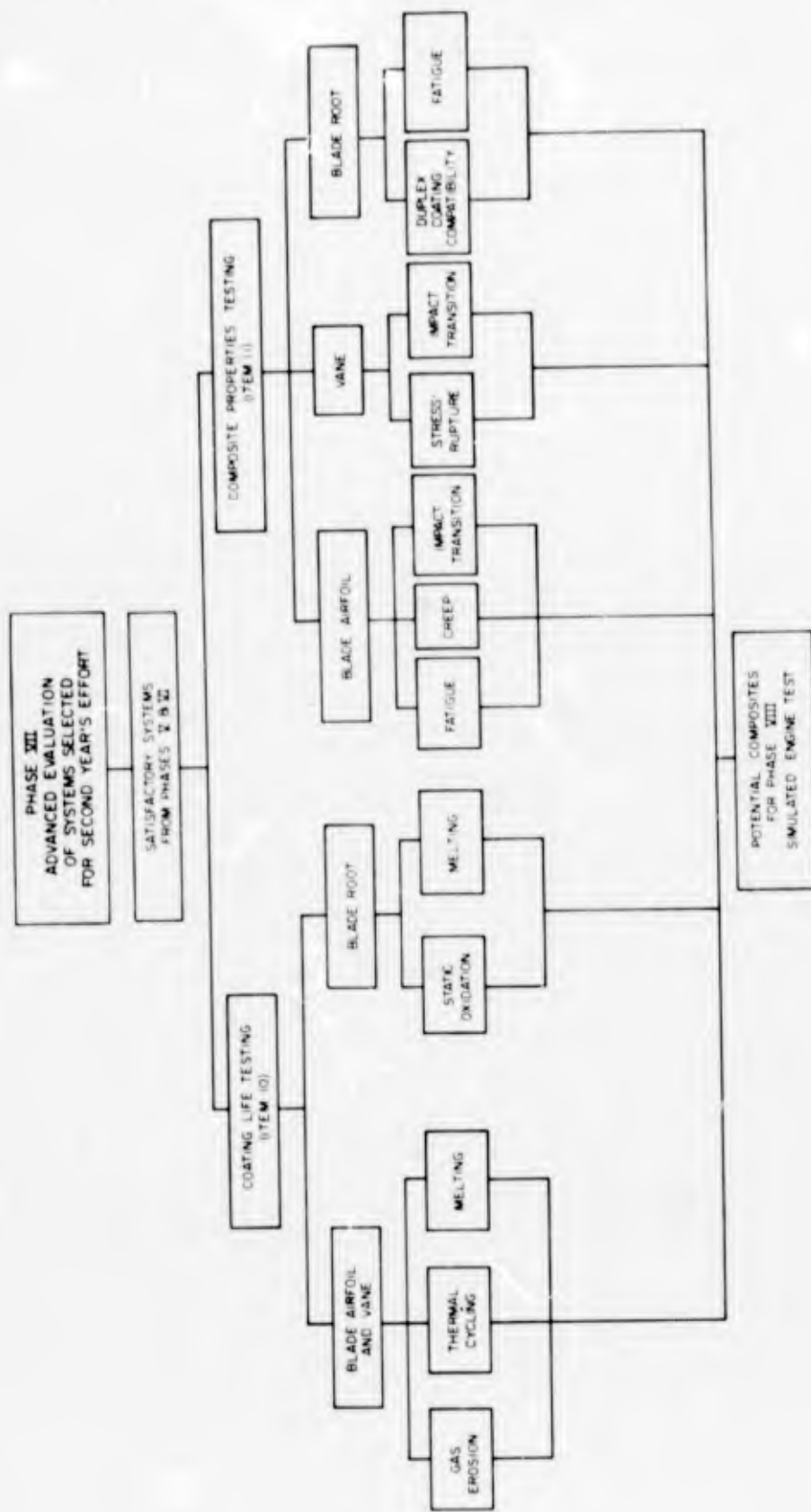


Figure 115. Flow Chart for Phase VII of Program (Items 10 and 11)

was chosen for vane evaluation, was based on these application features and coating properties:

- The slurry process is amenable to the coating of complex parts and, when necessary, to performing spot repairs.
- The coating application cycle of 2550°F for 1 hour should not significantly alter XB-88 substrate mechanical properties.
- The Sylvania SiCrTi coating was fully characterized and exhibited good reliability in oxidation-erosion and thermal fatigue evaluations on B-66 vane alloy.

The XB-88 alloy was selected for Phase VII because: (1) the Cb-132M blade alloy was evaluated in Phases III and IV of the program and it was desirable to obtain mechanical property data on an alternate high-strength columbium alloy, (2) good mechanical properties have been reported for XB-88 by Westinghouse Astronuclear Laboratory (Ref. 1, 2).

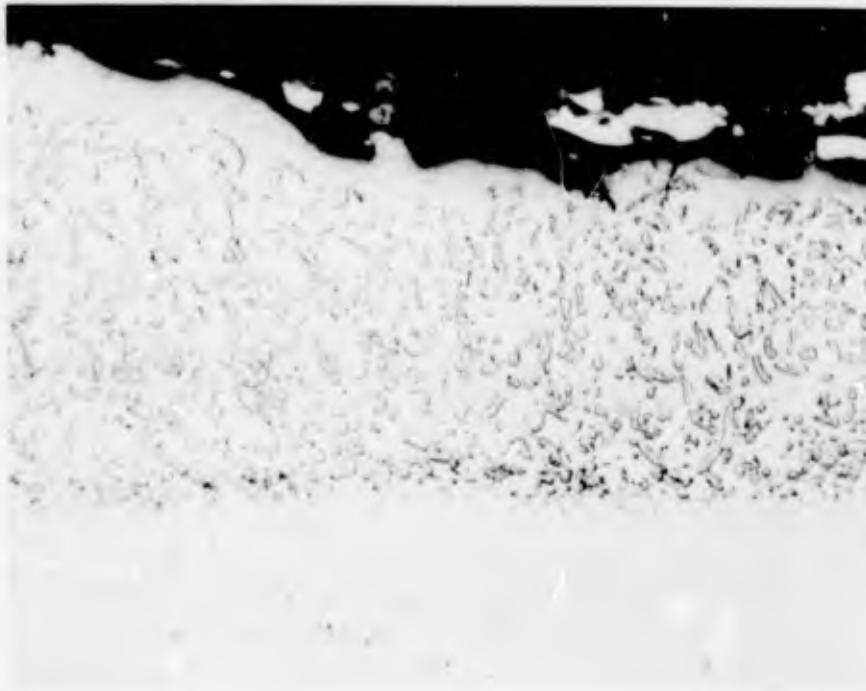
Characteristics of both the XB-88 and B-66 alloys are described in Item 8, paragraph 3.1. Substrate Materials.

5.2 COATINGS APPLICATION, HIGH-TEMPERATURE SYSTEMS

5.2.1 Vane System, Modified Sylvania SiCrTi Slurry/B-66

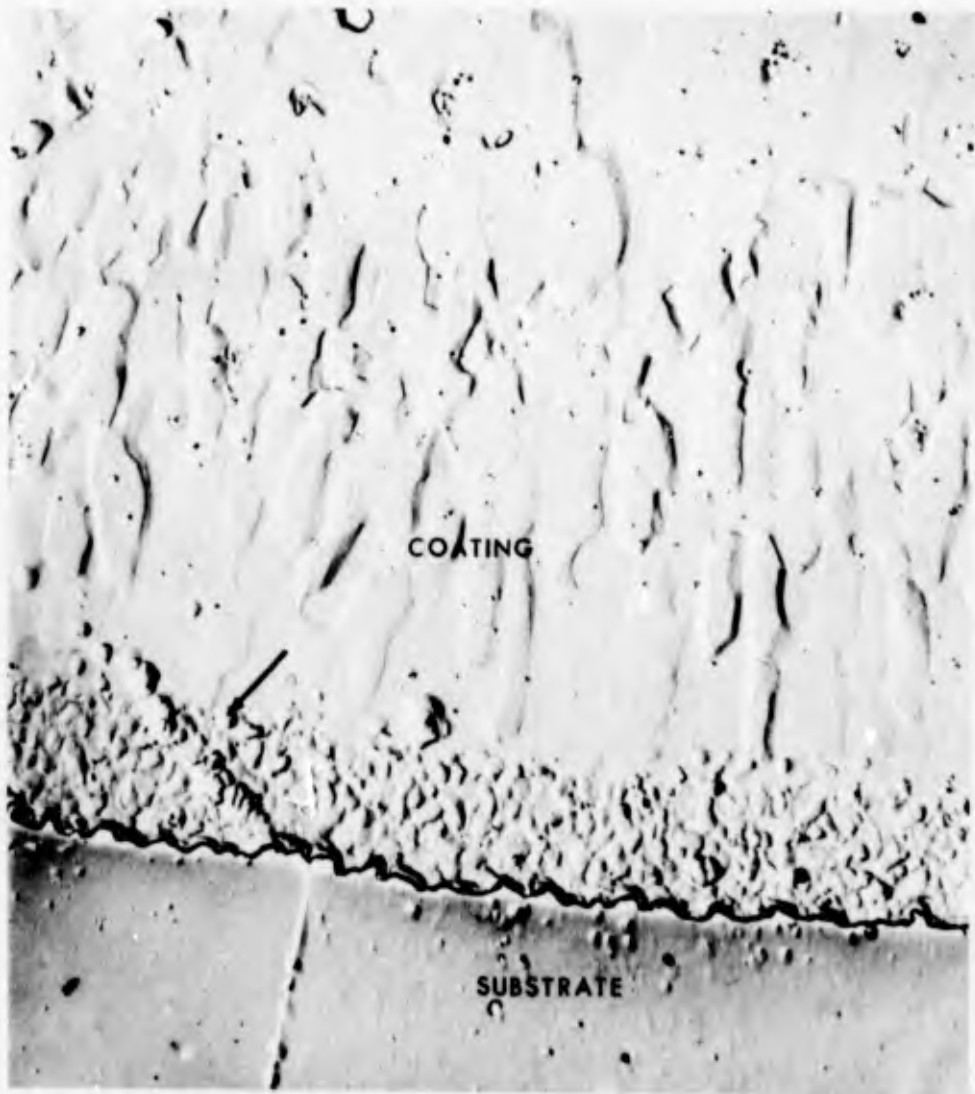
Application of a Si-20Cr-5Ti and vehicle mixture was performed at Sylvania by a spray technique. A 1-hour heat treatment at 2550°F in vacuum produced a metallic-gray coating on the B-66 alloy which was dense, continuous, and homogeneous in surface appearance. Coverage at the specimen edge and corner surfaces was excellent.

A metallographic examination of the resulting 4.5-mil-thick coating revealed a structure consisting of three distinct layers (Figure 116). A thin continuous diffusion zone of 0.19 mil thickness extended into the B-66 substrate. Electron metallography of this boundary region revealed coating diffusion across base-metal grain boundaries (Figure 117). The 1.1-mil-thick second zone, i.e. the intermediate coating layer, consisted of columnar-type grains exhibiting growth perpendicular to the coating-substrate interface. This coating region was completely void of second phases. The outer coating layer ranged in thickness from 3.0 to 3.4 mils. This zone contained precipitated particles in a matrix of equiaxed fine grains. Electron microscopy revealed diffusion "envelopes" surrounding all precipitated particles (Figure 118).



ETCH: 20% HYDROFLUORIC ACID, 20% NITRIC ACID, 60% WATER MAG: 500X

Figure 116. Typical Microstructure of Phase VII Sylvania SiCrTi Slurry Coating on B-66 Alloy

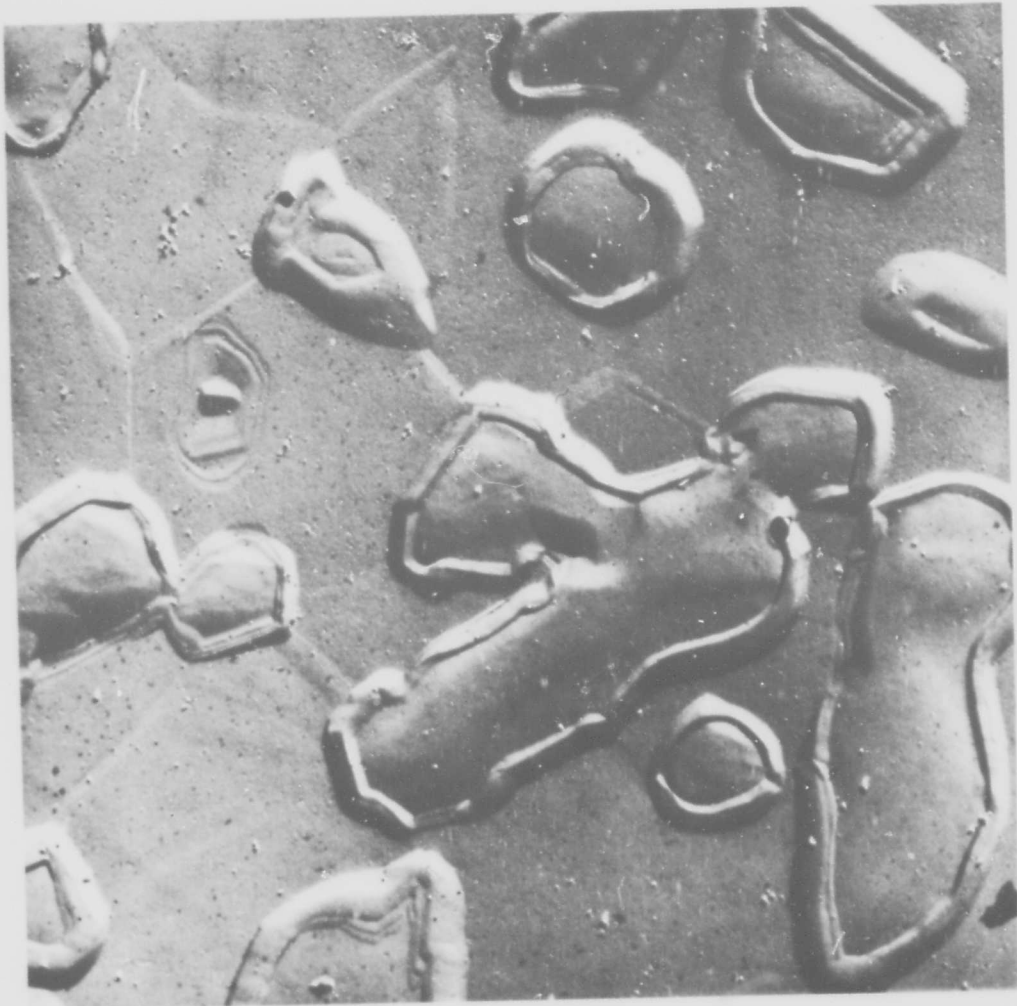


REPLICA: CHROMIUM-CARBON

MAG: 8,500X

Figure 117. Structure of As-Applied Phase VII Sylvania SiCrTi Slurry Coating on B-66 Alloy at the Coating-Substrate Interface

Note diffusion across base-metal grain boundary (arrow).



REPLICA: CHROMIUM-CARBON

MAG: 18,000X

Figure 118. Electron Micrograph of As-Applied Phase VII Sylvania SiCrTi Slurry Coating on B-66 Alloy Showing Regions of Diffusion Surrounding Precipitated Particles in the Outer Coating Region

Diamond pyramid hardness tests, utilizing a 20-gram load, were performed in each coating region with the following results:

<u>Region</u>	<u>Distance From Coating-Substrate Interface (mils)</u>	<u>Average or Range of Hardness (DPH)</u>
Outer coating layer	2.0 to 4.0	1038
Outer coating layer, precipitate particle	2.0 to 4.0	1235 to 1716
Intermediate coating layer	0.8	1493
Intermediate coating layer, columnar layer	0.4	1314
Coating layer adjacent to substrate	0.1	1038
Substrate	-0.2	239
Substrate	-2.0	221

The B-66 columbium alloy substrate was completely recrystallized due to the coating application process, i. e. the 2550°F, 1-hour heat treatment.

Concentration profiles obtained by electron microprobe scanning from the base metal through the coating to the nickel-plate overlay produced the results presented in Figure 119.

5.2.2 Blade Airfoil System, Modified Sylvania SiCrTi Slurry/XB-88

Using the same coating procedure as used for the Phase VII vane system, the application of a Si-20Cr-5Ti and vehicle mixture at Sylvania was followed by a 1-hour heat treatment at 2550°F in vacuum. The surface appearance of the coating on XB-88 alloy was dense and homogeneous with excellent coverage of corner and edge surfaces.

Three regions were observed metallographically in the 5.0-mil-thick coating (Figure 120). A 0.25-mil-thick continuous layer exhibiting columnar-type phase growth (Figure 121) was present at the coating-substrate interface. Above this diffusion zone, a 1.0-mil-thick continuous intermediate region, also exhibiting columnar-type phase growth, was denuded of second-phase material. The outer coating region of 3.5 to 3.75 mils in thickness contained second-phase particles in an equiaxed, continuous matrix. Concentration of the particles increased from the coating surface through the outer region to the intermediate coating layer.

Although the constitution of phases was similar to that reported above for the coating on the B-66 vane alloy, distinct differences were apparent: First, a large number of voids were present in the extreme outer portions of the coating, i. e. the

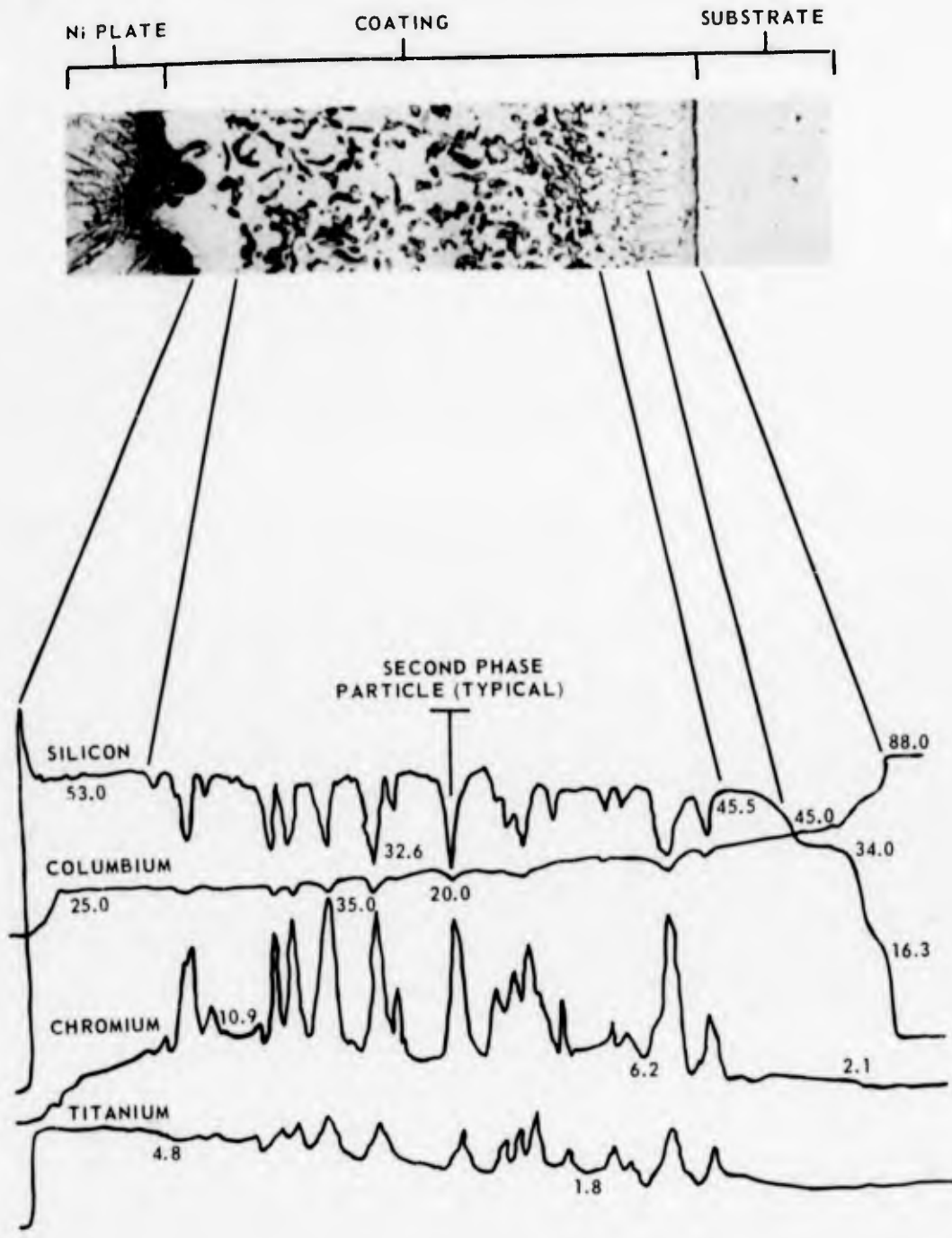
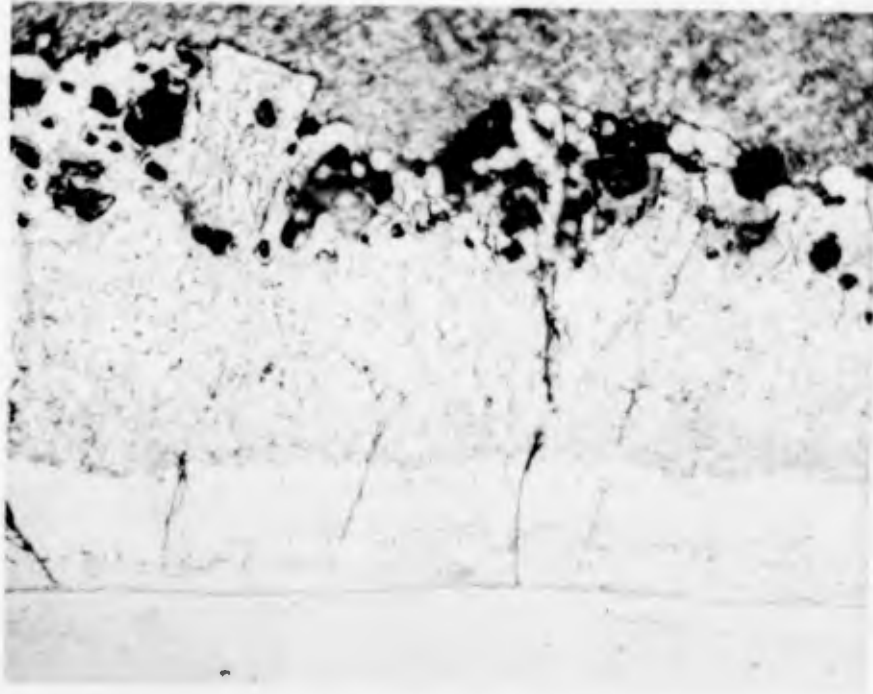


Figure 119. Concentration Profiles for Phase VII Sylvania SiCrTi Slurry Coated B-66 Alloy as Determined by Electron Microprobe Analyses

Weight percentage figures are given at representative points on traces.



ETCH: 20% HYDROFLUORIC ACID, 20% NITRIC ACID, 60% WATER MAG: 500X

Figure 120. Typical Microstructure of Phase VII Sylvania SiCrTi Slurry Coating on XB-88 Alloy



REPLICA: CHROMIUM-CARBON

MAG: 9000X

Figure 121. Electron Micrograph of As-Applied Phase VII Sylvania SiCrTi Slurry Coating on XB-88 Alloy Showing Columnar Growth Within the Diffusion Zone (A) and Intermediate Coating Layer (B)

outer 1.0 to 1.5 mils (Figure 120), and evidence of entrapped oxides was noted in some of these areas. Secondly, coating cracks were quite numerous and consisted of the two distinct types described below.

- Radial cracks: These separations were quite extensive and in some cases extended from the surface to the coating-substrate interface (Figure 122).
- Lateral cracks: Separations propagating parallel to the coating-substrate interface were of short length and appeared to be confined to the outer coating region (Figure 123).

A third dissimilarity was the absence of distinct diffusion envelopes encompassing the second-phase particles in the outer coating region (Figure 123). These envelopes, believed to be transition regions between silicide compounds, were observed in the SiCrTi coating on B-66 alloy (see Figure 118).

Diamond pyramid hardness tests were conducted in each coating region using a 20-gram load. The results are tabulated below.

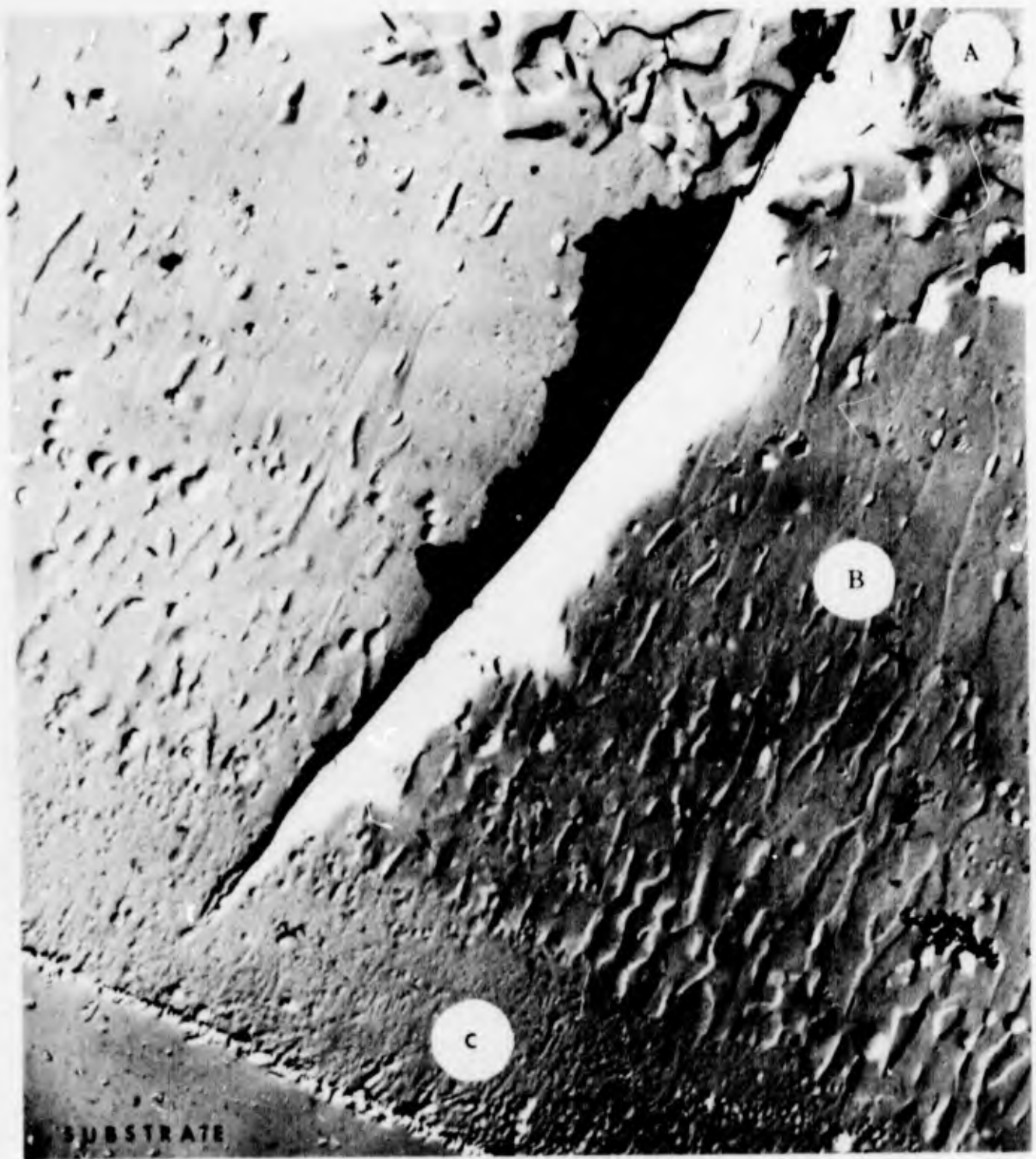
<u>Region</u>	<u>Distance From Coating-Substrate Interface (mils)</u>	<u>Average or Range of Hardness (DPH)</u>
Outer coating layer	1.5 to 4.0	538 to 695
Outer coating layer, second-phase particle	1.5 to 4.0	1038 to 1164
Intermediate coating layer	0.6	728 to 1099
Coating layer adjacent to substrate	0.1	1099
Substrate	-0.2	267
Substrate	-1.0	318
Substrate	-1.5 to -3.0	274 to 300

Electron microprobe scanning from the base metal through the coating to the nickel-plate overlay was performed to obtain concentration profiles for the three major coating elements (silicon, chromium, and titanium) and the two major alloy constituents (columbium and tungsten). These results are presented in Figure 124.

5.3 SYSTEMS EVALUATION, HIGH-TEMPERATURE SYSTEMS

5.3.1 Vane System, Modified Sylvania SiCrTi Slurry/B-66

As illustrated in the Phase VII flow chart (Figure 115), advanced evaluation of the Sylvania SiCrTi/B-66 vane system included oxidation-erosion, melting, thermal fatigue, ballistic impact, and stress-rupture tests. Results are summarized in the following sections.



REPLICA: CHROMIUM-CARBON

MAG: 5400X

Figure 122. Structure of As-Applied Phase VII Sylvania SiCrTi Slurry Coating on NB-88 Alloy Showing Surface Crack Penetration Through the Outer (A) and Intermediate (B) Coating Layers Into the Diffusion Zone (C)



REPLICA: CHROMIUM-CARBON

MAG. 5400X

Figure 123. Electron Micrograph of As-Applied Phase VII Sylvania SiCrTi Slurry Coating on XB-88 Alloy Showing Lateral Microcracks (Arrows) and the Absence of Diffusion Surrounding Precipitated Particles in the Outer Coating Region

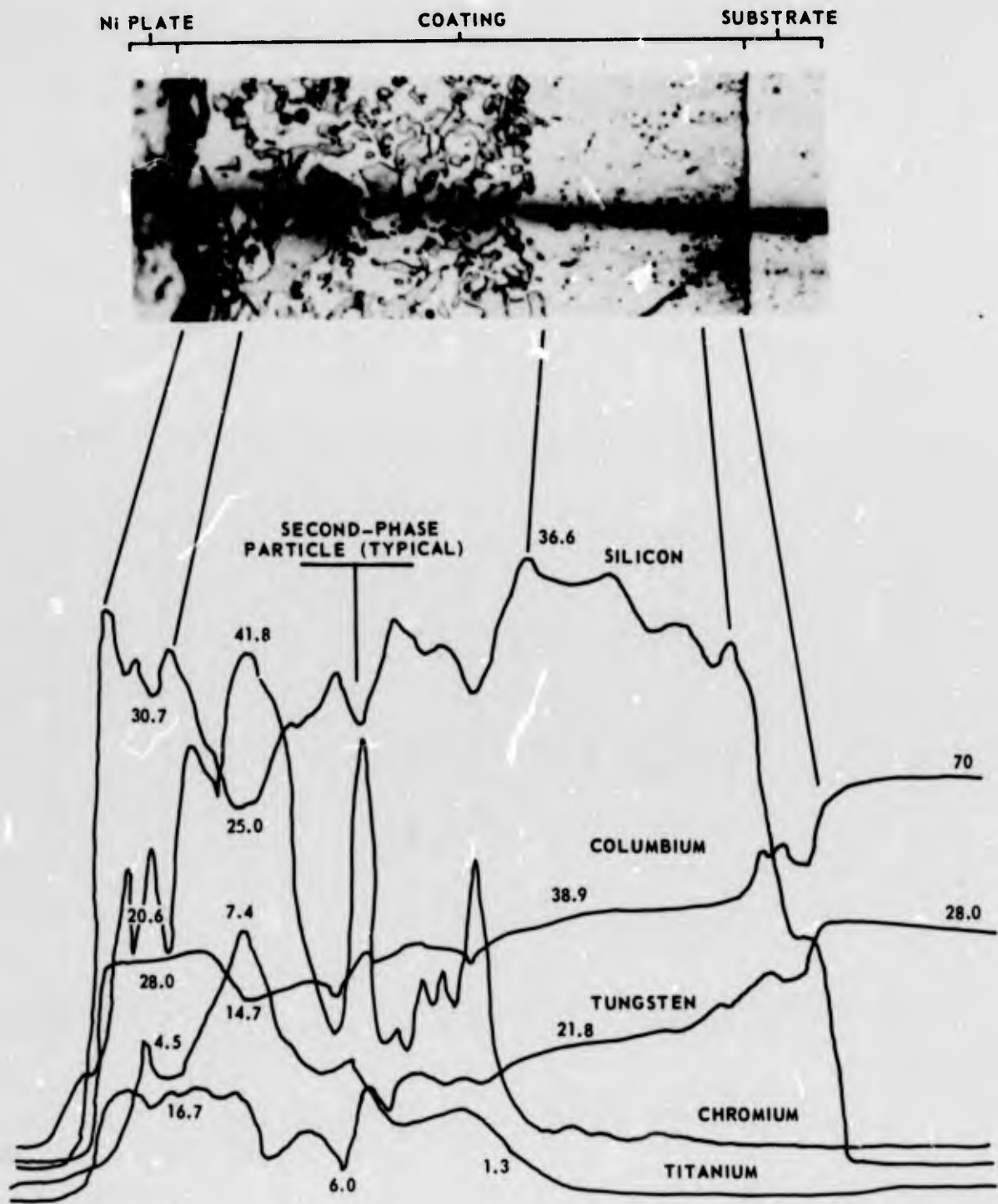


Figure 124. Concentration Profiles for Phase VII Sylvania SiCrTi Coated XB-88 Alloy as Determined by Electron Microprobe Analyses

Weight percentage figures are given at representative points on traces.

5.3.1.1 Oxidation-Erosion Test Results

Specimen configuration and the oxidation-erosion test procedure is described in paragraph 2.3.1. The Phase VII oxidation-erosion testing was conducted at 1800°, 2000°, 2200°, 2400°, and 2500°F in a combusted JP-5 fuel and air stream until failure.

Performance of the Sylvania SiCrTi/B-66 system (illustrated in Figure 125) was as follows:

- 1800°F: No airfoil failures for two specimens after 900 hours; test stopped due to extensive grip oxidation.
- 2000°F: Failures by localized oxidation along airfoil trailing edge surfaces after 380 and 400 hours.
- 2200°F: Failures by localized oxidation at airfoil trailing edge surfaces after 220 hours (Figure 126).
- 2400°F: Failures by oxidation at random airfoil locations after 140 hours (Figure 127).
- 2500°F: Failures by localized formation of substrate oxide, principally on specimen leading edge surfaces, after 53 hours (Figure 128).

Specimen condition after failure was generally good in that oxidation was confined to localized areas and was not progressing rapidly at test cessation.

5.3.1.2 Melting Test Results

Cyclic oxidation tests were performed for the Sylvania SiCrTi/B-66 system according to the procedure detailed in paragraph 2.3.3. The specimens were rotated at 1750 rpm in a combusted JP-5 fuel and air stream.

Failure by localized substrate oxidation occurred for four test specimens after 200 hours total time at 2200°F plus 50 minutes total transient time to 2600°F. Oxidation was primarily along airfoil trailing edge surfaces (Figure 129).

Comparison of these cyclic test results with the 2200°F isothermal oxidation-erosion performance revealed that the ten 5-minute transient periods to 2600°F during each 20 hours at 2200°F did not significantly reduce the reliability of the Sylvania SiCrTi slurry coating.

5.3.1.3 Thermal Fatigue Test Results

Unlike the Phase V and Phase VI thermal fatigue specimens, which were a welded sheet metal airfoil configuration (Figure 34), the Phase VII thermal fatigue tests were performed on forged B-66 paddle specimens of the type shown in Figure 13. Testing

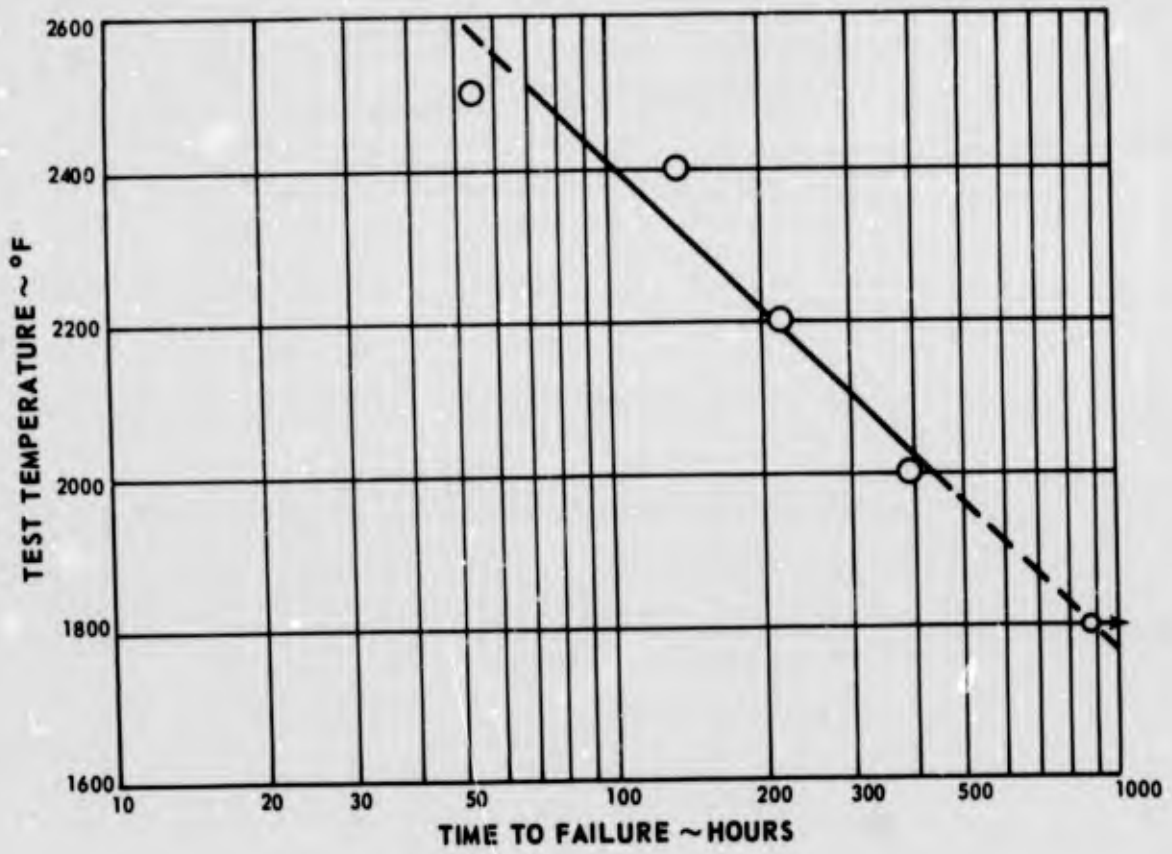
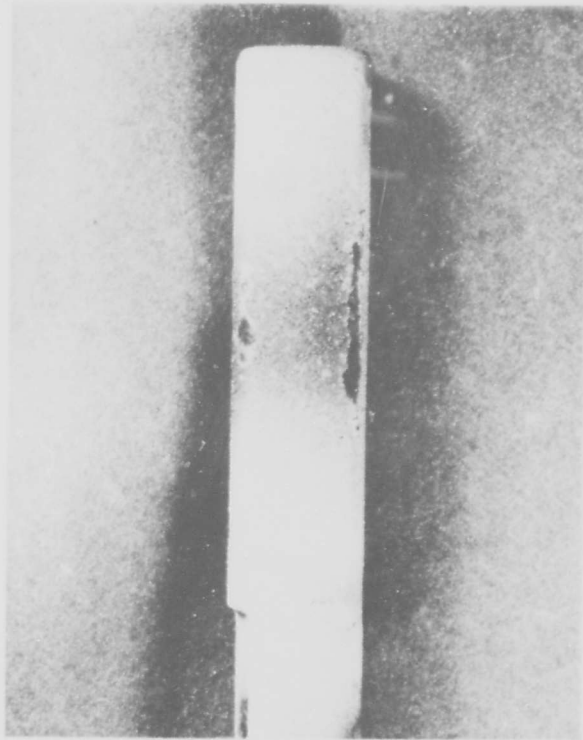


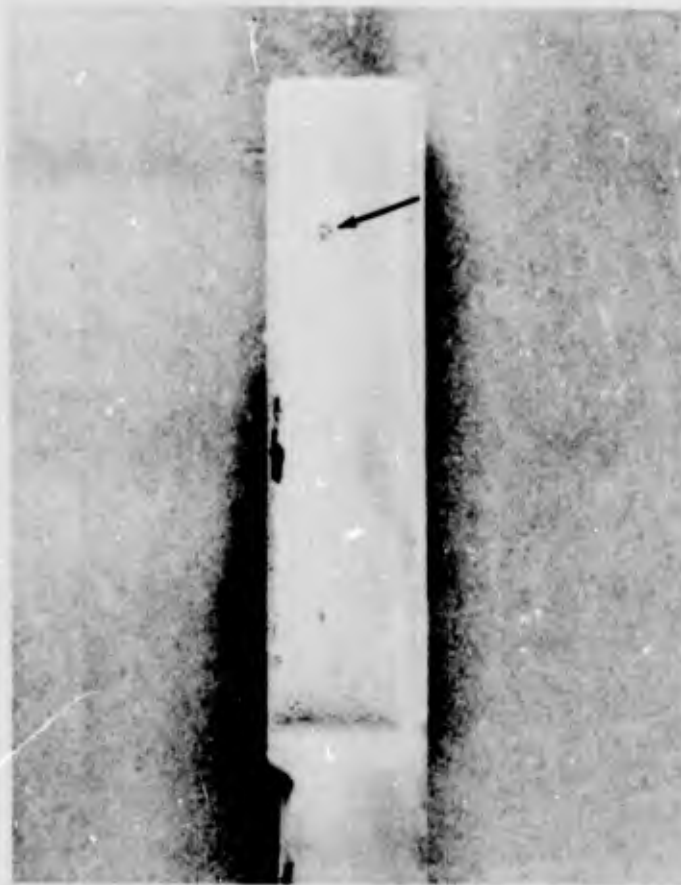
Figure 125. Oxidation-Erosion Life of Phase VII Sylvania SiCrTi Slurry Coated B-66 Alloy as a Function of Test Temperature



MAG: 1.6X

Figure 126. Phase VII Sylvania SiCrTi Slurry Coated B-66 Alloy Bar After Oxidation-Erosion Testing for 220 Hours at 2200°F

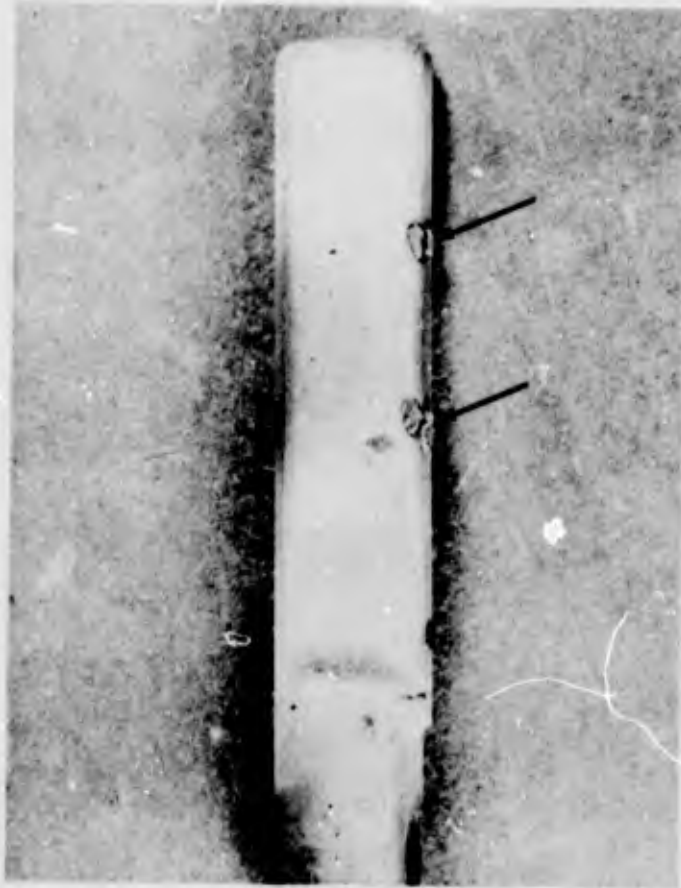
Failure resulted from oxidation along airfoil edge surfaces.



MAG: 1.6X

Figure 127. Phase VII Sylvania SiCrTi Slurry Coated B-66 Alloy Bar After Oxidation-Erosion Testing for 140 Hours at 2400°F

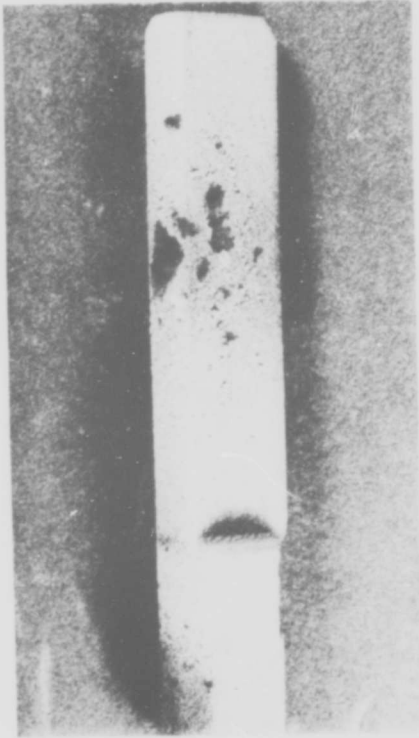
Substrate oxidation occurred along leading edge surfaces and on flat airfoil regions (arrow).



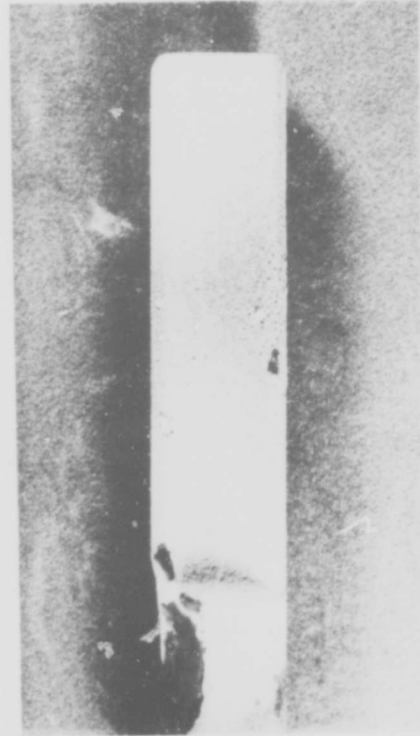
MAG: 1.6X

Figure 128. Phase VII Sylvania SiCrTi Slurry Coated B-66 Alloy Bar After Oxidation-Erosion Testing for 53 Hours at 2500°F

Failure resulted from localized substrate oxidation at the specimen leading edge surface (arrows).



SPECIMEN 1



SPECIMEN 4

MAG: 1.6X

Figure 129. Phase VII Sylvania SiCrTi Slurry Coated B-66 Alloy Bars After 200 Hours Total Time at 2200°F Plus 50 Minutes Total Transient Time to 2600°F

at 1800°, 2000°, 2200°, 2400°, and 2500°F was by a procedure identical to that described for the TRW TiCr-Si/Cb-132M system (paragraph 2.3.2). Each cycle consisted of 1 minute at the elevated temperature in a combusted JP-5 fuel and air stream followed by a 30-second cooling period.

The thermal fatigue results for two specimens per test temperature are presented in Figure 130 and are summarized below.

- 1800°F: No failures after 10,000 cycles; test stopped.
- 2000°F: No failures after 10,000 cycles; test stopped.
- 2200°F: Failures after 5800 and 6200 cycles.
- 2400°F: Failures after 3400 and 3600 cycles.
- 2500°F: Failures after 1400 cycles.

Thermal fatigue failures at 2200°, 2400°, and 2500°F occurred by oxidation along airfoil trailing edge surfaces. Prior to failure, outer coating layers in these regions were removed by the erosive gas stream. The results indicate that the Sylvania SiCrTi slurry coating on B-66 columbium alloy is relatively insensitive to rapid thermal cycling. This conclusion is supported by the melting test results reported in paragraph 5.3.1.2.

5.3.1.4 Ballistic Impact Test Results

Rectangular 0.050-inch-thick specimens were impacted at a velocity of 500 feet per second with 0.75-gram steel pellets. Four impacts at each of six temperatures (70°, 1600°, 2000°, 2200°, 2400°, and 2600°F) were performed after a 5-minute temperature stabilization. Spalling of outer silicide coating layers occurred on all specimens. The severity of spalling from the front and back specimen surfaces decreased as temperature was increased. Coating cracks extending into the B-66 substrate and radiating outward from the impact point occurred for all 70°F impacts. This behavior was caused in part by the decrease in ductility of the substrate due to recrystallization during the coating application process.

After impacting and subsequent inspection, all specimens were subjected to static oxidation exposure at 2200°F. The first appearance of substrate oxide constituted failure.

Oxidation surrounding all impact depressions occurred after a 1-hour exposure at 2200°F. Substrate oxidation radiating outward along surface cracks, which was severe for the 70°F, 500-ft/sec impacts on both the front and rear specimen surfaces at and directly behind the impact depressions (Figure 131), also occurred during the impact tests at 1600°F. Failure of the 2000°, 2200°, 2400°, and 2600°F impact areas, however, was confined to the front specimen surfaces in regions surrounding the impact

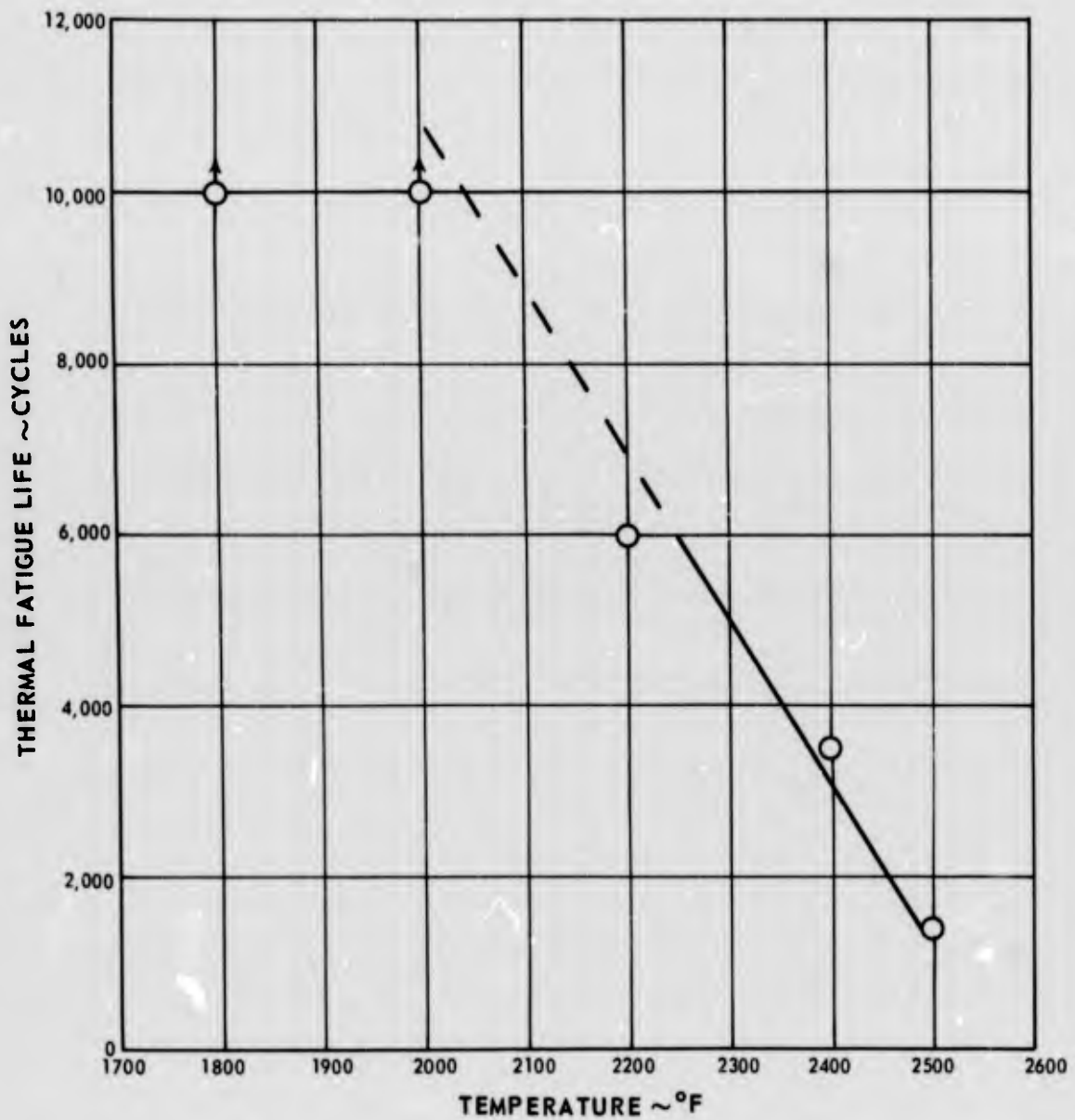
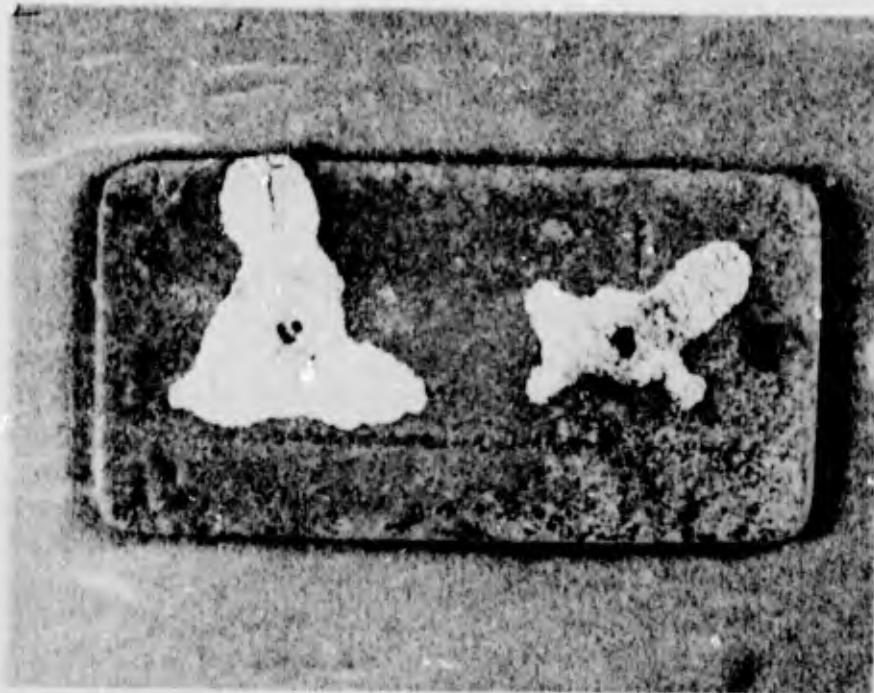
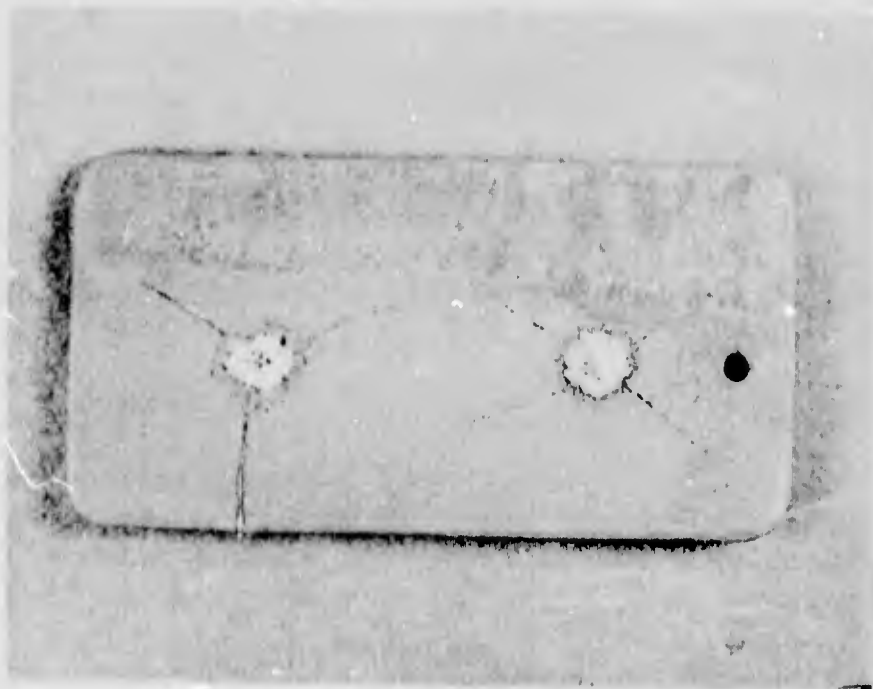


Figure 130. Thermal Fatigue Life of Phase VII Sylvania SiCrTi Slurry Coated B-66 Alloy as a Function of Test Temperature



POINTS OF IMPACT



SURFACE BEHIND IMPACT POINTS

Figure 131. Surfaces of Phase VII Sylvania SiCrTi Slurry Coated B-66 Alloy Test Specimens After Room Temperature Impacting at 500 Feet Per Second and Subsequent Static Oxidation Exposure For 1 Hour at 2200°F

depressions. Further exposure of the 2000°, 2200°, 2400°, and 2600°F impact specimens for 2 hours additional (total 3 hours) at 2200°F did not significantly degrade the test specimens further. This behavior appeared to be due to the adherent nature of the oxide surrounding the impact depression (Figure 132).

5.3.1.5 Stress-Rupture Test Results

Stress-rupture testing of the Sylvania SiCrTi/B-66 system was performed at 2200° and 2500°F at Metcut Research Associates. All tests were performed using 0.050-inch-thick sheet specimens. The specimen configuration is shown in Figure 133. Creep data were also obtained, though not required by the contract. A resistance-heated furnace was used for this testing at both temperatures. The specimens were placed in the furnace, aligned, and subjected to a small nominal load during the furnace heating cycle. After stabilization at the test temperature, the test load was applied using the specimen gage cross-sectional area prior to coating to establish the required stress level. Furnace temperature was monitored by an optical pyrometer which was calibrated by thermocouples for each test temperature. Creep extension of the specimen within the 1-inch-long gage section was measured optically.

Results of the creep-rupture testing at 2200° and 2500°F are summarized in Table XIII and illustrated in Figure 134. Included in Figure 134 are rupture and 1-percent-creep curves of uncoated stress-relieved 0.68-inch B-66 alloy sheet at 2200°F taken from published data (Ref. 3). Stress levels for 1- and 2-percent creep and rupture at 2200°F in 100 hours were 5000, 5800, and 9600 psi, respectively. At 2500°F the 100-hour 1- and 2-percent creep and rupture stress levels were 800, 1300, and 3900 psi, respectively. The rupture properties for Phase VII Sylvania SiCrTi slurry coated B-66 alloy at 2200° and 2500°F are inferior to those properties, at the same temperatures, of modified TRW TiCr-Si (vacuum) pack coated D-43 alloy, which was evaluated in Phase III of the program (see AFML-TR-66-186, Part I, paragraph 4.3.2.5, pages 181 and 186).

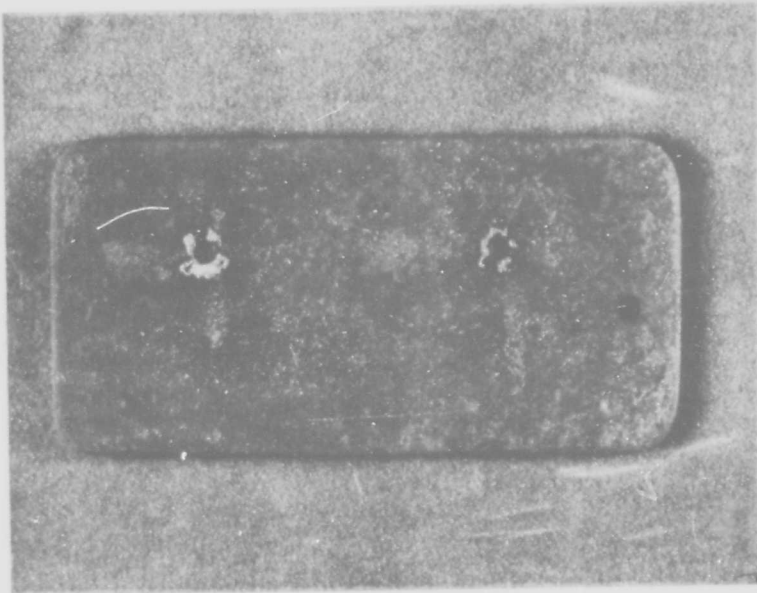
5.3.2 Blade Airfoil System, Modified Sylvania SiCrTi Slurry/XB-88

Advanced evaluation of the Sylvania SiCrTi/XB-88 blade airfoil system included oxidation-erosion, melting, thermal fatigue, ballistic impact, stress-rupture, and mechanical fatigue tests. In addition, Charpy impact tests were conducted, though not required by the contract.

5.3.2.1 Oxidation-Erosion Test Results

Oxidation-erosion testing of Sylvania SiCrTi/XB-88 utilized the test procedures described in paragraph 2.3.1. The tests were identical to those on the Sylvania SiCrTi/B-66 system. Performance of the Sylvania SiCrTi slurry coating on XB-88 alloy is illustrated in Figure 135. Test results are given below for each temperature.

- 1800°F: No airfoil failures after 900 hours; test stopped due to extensive grip area oxidation.



POINTS OF IMPACT



SURFACE BEHIND IMPACT POINTS

Figure 132. Surfaces of Phase VII Sylvania SiCrTi Slurry Coated B-66 Alloy After 2200°F Impacting at 500 Feet Per Second and Subsequent Static Oxidation Exposure for 3 Hours at 2200°F

Oxidation surrounding impact depressions (upper photograph) were first observed after 1 hour at 2200°F oxidation exposure.

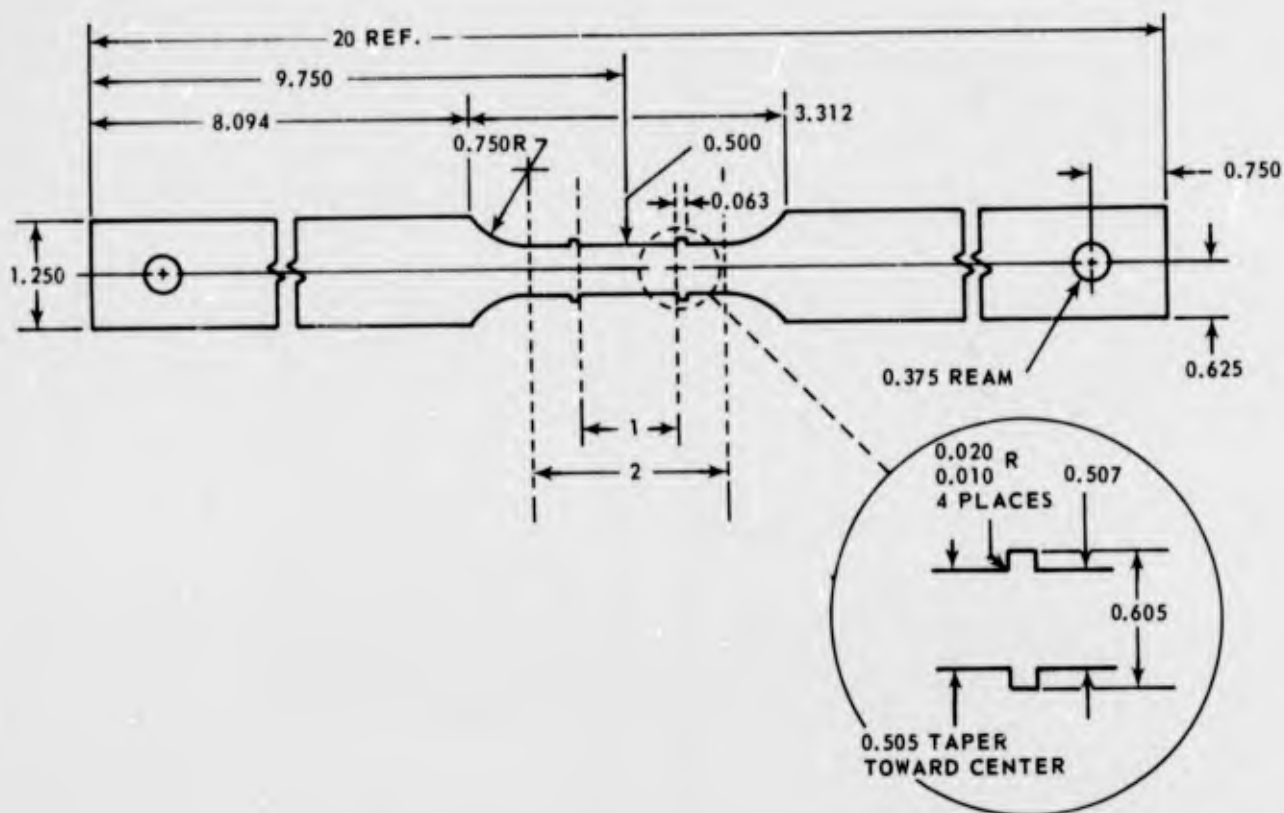


Figure 133. Sheet Creep-Rupture Specimen Configuration

TABLE XIII

RESULTS OF CREEP-RUPTURE TESTING OF PHASE VII
 SYLVANIA SiCrTi SLURRY COATED B-66 ALLOY

Test No.	Test Temperature (°F)	Stress (psi)	Time (hours)			
			0.5% Creep	1% Creep	2% Creep	Rupture
1	2200	14,000	---	3.1	4.0	27.5
2	2200	12,000	---	4.0	6.5	41.1
3	2200	10,000	2.5	6.0	13.0	93.8
4	2200	8,000	10.0	19.0	---	---
5	2200	6,000	---	45.0	---	---
6	2500	8,000	0.3	0.6	1.0	16.7
7	2500	6,000	1.0	1.9	2.8	34.6
8	2500	3,500	2.2	4.5	9.0	131.6
9	2500	2,000	8.0	17.0	34.0	---

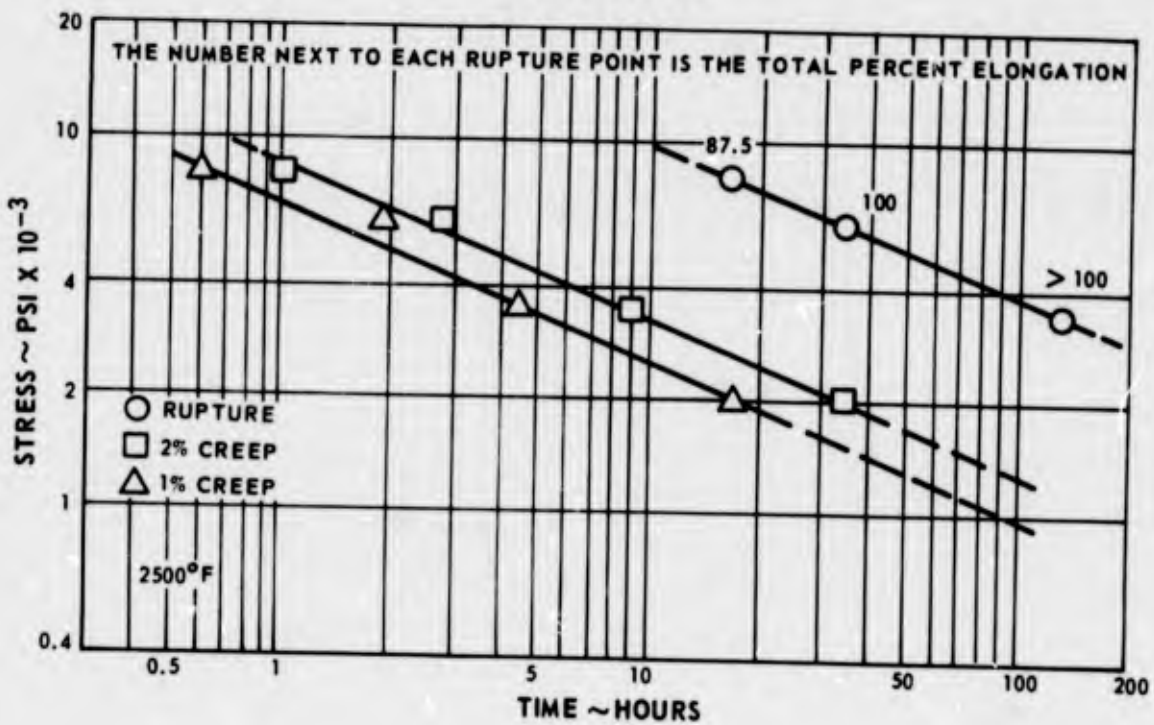
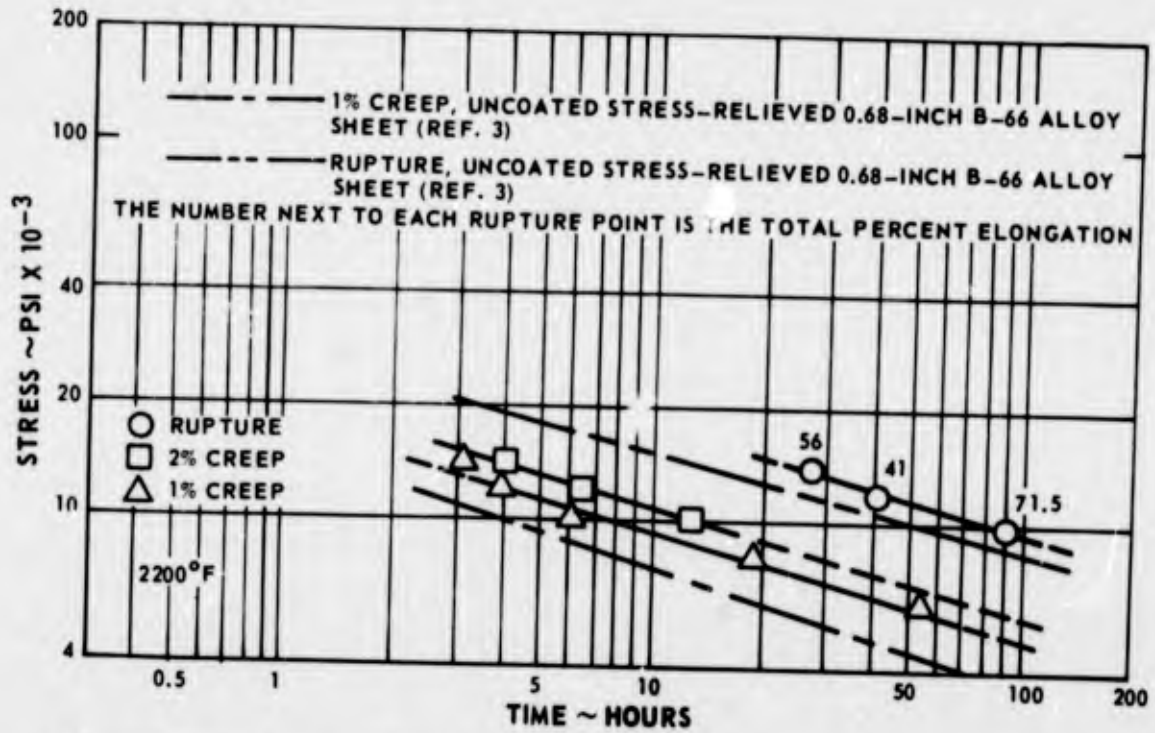


Figure 134. Creep-Rupture Properties of Phase VII Sylvania SiCrTi Slurry Coated B-66 Alloy at 2200° and 2500°F

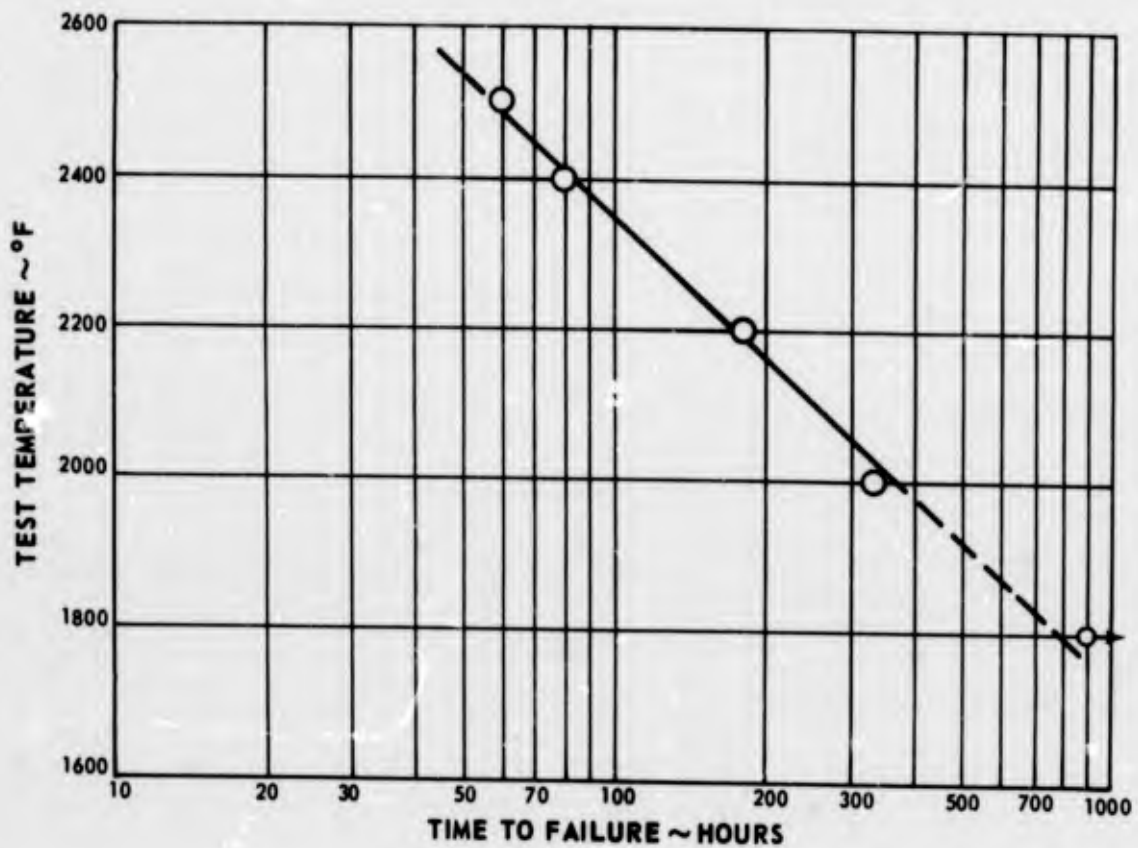


Figure 135. Oxidation-Erosion Life of Phase VII Sylvania SiCrTi Slurry Coated XB-88 Alloy as a Function of Test Temperature

- 2000°F: Failure after 280 and 380 hours for two specimens.
- 2200°F: Failure after 180 hours.
- 2400°F: Failure after 80 hours.
- 2500°F: Failure after 60 hours.

Up to 2400°F, failure occurred predominantly by localized oxidation along the airfoil trailing edge surfaces (Figure 136) and, in some cases, by the formation of point areas of substrate oxide (Figure 137). However, after 60 hours at 2500°F, more general oxidation occurred on airfoil edge surfaces (Figure 138). Erosion of outer coating layers during early stages of testing was observed at all temperatures. This condition remained through specimen failure as shown in Figure 137. Erosion was confined principally to the extreme outer regions of the coating, these regions containing numerous void areas and entrapped oxides (refer to paragraph 5.2.2, where coating application of the Sylvania SiCrTi coating on XB-88 alloy is discussed). Since coating removal was evident particularly at specimen corners and edges and since these were the predominant failure areas (Figures 136 through 138), coating erosion appears to have been the limiting factor for coating life.

5.3.2.2 Melting Test Results

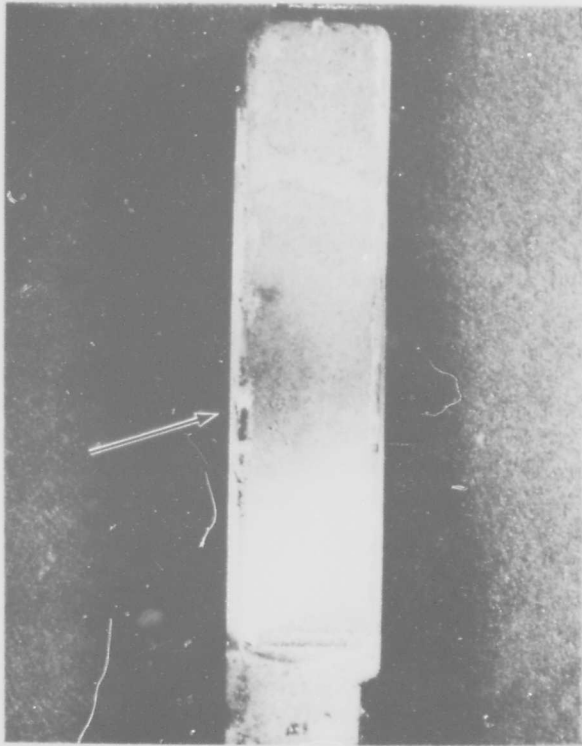
Oxidation-erosion testing at 2200°F with transient temperature overshoots to 2600°F was performed using the procedure described in paragraph 2.3.3. The Sylvania SiCrTi/XB-88 system demonstrated a performance of 140 hours at 2200°F plus 35 minutes total transient time to 2600°F for one specimen and 160 hours at 2200°F plus 40 minutes total transient time to 2600°F for three remaining specimens. Failure in all cases resulted from the formation of localized oxide on specimen airfoil surfaces (Figure 139).

Comparison of the cyclic oxidation-erosion performance with the 2200°F isothermal oxidation-erosion results indicates that the Sylvania SiCrTi slurry coating on XB-88 alloy was not significantly degraded by the cycling to 2600°F.

5.3.2.3 Thermal Fatigue Test Results

Thermal fatigue testing to 2200°, 2400°, and 2500°F was performed on forged paddle specimens of the configuration shown in Figure 13 according to test procedures described in paragraph 2.3.2. Results for two specimens at each temperature are summarized below. (Thermal fatigue tests were not conducted at 1800° and 2000°F on Sylvania SiCrTi/XB-88.)

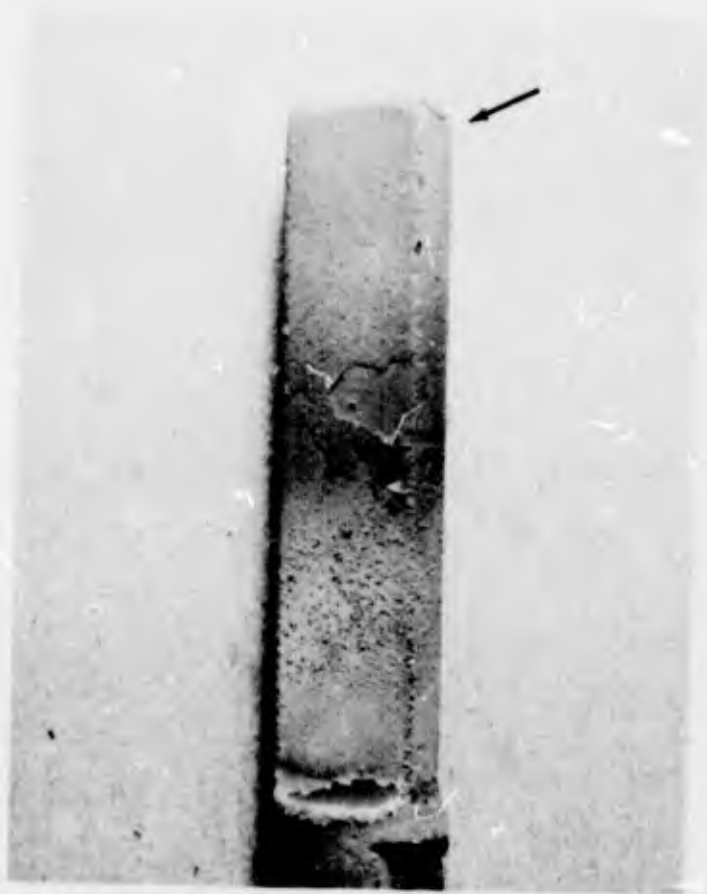
- 2200°F: Failure of both specimens after 2400 cycles.
- 2400°F: Failure of both specimens after 1800 cycles.
- 2500°F: Failure of both specimens after 1400 cycles.



MAG: 1.8X

Figure 136. Typical Surface Appearance of Phase VII Sylvania SiCrTi Slurry Coated XB-88 Alloy Bar After Oxidation-Erosion Testing for 180 Hours at 2200°F

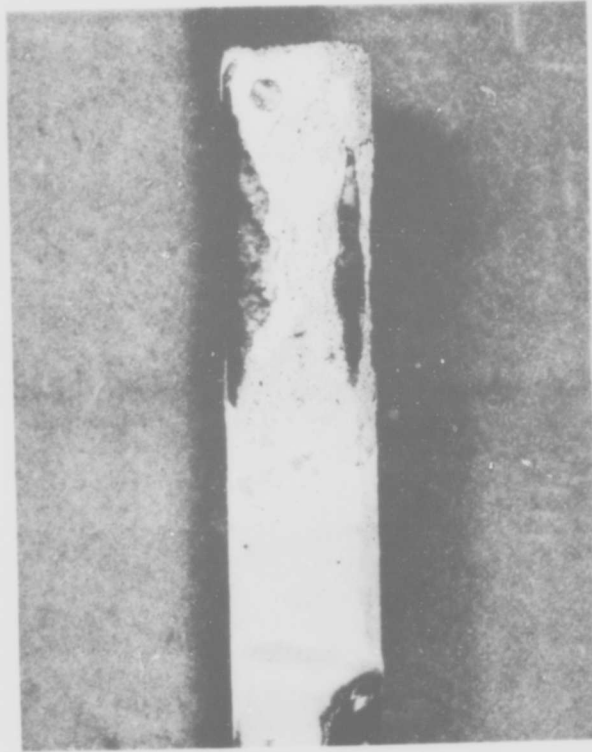
Note coating erosion and failure (arrow) along airfoil edge surfaces.



MAG: 1.8X

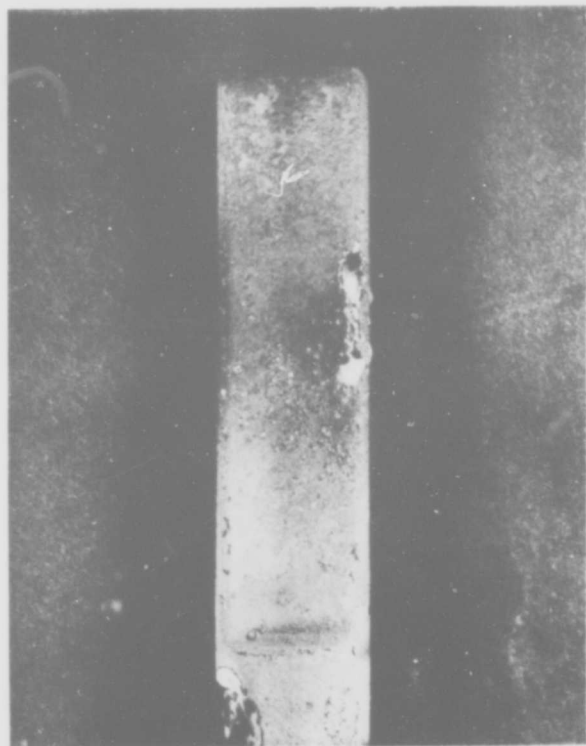
Figure 137. Typical Surface Appearance of Phase VII Sylvania SiCrTi Slurry Coated XB-88 Alloy Bar After Oxidation-Erosion Testing for 380 Hours at 2000°F

Note area of local oxidation at leading edge tip (arrow).



MAG: 1.8X

Figure 138. Surface Appearance of Phase VII Sylvania SiCrTi Slurry Coated XB-88 Alloy Bar After Oxidation-Erosion Testing for 60 Hours at 2500°F



MAG: 1.8X

Figure 139. Typical Surface Appearance of Phase VII Sylvania SiCrTi Slurry Coated XB-88 Alloy Bar After Melting (Transient Temperature Overshoot) Testing for 160 Hours at 2200°F Plus 40 Minutes Total Transient Time to 2600°F

Failure in all cases resulted from depletion of the coating and substrate oxidation along airfoil trailing edge surfaces.

5.3.2.4 Ballistic Impact Test Results

Test specimens (two per temperature) were impacted at 500 feet per second with a 0.75-gram steel pellet at 70°, 1600°, 2000°, 2200°, 2400°, and 2600°F. Impact procedure is described in paragraph 2.3.4. After impact and subsequent inspection, 2200°F oxidation exposure in static air resulted in failure for each test specimen after 1 hour exposure. Surface characteristics of the specimens after failure (Figure 140) were identical to those described for the Phase VII Sylvania SiCrTi slurry/B-66 vane system in paragraph 5.3.1.4.

5.3.2.5 Creep-Rupture Test Results

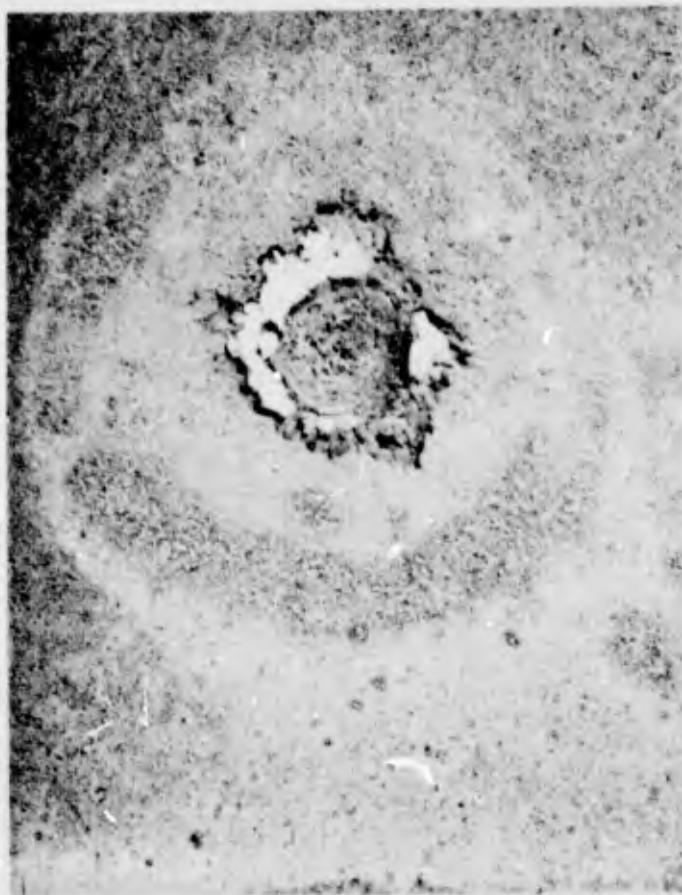
Creep testing in air at 1500°, 1800°, and 2200°F was performed at Metcut Research Associates using the specimen configuration shown in Figure 19. Testing was conducted in a resistance-heated furnace, and temperature was monitored with an optical pyrometer which had been calibrated with thermocouples prior to test initiation. The specimens were placed in the furnace, aligned, and placed under a nominal load during the furnace heating cycle. After temperature stabilization, the load was applied using the specimen gage cross-sectional area prior to coating to establish the required stress level.

As mentioned in the discussion of creep-rupture testing of the Phase IV Cb-132M alloy (paragraph 2.3.5), difficulties with the specimen grips limited the data obtained in creep-rupture testing. Creep-rupture data for Sylvania SiCrTi coated XB-88 alloy in air are presented in Table XIV, and tensile data are shown in Table XV. The creep-rupture data are plotted in Figure 141; for comparison purposes, Figure 141 includes data points for the TRW TiCr-Si coated Cb-132M alloy evaluated in Phase IV (paragraph 2.3.5).

5.3.2.6 Fatigue Test Results

Fatigue testing in air at 2200°F was performed using the specimen configuration shown in Figure 20. In a manner similar to the fatigue testing of the TRW TiCr-Si/Cb-132M system (paragraph 2.3.6), the Sylvania SiCrTi/XB-88 test specimens were calibrated utilizing static weight deflection, heated to 2200°F and stabilized at that temperature, and vibrated in reverse bending with a table shaker at a resonant frequency of 600 cycles per second.

The fatigue test results (Table XVI) indicate a fatigue limit between 45,000 and 50,000 psi. This stress level is approximately 65 percent of the ultimate strength for XB-88 alloy at 2200°F. The fracture surfaces of the two specimens which failed at a load of 50,000 psi had burnished and smooth areas indicative of fatigue failure (Figure 142).



MAG: 10X

Figure 140. Typical Surface Appearance of Phase VII Sylvania SiCrTi Slurry Coated XB-88 Alloy After 2000°F Impact Testing at 500 Feet Per Second and Subsequent Oxidation Exposure for 1 Hour at 2200°F

TABLE XIV

RESULTS OF CREEP-RUPTURE TESTING OF PHASE VII
SYLVANIA SiCrTi SLURRY COATED XB-88 ALLOY

Specimen No.	Test Temperature (°F)	Stress (psi)	Time (hours)					Elongation at Rupture (%)	
			0.1% Creep	0.2% Creep	0.5% Creep	1.0% Creep	2.0% Creep		Rupture
CR-7-5	1500	54,000	73	125	---	---	---	143.5 ^a	---
CR-7-3	1800	45,000	---	---	---	---	---	b	---
CR-7-2	1800	45,000	---	---	---	---	---	b	---
CR-7-6	2200	45,000	c	c	c	c	c	0.5	24.5
CR-7-9	2200	40,000	d	d	0.2	0.3	0.8	1.1	f
CR-7-10	2200	---	---	---	---	---	---	b	---
CR-7-11	2200	35,000	e	0.2	0.8	2.0	5.0	12.6	17.5
CR-7-8	2200	30,000	e	0.6	4.0	13.5	37.0	70.1	20.0

- Notes: a. Specimen removed without failure at time shown.
 b. Specimen failed on loading.
 c. 2% extension occurred on loading.
 d. 0.2% extension occurred on loading.
 e. 0.1% extension occurred on loading.
 f. Pin failure.

TABLE XV

TENSILE DATA FOR PHASE VII SYLVANIA SiCrTi
SLURRY COATED XB-88 ALLOY

Specimen No.	Test Temperature (°F)	Ultimate Tensile Strength (psi)	0.2% Yield Strength (psi)	Elongation (%)
CR-7-1	1500	59,500	54,200	1.5
CR-7-4	1800	58,200	44,300	2.0
CR-7-7	2000	12,600	---	---

Note: Specimen No. CR-7-7 failed before 0.2% yield stress was obtained.

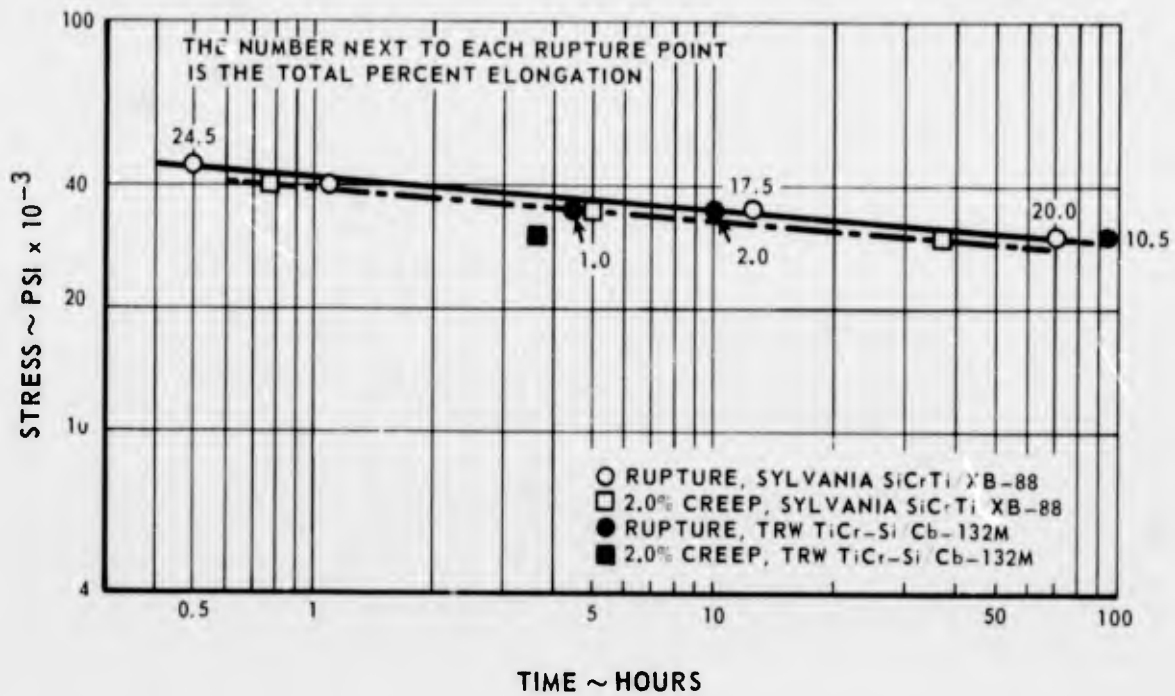


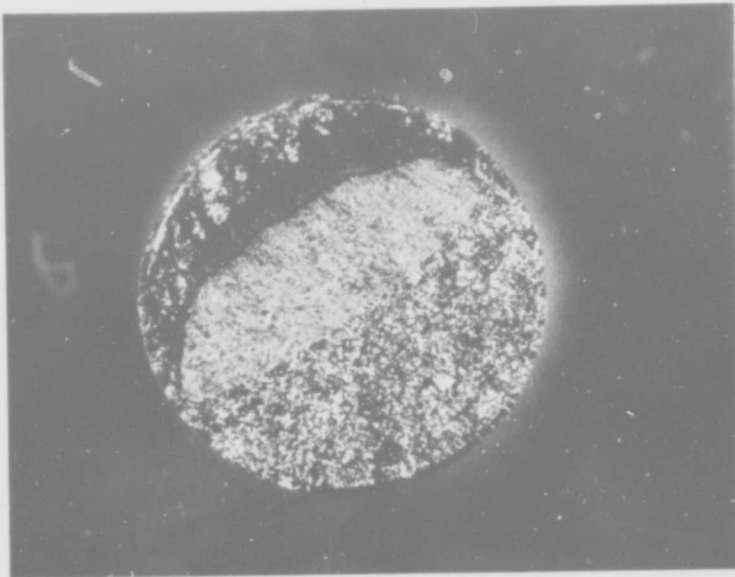
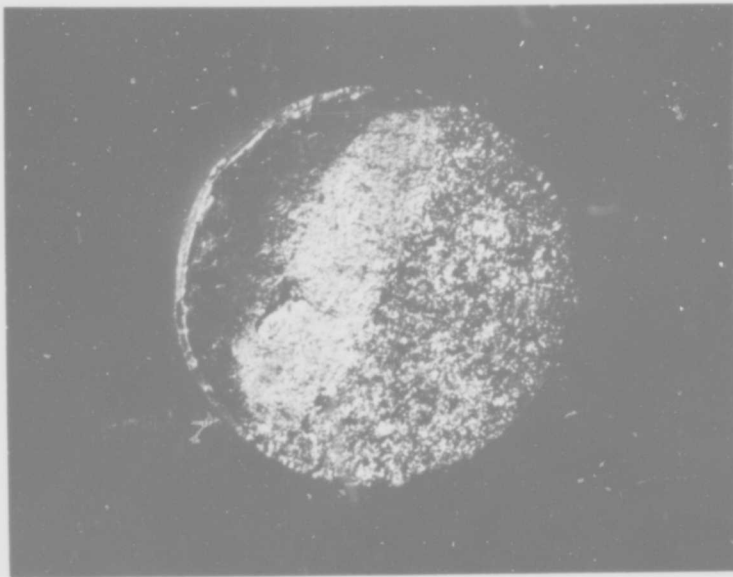
Figure 141. Creep-Rupture Properties of Phase VII Sylvania SiCrTi Slurry Coated XB-88 Alloy and Phase IV TRW TiCr-Si Coated Cb-132M Alloy at 2200°F

TABLE XVI

RESULTS OF FATIGUE TESTING OF PHASE VII
SYLVANIA SiCrTi SLURRY COATED XB-88 ALLOY IN AIR AT 2200°F

Test No.	Stress (psi)	Results
1	50,000	No failure after 10^7 cycles; test stopped
2	50,000	Failure after 0.54×10^7 cycles
3	50,000	Failure after 0.81×10^7 cycles
4	50,000	No failure after 10^7 cycles; test stopped
5	45,000	No failure after 10^7 cycles; test stopped
6	45,000	No failure after 10^7 cycles; test stopped
7	45,000	No failure after 10^7 cycles; test stopped
8	45,000	No failure after 10^7 cycles; test stopped

Note: All tests were conducted in reverse bending using a resonant frequency of 600 cycles per second.



MAG: 10X

Figure 142. Fracture Surfaces of Phase VII Sylvania SiCrTi Slurry Coated XB-88 Alloy After Fatigue Testing at 50,000 Psi Stress in Air at 2200°F

Failure occurred after 0.54×10^7 cycles for the specimen in the upper photograph and after 0.81×10^7 cycles for the lower specimen.

An anomaly was observed in fatigue testing of the Sylvania SiCrTi/XB-88 system. During early stages of reversed bending, vibration amplitude of all test specimens decreased markedly, indicating an increase in the alloy modulus of elasticity. Although the testing apparatus was thoroughly rechecked and all instrumentation recalibrated, this behavior persisted. All specimens were recalibrated after the vibration amplitude stabilized, and testing was continued until failure or runout. The cause of this behavior is undetermined, but all test data point to this being a condition resulting from the XB-88 columbium alloy material rather than from the testing apparatus. This conclusion is supported by the complete absence of this condition during testing of the Phase IV TRW TiCr-Si coating on Cb-132M columbium alloy at 2200°F.

5.3.2.7 Charpy Impact Test Results

Smooth Charpy impact testing of Sylvania SiCrTi coated XB-88 columbium alloy was performed in air at 70°, 1400°, 1700°, and 2000°F. Two uncoated specimens were also impacted at 70°F. Impact test results (Table XVII) indicate a ductile-brittle transition between 70°F and 1400°F. Very good toughness was indicated at 1400°, 1700°, and 2000°F; no failures were noted (Figure 143).

5.4 COMPOSITE MATERIALS, LOW-TEMPERATURE SYSTEMS

As a result of the Phase V preliminary screening evaluation of blade root coatings, the Sylvania SiCrFe slurry and TRW TiAl (vacuum) pack coatings were selected for advanced evaluation. Both coatings on Cb-132M columbium alloy exhibited good performance in the oxidation screening tests at 1300° and 1600°F, adequate prestrain capability, and good resistance to the imposed wear-galling conditions. Except for the NiCr and NiPt coatings, all of the blade root coatings had a detrimental effect on the ductility of the Cb-132M alloy to some degree. However, since the ductility of the uncoated Cb-132M alloy was marginal and inconsistent, a decision was made to perform the Phase VII advanced evaluation tests on XB-88 columbium alloy. The Air Force Materials Laboratory concurred in this decision and in the choice of the SiCrFe and TiAl coating systems.

5.5 COATINGS APPLICATION, LOW-TEMPERATURE SYSTEMS

5.5.1 Sylvania SiCrFe Slurry/XB-88

The Sylvania SiCrFe coating was applied to XB-88 alloy using a Si-20Cr-20Fe-mixture vehicle slurry and heat treating for 1 hour at 2550°F. Excellent coverage of specimen corners and edges was obtained. Five distinct regions were noted during metallographic examination of the 4.2-mil-thick coating (Figure 144). Above a continuous 0.2-mil-thick region at the coating-substrate interface, a continuous dark-colored 0.2-mil-thick region extended into a 0.3-mil third coating layer of dendritic appearance. Above this third layer, a 1.3-mil fourth layer appeared continuous and homogeneous. The two-phased outer coating region was 2.2 mils thick.

TABLE XVII

RESULTS OF SMOOTH CHARPY IMPACT TESTING OF PHASE VII
 SYLVANIA SiCrTi SLURRY COATED XB-88 ALLOY

Test No.	Specimen Condition	Specimen Temperature at Impact (°F)	Impact Strength (ft-lb)
1	Uncoated	70	3.0
2	Uncoated	70	10.5
3	Coated	70	2.5
4	Coated	70	2.0
5	Coated	1400	>60*
6	Coated	1400	>60*
7	Coated	1700	>120*
8	Coated	1700	>120*
9	Coated	2000	>120*
10	Coated	2000	>120*

*The coated specimens tested at 1400°, 1700°, and 2000°F did not fail.



MAG: 1.5X

Figure 143. Appearance of Phase VII Sylvania SiCrTi Slurry Coated XB-88 Alloy After Charpy Impact Testing at 1400°F, 60 Ft-Lb (Left); 1700°F, 120 Ft-Lb (Center); and 2000°F, 120 Ft-Lb (Right)

Ni PLATE



ETCH: 33% HYDROFLUORIC ACID, 33% NITRIC ACID, 33% WATER MAG: 500X

Figure 144. Typical Microstructure of As-Applied Sylvania SiCrFe Slurry Coating on XB-88 Alloy

5.5.2 TRW TiAl (Vacuum) Pack/XB-88

Application of the TiAl coating was performed at TRW utilizing the following parameters:

- Cycle 1: Titanium was deposited at 2000°F for 13 hours in an argon atmosphere.
- Cycle 2: Aluminum was deposited from a 56Cr-44Al prealloyed pack at 1900°F for 4 hours in a partial vacuum.

Specimen edges and corners appeared to have excellent coverage.

Metallographic examination revealed three distinct coating regions in the 5.5-mil-thick coating (Figure 145). A 1.2-mil-thick solid solution zone was present adjacent to the substrate. Above this solid solution zone, a 3.0-mil-thick intermediate coating layer was observed, consisting primarily of a transformed beta-type titanium structure with spheroidal precipitates dispersed throughout. The outer 0.8-mil-thick coating layer was very irregular and contained numerous cracks penetrating to the intermediate coating region.

5.6 SYSTEMS EVALUATION, LOW-TEMPERATURE SYSTEMS

Three test procedures were utilized in advanced evaluations: 1400° and 1600°F static oxidation, cyclic oxidation including transient overshoot periods above 1600°F, and fatigue testing at 1250° and 1600°F. The fatigue tests used both smooth and notched specimen configurations for both blade root coatings and coating overlap joints with the Sylvania SiCrTi slurry blade airfoil coating.

5.6.1 Static Oxidation Test Results

Oxidation testing was conducted at 1400° and 1600°F in static air using 0.75-inch-diameter, 0.25-inch-thick disk coupons. Five specimens of each coating-substrate system were tested at each temperature. Specimens were removed from the furnace and inspected at 24-hour intervals. Failure was defined as the first appearance of substrate oxide on the specimen surface. Test results are presented in Table XVIII.

The SiCrFe coating performed adequately for the intended application, with the first failure occurring at 571 hours of test. In addition, only one of the remaining specimens failed during testing, and that after 960 test hours. The TiAl coating did not perform as well, with the initial failure occurring at 77 hours and only five of the ten test coupons surviving the total exposure. Failures of the SiCrFe and the TiAl coatings on XB-88 are shown in Figures 146 and 147.

Stability of both the SiCrFe and the TiAl coatings was evaluated by metallographic examination of specimens exposed in excess of 1100 hours at 1600°F. The TiAl coating developed a substantial precipitate in the intermediate coating layer (Figure 148), but no significant depletion of the coating was observed. The SiCrFe coating exhibited



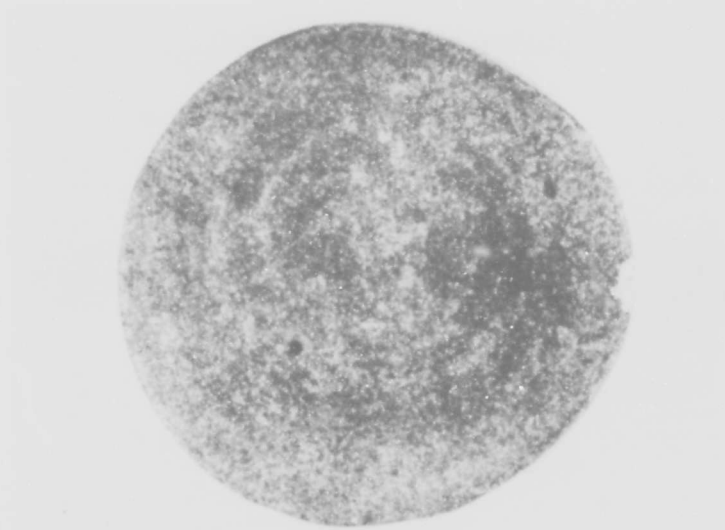
ETCH: 33% HYDROFLUORIC ACID, 33% NITRIC ACID, 33% WATER MAG: 500X

Figure 145. Typical Microstructure of As-Applied TRW TiAl (Vacuum) Pack Coating on XB-88 Alloy

TABLE XVIII

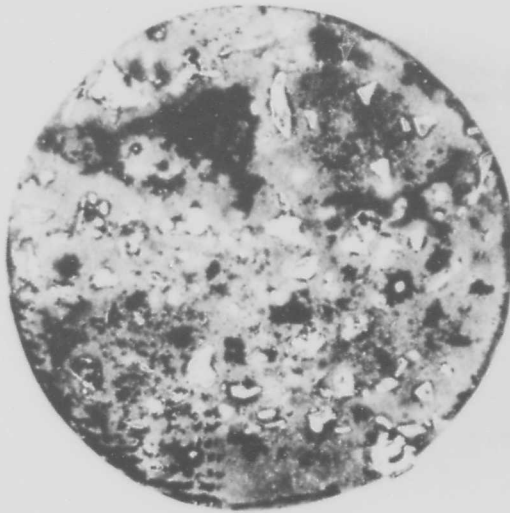
RESULTS OF STATIC OXIDATION TESTING OF
PHASE VII BLADE ROOT SYSTEMS

Coating-Substrate System	Temperature (°F)	Test Results
Sylvania SiCrFe/XB-88	1400	One edge failure after 960 hours; no failures on remaining four specimens after 1152 hours; test stopped
	1600	One edge failure after 571 hours; no failures for remaining four specimens after 1176 hours; test stopped
TRW TiAl/XB-88	1400	Edge or surface failures after 365 and 1162 hours; no failures on remaining three specimens after 1162 hours; test stopped
	1600	Edge or surface failures after 77, 653, and 940 hours; no failures on remaining two specimens after 1162 hours; test stopped



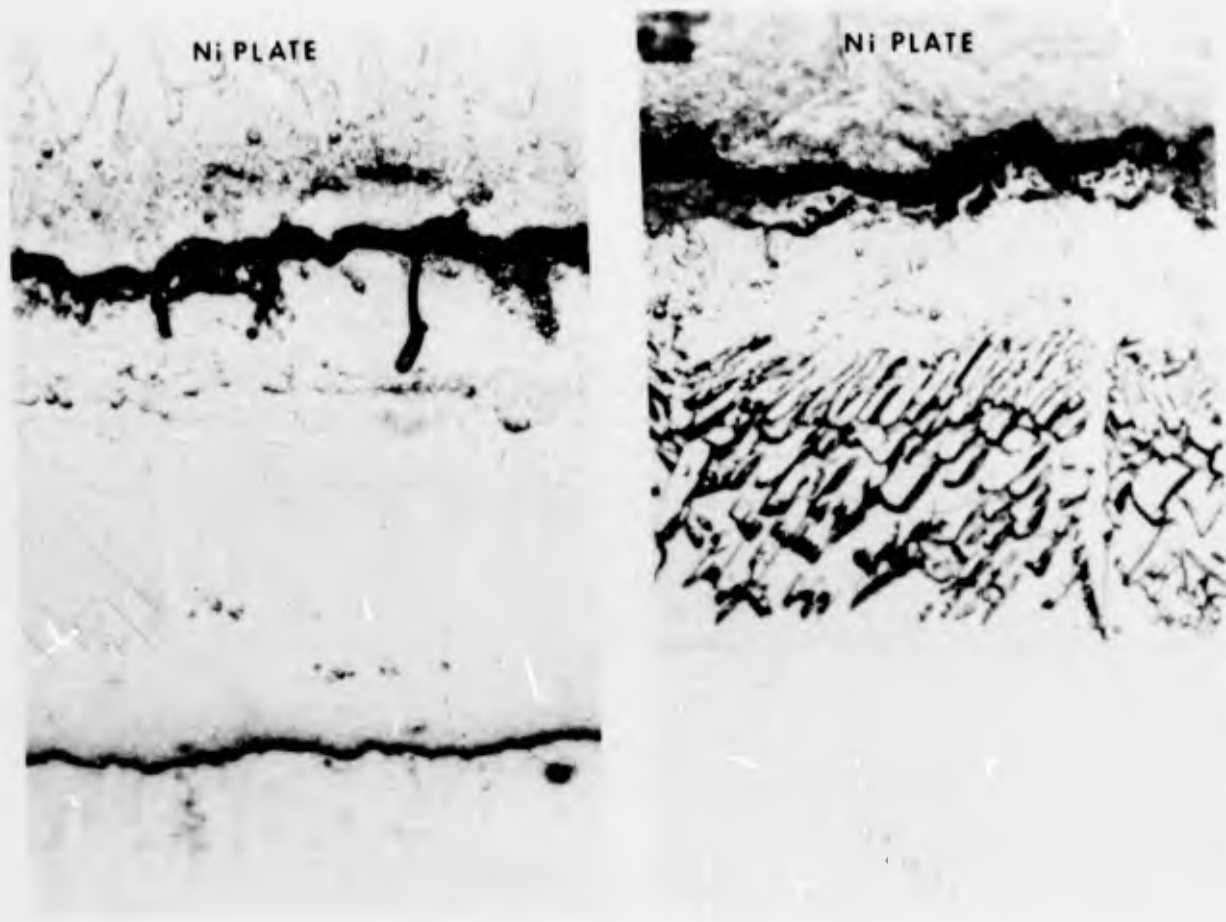
MAG: 3X

Figure 146. Sylvania SiCrFe Slurry Coated XB-88 Alloy Specimen Showing Edge Failure After 571 Hours Static Oxidation Exposure at 1600°F



MAG: 3X

Figure 147. TRW TiAl (Vacuum) Pack Coated XB-88 Alloy Specimen Showing Edge Failure After 77 Hours Static Oxidation Exposure at 1600°F



ETCH: 33% HYDROFLUORIC ACID, 33% NITRIC ACID, 33% WATER MAG: 500X

Figure 148. Typical Microstructure of As-Applied (Left) and Exposed (Right) TRW TiAl (Vacuum) Pack Coated XB-88 Alloy

Exposure was for 1162 hours in air at 1600°F.

oxidation of approximately 1 mil of the outer coating layer (Figure 149), but no significant microstructural changes in the coating-substrate composite were evident.

5.6.2 Cyclic Oxidation Test Results

Coupons similar to those described in the discussion of static oxidation testing (paragraph 5.6.1) were cycled from 1400° and 1600°F to 2000°F. Cycling was performed by transferring coupons between furnaces stabilized at the appropriate temperatures. Transfer time was approximately 1 minute. After five cycles, each consisting of 1 hour at 1400° or 1600°F followed by 1 hour at 2000°F, the specimens were exposed in still air at the lower temperature until failure. Five specimens of each coating were tested at each cyclic condition.

No failures resulted for either the Sylvania SiCrFe or the TRW TiAl coatings after the five cyclic periods of both the 1400°-2000°F and 1600°-2000°F tests. Results of the subsequent testing at 1400° and 1600°F are summarized in Table XIX.

Although there was an edge failure after 24 hours of test at 1600°F on one of the SiCrFe coated specimens (Figure 150), this system performed well, with the remaining nine specimens all surviving the test period. The TiAl coated specimens did not perform satisfactorily, with failure occurring at 24, 48, and 96 hours and only one of the ten specimens surviving the test period. Figures 151 and 152 illustrate failures of the TiAl coating at 1400° and 1600°F exposure, respectively.

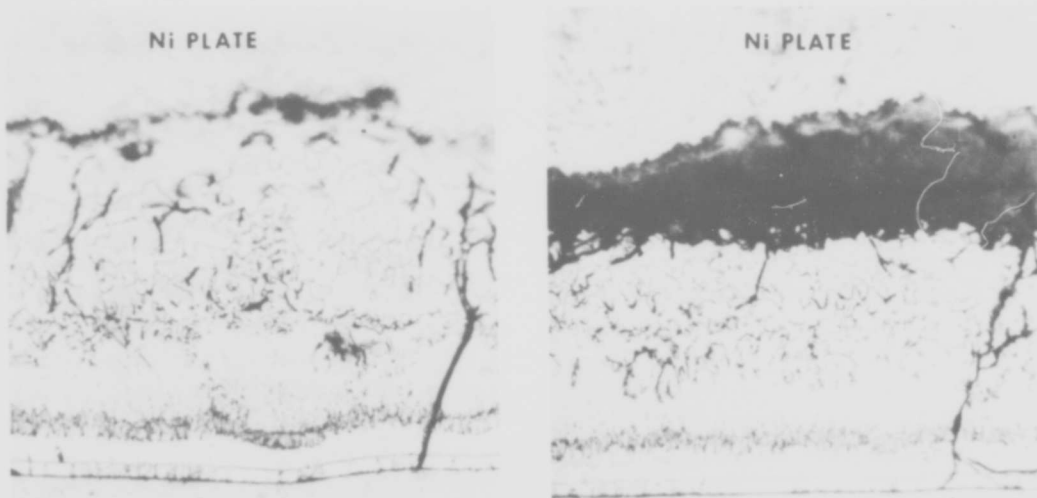
5.6.3 Fatigue Test Results

Fatigue testing of the Sylvania SiCrFe/XB-88 and the TRW TiAl/XB-88 systems was conducted in air at 1250° and 1600°F using smooth and notched ($K_t = 3.2$) specimens (Figure 153). The specimens were calibrated utilizing static weight deflection, heated to the desired test temperature, and vibrated in reverse bending at a frequency of 120 cycles per second. Test results are presented in Tables XX and XXI.

At 1200°F the Sylvania SiCrFe coated notched XB-88 alloy specimens exhibited a fatigue limit of about 49,000 psi, which is approximately 90 percent of the 0.2-percent yield strength of uncoated XB-88 at 1250°F. After test, all specimens were fractured and examined for evidence of fatigue. The fracture surfaces of specimens which had been fatigue tested for 10^7 cycles are shown in Figure 154.

At 1250°F the TRW TiAl coated notched XB-88 alloy specimen exhibited a fatigue limit of less than 30,000 psi, while the smooth specimens had a fatigue limit greater than 55,000 psi, which is approximately equal to the yield strength of the uncoated alloy. The fracture surfaces of the notched specimens after test and room temperature fracture showed small oxidized areas of fatigue progression (Figure 155).

The TRW TiAl and the Sylvania SiCrFe coated smooth XB-88 alloy fatigue specimens exhibited similar results in 1600°F air testing. Both systems had a fatigue limit in excess of 48,500 psi, which is greater than 90 percent of the yield strength



ETCH: 33% HYDROFLUORIC ACID, 33% NITRIC ACID, 33% WATER MAG: 500X

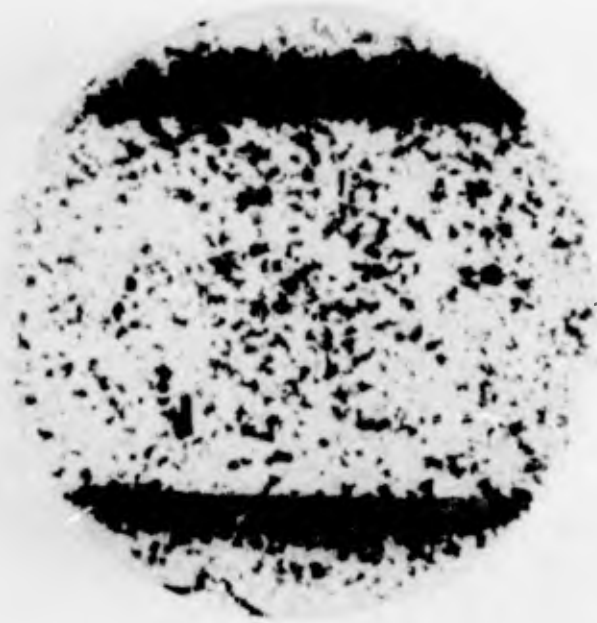
Figure 149. Typical Microstructure of As-Applied (Left) and Exposed (Right) Sylvania SiCrFe Slurry Coated XB-88 Alloy

Exposure was for 1176 hours in air at 1600°F.

TABLE XIX

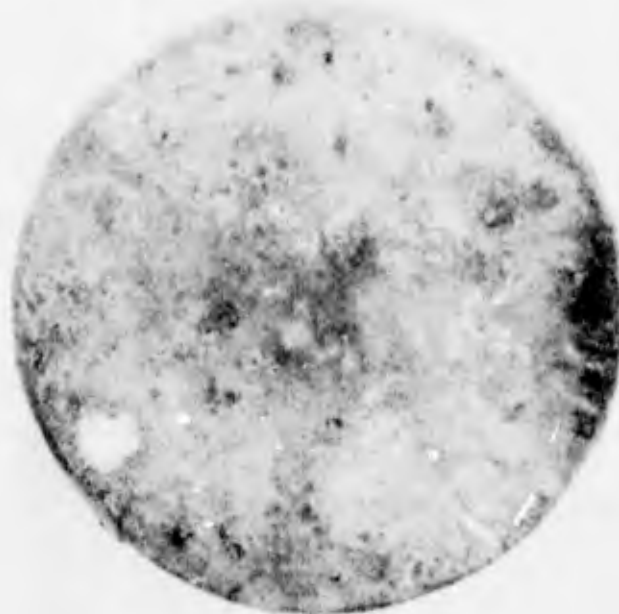
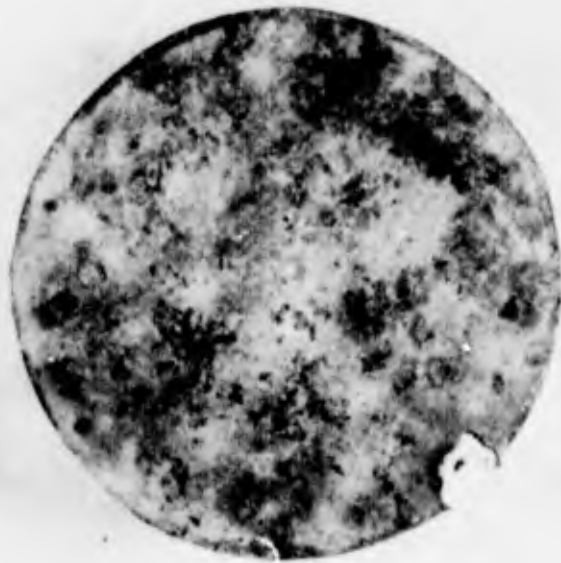
RESULTS OF CYCLIC OXIDATION TESTING OF
PHASE VII BLADE ROOT SYSTEMS

Coating-Substrate System	Temperature (°F)	Postcyclic Exposure Results
Sylvania SiCrFe/XB-88	1400	No failures after 1013 hours; test stopped
	1600	One edge failure after 24 hours; no failures on remaining four specimens after 1013 hours; test stopped
TRW TiAl/XB-88	1400	Edge or surface failures after 96, 168, 216, and 1013 hours; no failure on remaining specimen after 1013 hours; test stopped
	1600	Edge or surface failures after 24, 48, 168, 168, and 821 hours



MAG: 3X

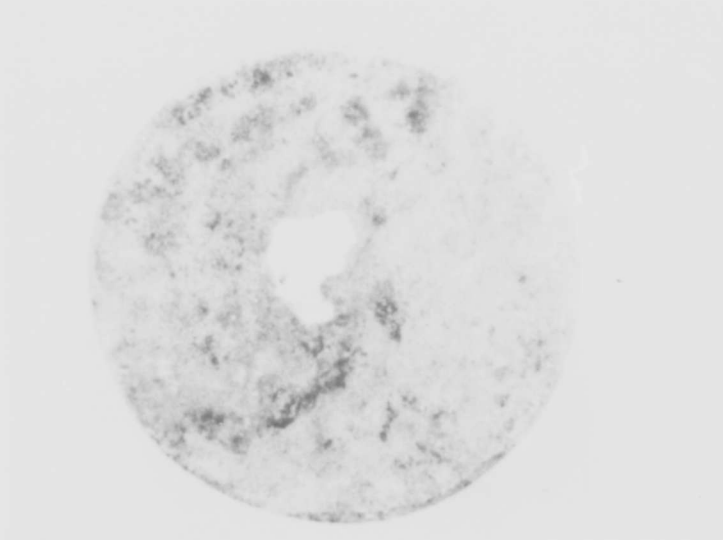
Figure 150. Sylvania SiCrFe Slurry Coated XB-88 Alloy Specimen Showing Edge Failure After 24-Hour Postcyclic Exposure at 1600°F



MAG: 3X

Figure 151. TRW TiAl (Vacuum) Pack Coated XB-88 Alloy Specimens Showing Edge and Surface Failures After Postcyclic Exposure at 1400°F

The specimen at top failed after 168 hours exposure; the specimen at bottom failed after 96 hours exposure.



MAG: 3X

Figure 152. TRW TiAl (Vacuum) Pack Coated XB-88 Alloy Specimens Showing Typical Edge and Surface Failures After Postcyclic Exposure at 1600°F

The specimen at top failed after 168 hours exposure; the specimen at bottom failed after 48 hours exposure.

TABLE XX

RESULTS OF FATIGUE TESTING OF PHASE VII
COATED XB-88 ALLOY AT 1250°F

Specimen Coating	Specimen Configuration	Stress (psi)	Results
Sylvania SiCrFe	Notched	34,500	No failure after 10^7 cycles; test stopped
Sylvania SiCrFe	Notched	42,500	No failure after 10^7 cycles; test stopped
Sylvania SiCrFe	Notched	49,000	No failure after 10^7 cycles; test stopped
Sylvania SiCrFe	Notched	54,500	Failure after 2.1×10^6 cycles
Sylvania SiCrFe/SiCrTi overlap joint	Smooth	59,000	Failure after 1.3×10^5 cycles
TRW TiAl	Notched	26,000	No failure after 10^7 cycles; test stopped
TRW TiAl	Notched	30,000	Failure after 4.0×10^6 cycles
TRW TiAl	Smooth	55,000	No failure after 10^7 cycles; test stopped
TRW TiAl	Smooth	55,000	No failure after 10^7 cycles; test stopped
TRW TiAl/Sylvania SiCrTi overlap joint	Smooth	50,000	Failure after 3.0×10^5 cycles
TRW TiAl/Sylvania SiCrTi overlap joint	Smooth	54,000	Failure after 3.5×10^6 cycles

TABLE XXI

RESULTS OF FATIGUE TESTING OF PHASE VII
COATED XB-88 ALLOY AT 1600°F

Specimen Coating	Specimen Configuration	Stress (psi)	Results
Sylvania SiCrFe	Smooth	48,000	No failure after 10^7 cycles; test stopped
Sylvania SiCrFe	Smooth	48,500	No failure after 10^7 cycles; test stopped
Sylvania SiCrFe	Smooth	55,000	Failure after 3.8×10^6 cycles
Sylvania SiCrFe/ SiCrTi overlap joint	Smooth	54,000	No failure after 10^7 cycles; test stopped
TRW TiAl	Smooth	46,000	No failure after 10^7 cycles; test stopped
TRW TiAl	Smooth	48,500	No failure after 10^7 cycles; test stopped
TRW TiAl	Smooth	52,500	Failure after 6.1×10^5 cycles
TRW TiAl	Smooth	56,000	Failure after 1.3×10^5 cycles



MAG: 10 X

Figure 154. Sylvania SiCrFe Slurry Coated XB-88 Alloy Notched ($K_t = 3.2$) Fatigue Specimens Showing Room Temperature Fracture Surface After Testing in Air at 1250°F

Neither specimen had failed after 1.0×10^7 cycles. The specimen at top ran at a stress of 49,000 psi; the specimen at bottom ran at a stress of 42,500 psi.



MAG: 10X

Figure 155. TRW TiAl (Vacuum) Pack Coated XB-88 Alloy Notched ($K_t = 3.2$) Fatigue Specimen Showing Room Temperature Fracture Surface After Testing at 30,000 Psi in Air at 1250°F

Failure occurred after 4.0×10^6 cycles. Arrows indicate areas of fatigue.

of the uncoated XB-88 alloy. Fracture surfaces of the specimens indicated fatigue progression (Figures 156 and 157).

Fatigue specimens were prepared to simulate the overlap area between a blade airfoil coating (Sylvania SiCrTi) and the candidate blade root coatings (Sylvania SiCrFe and TRW TiAl). Two TiAl/SiCrTi smooth overlap specimens were tested at 1250°F (Figure 158). One specimen failed in the overlap area and one failed in the TiAl coated area. The failure point of 3.5×10^6 cycles at 54,000 psi indicates that there are no serious problems in the overlap area with the TiAl/SiCrTi systems.

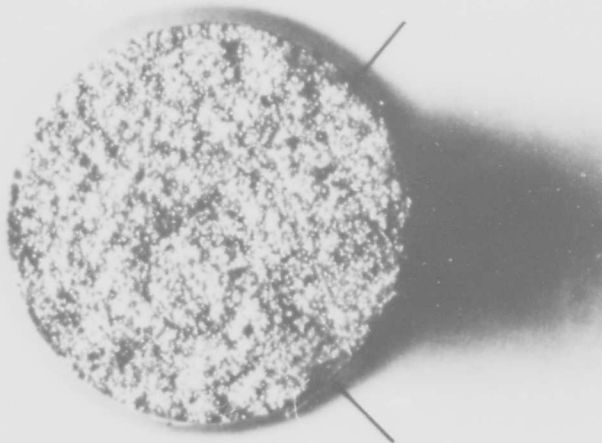
Two SiCrFe/SiCrTi smooth overlap specimens were also tested, one at 1250°F and one at 1600°F. The 1600°F specimen exhibited a fatigue limit in excess of 54,000 psi while the 1250°F specimen failed in the overlap area (Figure 159) after 1.3×10^5 cycles at 59,000 psi. The fracture surface of the latter specimen (Figure 160) indicates multiple fatigue origins. These tests indicate that the SiCrFe/SiCrTi coating systems are compatible in fatigue.



MAG: 10X

Figure 157. TRW TiAl (Vacuum) Pack Coated XB-88 Alloy Smooth Fatigue Specimen Showing Room Temperature Fracture Surface After Testing at 52,500 Psi Stress in Air at 1600°F

Failure occurred after 6.1×10^5 cycles. Dark areas are the areas of fatigue.



MAG: 10X

Figure 156. Sylvania SiCrFe Slurry Coated XB-88 Alloy Smooth Fatigue Specimen Showing Room Temperature Fracture Surface After Testing at 55,000 Psi Stress in Air at 1600°F

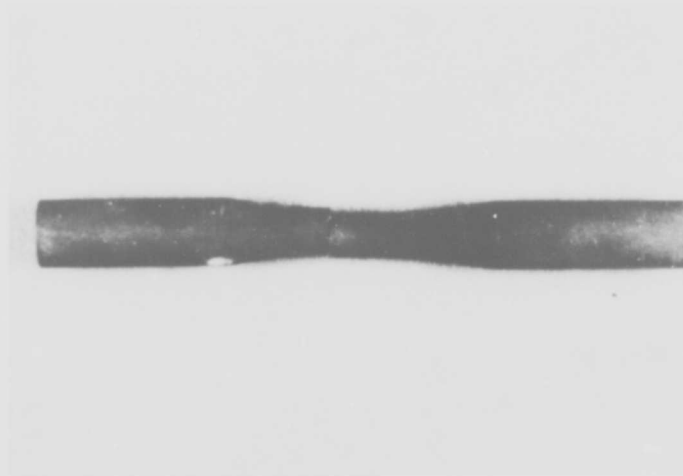
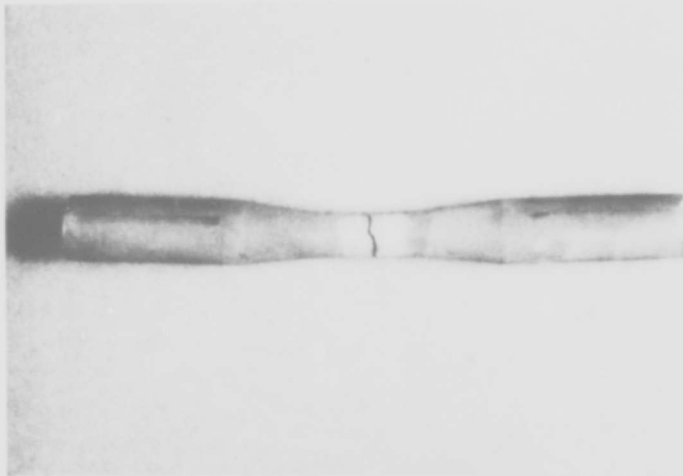
Failure occurred after 3.8×10^6 cycles. Arrows indicate areas of fatigue.



MAG: 1X

Figure 158. TRW TiAl (Vacuum) Pack Plus Sylvania SiCrTi Slurry Coated Compatibility Fatigue Specimens After Testing in Air at 1250°F

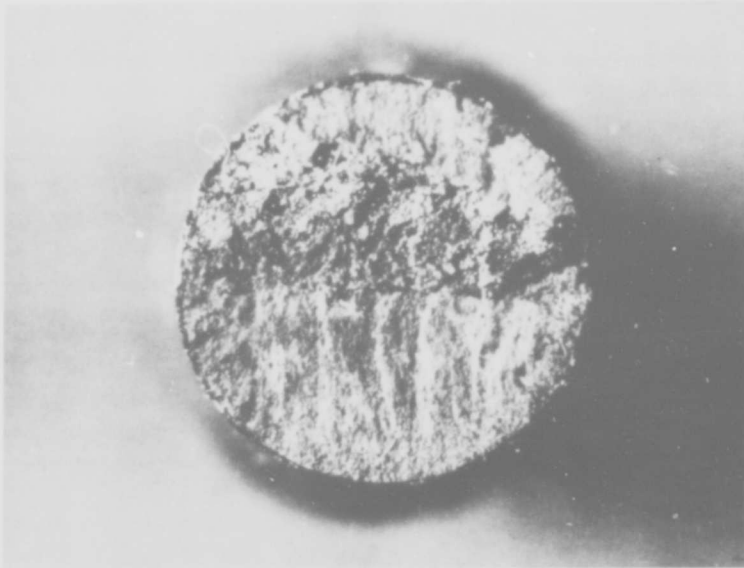
The specimen at top was tested at a stress of 50,000 psi and failed after 3.0×10^5 cycles. The specimen at bottom was tested at a stress of 54,000 psi and failed after 3.5×10^6 cycles.



MAG: 1X

Figure 159. Sylvania SiCrFe Slurry Plus Sylvania SiCrTi Slurry Coated Compatibility Fatigue Specimens After Testing in Air

The specimen at top was tested at a stress of 54,000 psi at 1600°F and had not failed after 1.0×10^7 cycles. The specimen at bottom was tested at a stress of 59,000 psi at 1250°F and failed after 1.3×10^5 cycles.



MAG: 10X

Figure 160. Sylvania SiCrFe Slurry Plus Sylvania SiCrTi Slurry Coated Compatibility Fatigue Specimen Showing Room Temperature Fracture Surface After Testing at 59,000 Psi Stress in Air at 1250°F

Failure occurred after 1.3×10^5 cycles. Dark areas are the areas of fatigue.

SECTION IV

CONCLUSIONS AND RECOMMENDATIONS

1. CONCLUSIONS

The following conclusions have been drawn based on the performance of the vane, blade airfoil, and blade root coating-substrate systems evaluated during the second year of the program:

- The Sylvania SiCrTi slurry coating on B-66 columbium alloy exhibits the best performance of the vane systems evaluated during the two-year effort. The oxidation life of this system was uniquely insensitive to thermal cycling. Although increasing the thickness of the SiCrTi coating does not increase the maximum oxidation-erosion and thermal fatigue lives, it does significantly improve reliability.
- The Sylvania SiCrTi slurry coated B-66 columbium alloy has marginal strength for turbine vane application above an average metal temperature of 2200°F, based on the 1-percent and 2-percent creep and stress-rupture lives.
- Overall performance of the Sylvania SiCrTi slurry coating is superior to that of the TRW TiCr-Si (vacuum) pack coatings (60Cr-40Ti and 50Cr-50Ti packs) on XB-88 columbium alloy. This conclusion is based largely on the significantly better thermal fatigue performance of the Sylvania SiCrTi coating.
- In oxidation-erosion, the Sylvania SiCrTi slurry coating life is approximately 10 percent greater when the coating is applied to B-66 than when applied to XB-88 columbium alloy. The oxidation life of the coating on XB-88 appeared limited by erosion of the outer coating layers. This behavior is attributed to the high tungsten content (28 percent nominal) of the XB-88 alloy.
- Transient temperature overshoots to 2600°F do not significantly affect the 2200°F oxidation-erosion life of Sylvania SiCrTi slurry coated B-66 and XB-88 columbium alloys.
- The Solar V-CrTi-Si/Cb-132M system does not show promise for blade airfoil application, based on its poor performance in oxidation-erosion and thermal fatigue tests. However, an extracontractual Solar V-(CrTi)-Si coating, which is believed to be a modification of the Phase V V-CrTi-Si coating, demonstrated good oxidation-erosion life and warrants further testing in thermal fatigue.
- The Sylvania SiCrV slurry coated Cb-132M alloy system performance is adequate in oxidation-erosion and excellent in resistance to thermal fatigue.

- All of the Sylvania slurry coated systems evaluated in blade airfoil and vane tests, i. e. SiCrTi/B-66, SiCrTi/XB-88, and SiCrV/Cb-132M, are relatively insensitive to the cyclic conditions used in the thermal fatigue evaluations. As mentioned in the first conclusion, the SiCrTi/B-66 system was particularly good in this regard.
- The Solar MoTi-Si (TNV-12SE4) coated Cb-132M alloy supplemental system exhibited the best oxidation-erosion and thermal fatigue performance of all vane and blade airfoil systems. As a supplemental system it was not a candidate for advanced evaluation. Protection appears to be enhanced by the presence of a high-viscosity glassy phase which devitrifies as glassy nodules on the coating surface on cooling.
- The smooth reverse-bending fatigue strengths of both the Sylvania SiCrTi/XB-88 and TRW TiCr-Si/Cb-132M systems are adequate for blade airfoil application. The 10^7 -cycle fatigue limits at 2200°F were 45,000 and 35,000 psi, respectively.
- The creep and stress-rupture strengths of the Sylvania SiCrTi/XB-88 and TRW TiCr-Si/Cb-132M systems are adequate for turbine blade airfoil applications to approximately 2200°F. However, tensile and creep-rupture ductilities in the intermediate temperature range (1300°-1800°F) are very low for both systems, ranging from nil to 1 percent. For this reason, these composites would be susceptible to premature failure during thermal cycling in a turbine blade airfoil environment.
- Smooth Charpy impact energy absorptions for TRW TiCr-Si coated Cb-132M alloy were very low from 70° to 2000°F (maximum of 5 ft-lb). The Sylvania SiCrTi/XB-88 system showed a brittle-ductile transition between 70° and 1400°F. Strengths at 70°F were approximately 2 ft-lb, while at 1400°-2000°F values were greater than 60 ft-lb. The excellent impact ductility of Sylvania SiCrTi coated XB-88 at 1400°F is not inconsistent with the above noted poor tensile strain capability of the system at this temperature in view of the findings of Allen and Bartlett (Ref. 4). A similar strain rate effect was documented in their work and attributed principally to the longer exposure of coating-substrate cracks to air at a lower strain rate.
- The ballistic impact performance of Sylvania slurry coatings was in general inferior to that of both Solar and TRW coatings. This trend is attributed to the highly oxidation-resistant layers adjacent to the substrate for the latter coatings, which are apparently less prone to impact damage.
- The Sylvania SiCrFe, Sylvania SiCrV, and TRW TiAl coatings are superior to the TRW TiCr, TRW TiCr-Al, and TRW TiCr-Si coatings in oxidation resistance at 1300° and 1600°F. The Sylvania SiCrFe coating exhibited the best performance, with lives in excess of 1000 hours at 1400°-1600°F for 17 of the 20 specimens tested.

- All coatings investigated for the blade root application, metallic and silicide types, demonstrated adequate wear-galling resistance.
- Qualitatively, the NiCr and NiPt blade root coatings tested have considerably less detrimental effect on composite ductility (Cb-132M alloy substrate) than the pack- or slurry-applied metallic and silicide coatings. However, the 1300° and 1600°F oxidation performance of the NiCr and NiPt coatings was very poor, primarily because the application techniques which were employed in this program had not been optimized.
- The Sylvania SiCrFe and TRW TiAl/XB-88 systems, including areas of overlap with the Sylvania SiCrTi blade airfoil coating, have adequate high-cycle reverse-bending fatigue strengths for turbine blade root application. The strength of Sylvania SiCrFe coated XB-88 alloy was outstanding: 10^7 cycles without failure for a notched ($K_t=3.2$) specimen loaded to 49,000 psi.

2. RECOMMENDATIONS

Based on the results obtained during the two-year evaluation effort, it is recommended that:

- The Sylvania SiCrTi slurry be engine tested as a vane coating on a substrate to be selected in Phase VIII, Component Design and Simulated Engine Test.
- The insensitivity of Sylvania SiCrTi coated B-66 alloy to thermal cycling be investigated to aid in the development of advanced columbium composites for turbine engine applications.
- Solar MoTi-Si (TNV-12SE4) and Solar V-(CrTi)-Si be investigated further as candidate vane and blade airfoil coatings.
- Additional effort be expended to develop application techniques for nickel-chromium and precious metal coatings for turbine blade roots.
- Studies be initiated to further develop the applicable coatings and high-creep-strength columbium alloys for turbine blade use with emphasis on resistance to thermal fatigue. Toward this end, coating ductility in the 1200°-2000°F range should be improved without sacrifice in 2000°-2400°F oxidation life, and alloy composition and processing variables should be tailored to ensure a reproducible combination of low- and intermediate-temperature (70°-2000°F) ductility and elevated temperature (2000°-2400°F) creep strength. A realistic target for ductility as described above would be minimum true tensile and creep strain capabilities of 2 percent throughout the operating temperature range.

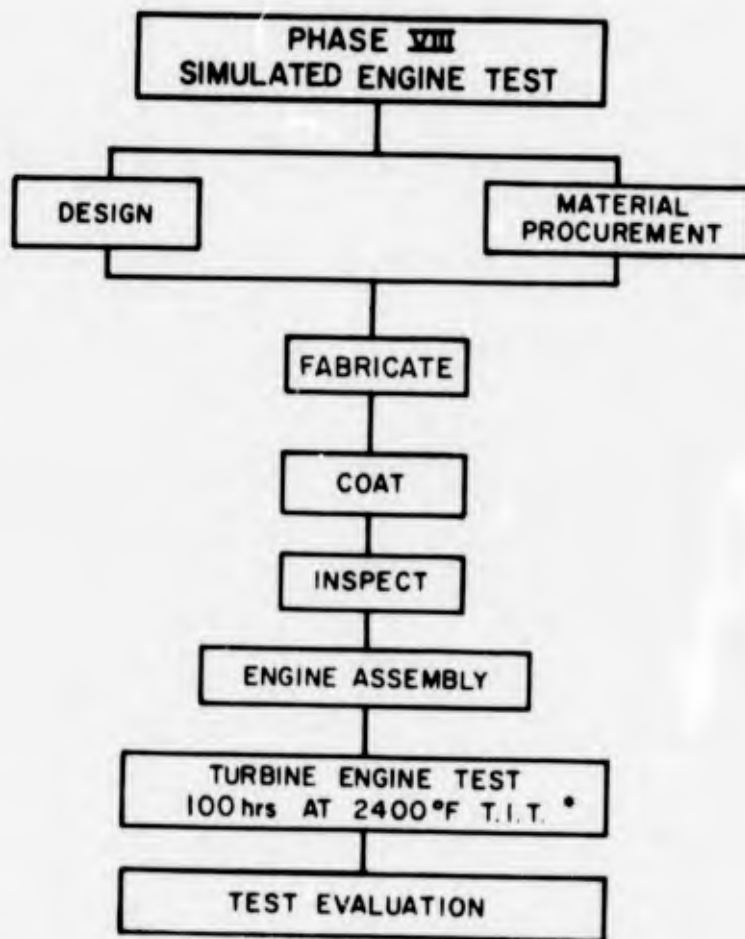
Of the five recommendations listed above, the last four are outside the scope of this contract.

SECTION V

FUTURE WORK

Item 12, Preliminary Test Design and Material Procurement, and Item 13, Simulated Engine Test, are Phase VIII of the program (see Figure 161). The appropriate coating-substrate system(s) for engine testing will be selected with approval of the Air Force Materials Laboratory Project Engineer.

Turbine components will be designed with the aid of the advanced evaluation mechanical test data and the necessary substrate material purchased for the fabrication of engine test hardware under Item 12. Upon receipt of specific authorization from the Air Force, a number of components will be fabricated under Item 13. These parts will be installed in a turbine development engine and tested at temperatures approaching substrate alloy limits to establish short-time, high-performance capability under actual engine conditions and to provide an indication, by correlation with longer term laboratory test data, of the multihundred-hour performance of this hardware.



* TURBINE INLET TEMPERATURE

Figure 161. Flow Chart for Phase VIII of Program (Items 12 and 13)

REFERENCES

1. R. T. Begley, J. L. Godshall, and D. Harrod, Development of Columbium Base Alloys, Technical Report AFML-TR-65-385, Westinghouse Astronuclear Laboratory, January 1966.
2. Private communication with Westinghouse Astronuclear Laboratory.
3. R. L. Stephenson, Comparative Creep-Rupture Properties of D-43 and B-66 Alloys, Report ORNL-TM-944, Contract Number W-7405-eng-26, Union Carbide Corporation, Oak Ridge National Laboratory, November 1964; DMIC Memorandum 203, 26 April 1965.
4. B. C. Allen and E. S. Bartlett, "Elevated Temperature Tensile Ductility Minimum in Silicide Coated Cb-10W and Cb-10W-2.5Zr," Transactions of the American Society of Metals, V. 60, pp. 295-304, September 1967.

UNCLASSIFIED

Security Classification

DOCUMENT CONTROL DATA - R&D

(Security classification of title, body of abstract and indexing annotation must be entered when the overall report is classified)

1 ORIGINATING ACTIVITY (Corporate author) Pratt & Whitney Aircraft Division of United Aircraft Corporation		2a. REPORT SECURITY CLASSIFICATION UNCLASSIFIED	
		2b. GROUP N/A	
3 REPORT TITLE EVALUATION AND IMPROVEMENT OF COATINGS FOR COLUMBIUM ALLOY GAS TURBINE ENGINE COMPONENTS			
4 DESCRIPTIVE NOTES (Type of report and inclusive dates) Second Summary Technical Report, 1 May 1966 to 31 December 1967			
5 AUTHOR(S) (Last name, first name, initial) Hauser, H. A. and Holloway, J. F., Jr.			
6 REPORT DATE May 1968	7a. TOTAL NO OF PAGES 254	7b. NO OF REFS 4	
8a. CONTRACT OR GRANT NO. AF33(615)-2117	8a. ORIGINATOR'S REPORT NUMBER(S) AFML-TR-66-186, Part II		
b. PROJECT NO. 7312	8b. OTHER REPORT NO(S) (Any other numbers that may be assigned this report) PWA-3172		
c. Task No. 731201			
d.			
10 AVAILABILITY/LIMITATION NOTICES This document is subject to special export controls and each transmittal to foreign governments or foreign nationals may be made only with prior approval of the Metals and Ceramics Division (MAM), Air Force Materials Laboratory, Wright-Patterson AFB, Ohio 45433.			
11 SUPPLEMENTARY NOTES N/A		12 SPONSORING MILITARY ACTIVITY Air Force Materials Laboratory (MAMP) Wright-Patterson AFB, Ohio 45433	
13 ABSTRACT (This abstract is continued on the following sheet.) Data generated using laboratory tests such as oxidation-erosion, thermal fatigue, ballistic impact, and wear-galling to simulate turbine engine environments are reported for 14 coated columbium alloy composites, 12 in preliminary screening evaluations, 3 of which were pursued through advanced evaluation, and 2 others involved only in the advanced evaluation. Applications considered were turbine vane and turbine blade airfoils operating in the 1800°-2500°F temperature range and turbine blade roots at 1300°-1600°F. Oxidation-erosion, thermal fatigue, and ballistic impact test results for five vane and blade airfoil coating-substrate systems are reported and reviewed through preliminary screening and, where applicable, coating improvement phases. The Sylvania SiCrTi slurry/B-66 alloy and Solar MoTi-Si(TNV-12SE4)/Cb-132M alloy systems demonstrated the best overall performance of the five systems evaluated. As a result of the advanced evaluation program, it was recommended that the Sylvania SiCrTi slurry coating be engine tested on columbium alloy turbine vanes in the final phase of the contract program. Both the TRW TiCr-Si/Cb-132M and the Sylvania SiCrTi/XB-88 systems demonstrated potential for turbine blade application based on adequate oxidation-erosion, thermal fatigue, and 2200°F mechanical fatigue, creep, and stress-rupture performance in advanced evaluation. However, low ductility was observed in tensile tests at intermediate temperatures (1300°-1800°F). Since this characteristic would cause a high risk of premature failure during thermal cycling of a turbine blade, it was recommended that			

DD FORM 1473
1 JAN 64

UNCLASSIFIED

Security Classification

14.	KEY WORDS	LINK A		LINK B		LINK C	
		ROLE	WT	ROLE	WT	ROLE	WT
		Columbian Alloys Coatings (Oxidation-Resistant) Gas Turbine Engines					

INSTRUCTIONS

1. ORIGINATING ACTIVITY: Enter the name and address of the contractor, subcontractor, grantee, Department of Defense activity or other organization (*corporate author*) issuing the report.

2a. REPORT SECURITY CLASSIFICATION: Enter the overall security classification of the report. Indicate whether "Restricted Data" is included. Marking is to be in accordance with appropriate security regulations.

2b. GROUP: Automatic downgrading is specified in DoD Directive 5200.10 and Armed Forces Industrial Manual. Enter the group number. Also, when applicable, show that optional markings have been used for Group 3 and Group 4 as authorized.

3. REPORT TITLE: Enter the complete report title in all capital letters. Titles in all cases should be unclassified. If a meaningful title cannot be selected without classification, show title classification in all capitals in parentheses immediately following the title.

4. DESCRIPTIVE NOTES: If appropriate, enter the type of report, e.g., interim, progress, summary, annual, or final. Give the inclusive dates when a specific reporting period is covered.

5. AUTHOR(S): Enter the name(s) of author(s) as shown on or in the report. Enter last name, first name, middle initial. If military, show rank and branch of service. The name of the principal author is an absolute minimum requirement.

6. REPORT DATE: Enter the date of the report as day, month, year; or month, year. If more than one date appears on the report, use date of publication.

7a. TOTAL NUMBER OF PAGES: The total page count should follow normal pagination procedures, i.e., enter the number of pages containing information.

7b. NUMBER OF REFERENCES: Enter the total number of references cited in the report.

8a. CONTRACT OR GRANT NUMBER: If appropriate, enter the applicable number of the contract or grant under which the report was written.

8b, 8c, & 8d. PROJECT NUMBER: Enter the appropriate military department identification, such as project number, subproject number, system numbers, task number, etc.

9a. ORIGINATOR'S REPORT NUMBER(S): Enter the official report number by which the document will be identified and controlled by the originating activity. This number must be unique to this report.

9b. OTHER REPORT NUMBER(S): If the report has been assigned any other report numbers (*either by the originator or by the sponsor*), also enter this number(s).

10. AVAILABILITY/LIMITATION NOTICES: Enter any limitations on further dissemination of the report, other than those

imposed by security classification, using standard statements such as:

- (1) "Qualified requesters may obtain copies of this report from DDC."
- (2) "Foreign announcement and dissemination of this report by DDC is not authorized."
- (3) "U. S. Government agencies may obtain copies of this report directly from DDC. Other qualified DDC users shall request through _____."
- (4) "U. S. military agencies may obtain copies of this report directly from DDC. Other qualified users shall request through _____."
- (5) "All distribution of this report is controlled. Qualified DDC users shall request through _____."

If the report has been furnished to the Office of Technical Services, Department of Commerce, for sale to the public, indicate this fact and enter the price, if known.

11. SUPPLEMENTARY NOTES: Use for additional explanatory notes.

12. SPONSORING MILITARY ACTIVITY: Enter the name of the departmental project office or laboratory sponsoring (*paying for*) the research and development. Include address.

13. ABSTRACT: Enter an abstract giving a brief and factual summary of the document indicative of the report, even though it may also appear elsewhere in the body of the technical report. If additional space is required, a continuation sheet shall be attached.

It is highly desirable that the abstract of classified reports be unclassified. Each paragraph of the abstract shall end with an indication of the military security classification of the information in the paragraph, represented as (TS), (S), (C), or (U).

There is no limitation on the length of the abstract. However, the suggested length is from 150 to 225 words.

14. KEY WORDS: Key words are technically meaningful terms or short phrases that characterize a report and may be used as index entries for cataloging the report. Key words must be selected so that no security classification is required. Identifiers, such as equipment model designation, trade name, military project code name, geographic location, may be used as key words but will be followed by an indication of technical context. The assignment of links, roles, and weights is optional.

UNCLASSIFIED

Security Classification

DOCUMENT CONTROL DATA - R&D		
<i>(Security classification of title, body of abstract and indexing annotation must be entered when the overall report is classified)</i>		
1. ORIGINATING ACTIVITY (Corporate author)	2a. REPORT SECURITY CLASSIFICATION	
	2b. GROUP	
3. REPORT TITLE		
4. DESCRIPTIVE NOTES (Type of report and Inclusive dates)		
5. AUTHOR(S) (Last name, first name, initial)		
6. REPORT DATE	7a. TOTAL NO. OF PAGES	7b. NO. OF REFS
8a. CONTRACT OR GRANT NO.	8a. ORIGINATOR'S REPORT NUMBER(S)	
b. PROJECT NO.		
c.	8b. OTHER REPORT NO(S) (Any other numbers that may be assigned this report)	
d.		
10. AVAILABILITY/LIMITATION NOTICES		
11. SUPPLEMENTARY NOTES		12. SPONSORING MILITARY ACTIVITY
13. ABSTRACT Continued		
<p>testing of coated columbium alloy turbine blades not be conducted under this contract. Of eight candidate turbine blade root systems evaluated, the Sylvania SiCrFe slurry coated alloy composites proved superior in 1300°-1600°F oxidation, wear-galling resistance, and fatigue performance. The NiCr and NiPt coatings demonstrated potential for the blade root application, especially with regard to coating ductility and minimum effect on composite properties, but, as applied in this program, were poor in 1300° and 1600°F oxidation. Additional development work on these two systems was recommended.</p> <p>This abstract is subject to special export controls and each transmittal to foreign governments or foreign nationals may be made only with prior approval of the Metals and Ceramics Division (MAM), Air Force Materials Laboratory, Wright-Patterson AFB, Ohio 45433.</p>		

DD FORM 1473
1 JAN 64

UNCLASSIFIED

Security Classification